CP-1249 Final Report

Adaptive Grid Modeling and Direct Sensitivity Analysis for Predicting the Air Quality Impacts of DoD Activities

Prepared by:

Alper Unal

and

M. Talat Odman

School of Civil and Environmental Engineering
Georgia Institute of Technology
Atlanta, GA 30322-0512

February 13, 2004

Report Documentation Page		*Form Approved* *OMB No. 0704-0188*

Public reporting burden for the collection of information is estimated to average 1 hour per response, including the time for reviewing instructions, searching existing data sources, gathering and maintaining the data needed, and completing and reviewing the collection of information. Send comments regarding this burden estimate or any other aspect of this collection of information, including suggestions for reducing this burden, to Washington Headquarters Services, Directorate for Information Operations and Reports, 1215 Jefferson Davis Highway, Suite 1204, Arlington VA 22202-4302. Respondents should be aware that notwithstanding any other provision of law, no person shall be subject to a penalty for failing to comply with a collection of information if it does not display a currently valid OMB control number.

1. REPORT DATE **13 FEB 2004**	2. REPORT TYPE	3. DATES COVERED **00-00-2004 to 00-00-2004**

4. TITLE AND SUBTITLE	5a. CONTRACT NUMBER
Adaptive Grid Modeling and Direct Sensitivity Analysis for Predicting the Air Quality Impacts of DoD Activities	5b. GRANT NUMBER
	5c. PROGRAM ELEMENT NUMBER
6. AUTHOR(S)	5d. PROJECT NUMBER
	5e. TASK NUMBER
	5f. WORK UNIT NUMBER

7. PERFORMING ORGANIZATION NAME(S) AND ADDRESS(ES) **Georgia Institute of Technology,School of Civil and Environmental Engineering,Atlanta,GA,30332-0512**	8. PERFORMING ORGANIZATION REPORT NUMBER

9. SPONSORING/MONITORING AGENCY NAME(S) AND ADDRESS(ES)	10. SPONSOR/MONITOR'S ACRONYM(S)
	11. SPONSOR/MONITOR'S REPORT NUMBER(S)

12. DISTRIBUTION/AVAILABILITY STATEMENT
Approved for public release; distribution unlimited

13. SUPPLEMENTARY NOTES

14. ABSTRACT

15. SUBJECT TERMS

16. SECURITY CLASSIFICATION OF:			17. LIMITATION OF ABSTRACT	18. NUMBER OF PAGES	19a. NAME OF RESPONSIBLE PERSON
a. REPORT **unclassified**	b. ABSTRACT **unclassified**	c. THIS PAGE **unclassified**	**Same as Report (SAR)**	**201**	

Table of Contents

1 Executive Summary

Air pollutants emitted from Department of Defense (DoD) facilities can interfere with military activities or in some cases even threaten life and property. These emissions can contribute to local concerns on the military base and neighboring communities, and regional air quality problems can occur through long-range transport and transformation processes. In some cases, operations performed for the benefit of one component of the ecosystem may have adverse effects. For example, prescribed burnings performed on a base primarily to save the habitat of an endangered species may have contributed to the air quality problem in a nearby metropolitan area. Faced with such complex problems, DoD needs reliable tools to determine the impact of its operations on the environment. In particular, air quality simulation models are needed that can help determine the impacts of various types of emissions from military installations on air quality. Existing air quality models have limited reliability to respond to such needs.

The objective of this project was to enhance current air quality models in order to simulate the air quality impacts of military activities. Two techniques developed earlier, adaptive grid modeling and direct sensitivity analysis, have the potential to improve the ability of the models to capture source-receptor relationships between emissions at local scales and air quality at the regional scale. While adaptive grid modeling can fill the gaps between local and regional scales, the direct sensitivity analysis allows the impacts of specific sources to be discerned from cumulative effects on regional air quality.

In this study, a new air quality model that incorporates the adaptive grid and sensitivity analysis techniques was developed. A code review was conducted and test simulations were performed to verify that the new model fulfills the design requirements. August 15-18, 2000 period was simulated to determine the air quality impacts of the prescribed burning operation at Fort Benning, Georgia. The impact on Columbus metropolitan area is of particular interest. Ozone levels as well as their sensitivity to nitrogen oxide (NO_x) and volatile organic compound (VOC) emissions from the fires were modeled. Emission rates from the burns were estimated from the fire data which include the location, time and acreage of the burns, using the First Order Fire Effects Model (FOFEM). Data for other emissions in the region were obtained from an ongoing air quality study. Several simulations were performed with air quality model that is equipped with the new techniques as well as the base model. The adaptive grid in the new model enabled better resolution of the plumes caused by prescribed burns. The sensitivity of ozone concentrations to the fires was also better resolved in comparison to the brute-force method which takes the difference between two old-model simulations: one without and another with the fires. The adaptive model with direct sensitivity captured the near-source reduction and downwind increase in ozone concentrations due to the fires. This non-linear response of ozone, which is also observed in power plant plumes, was totally missed by the base model. In view of these results, it was concluded that the new model, enhanced by adaptive grid and sensitivity analysis techniques, can be used for accurate assessment of the air quality impacts of most DoD activities.

The results from this effort are expected to directly benefit the management of prescribed burning at Fort Benning. Additionally, the techniques developed can be used for the general purpose of predicting the fate of air pollutant emissions from aviation, ship, or coastal operations. Products can be developed to assist site managers in responding to immediate needs as well as in planning future emissions that will minimize the negative impacts on local and regional air quality. This project was completed in FY 2002.

2 Introduction

This project is about the fate of air pollutants associated with the Department of Defense (DoD) activities. Emissions from military installations may directly interfere with military activities such as training exercises, or in some cases even threaten life and property. They may jeopardize wildlife on the base and pose a risk to the neighboring communities. Further, through long-range transport and transformation processes, these emissions may contribute to regional air-quality problems. In some cases, operations performed for the benefit of one component of the ecosystem may have adverse effects on another component. For example, as will be described below, prescribed burnings performed on a base primarily to save the habitat of an endangered species may have contributed to the air quality problem in a nearby metropolitan area. Faced with such complex problems, DoD needs reliable tools to determine the impact of its operations on the environment. In particular, air quality simulation models are needed that can help determine the air quality impacts of emissions from military installations.

At their current state, existing air quality models would fall short of responding to DoD needs such as those described above. Our objective is to improve the ability to predict the impacts of air pollutants emitted as a result of military operations on the surrounding environment. The atmospheric and chemical modeling systems currently used by various agencies tend to focus on a single scale that seems to be the most relevant to a particular air pollution problem (e.g., global climate models or local scale accidental release models). However, the study of the impact of DoD facilities requires the investigation of the interaction between various scales due to the fact that both the location of the facilities and the lifetimes of emitted pollutants are conducive to long-range transport. Existing modeling systems need improvement in their representation of source-receptor relationships over a wide range of scales in order to predict accurately the ultimate fate of pollutants emitted from specific sources such as DoD facilities.

Recently, we have developed two unique techniques that would improve current air quality models by filling the gaps between the scales from local to regional and by discerning the impacts of specific sources from cumulative effects on regional air quality. These techniques are: 1) Adaptive grid modeling, and 2) Direct sensitivity analysis. We have developed both of these techniques to a level where they have been successfully applied to very relevant air quality problems. However, for application to DoD-related systems, a proof-of-concept was necessary to show that the techniques would work under the unique conditions of DoD operations. Although the techniques were developed with similar applications in mind, the primary objective has not been, for example, source apportionment at the facility level. This project aims to provide an early assessment of potential benefits.

To achieve the objectives stated above, we tested the two techniques within an advanced air quality model, in an urban-to-local scale application, to determine the impact of the prescribed burning operation on the ozone levels in a downwind metropolitan area. We assessed the potential of these new techniques in bringing the models to the desired level of reliability. This application is particularly important since the metropolitan area was recently declared a non-attainment area, and intends to get back in compliance with the national air quality standards as quickly as possible. There are several other sources affecting the ozone levels and it is critical to determine the incremental contribution of the DoD operation to develop a strategy for attainment.

In this project, the particular focus was on prescribed burning emissions from a military reservation at Fort Benning, Georgia, and their impact on local and regional air quality. However, the techniques are general enough for application to other military operations. We could target

other types of emissions, for example from aviation, ship, or coastal operations at various locations, in this project. Once the concept is proven, the techniques can be used for the general purpose of predicting the fate of air pollutant emissions from various military sources. Products can be developed that can assist site managers in responding to immediate needs, as well as being able to plan future emissions that will minimize the impact on the environment. This would be particularly advantageous in regions where such facilities must meet local pollution standards and where ambient concentrations of some pollutants are already high due to contributions from other anthropogenic and/or natural sources.

3   Problem Statement

3.1   Prescribed Burnings at Fort Benning

The reasons for prescribed burning at Fort Benning include to improve and maintain endangered species habitat, reduce hazardous fuels, prepare sites for seeding and planting, manage understory hardwoods, control disease, improve forage for grazing, enhance appearance, and improve access. The objective is to convert the landscape as close to its pre-settlement condition (a pine overstory with grasses, legumes, and other herbaceous vegetation as a ground cover) as possible. In 1994, Fort Benning received a Biological Opinion from the Fish and Wildlife Service stating that the actions on the base were likely to jeopardize the endangered red-cockaded woodpecker (RCW) habitat. One of the most economical means of maintaining the longleaf pine habitats is prescribed burning. Approximately 30,000 acres must be prescribed burned each year, during the growing season (March through August). This period falls within the "ozone season." In order to restore the RCW habitat, longleaf seedlings are planted. Prescribed burnings continue from August trough October for site preparation purposes which also overlaps with the ozone season. These fires reduce unwanted vegetation that would compete with longleaf seedlings.

Prescribed burning is an efficient and effective means to reduce fire fuel build-up. Heavy roughs can build up posing a serious threat from wildfire to lives, property, and all natural resources. A burning rotation of approximately 3 years is usually adequate to fire proof pine stands and reduce this threat. Prescribed burning helps control undesirable species which compete with pines. It also controls brownspot disease, which is a fungal infection that weakens and eventually kills longleaf seedlings. Burning increases the yield and quality of herbage, legumes, and browse from hardwood sprouts. Wildlife species such as deer, turkey, quail, and doves also benefit from prescribed burning. Prescribed burning on a regular basis also serves a military need by providing a safer training environment with improved access and visibility. Lastly, growing season burns have significantly reduced the tick population on the installation.

Operational and safety constraints limit the burnings to an average of 300 acres per day (Environmental Management Division, 2000). For example, although an attempt is made to burn all RCW clusters during the growing season it is logistically impossible due to the number of clusters (75-80 annually) and scheduling conflicts with training. Currently, ignition is accomplished with hand crews and drip torches. While this provides better control with respect to where the fire is applied and when, it is difficult to control the intensity of the fire. Natural firebreaks such as roads, trails, drains, and creeks dictate the size of burn areas. All these limitations make it necessary to continue the burnings throughout the year. In realization of the Columbus ozone problem, the majority of the burnings (70-75%) were shifted to the January-April period, which is outside the "ozone season."

Currently, the only external constraint on prescribed burning arises as a result of smoke management concerns. Smoke complaints and the threat of litigation from smoke-related incidents / accidents are the primary concerns. Fort Benning follows voluntary (not mandated by state or federal government) smoke management guidelines in an effort to minimize the adverse impacts from smoke. An additional concern is the effect of prescribed burning on ozone levels in Columbus. Forest fires produce nitrogen oxide and hydrocarbon emissions that form ozone (Cheng *et al.*, 1998; Battye and Battye, 2002; Ottmar, 2001). These pollutants may be transported downwind, mix with emissions from other sources and contribute to the poor air quality in urban areas. Sulfur dioxide and particulate matter emissions from forest fires are also of concern but, in general, they do not have a direct influence on the urban ozone problem. The ozone alert season is from 1 May through 30 September in Georgia. It is during this season that emissions from prescribed burning operations could affect smog levels in Columbus. In collaboration with the Partnership for a Smog-Free Georgia (PSG), Fort Benning is avoiding prescribed burns when meteorological conditions are conducive to ozone buildup. If Columbus shows a trend toward more days with elevated ozone levels, it will become more critical to design burning strategies that can adapt to changing weather parameters.

3.2   Limitations of Current Air Quality Models

The atmospheric and chemical modeling systems currently used by various agencies tend to focus on a single scale that seems to be the most relevant to a particular air pollution problem. Global scale models address climate issues while regional scale models are used for the tropospheric ozone, regional haze or acid deposition studies. Urban scale smog models are being replaced with urban-to-regional scale models in most places where transport from other upwind sources play an important role. On the local scale, models are used to deal with problems such as accidental releases. The domains of local scale models are limited by design; therefore, they cannot be used for regional scale impact studies.

One of the most advanced urban-to-regional scale models is the Multiscale Air Quality Simulation Platform (MAQSIP) (Odman and Ingram, 1996). Urban-to-regional scale models are used in developing emission control strategies for problems such as urban and regional ozone, acid deposition, or regional haze which is attributed to primary (emitted) and secondary (formed in the atmosphere) fine particulate matter. While these models are equipped with special tools to treat emissions from large power plants (Karamchandani *et al.*, 2000), they lack the ability to resolve emissions from relatively small area sources such as those from prescribed burnings. To account for such area sources, the models rely on grid resolution. Prescribed burnings are performed over areas as small as one square kilometer (approximately 200 acres). This scale is too small for typical regional applications. Therefore, emissions from prescribed fires are blended with emissions from many other sources within the same grid cell of regional scale models. This would make it impossible to conduct an impact study that would target emissions from biomass burnings.

Another limitation of current air quality models is related to numerical errors involved during the simulations. Let us suppose that the grid cell size could be reduced to one square kilometer by using nested-grid techniques (Odman *et al.*, 1997). In that case, a typical prescribed burning unit would cover a single grid cell. The effect of having or not having prescribed burning emissions from a single grid cell would be a small perturbation for air quality models. As the perturbation gets smaller in size, numerical errors that affect the simulation results become more important. The results of an impact study such as the one here would be highly uncertain if the models were used as is. Therefore, urban-to-regional scale models, in their current state, are not very reliable tools for determining the impact of prescribed burning emissions to the surrounding environment.

The study of the impact of biomass burning from DoD facilities requires investigation of the interaction between various scales due to the fact that both the location of the facilities and the lifetimes of emitted pollutants are conducive to long-range transport. Below, we describe a methodology to improve current urban-to-regional scale air quality models with two modeling techniques. These techniques improve representation of the transport and transformation processes over a wide range of scales and provide more reliable source-receptor relationships. The product is a more reliable tool that can predict accurately the ultimate fate of pollutants emitted from specific sources such as DoD facilities.

4 Methodology

Recently, we have developed two unique techniques that can improve the air quality models by filling the gaps between the scales from local to regional and by discerning the impacts of specific sources from cumulative effects on regional air quality. They are: 1) Adaptive grid modeling, and 2) Direct sensitivity analysis. These techniques improve representation of the transport and transformation processes over a wide range of scales and provide more reliable source-receptor relationships. An air quality model equipped with these two techniques would be a more reliable tool that can predict accurately the ultimate fate of pollutants emitted from specific sources such as DoD facilities. In this section we describe the two techniques in detail and overview the air quality modeling platform.

4.1 Adaptive Grid Modeling

We developed an adaptive grid modeling approach to reduce the uncertainty in air quality predictions. By clustering the grid nodes in regions that would potentially have large errors in pollutant concentrations, the model is expected to generate much more accurate results than the traditional fixed, uniform grid counterparts. The repositioning of grid nodes is performed automatically through the use of a weight function that assumes large values when the curvature (change of slope) of the pollutant fields is large. The nodes are clustered around regions where the weight function bears large values, thereby increasing the resolution where the error is large. Since the number of nodes is fixed, refinement of grid scales in regions of interest is accompanied by coarsening in other regions where the weight function has smaller values. This yields a continuous multiscale grid where the scales change gradually. Unlike nested grids, there are no grid interfaces, which may introduce numerous difficulties due to the discontinuity of grid scales. The availability of computational resources determines the number of grid nodes that can be afforded in any model application. By clustering grid nodes automatically in regions of interest, the adaptive grid technique uses computational resources in an optimal fashion throughout the simulation.

A detailed description of the technique can be found in Srivastava *et al.* (2000). Here we will not repeat that information; instead, we will try to illustrate the technique and its potential with relevant applications. The adaptive technique was applied to problems with increasing complexity and relevance to air quality modeling. First, it was applied to pure advection tests (Srivastava *et al.*, 2000). In a rotating cone test, the adaptive grid solution was more accurate than the fixed uniform grid with the same number of grid nodes. The error in maintaining the peak of the cone was only 13% compared to 39% with the fixed grid: an accuracy that could only be achieved by using 22 times more grid nodes with a fixed uniform grid. In a second test, four cones were rotated to measure the performance of the algorithm in following multiple features. Once again, the peak accuracy was better than the fixed uniform grid alternative. The peak error increased to 23% since the grid nodes, whose number was the same as in the previous test, were being

4

clustered around four cones instead of one. Srivastava *et al.* (2001a) conducted a third test with concentric conical puffs of NO_x and VOCs reacting in a rotational wind field. The parameters of this problem are such that, after a certain time, ozone levels drop below the background near the base of the conical puffs but they peak near the vertex of the cones. This feature was resolved by the adaptive grid solution while it was completely missed by the uniform fixed grid solution. When nine times more grid nodes were used, the fixed grid was finally able to reveal this feature but not as accurately as the adaptive grid technique. The overhead involved in adaptive grid computations is much smaller than the time spent in computing the chemical kinetics for these additional nodes. Overall, the adaptive grid algorithm is about 10 times more efficient than the uniform grid alternative for the same level of accuracy.

Next, the adaptive grid technique was applied to the simulation of a power plant plume (Srivastava *et al.*, 2001b). A two dimensional plume with a VOC/NO_x emission ratio of 14% was advected with uniform winds and diffused over a background with a VOC/NO_x ratio of 35. Other parameters were chosen to make the dispersion as realistic as possible. After about 12 hours of simulation, the composition of the plume was analyzed taking cross sections at various downwind distances. At 10 km downwind, the adaptive grid solution showed a NO_x rich, but ozone deficient core. This feature, which is also observed in actual power plant plumes, was completely missing in the uniform grid solution, which artificially diffused the NO_x and displayed highest ozone levels at the core of the plume. The adaptive grid, on the other hand, had ozone bulges developing near the plume edges. At a downwind distance of 30 km, these bulges continued to grow as NO_x diffused slowly from the core to the edges (at a rate more in line with physical diffusion) and radicals were entrained into the plume. This plume structure started disappearing after about 80 km. At a downwind distance of 135 km, the plume was fully *matured* with an ozone peak at the center. The peak ozone concentration was larger than one predicted by the fixed uniform grid. A similar evolution of the plume was observed in the fixed uniform grid solution when the number of grid nodes was increased by a factor of nine. However, this solution was about five times more expensive than the adaptive grid solution.

Another relevant application was the multiple source test, where an imaginary city was placed at the center of a domain with diagonal winds (Odman *et al.*, 2000b). The city consists of an inner circular source representing urban conditions and an outer circle representing suburban conditions. The VOC/NO_x emission ratios are 5 and 9, respectively. There are two identical point sources with a VOC/NO_x emission ratio of 14%: one is located upwind and the other downwind from the city. The background has a VOC/NO_x ratio of 10. Figure 2 of Section 5.b shows the adaptive grid at the beginning of the simulation and 12 hours later. The locations of the sources are clearly visible in the initial grid. Note that the grid nodes are clustered around the point sources and at the transitions from the background to the outer suburban circle and from the suburban to the urban circles. Once the simulation started, the nodes continued to cluster around the upwind source but moved away from the downwind source towards the upwind end of the city. This behavior was mostly due to a more uniform ozone field downwind of the city.

After these and other testing of the algorithm (Odman *et al.*, 2001; Khan et al, 2003), finally an adaptive grid AQM was developed (Odman *et al.*, 2002). The model was applied to an ozone simulation in the Tennessee Valley (Khan and Odman 2003). Ozone results from this application were evaluated and showed significant improvement over those from fixed grid models, even those employing up to four times more grid cells. In several cases the agreement with observations was better compared to fixed grid models. When the reasons were investigated it was found that the complex source-receptor relationships, especially the long-range ones were much better resolved with the adaptive grid.

4.2 Direct Sensitivity Analysis

Sensitivity analysis is essential in determining source-receptor relationships and designing emission control strategies. The traditional "brute-force" method involves running the model several times, each time perturbing one type of emission (e.g., NO_x or VOC) from a different source. If the perturbation is small, the brute-force method may not yield accurate sensitivities due to numerical errors propagating in the model. Our group has developed a new and powerful direct sensitivity analysis technique to study the response of air quality to various types of emissions (Yang *et al.,* 1997). Unlike the brute force approach, this technique is not limited by the magnitude of the perturbation and, in theory, it can be used for even infinitesimal changes in emissions. Therefore, the technique has the potential of improving current models to a level where they can be used for impact analysis of relatively small sources such as military installations.

Air quality models are based on the atmospheric diffusion equation:

$$\frac{\partial c_i}{\partial t} + \nabla \cdot (\mathbf{u} c_i) = \nabla \cdot (\mathbf{K} \nabla c_i) + R_i + S_i. \tag{1}$$

Here, c_i is the concentration of the ith pollutant species, $\mathbf{u}$ describes the velocity field, $\mathbf{K}$ is the diffusivity tensor, $R_i(c_1, c_2, ...)$ is the chemical reaction term and S_i is a source term for certain types of emissions. The local sensitivity of the concentration of a species (e.g., ozone) to a certain emission type (e.g., NO_x or VOC) from a particular source can be defined as:

$$s_{ij}(t) = \frac{\partial c_i(t)}{\partial E_j}. \tag{2}$$

Here, s_{ij} is the sensitivity of c_i to emission E_j. Using direct derivatives of Equation (1) the following equation can be obtained for sensitivities.

$$\frac{\partial s_{ij}^*}{\partial t} = -\nabla(\mathbf{u} s_{ij}^*) + \nabla(\mathbf{K} \nabla s_{ij}^*) + J_{ik} s_{kj}^* + \frac{\partial R_i}{\partial \varepsilon_j} + \frac{\partial S_i}{\partial \varepsilon_j} - \nabla(\mathbf{u} c_i)\delta_{ij} + \nabla(\mathbf{K} \nabla c_i)\delta_{ij} \tag{3}$$

Here, s_{ij}^* is the semi-normalized sensitivity coefficient, J_{ik} is the Jacobian matrix, ε_j is a scaling variable with a nominal value of 1, and δ_{ij} is a binary variable (either 1 or 0). Since the sensitivities to different emissions can vary by many orders of magnitude, it was necessary to define semi-normalized sensitivity coefficients, s_{ij}^*.

The similarities between Equations (1) and (3) allows us to use the same or very similar numerical solution techniques and calculate local sensitivities to emission sources simultaneously along with the species concentrations. This also makes the implementation of the technique in any model relatively straightforward. The technique is also computationally efficient because several of these sensitivities (the number being limited by available core memory) can be calculated simultaneously with a fractional increase in CPU time. The emission sources can be discerned by type as point, area, mobile, or biogenic, and by composition such as SO_2, NO_x, or VOC. Also, the location of the emission source can be specified, for example, as the boundaries of a DoD facility (to the grid scale resolution). The technique would predict the sensitivity of air

quality at any desired location in the modeling domain (e.g., sensitivity of ozone concentrations at a downwind urban center) to a fractional change in the emissions from the source of interest.

The technique has been evaluated in an application to the Southern California where the sensitivities of ozone concentrations to the domain wide reductions of mobile and area sources of NO_x were compared to a brute-force method (Yang *et al.*, 1997). This technique was used in an integrated modeling system focusing, simultaneously, on ozone, particulate matter and acid deposition (Boylan, *et al.*, 2001). We investigated the sensitivity of particulate matter concentrations to the reductions of SO_2 and NO_x emissions in the Southern Appalachian Mountains region. We also investigated the sensitivity of ozone concentrations to NO_x and VOC emissions from different states, using state boundaries as sub-regions. As part of that project, we compared our method to the brute-force approach for ozone sensitivities to domain wide NO_x and VOC emissions. The general agreement between the direct sensitivity and the brute-force method shows that the former is a reliable tool. Whenever we observed differences, we were able to relate the difference to the numerical errors associated with the brute force technique and show that the direct sensitivity method yields results that are more accurate.

Note that in all of the applications thus far, we have focused on a relatively large perturbation such as a reduction over the entire domain or an entire state in a region as big as the Eastern U.S. When the focus is shifted to a small contributor, such as a single DoD facility in a large region, the results of a brute-force analysis would be very unreliable. This is more so if the facility is surrounded by other sources of emissions of the same type. As mentioned several times before, the reason is that the perturbation may be below the numerical detection limit of the model. It is very likely that numerical errors in the model would be larger than the perturbation so that a noise is obtained, instead of an accurate response, from the brute-force analysis. The direct sensitivity analysis on the other hand is not subject to such a limitation and even the response of an infinitesimal change in emissions can be detected accurately.

4.3 Air Quality Modeling

The platform of choice for the incorporation of the adaptive grid modeling and direct sensitivity analysis techniques is the Multiscale Air Quality Simulation Platform (MAQSIP) (Odman and Ingram, 1996), which is an early prototype of the Community Multiscale Air Quality (CMAQ) (Byun and Ching, 1999). MAQSIP is a state-of-the-art pollutant transport and chemistry model. The following attributes of MAQSIP distinguish it from other models.

1) **Modular**: MAQSIP is a truly modular platform where physical/chemical processes are cast into modules following the time-splitting approach. Each process module operates on a common concentration field. Other variables are encapsulated within each module.

2) **Flexible**: MAQSIP has alternative modules for various processes.

3) **Expandable**: New modules can be (and are being) added to the platform by scientists using MAQSIP in their research.

4) **Multiscale**: MAQSIP supports multiple, multi-level nested grids.

5) **Generalized Coordinates**: MAQSIP can support practically any coordinate system.

The MAQSIP model offers the user a choice among the CB-4 and SAPRC-99 chemical mechanisms. For the type of emissions involved in prescribed burning, both mechanisms offer similar ozone formation pathways. In an application to California, CB-4 and SAPRC-99 mechanisms gave essentially the same results for ozone, and while the SAPRC mechanism offers more detail, the CB-4 mechanism is computationally faster. Investigating the effect of different chemical mechanisms on the results is beyond the scope of this project and since their ozone pathways are very similar either mechanism could be used. For this study CB-4 mechanism was selected.

The adaptive grid version of MAQSIP is described in detail elsewhere (Odman et al., 2001 and 2002). The grid adaptation was restricted to the horizontal plane and the same grid structure was used for all vertical layers. Air quality models such as MAQSIP have unequally spaced vertical layers designed to better resolve mixing in the Planetary Boundary Layer. Typically, starting from about 20 m at the surface, layer thickness increases as the model is extending to the upper troposphere. Adaptation in the horizontal plane has no direct effect on this vertical resolution.

A weight function determines where grid nodes must be clustered to obtain a more accurate solution. In this study, the curvature in the concentrations of an inert fire tracer was used to calculate the weight function that drives the adaptation. The tracer is assumed to be a product of the fires at Fort Benning emitted at the same rate as the NO emissions from the fire. The tracer is transported and deposited in the same way as other fire species but it is non reactive.

The presence of convective clouds is an important factor that affects pollutant levels. Cloud scavenging of gaseous pollutants and aerosol formation in clouds are important processes that must be characterized in air quality models. However, for the ozone episode that was investigated in this proof-of-concept study, clouds and precipitation were not major factors. The scenario simulated had clear sky conditions conducive to photochemical ozone formation. A follow on project, which addresses secondary PM formation, can thoroughly investigate the processes related to clouds and precipitation. In addition, in relation to the adaptive grid modeling, the presence of clouds presents a good reason for developing three-dimensional adaptation techniques.

5 Accomplishments

5.1 Data Preparation

The episode selection is based primarily on the availability and quality of meteorological and emissions data as well as the impact potential of prescribed burns at Fort Benning on regional air quality. As part of Fall Line Air Quality Study (FAQS), we have already simulated several episodes during summer of 1999 and 2000 in Georgia using MM5 meteorological model and SMOKE emissions model. The ideal scenario for our case study is one with southeasterly winds, biomass burning performed at Fort Benning and high ozone levels observed at Columbus. The Host Site Coordinator of the SERDP Ecosystem Management Project (SEMP) at Fort Benning, Mr. Hugh Westbury, was very instrumental in providing the fire data for the years 2000-2001. Based upon meteorological conditions and fire data a four-day period, August 15-18 2000, was selected for modeling. Fires were reported at Fort Benning on those days and there are periods during which the winds were southeasterly hence it is possible that fires may have affected air quality in Columbus. Table 1 shows the data for the fire events on those days.

Table 1. Fire data during the August 15-18 2000 period.

Fire	Date	Time (GMT)	Area (km^2)
1	8/15/00	17:00 –20:00	0.142
2	8/15/00	18:00	0.079
3	8/16/00	17:00	0.039
4	8/18/00	1:00 –3:00	0.002
5	8/18/00	1:00 –3:00	0.001
6	8/18/00	1:00 –3:00	0.139
7	8/18/00	1:00 –3:00	0.097
8	8/18/00	12:00	0.039

Data preparation efforts included meteorological and emissions data preparation as well as post-processing. Meteorological data were obtained from FAQS. Detailed information on meteorological data preparation is given elsewhere (Hu *et al.*, 2003a). Similarly emissions data were obtained from FAQS study. More information on emissions data can be obtained elsewhere (Unal *et al.*, 2003; Hu *et al.*, 2003b). For biomass burning emissions First Order Fire Effects Model (FOFEM) Version 5, developed by Intermountain Fire Sciences Laboratory was utilized. In this model fuel type was assumed as natural fuel with long leaf pine trees. For some of the pollutants, such as speciated VOCs and NO_x, emission factors provided by Battye and Battye (2002) were utilized. Table 2 shows the estimated emissions for biomass burning.

Table 2. Estimated emissions for the fire events during the August 15-18 2000 period.

Fire	Pollutants (kg/hr)											
	CH$_4$	CO	NO	NO$_2$	PAR	OH	HCHO	ALD	TOL	XYL	OLE	CRE
1	34.6	745	9.08	1.01	6.82	2.94	5.19	3.03	1.70	0.19	0.57	0.93
2	17.9	387	4.72	0.52	3.54	1.53	2.69	1.57	0.88	0.10	0.30	0.48
3	11.9	257	3.14	0.35	2.36	1.02	1.79	1.05	0.59	0.07	0.20	0.32
4	0.73	15.6	0.19	0.02	0.14	0.06	0.11	0.06	0.04	0.00	0.01	0.02
5	0.20	4.25	0.05	0.01	0.04	0.02	0.03	0.02	0.01	0.00	0.00	0.01
6	54.3	1170	14.3	1.58	10.7	4.62	8.14	4.76	2.66	0.30	0.90	1.45
7	37.8	814	9.93	1.10	7.46	3.21	5.67	3.31	1.85	0.21	0.63	1.01
8	8.9	193	2.35	0.26	0.04	0.04	0.01	0.00	0.04	0.00	0.01	0.00

5.2 Model Preparation

The task here was to install the direct sensitivity analysis technique, which we have previously developed for a static grid model, into the adaptive grid version of MAQSIP. This required several modifications to the algorithm and the computer code. The most important change is the treatment of the emission source during the calculation of sensitivity to that source. Since an emission source is fixed with respect to the static grid, in the old code the grid cells overlapping the emission source (e.g., location of the fire) were being flagged before the simulation. Then, the sensitivity of the emitted species in the flagged cells was being set equal to the emission rate into that cell. In the adaptive grid model, since the grid nodes are constantly moving, the grid cells cannot be flagged beforehand. Also the intersection of the emission source with each cell keeps changing. An algorithm was devised to find this intersection. In the new code, the sensitivity of the emitted species in each cell is being set equal to the emissions per unit area times the intersection area of the cell with the emission source. Another change worth noting is the addition of an inert fire tracer species to drive the grid adaptation. This tracer is transported just like the other species and the grid is adapted to the curvature in the tracer's concentration.

In order to verify the new model which incorporates the adaptive grid and sensitivity analysis techniques, a test simulation was performed with fire emissions under controlled meteorological conditions (i.e., constant winds). The sensitivity results obtained with the new model have been compared to the "brute-force" sensitivity (i.e., the difference between two runs: one with and another without the fire emissions) obtained from the old model (i.e., static grid MAQSIP). Initially, the sensitivities from the two models were significantly different so the new model could not be verified. A quick review of the critical modules revealed several programming mistakes or "bugs." To identify the few remaining "bugs", the computer program was reviewed by the principal investigator and a programmer. In this review, the flow of the program was followed through a debugger during a typical simulation. After the remaining bugs were found and fixed, it was concluded that the program properly executed the operations described in the algorithm. In addition, the results of test simulations showed that the computer program fulfills the requirements of the original design. Therefore, the new model was declared "verified" and ready for simulations.

5.3 Simulations

Emissions and meteorology data were processed to prepare the inputs required to run the air quality model. Simulations were conducted in three stages:
(1) Simulation of the selected episode with 4×4 km^2 static grid version of the MAQSIP model;
(2) Simulation of the selected episode with the new version of the MAQSIP model incorporating the adaptive grid and direct sensitivity analysis techniques.

Static Grid Simulations

To be used for comparison in the evaluation of the new model, the selected episode was simulated with a 4×4 km^2 static grid version of the MAQSIP model. Lambert Conformal projection with parameters of 30^0N, 60^0N, and 90^0W, centered at 40^0N and 90^0W, was utilized for the domain. The 4×4 km^2 grid has 102 columns and 78 rows with 13 vertical layers. The results of the static grid run were compared with outputs from CMAQ model for the same location and time

period generated during the FAQS project. The comparison showed that static grid results were similar to the CMAQ results. Since CMAQ results were already compared with observed air quality data and found to be an accurate representation of actual conditions, no further evaluation of the static grid MAQSIP results (i.e., with observations) was performed. A second run was also made including emissions from the fires at Fort Benning. The difference between the concentrations of these two simulations yields the static grid "brute-force" sensitivities.

Adaptive Grid Simulations

The adaptive grid also used the same domain definitions as for the static grid. In adaptive runs the concentration of an inert fire tracer was used to calculate the weight function that drives the adaptation. The tracer is assumed to be a product of the fires at Fort Benning emitted at the same rate as the NO from the fires. The tracer is transported and deposited in the same way as the other fire species but it is non reactive. Two different runs were made with the adaptive grid model. These runs include: one run with base emissions; and one run with base emissions plus fire emissions, which also has the direct sensitivity calculations. In both runs the grid adapted to the same fire tracer, therefore the grids are identical in both simulations. The difference between the concentrations of these two simulations yields the adaptive grid "brute-force" sensitivities. Direct sensitivity results were compared with "brute-force" and it was observed that differences were within the bounds of previously reported differences (Hakami *et al.*, 2003). Only direct sensitivities will be used hereafter.

Simulation Results

First we compared the adaptive grid model with the static grid model. The tracer concentrations calculated by the two models as a result of fires at Fort Benning on August 15, 2000 at 19:00 Greenwich Mean Time (GMT) are shown in Figures 1 and 2. During this period two different fires happened at two different locations. The fire to the south is emitting at a higher rate than the northern one since the area burnt is almost 1.5 times bigger. The location of these fires can be seen in both static and adaptive simulation results.

One of the significant differences between these simulations is the fact that static grid distributes emissions uniformly to the 4×4 km^2 cell area where the fire takes place. Adaptive grid, on the other hand, increases the grid resolution around the fire location as shown in Figure 2. At the points where fires occur, adaptive grid reduces cell size to approximately 400 m or one tenth of the static grid size. This provides adaptive grid the capability to distinguish two distinct plumes from the fires. For this reason concentration gradients are much better resolved by the adaptive grid model than by the static grid model. Simulation results for other hours are presented in Appendices.

Another objective of this study was to utilize direct sensitivity method to estimate sensitivity of ozone to NO emissions from fires. We made a comparison between static "brute-force" and adaptive direct sensitivity results. Figures 3 and 4 present sensitivity of ozone concentration to fire emissions as estimated by static and adaptive grids respectively on August 15, 19:00 (GMT). While the fires reduce the ozone concentrations near the source by as much as 8 parts per billion (ppb), they result in an increase by as much as 7 ppb further downwind for this particular time period. Such a distinction between the near and the far field impacts is not so clear in the "brute-force" sensitivities calculated by the static grid model shown in Figure 3. Simulation results for other hours are presented in Appendices.
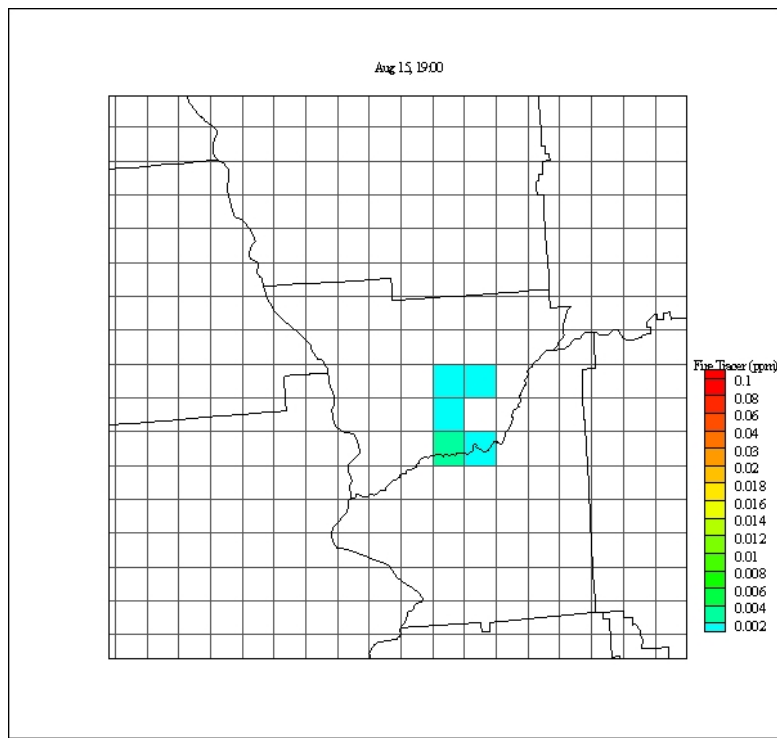
11

Figure 1. Static Grid Result for Inert Fire Tracer Concentrations (ppm)
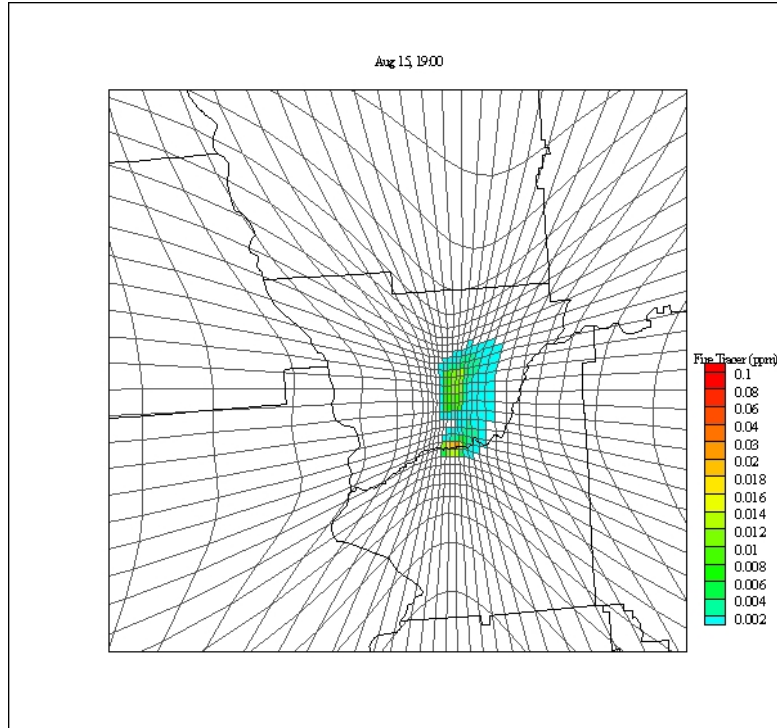
Figure 2. Adaptive Grid Result for Inert Fire Tracer Concentrations (ppm)
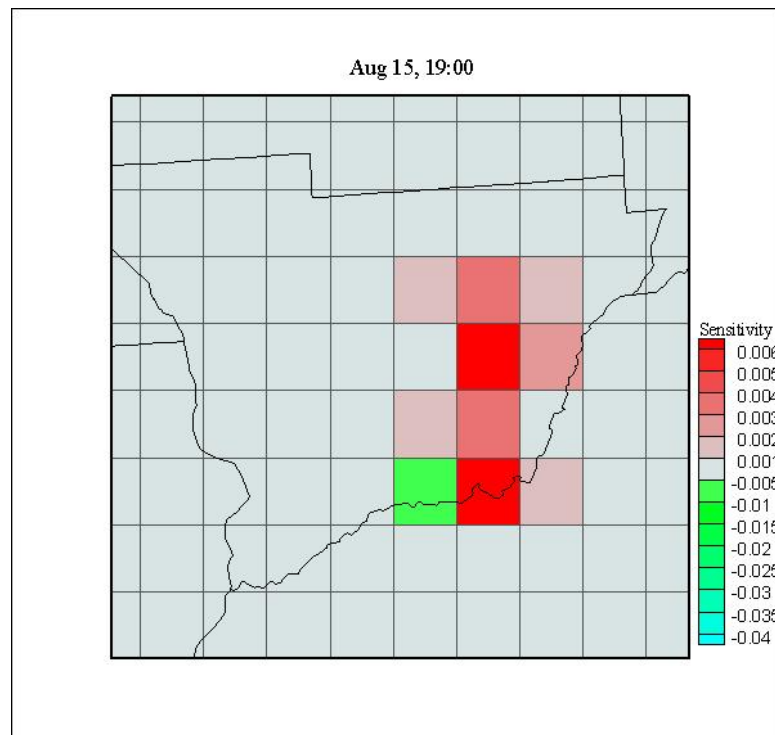
Figure 3. Static Grid Result for Brute-Force Sensitivity of O$_3$ (ppm) to Fire Emissions
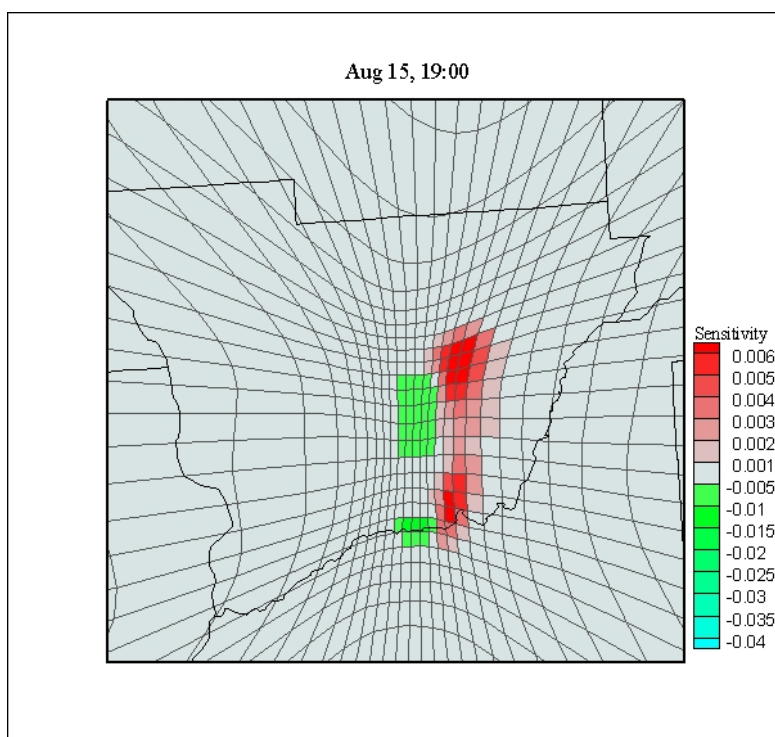
Figure 4. Adaptive Grid Result for Direct Sensitivity of O$_3$ (ppm) to Fire Emissions

5.4 Analysis of Results

There are no special measurements taken along the trajectory of the fire plumes during the simulated period. The only data available for evaluation are the routine air quality observations from the existing monitoring network. The differences between new and old model simulation results were very small at the monitoring locations, therefore it was difficult to judge if the new model is performing better than the old model solely based on observations. In the absence of measurements, we performed the following evaluations in the vicinity of the fires.

Comparison of Ozone Estimates

We performed statistical analysis to determine the differences between static and adaptive grid simulation results. For this purpose, we identified the adaptive cells that intersect with each static cell. Figure 5 presents an example for intersection of static grid cell with adaptive cells. For this particular case, there are about 40 adaptive cells that fall in one static cell. For the intersected cells we recorded individual adaptive cell concentrations and also estimated a weighted average, based upon area, in order to compare to static cell values. Note that in this analysis we selected a region where changes in O_3 concentration occurred due to fire events. Adaptive grid O_3 concentrations are very similar to static grid simulation results in the rest of the domain.

Figure 6 presents a scatter plot of O_3 concentration values for static and corresponding adaptive cell values for August 15, 21:00 (GMT). In this figure both average values as well as minimum and maximum values of adaptive cells within each 4×4 km^2 static cell are shown. One of the important finding in Figure 6 is that O_3 concentrations of adaptive cell averages are very close to static cell results. The correlation coefficient of the regression is 0.9 and has a slope of 0.9 which is an indication of a strong linear relationship between average adaptive and static cell results. However, it should also be noted that adaptive cell averages tends to over predict lower concentrations and under predict higher concentrations as compared to static cell values. In other words, the variation in average adaptive results is slightly smaller than the variation in static cell results. For this particular case, coefficient of variation, which is defined as the ratio of the standard deviation to the mean, is 8.1 percent in adaptive case and 8.6 percent in static case. The coefficient of variation in maximum and minimum values together is slightly greater with a value of 8.9 percent. These values suggest that variability is about the same with maximum-minimum values of adaptive cells having the highest variability. It should be noted however that the number of data for this category is twice the static and average adaptive cells. Another important point is the range of variability. Static grid O_3 concentrations change between 62 ppb and 95 ppb, whereas average adaptive cells range between 63 ppb and 92 ppb. For the max/min values this range is between 62 ppb and 96 ppb. Similar results were obtained for other periods of simulation where fire events were observed and they are provided in Appendices.
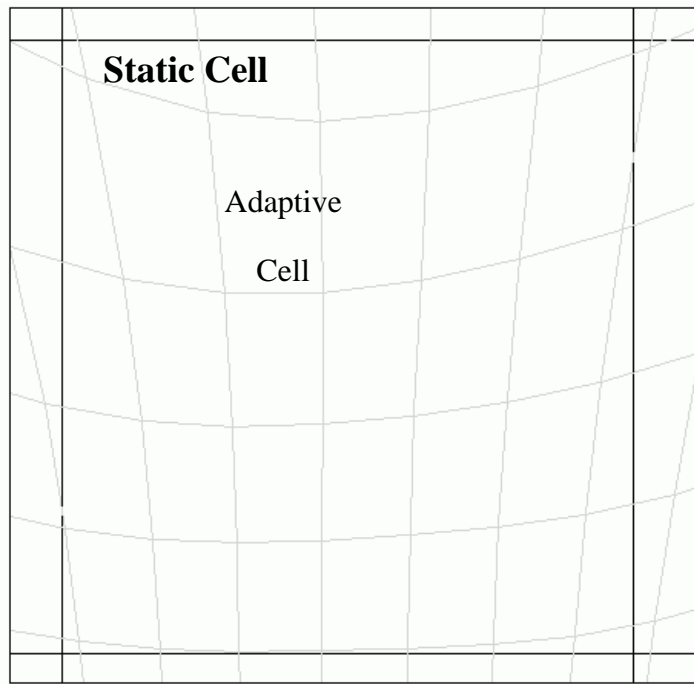
Figure 5. Intersections of Static and Adaptive Cells
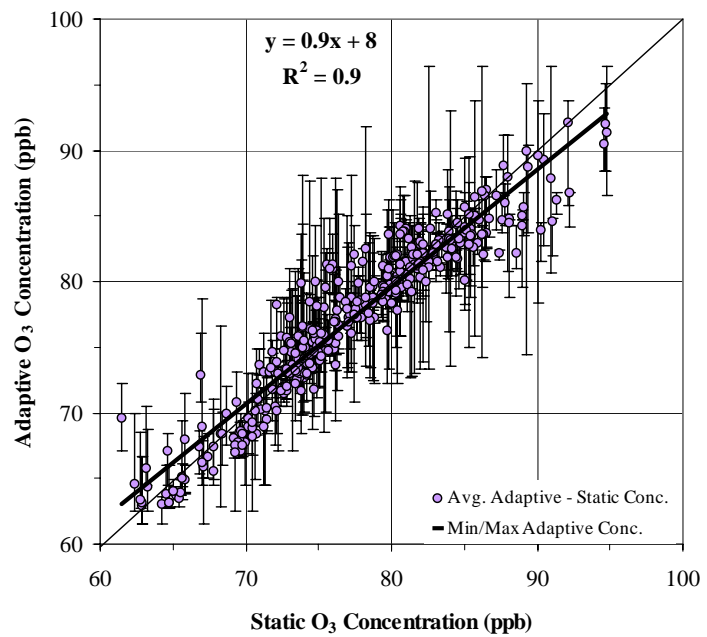
Figure 6. Adaptive versus Static Grid O_3 Concentrations (ppb) for August 15, 21:00

Table 3. Comparison of Static versus Adaptive for O_3 Concentration

Date	Time	Range of O_3 (ppb)			Linear Regression (Adaptive Average vs. Static)	
		Adaptive Average	Adaptive Max/Min	Static	R^2	Slope
15	19:00	69 – 100	66 – 106	68 – 103	0.96	0.94
15	20:00	66 – 99	66 – 104	67 – 101	0.92	0.92
15	21:00	63 – 92	61 – 96	62 – 95	0.90	0.90
16	18:00	55 – 99	55 – 101	55 – 100	0.97	1.04
16	19:00	55 -100	54 – 103	55 – 97	0.95	1.01
16	20:00	54 – 101	54 – 106	54 – 97	0.96	1.02
16	21:00	54 – 102	54 – 104	53 – 101	0.96	1.00
16	22:00	48 – 104	47 – 108	39 – 103	0.95	0.97
16	23:00	26 – 103	18 – 105	10 – 100	0.90	0.94
18	2:00	10 – 68	3 – 73	2 – 76	0.92	0.90
18	3:00	7 – 64	2 – 72	2 – 75	0.91	0.91
18	4:00	5 – 64	1 – 64	1 – 72	0.91	0.91
18	5:00	32 – 64	27 -70	31 – 61	0.83	0.97
18	6:00	45 – 63	43 – 65	40 – 61	0.65	0.82
18	7:00	47 – 64	44 – 64	41 – 62	0.68	0.72
18	8:00	43 – 60	42 – 61	39 – 59	0.66	0.73
18	9:00	42 – 57	42 – 58	37 – 55	0.69	0.69
18	10:00	35 – 58	34 – 58	31 – 55	0.93	0.82
18	13:00	38 – 67	36 – 67	29 – 66	0.93	0.91
18	14:00	53 – 75	51 – 77	44 – 74	0.91	0.90

Table 3 summarizes the comparison between adaptive and static grids for 20 different hours when fires occurred. As seen in Table 3, the range of variation is similar in adaptive maximum-minimum values and static values. The range is slightly smaller in adaptive averages. Parameters of regression between adaptive averages and static values are also given in Table 3. In most cases (15 out of 20) R^2 values are greater than or equal to 0.9, and slopes are between 0.9 and 1.04. There are, however, nighttime fire events where R^2 is less than 0.85 and slope is less than 0.8. In general, it is observed that there is a strong linear relationship between adaptive averages and static values. In 16 cases, the slope of regression is less than 1.0 indicating that the adaptive average O_3 concentration is less than the static cell values. These results are in agreement with the study conducted by Jang *et al.* (1995) where they found that lumped finer-scale grid (i.e., 20km) produced less O_3 than coarser grid (i.e., 80km) for equal size area.

Another implication of the differences in adaptive and static predictions is at the local scale. Figure 7 shows O_3 concentrations from adaptive and static grid simulations at a cell near the fires for selected time periods. Adaptive cell averages as well as minimum and maximum values of adaptive cells that fall in the 4×4 km^2 static cell are presented. Adaptive averages are 4 ppb more than static values on the average, and the difference ranges from -2 ppb to +18 ppb. For minimum and maximum adaptive values the average difference from static concentration is +6 ppb, and it ranges from -6 ppb to +28 ppb. These findings suggest that there can be significant differences in O_3 between adaptive and static grids at the local scale. For example, one static grid O_3 is 47 ppb whereas one of the adaptive cells inside that static cell has a value of 75. This 28 ppb difference may have important implications from a policy perspective.
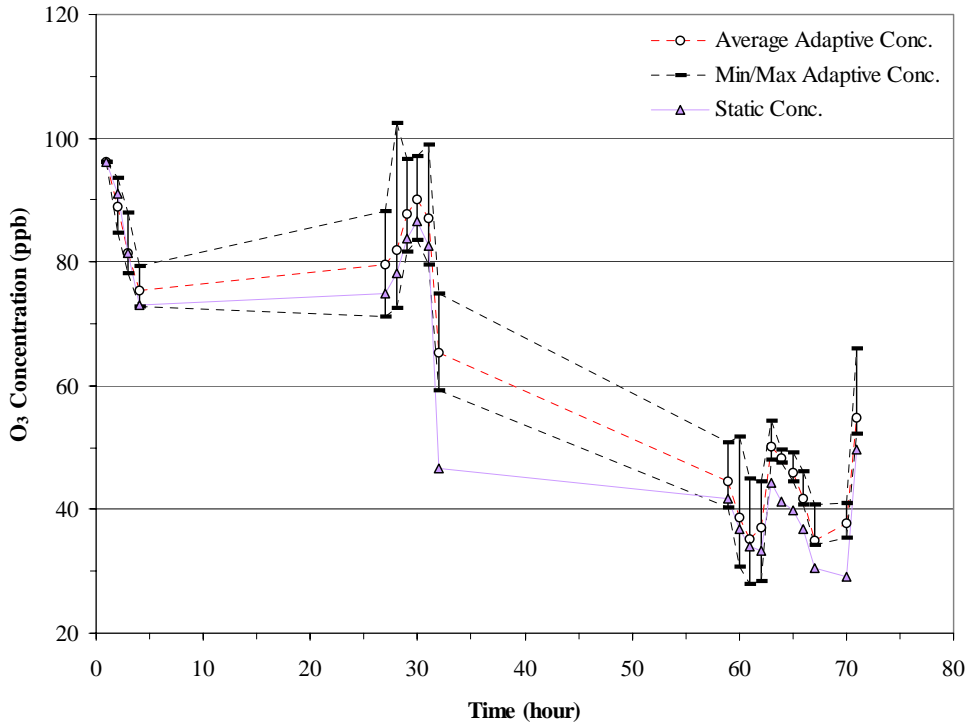
Figure 7. Static versus Adaptive O_3 predictions (ppb) for a specific cell near the fires

Comparison of Ozone Sensitivities

We did a similar analysis to compare sensitivity results from static and adaptive simulations. Figure 8 presents the comparison for the selected region on August 15, 21:00 (GMT). As in the case for O_3 predictions, R^2 and slope values indicate that there is a linear relationship between adaptive averages and static values for sensitivity. However, there is a high variability in individual adaptive cell values as shown by the minimum and maximum sensitivity values. Variation ranges from -8 ppb to +6 ppb for the maximum-minimum adaptive values, whereas it is between -6 ppb and +5 ppb in static grid. For the adaptive averages the range of variation is between -6 ppb and +5 ppb. Similar results were obtained for other periods of simulation where fire events occurred and they are provided in Appendices. Table 4 presents a summary of these events. As seen in Table 4, variability in O_3 sensitivity is smallest in adaptive averages. Maximum-minimum adaptive values have a higher variability than static values. Table 4 also presents parameters of regression between adaptive averages and static values. It is seen that most of the cases (15 out of 20) have R^2 values greater than 0.85 and slope values are greater than 0.70. There are several fire events where there is weak correlation between adaptive averages and static values. One R^2 value is 0.14 at the beginning of a fire. Others are during the nighttime events. In all these cases the sensitivity is mostly negative. The differences in the sensitivities estimated by static and adaptive grids are indicative of the scale-related uncertainty in modeling the impact of prescribed burns.
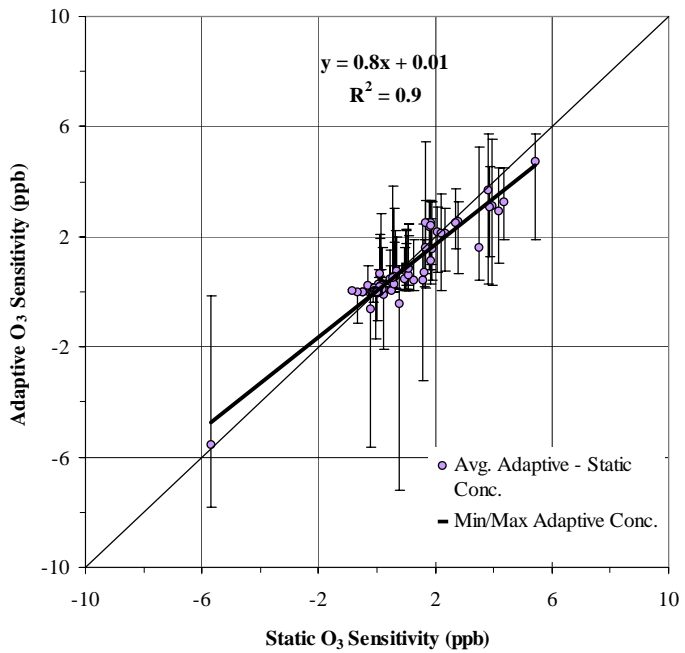
Figure 8. Static versus Adaptive O_3 Sensitivities (ppb) for August 15, 21:00

Table 4. Comparison of Static versus Adaptive for O_3 Sensitivity

Date	Time	Range of O_3 Sensitivity (ppb)			Linear Regression (Adaptive Average vs. Static)	
		Average Adaptive	Max/Min Adaptive	Static	R^2	Slope
15	19:00	-9 – 4	-13 – 8	-8 – 7	0.69	0.77
15	20:00	-5 – 5	-7 – 8	-5 – 6	0.88	0.78
15	21:00	-6 – 5	-8 – 6	-6 – 5	0.90	0.85
16	18:00	-2 – 2	-5 – 3	-2 – 4	0.14	0.23
16	19:00	0 – 6	0 – 8	0 – 6	0.77	0.71
16	20:00	0 – 3	0 – 5	0 – 4	0.93	0.81
16	21:00	0 – 2	0 – 3	0 – 3	0.90	0.73
16	22:00	0 – 2	0 – 3	0 – 2	0.88	0.74
16	23:00	0 – 1	0 – 2	0 – 1	0.91	0.74
18	2:00	-30 – 0	-33 – 0	-48 – 0	0.84	0.52
18	3:00	-33 – 0	-38 – 0	-48 – 0	0.78	0.54
18	4:00	-35 – 0	-40 – 0	-47 – 0	0.76	0.58
18	5:00	-15 – 0	-18 – 0	-15 – 0	0.98	0.96
18	6:00	-8 – 0	-9 – 0	-8 – 0	0.98	0.98
18	7:00	-4 – 0	-4 – 0	-4 – 0	0.97	1.00
18	8:00	-3 – 0	-3 – 0	-3 – 0	0.97	0.97
18	9:00	-2 – 0	-2 – 0	-2 – 0	0.96	0.95
18	10:00	-1 – 0	-1 – 0	-1 – 0	0.96	0.89
18	13:00	-9 – 0	-12 – 0	-16 – 0	0.87	0.49
18	14:00	0 – 2	0 – 2	0 – 3	0.95	0.67

6   Conclusions

Our objective was to bring current air quality models to a level where they can be used to predict the impact on the surrounding environment of air pollutants emitted from military installations. We improved the models' ability to capture source-receptor relationships between emissions at local scales and air quality at regional scale. In this project, we focused on the prescribed burning emissions from Fort Benning as a case study. The immediate questions we answered are:

- Can our recently developed techniques bridge the gap between the current state of the models and DoD's needs of determining the fate of emissions from military operations?

- If so, do the prescribed burning operations have an impact to the air quality in Columbus metropolitan area?

The answer to the first question is positive but the study was inclusive for the second question. Now that the first phase objectives are achieved, follow-on research in a second phase should address the following questions:

- What extensions are necessary for the techniques to be applied to other DoD activities such as aviation, ship and coastal operations?

- Can we develop reliable tools to help site managers not only to plan their operations but adapt them as necessary for minimizing adverse effects to the environment?

The development of this impact analysis technology has many upside potentials. A user-friendly product tailored to DoD needs can be developed, along with a detailed plan for the transfer of this technology to DoD facilities. The technology can be implemented in U.S. EPA's Community Multiscale Air Quality (CMAQ) model and applied to many other sectors including energy, agriculture and homeland security.

In conclusion, the new model (i.e., MAQSIP enhanced by adaptive grid and sensitivity analysis techniques) can be used for accurate assessment of the air quality impacts of most DoD activities.

7   References

Battye, W. and Battye, R. (2002) "*Development of Emissions Inventory Methods for Wildland Fires*", Report Prepared for U.S. Environmental Protection Agency, Durham, NC.

Boylan, J., Wilkinson, J., Yang, Y.-J., Odman, T. and Russell, A. (2000) Particulate matter and acid deposition modeling for the Southern Appalachian Mountains Initiative. *A&WMA Annual Conference and Exhibition*, Salt Lake City, Utah, June 18-22, 2000.

Boylan, J., Wilkinson, J., Odman, T., Russell, A., Imhoff, R. (2001) Response and sensitivity of $PM_{2.5}$ in the southern Appalachian mountains. *A&WMA Annual Conference and Exhibition*, Orlando, Florida, June 24-28, 2001.

Byun, D. W. and Ching, J. K. S. (1999) *Science Algorithms of the EPA Models-3 Community Multiscale Air Quality (CMAQ) Modeling System*, EPA/600/R-99/030, U. S. EPA, Washington.

Cheng L., McDonald K.M., Angle R.P. and Sandhu H.S. (1998) Forest fire enhanced photochemical air pollution: A case study. *Atmospheric Environment* **32**, 673-681.

Environmental Management Division (2000) *Prescribed Burning Operational Plan*, Fort Benning, Georgia, June 28, 2000.

Hakami A., Odman M. T. and Russell A. G., "High-order, direct sensitivity analysis of multidimensional air quality models," Environmental Science and Technology, vol. 37, no. 11, pp. 2442-2452, June 2003.

Hu, Y., Odman, M. T., and Russell, A. (2003a) "*Air Quality Modeling of the First Base Case Episode for the Fall Line Air Quality Study*," Prepared for Georgia Department of Natural Resources, Environmental Protection Division, June 2003.

Hu, Y., Odman, M. T., and Russell, A. (2003b) "*Meteorological Modeling of the First Base Case Episode for the Fall Line Air Quality Study*," Prepared for Georgia Department of Natural Resources, Environmental Protection Division, February 2003.

Jang, J. C., Jeffries, H. E., Byun, D., and Pleim, J. E. (1995) "Sensitivity of Ozone to Model Grid Resolution-I. Application of High-Resolution Regional Acid Deposition Model," *Atmospheric Environment*, **Vol. 29**, No. 21, 3085-3100.

Khan, N. K., Odman, M. T. and Karimi, H. (2001) Reducing uncertainty of air quality models through coupling adaptive grids with GIS techniques. *International Journal of Geographical Information Science*, submitted.

Khan, N. K., Odman, M. T. and Karimi, H. (2003) Evaluation of algorithms developed for adaptive grid air quality modeling using surface elevation data," *Computers, Environment and Urban Systems*, in press.

Karamchandani, P., Santos, I., Sykes, I., Zhang, Y., Tonne, C. and Seigneur, C. (2000) Development and evaluation of a state-of-the-science reactive plume model. *Environmental Science and Technology* **34**, 870-880.

Larimore, R. (2000) Prescribed burning on the Fort Benning military reservation. Presentation to the Columbus Environmental Committee, August 8, 2000.

Odman, M. T. and Ingram, C. L. (1996), *Multiscale Air Quality Simulation Platform (MAQSIP): Source Code Documentation and Validation*. Technical Report, ENV-

96TR002, MCNC—North Carolina Supercomputing Center, Research Triangle Park, NC, 83 pp.

Odman, M. T., Mathur, R., Alapaty, K., Srivastava, R. K., McRae, D. S. and Yamartino, R. J. (1997) Nested and adaptive grids for multiscale air quality modeling. *Next Generation Environmental Models Computational Methods*, G. Delic and M. F. Wheeler, SIAM, Philadelphia, p. 59-68.

Odman, T., Boylan, J., Wilkinson, J., Yang, Y.-J., Russell, A., Doty, K. and Mcnider R. (2000a) Ozone modeling for the Southern Appalachian Mountains Initiative. *A&WMA Annual Conference and Exhibition*, Salt Lake City, Utah, June 18-22, 2000.

Odman, M. T., Khan M. N., and McRae, D. S. (2000b) Adaptive grids in air pollution modeling: Towards an operational model. *Millennium NATO/CCMS International Technical Meeting on Air Pollution Modelling and Its Application*, Boulder, Colorado, May 15-19, 2000.

Odman, M. T., Khan M. N., and McRae, D. S. (2001) Adaptive grids in air pollution modeling: Towards an operational model," in Air Pollution Modeling and Its Application XIV, pp. 541-549, (S.-E. Gryning and F. A. Schiermeier, Eds.), New York: Kluwer Academic/Plenum Publishers.

Odman, M. T., Khan, M. N., Srivastava, R. K. and McRae, D. S. (2002) Initial application of the adaptive grid air pollution model," in Air Pollution Modeling and its Application XV, pp. 319-328 (C. Borrego and G. Schayes, Eds.), New York: Kluwer Academic/Plenum Publishers

Ottmar, R. D. (2001) "Smoke Source Characteristics" *2001 Smoke Management Guide for Prescribed and Wildland Fire*, Prepared by National Wildfire Coordinating Group, NFES-1279.

Srivastava, R. K., McRae, D. S. and Odman, M. T. (2000) An adaptive grid algorithm for air quality modeling. *Journal of Computational Physics* **165**, 437-472.

Srivastava, R. K., McRae, D. S. and Odman, M. T. (2001a) Simulation of a reacting pollutant puff using an adaptive grid algorithm. *Journal of Geophysical Research*, in press.

Srivastava, R. K., McRae, D. S. and Odman, M. T. (2001b) Simulation of dispersion of a power plant plume using an adaptive grid algorithm. *Atmospheric Environment*, revisions submitted.

Unal, A., Tian, D., Hu, Y., Russell, T. "*2000 Emissions Inventory for Fall Line Air Quality Study (FAQS),*" Prepared for Georgia Department of Natural Resources, Environmental Protection Division, April 2003.

Yang, Y.-J., J. G. Wilkinson and A. G. Russell, Fast direct sensitivity analysis of multidimensional photochemical models, *Environ. Sci. Technol*. **31**, 2859-68, 1997.

8   Appendices

8.1   Simulation Results

8.2   Analysis Results

8.3   Publications

a) Conference Paper (Submitted to 2nd International Wildland Fire Ecology and Fire Management Congress, Orlando, FL 16-20 November 2003)

b) Conference Presentation (Presented at 2nd International Wildland Fire Ecology and Fire Management Congress, Orlando, FL 16-20 November 2003)

c) Journal Paper (Submitted to either "Journal of Agricultural and Forest Meteorology" or "International Journal of Wildland Fire")

8.1   Simulation Results
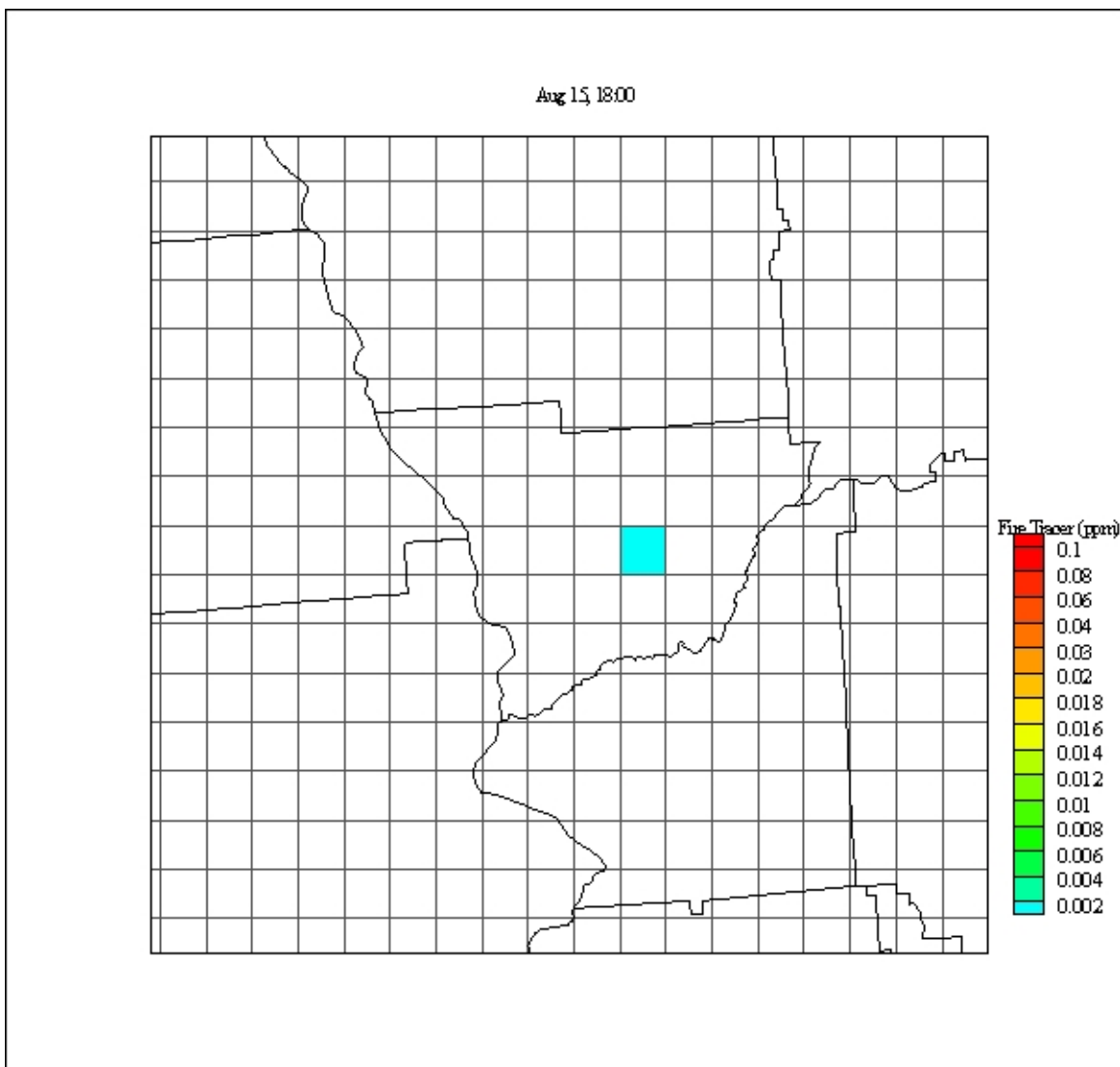
Figure 1 Static Grid Result for Inert Fire Tracer Concentrations (ppm) for August 15, 18:00
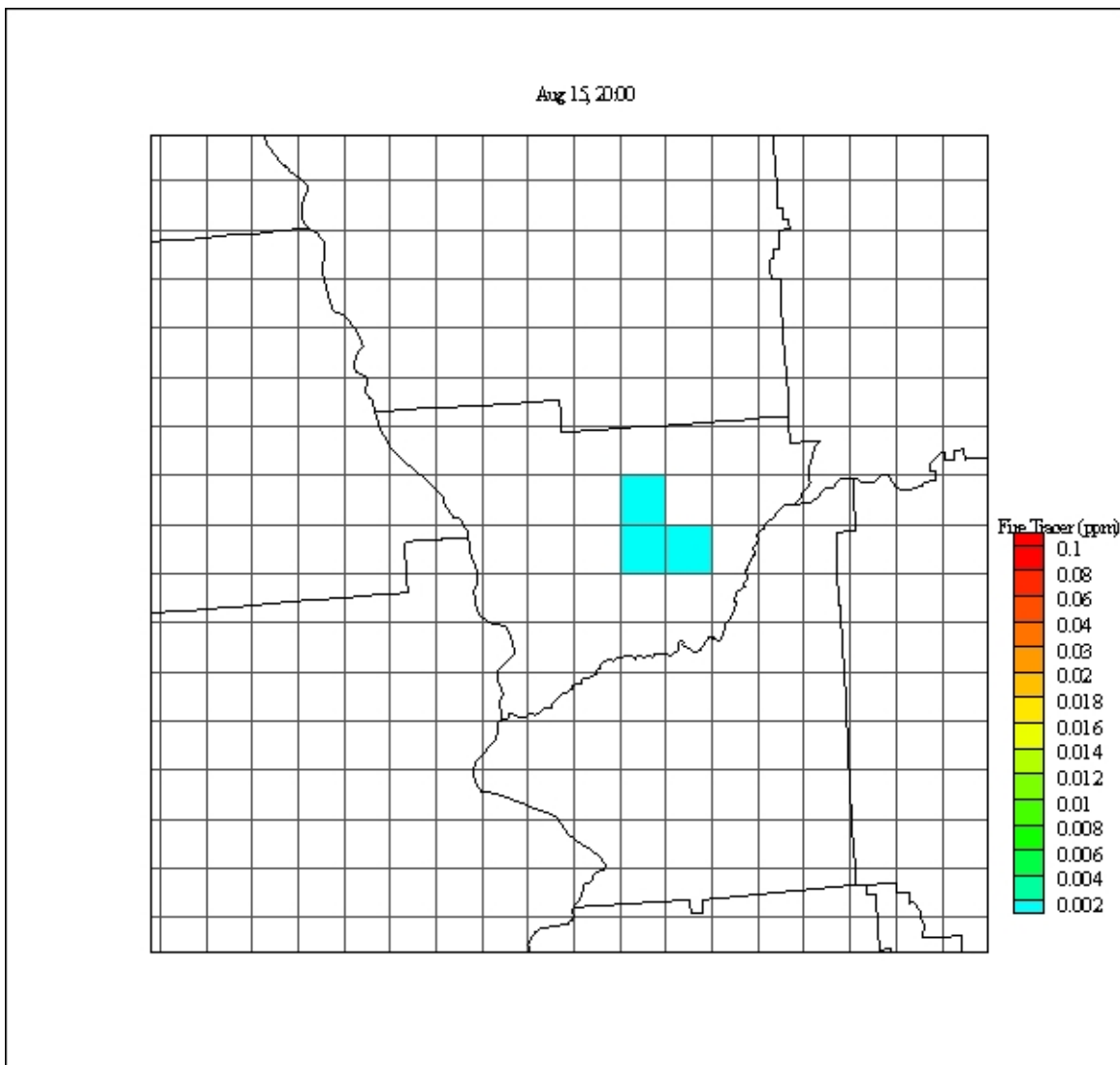
Figure 2 Static Grid Result for Inert Fire Tracer Concentrations (ppm) for August15, 20:00
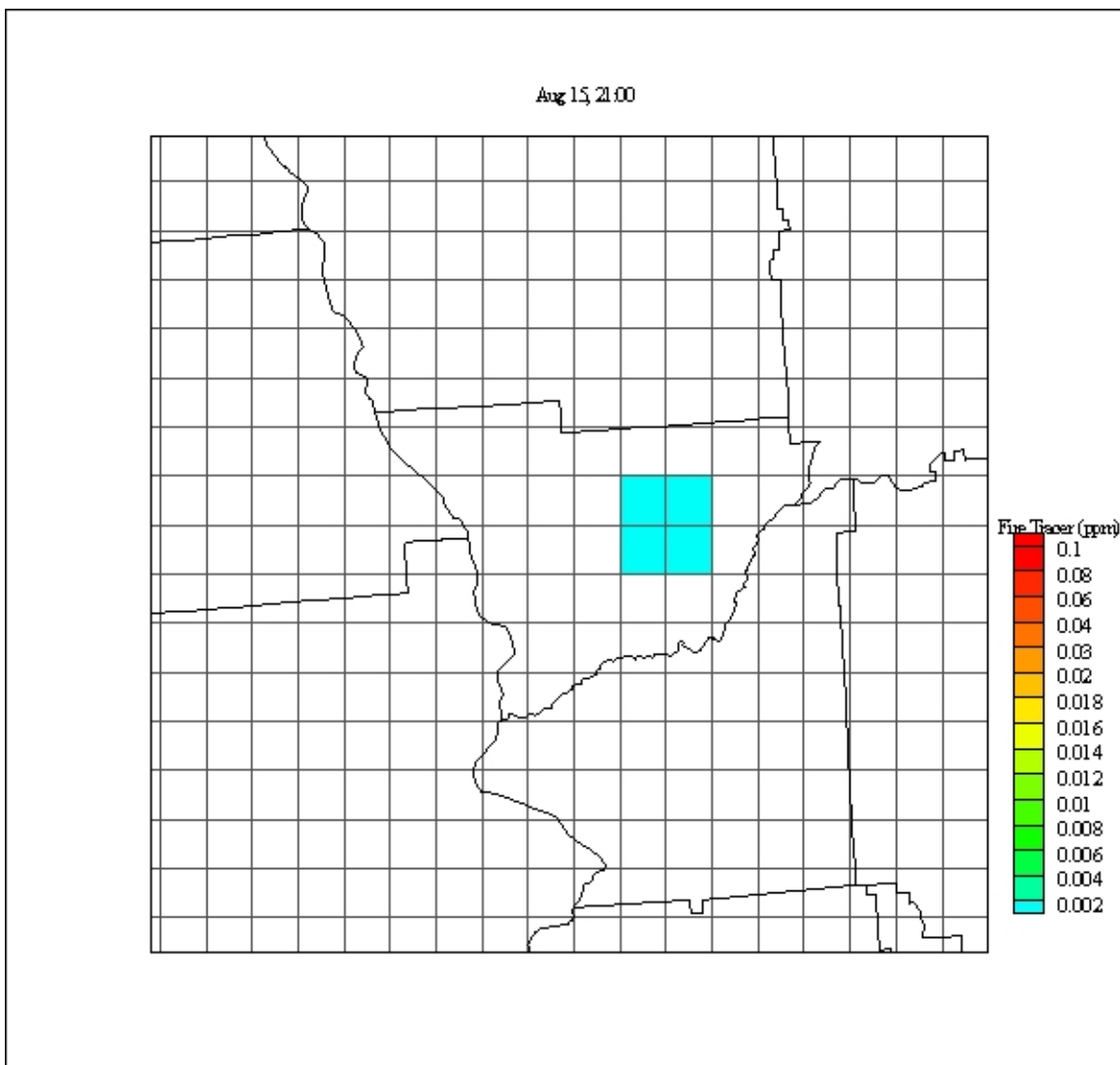
Figure 3 Static Grid Result for Inert Fire Tracer Concentrations (ppm) for August15, 21:00
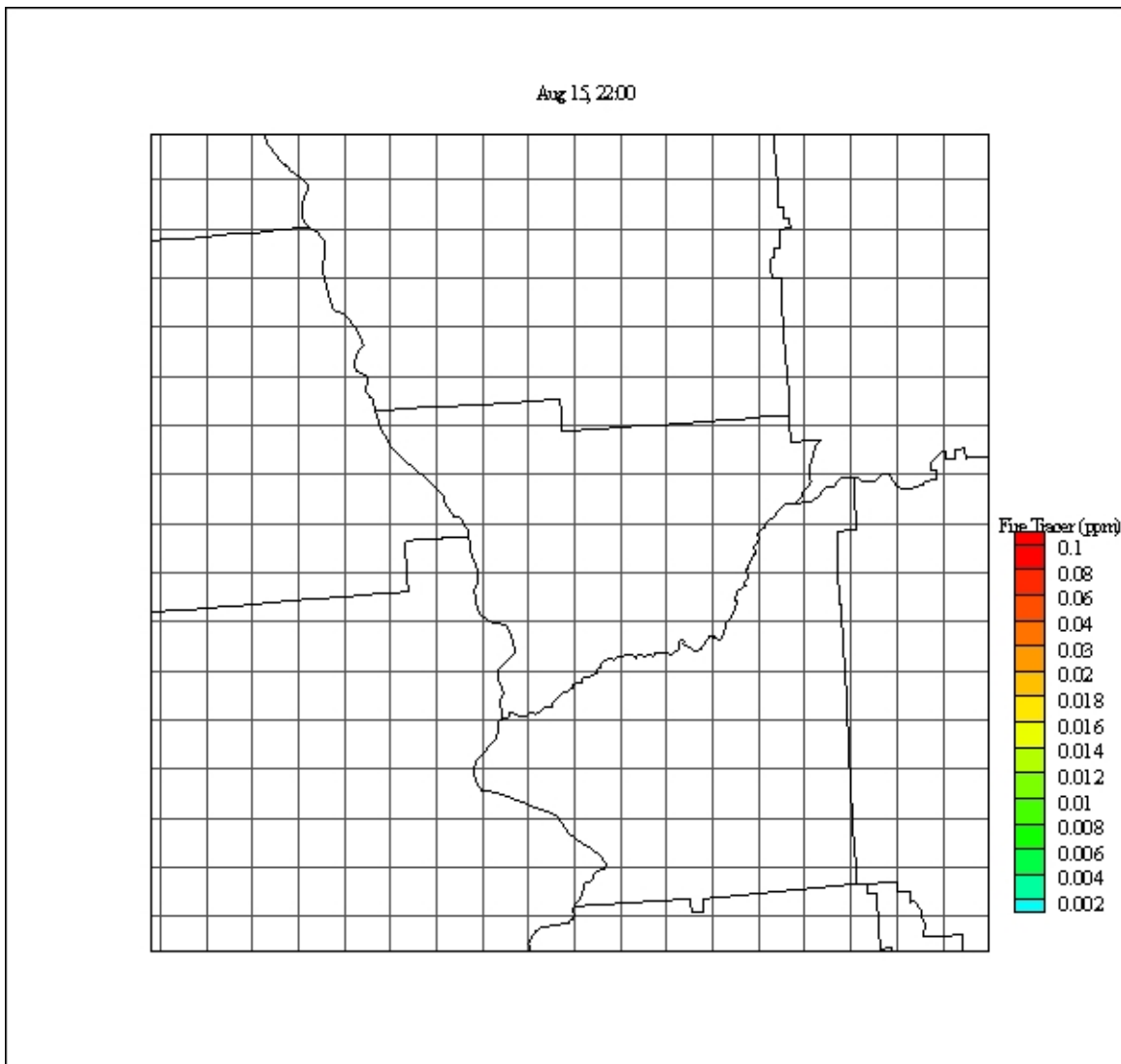
Figure 4 Static Grid Result for Inert Fire Tracer Concentrations (ppm) for August15, 22:00
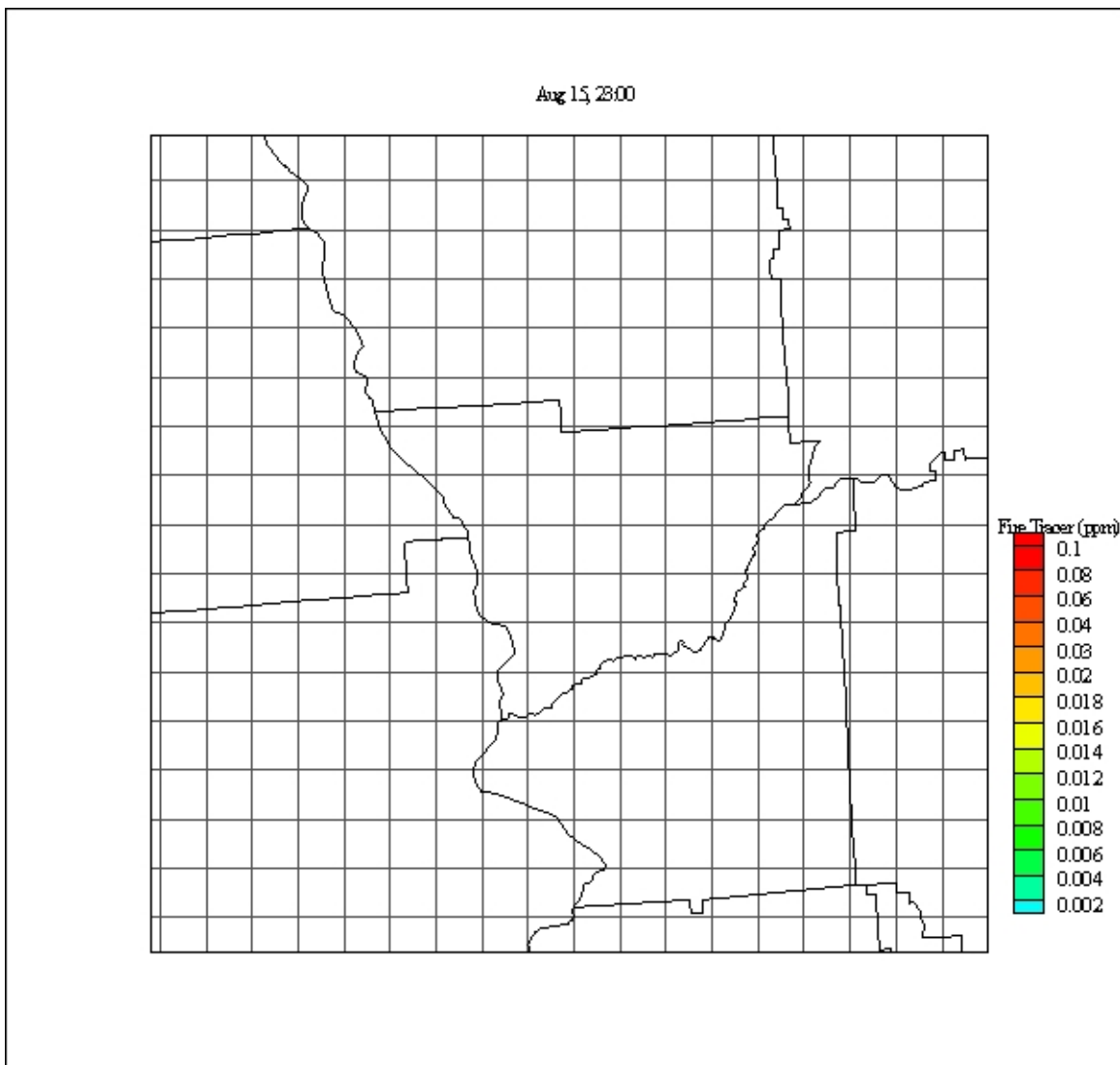
Figure 5 Static Grid Result for Inert Fire Tracer Concentrations (ppm) for August15, 23:00

Aug 16, 0:00

Fire Tracer (ppm)
0.1
0.08
0.06
0.04
0.03
0.02
0.018
0.016
0.014
0.012
0.01
0.008
0.006
0.004
0.002
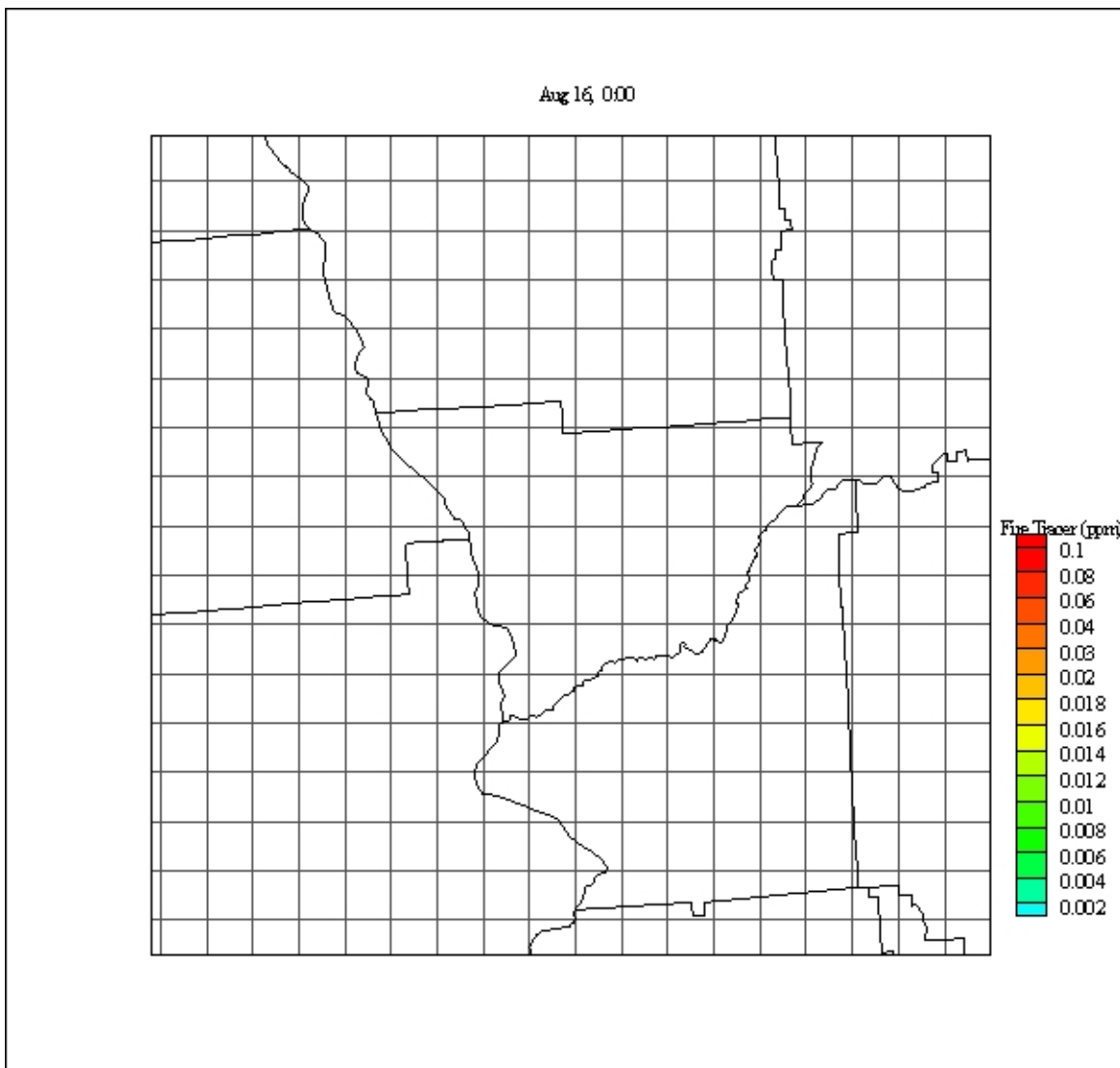
**Figure 6 Static Grid Result for Inert Fire Tracer Concentrations (ppm) for August16, 00:00**
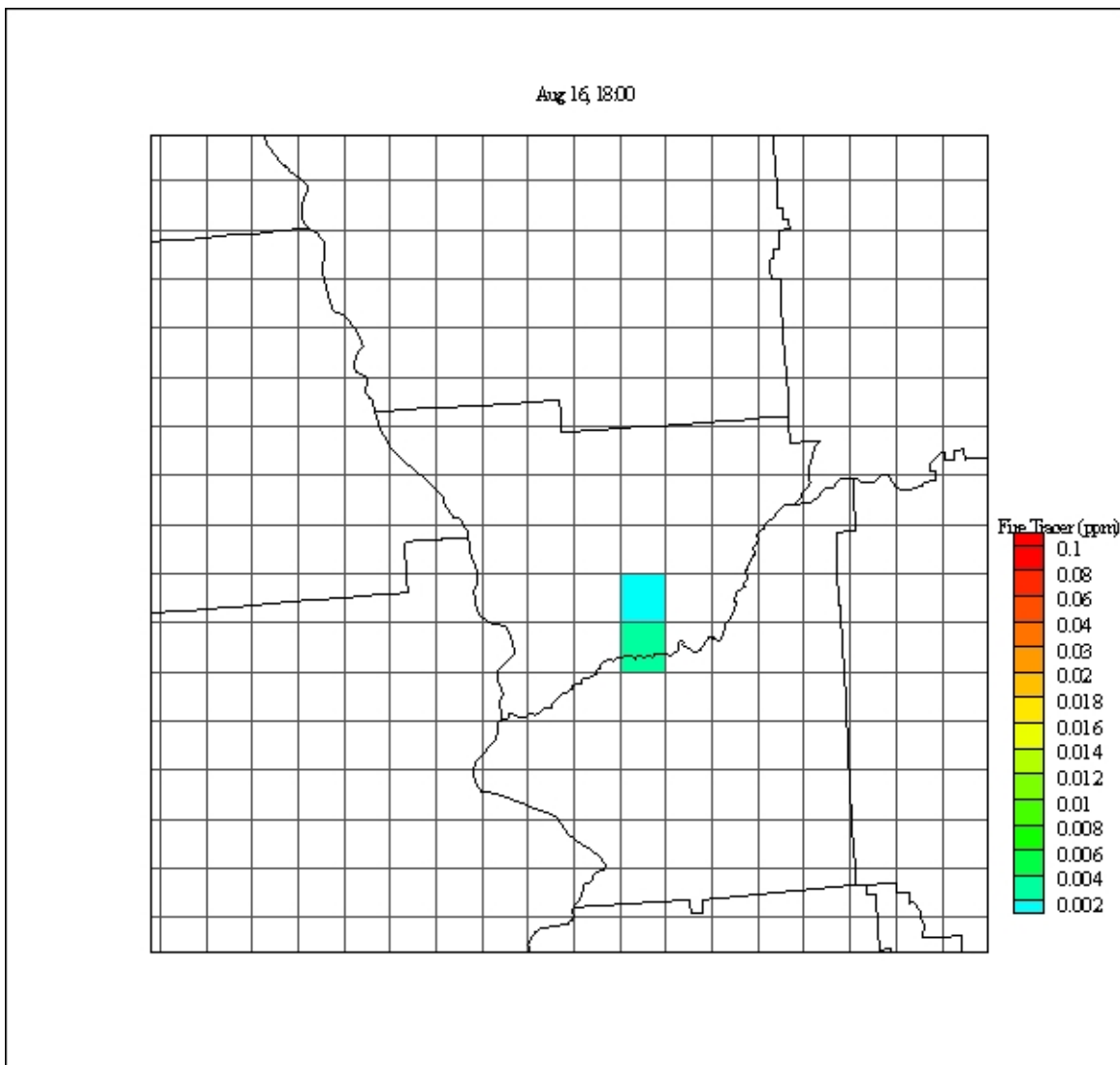
Figure 7 Static Grid Result for Inert Fire Tracer Concentrations (ppm) for August 16, 18:00

Aug 16, 19:00

Fire Tracer (ppm)
0.1
0.08
0.06
0.04
0.03
0.02
0.018
0.016
0.014
0.012
0.01
0.008
0.006
0.004
0.002
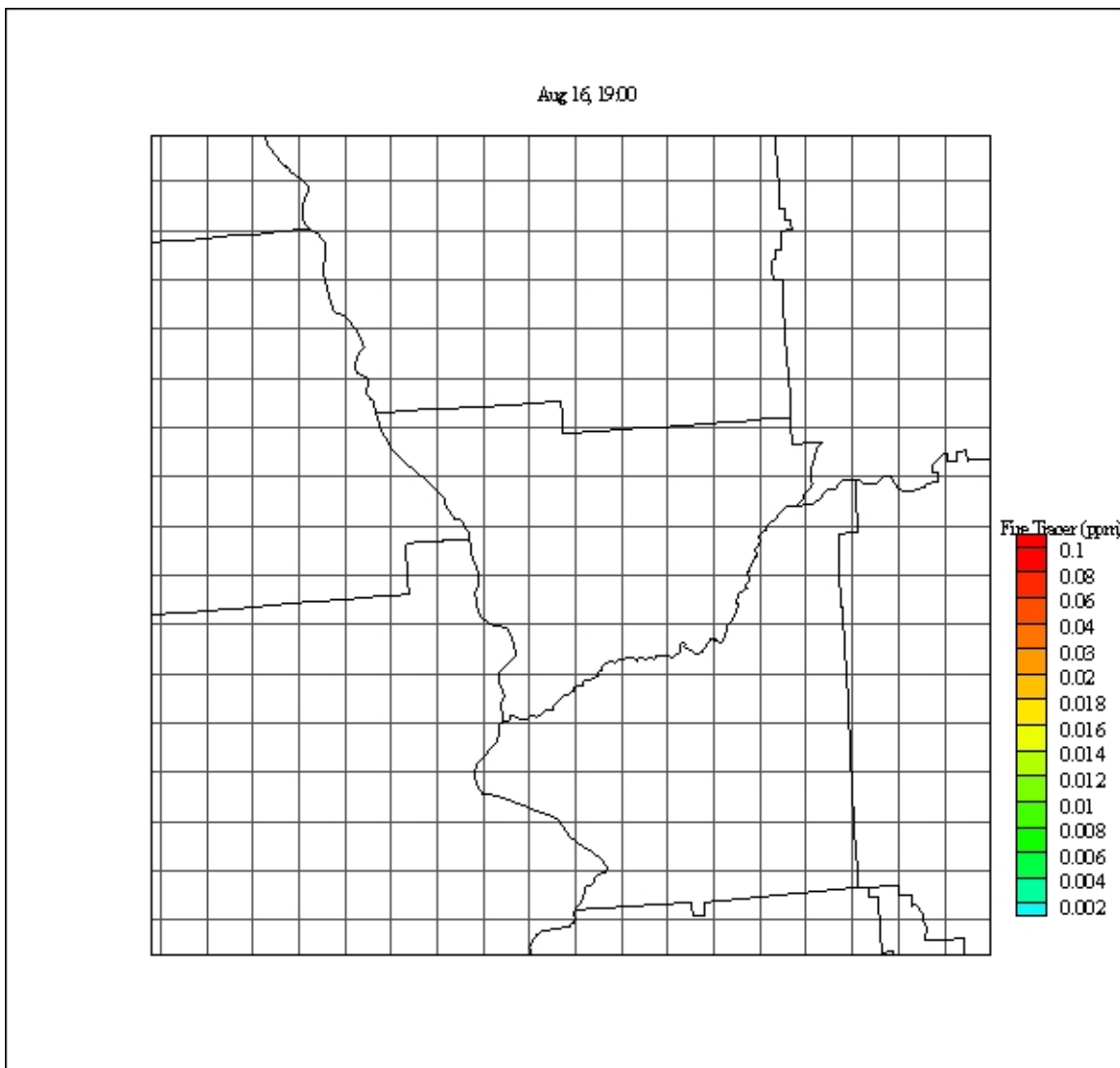
**Figure 8 Static Grid Result for Inert Fire Tracer Concentrations (ppm) for August 16, 19:00**
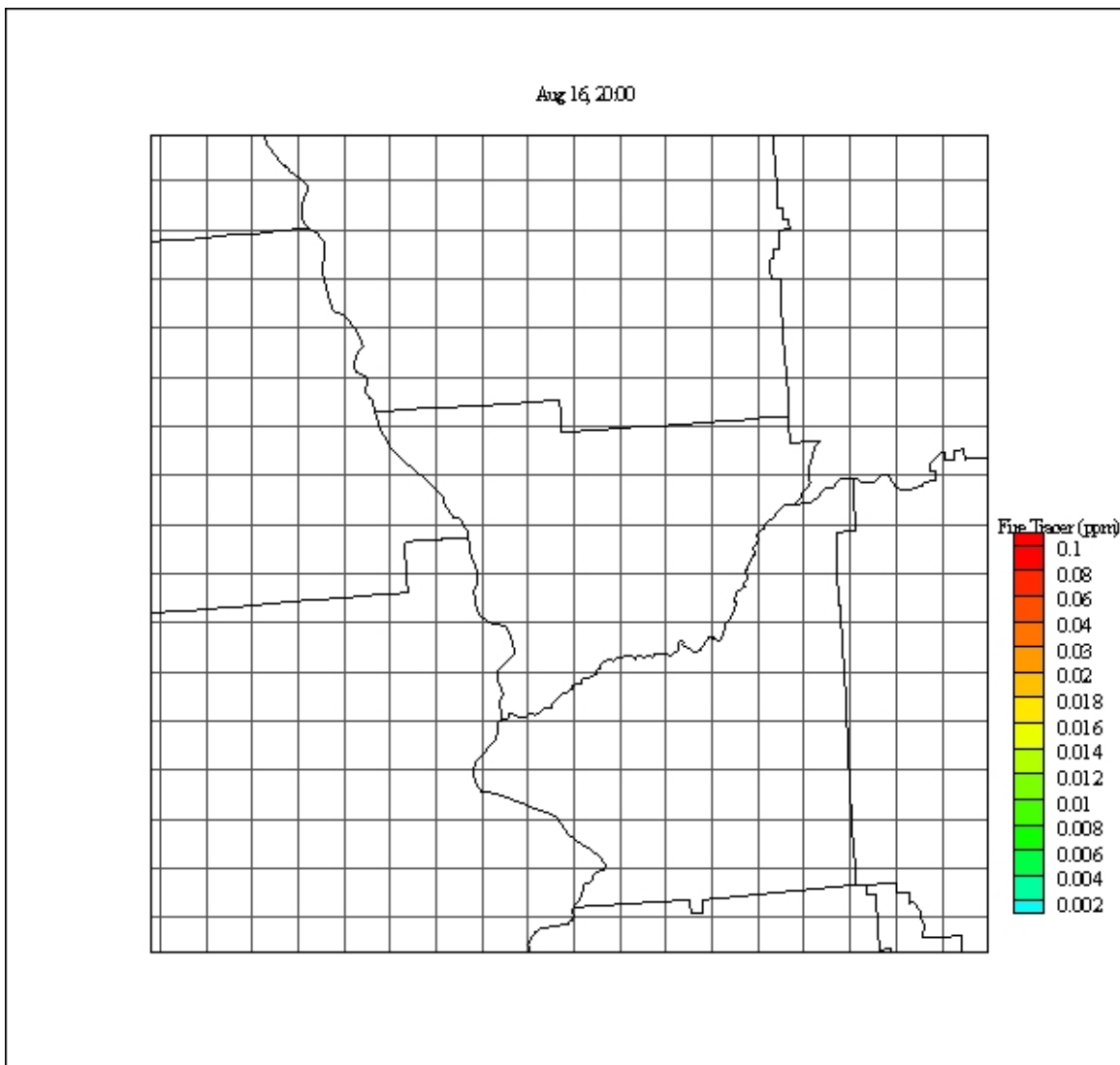
Figure 9 Static Grid Result for Inert Fire Tracer Concentrations (ppm) for August 16, 20:00
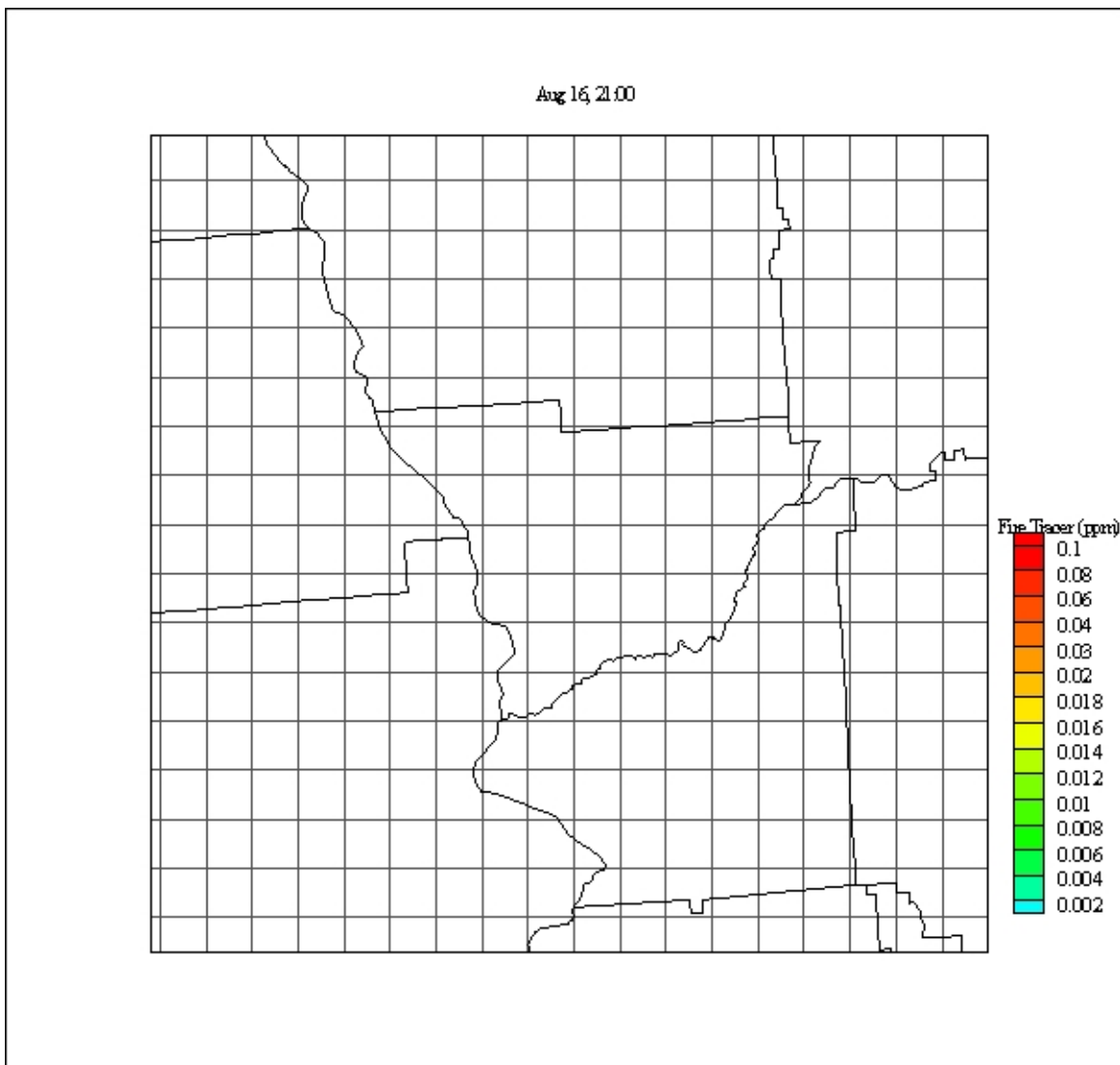
Figure 10 Static Grid Result for Inert Fire Tracer Concentrations (ppm) for August 16, 21:00
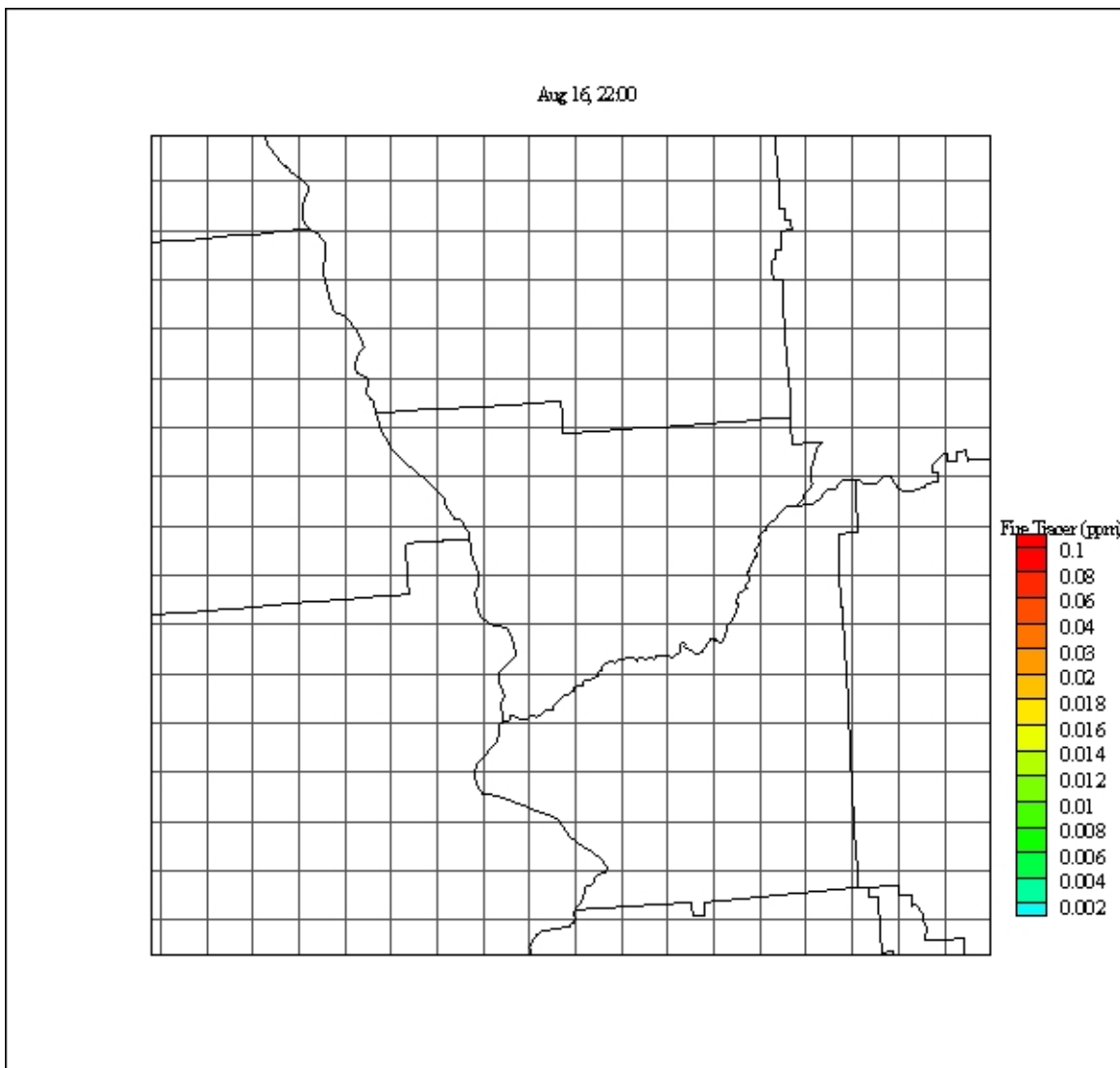
Figure 11 Static Grid Result for Inert Fire Tracer Concentrations (ppm) for August 16, 22:00

Aug 16, 23:00

Fire Tracer (ppm)
0.1
0.08
0.06
0.04
0.03
0.02
0.018
0.016
0.014
0.012
0.01
0.008
0.006
0.004
0.002
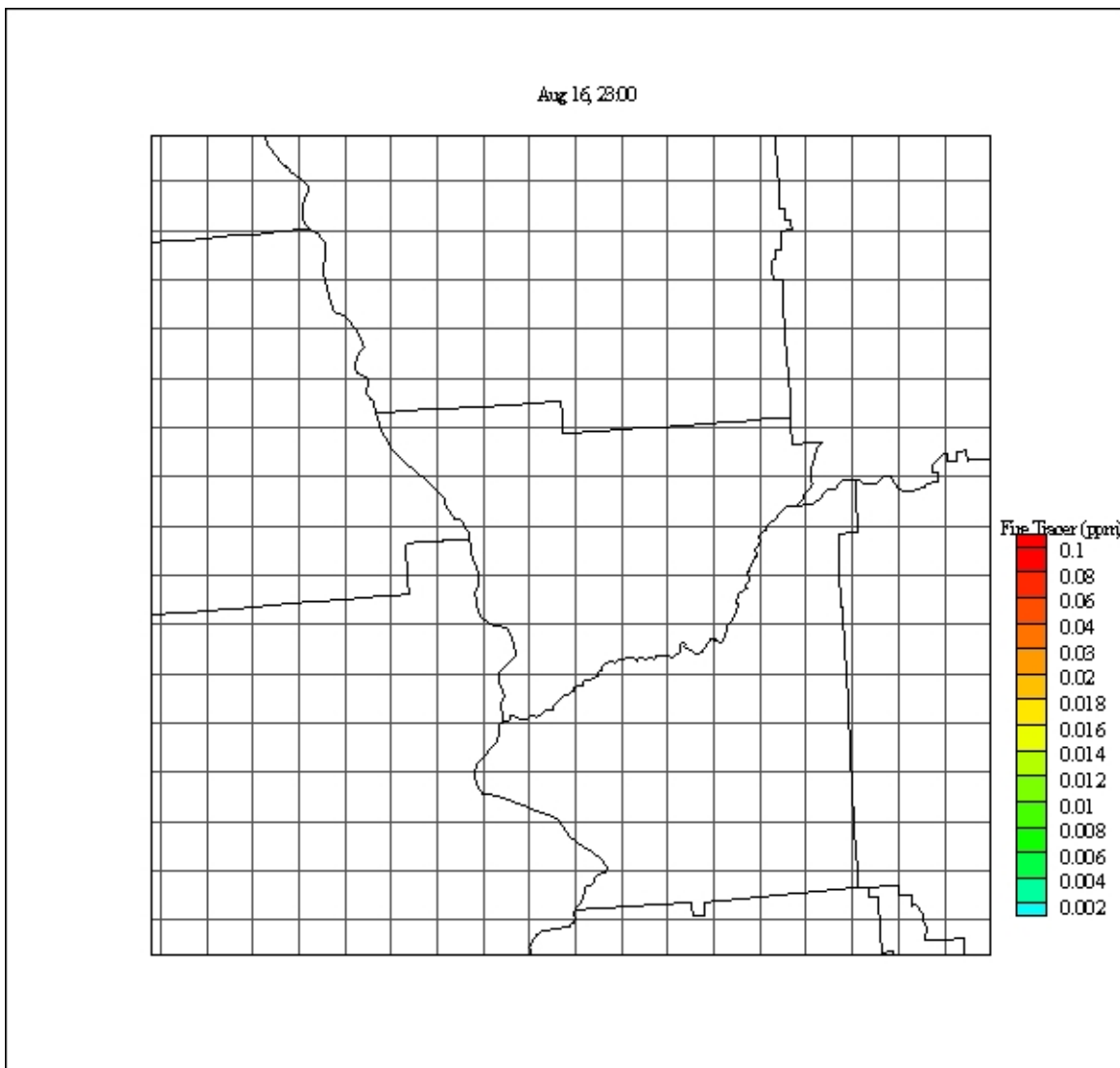
**Figure 12 Static Grid Result for Inert Fire Tracer Concentrations (ppm) for August 16, 23:00**
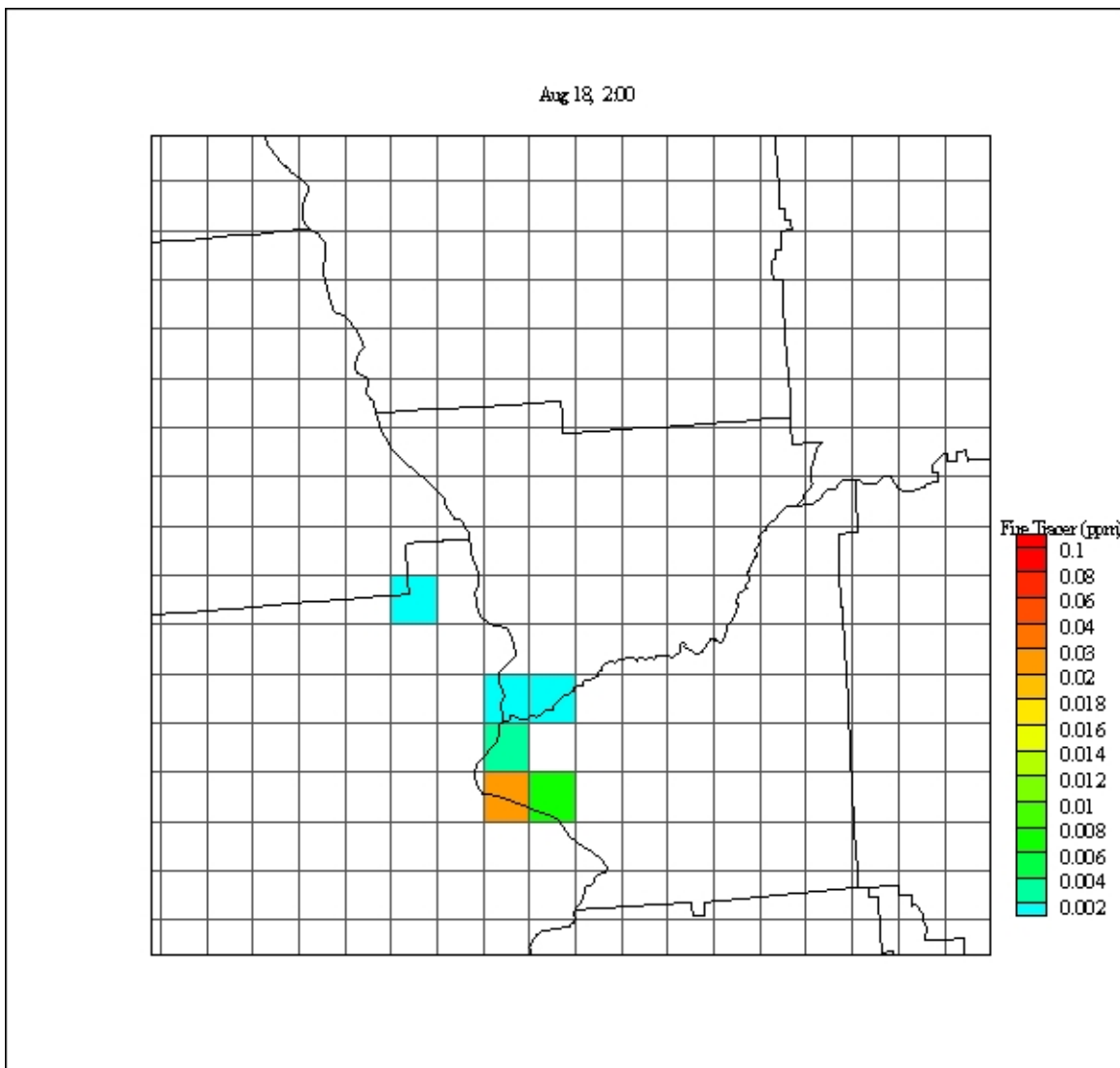
Figure 13 Static Grid Result for Inert Fire Tracer Concentrations (ppm) for August 18, 2:00
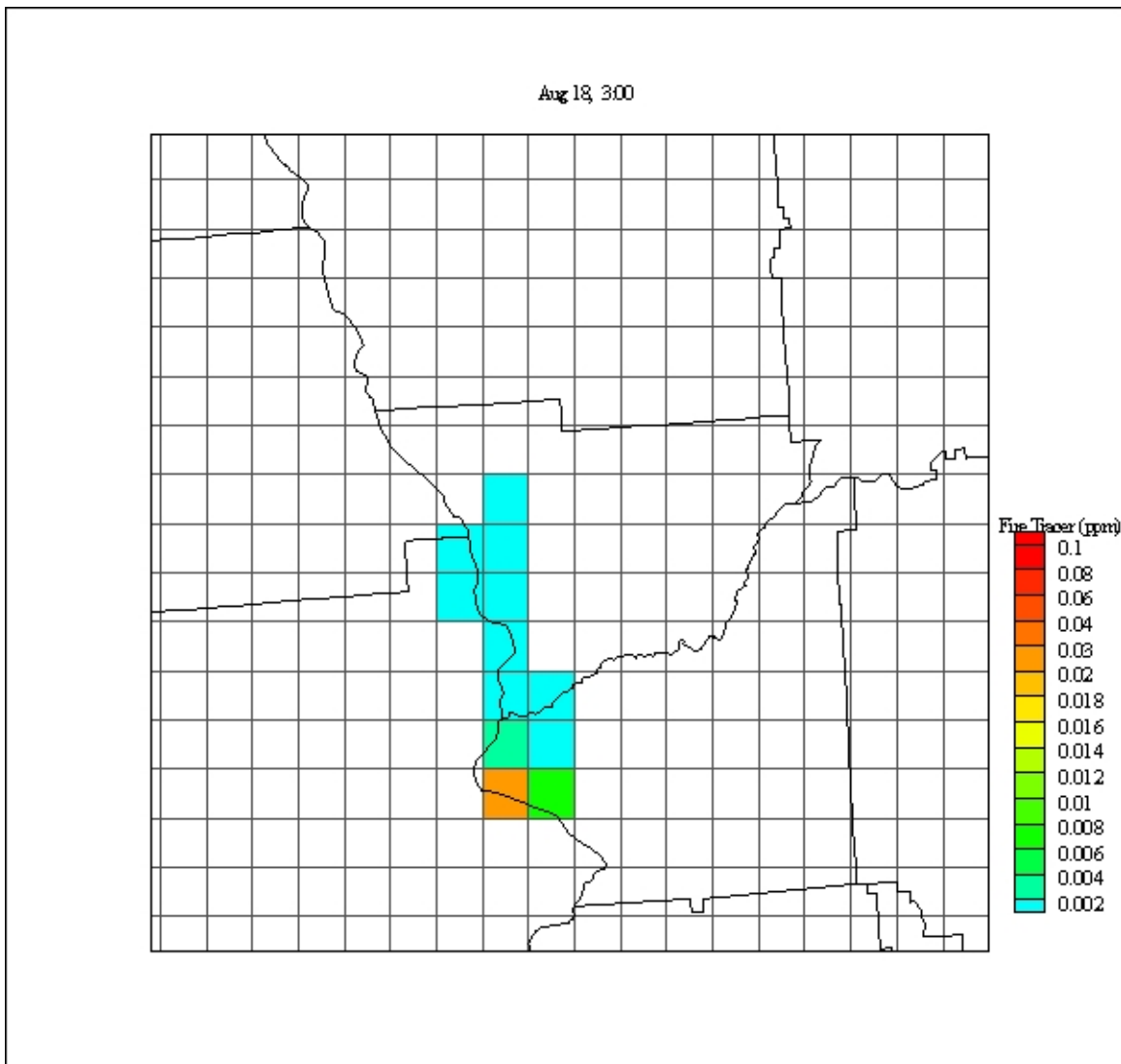
Figure 14 Static Grid Result for Inert Fire Tracer Concentrations (ppm) for August 18, 3:00
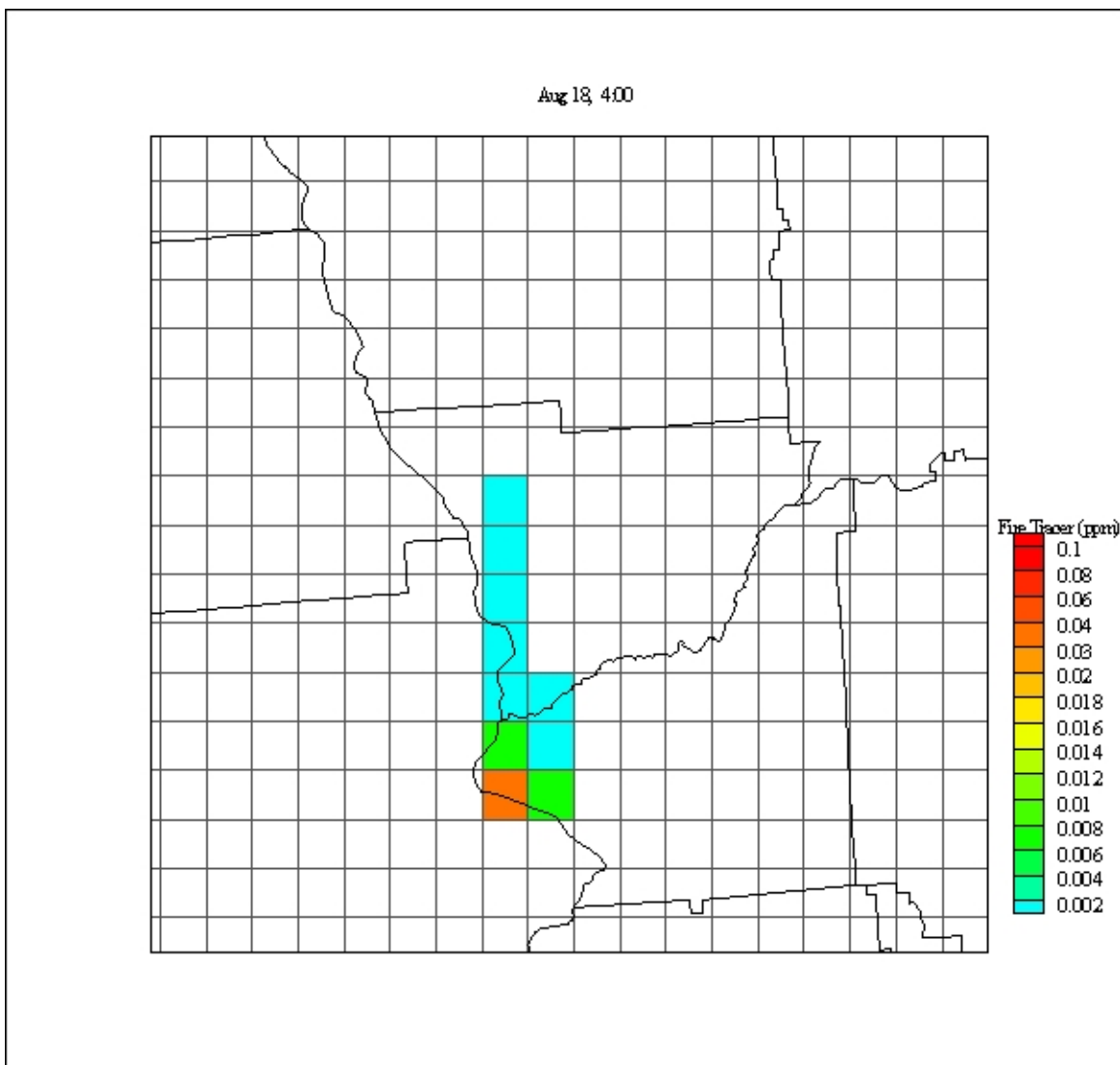
Figure 15 Static Grid Result for Inert Fire Tracer Concentrations (ppm) for August 18, 4:00
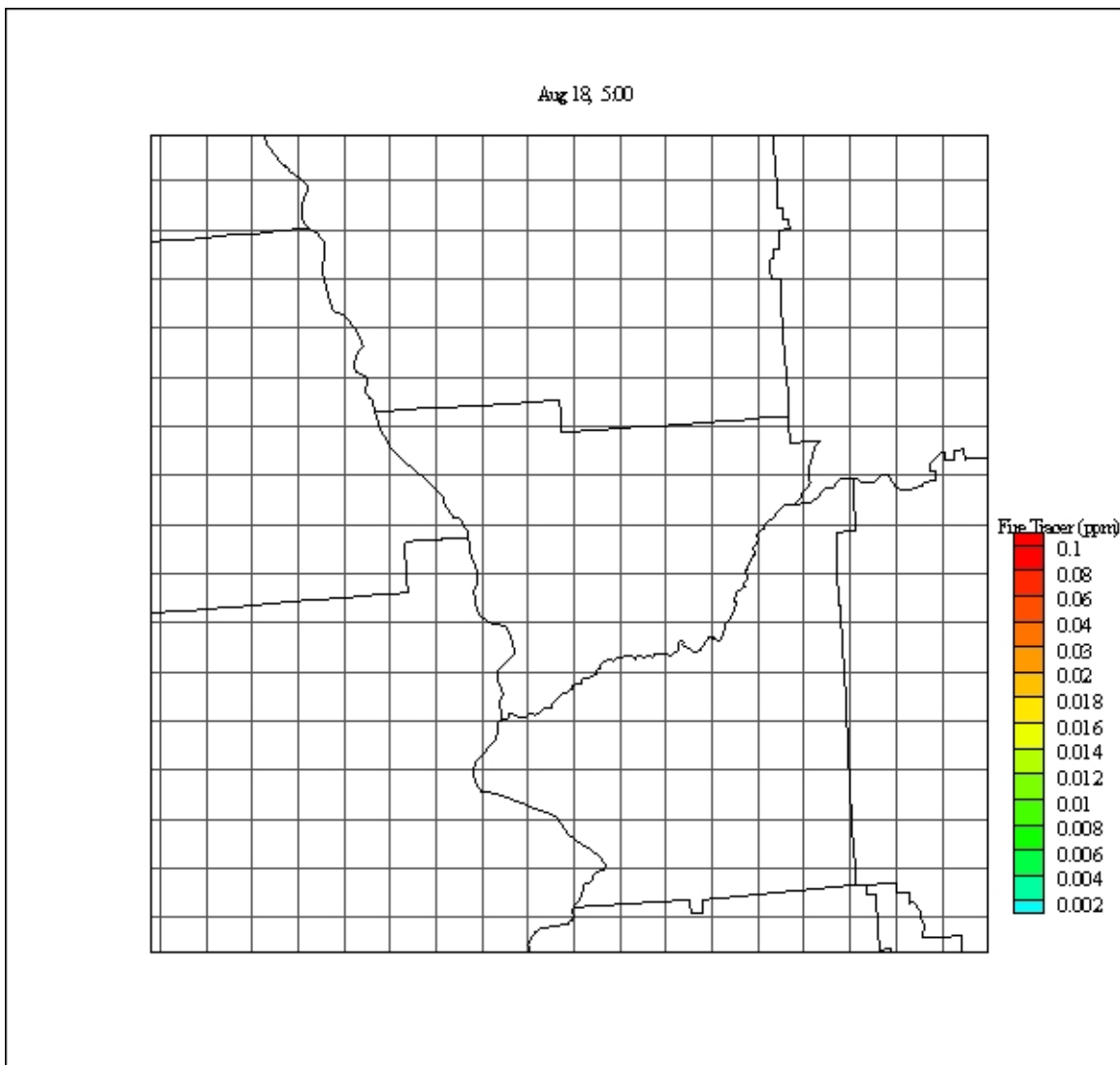
Figure 16 Static Grid Result for Inert Fire Tracer Concentrations (ppm) for August 18, 5:00
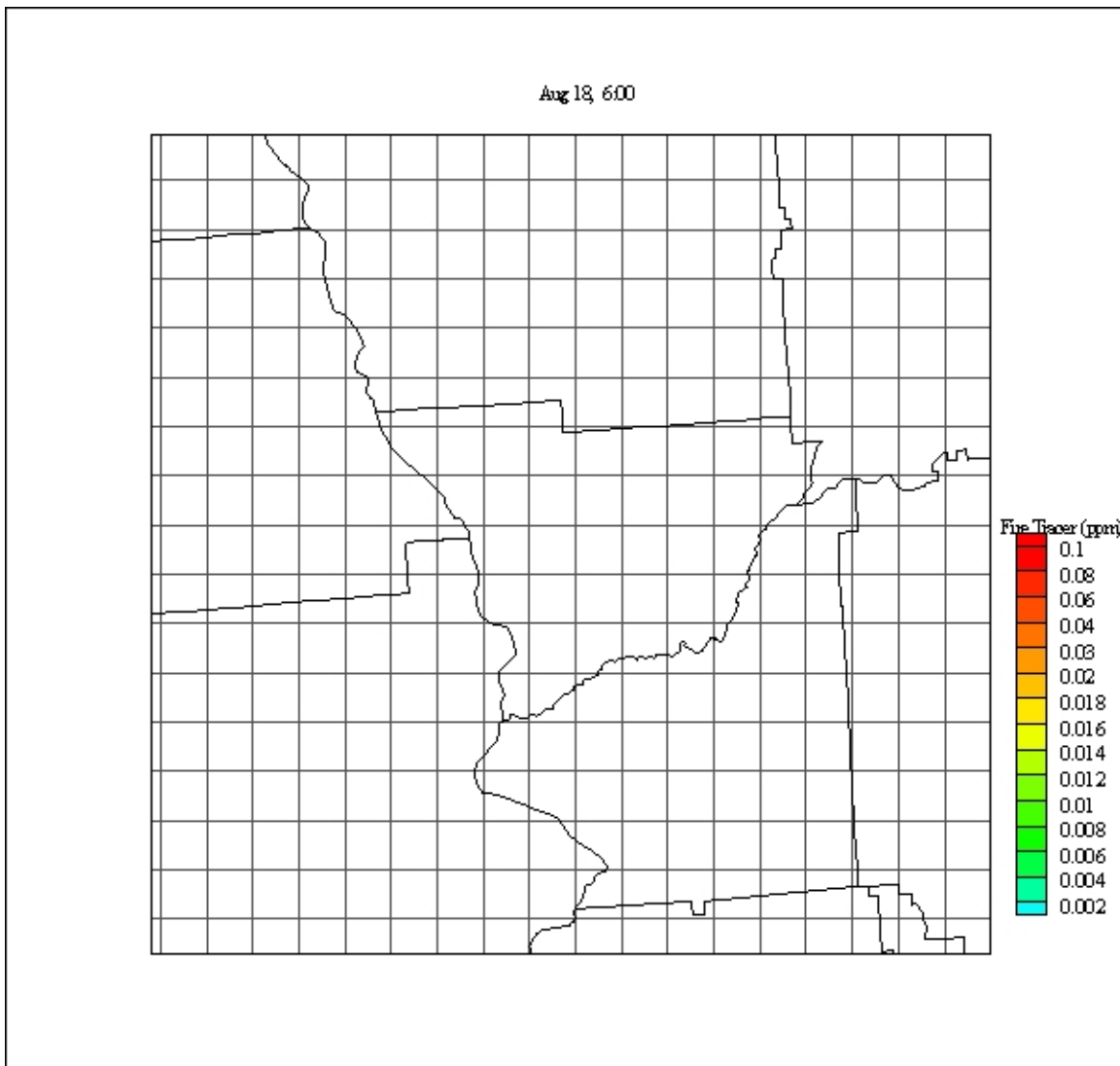
**Figure 17 Static Grid Result for Inert Fire Tracer Concentrations (ppm) for August 18, 6:00**
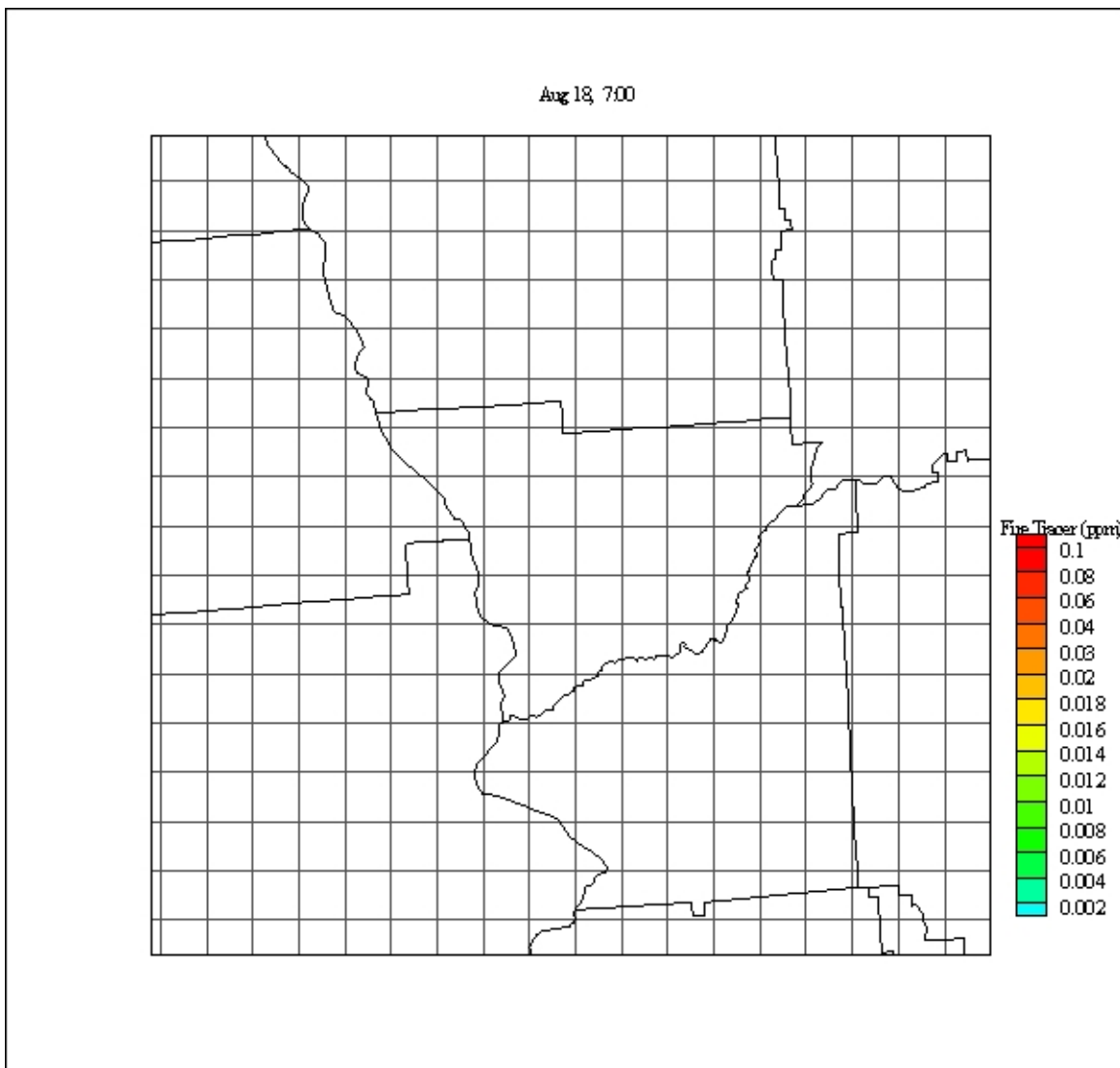
Figure 18 Static Grid Result for Inert Fire Tracer Concentrations (ppm) for August 18, 7:00
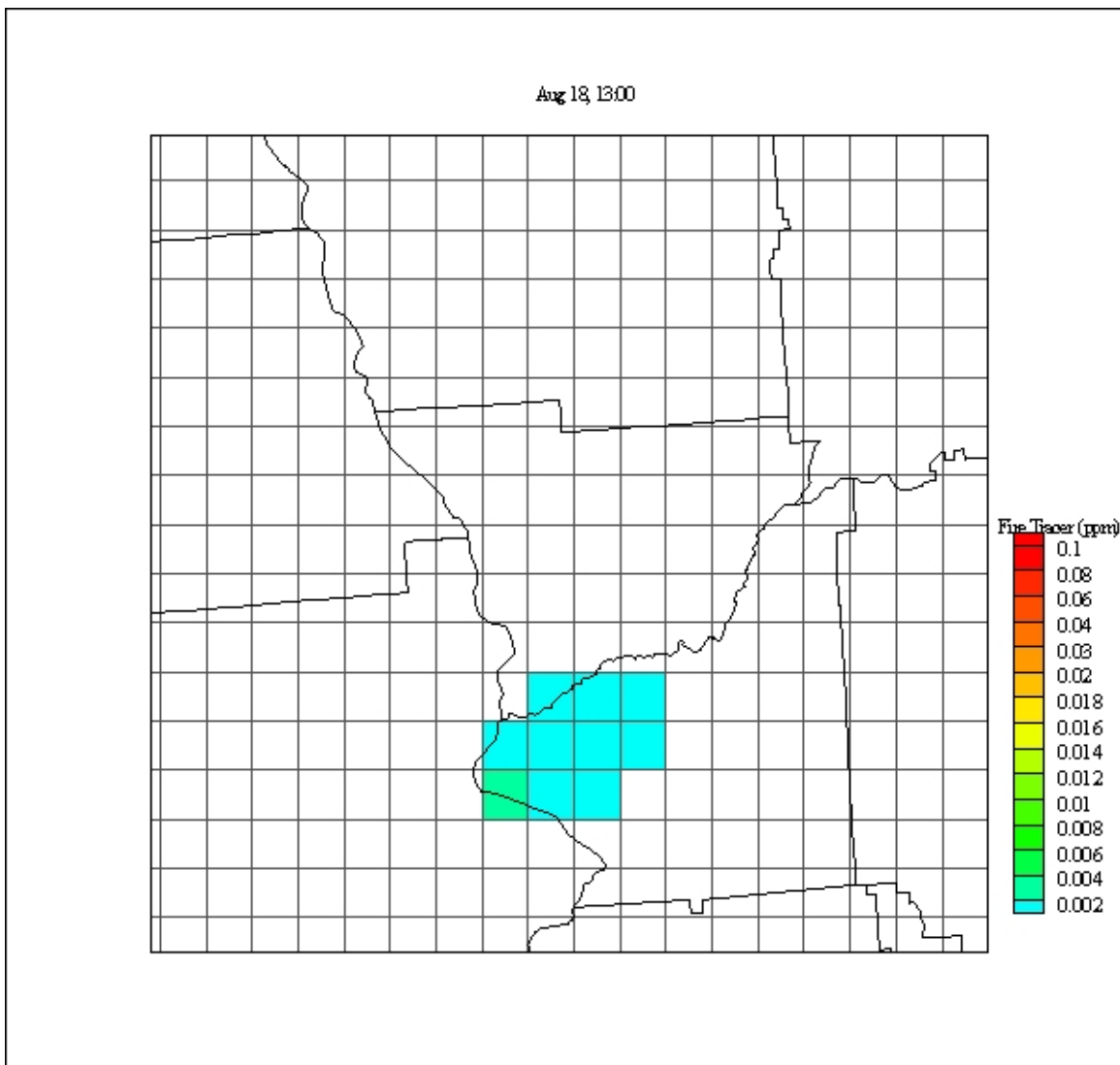
Figure 19 Static Grid Result for Inert Fire Tracer Concentrations (ppm) for August18, 13:00
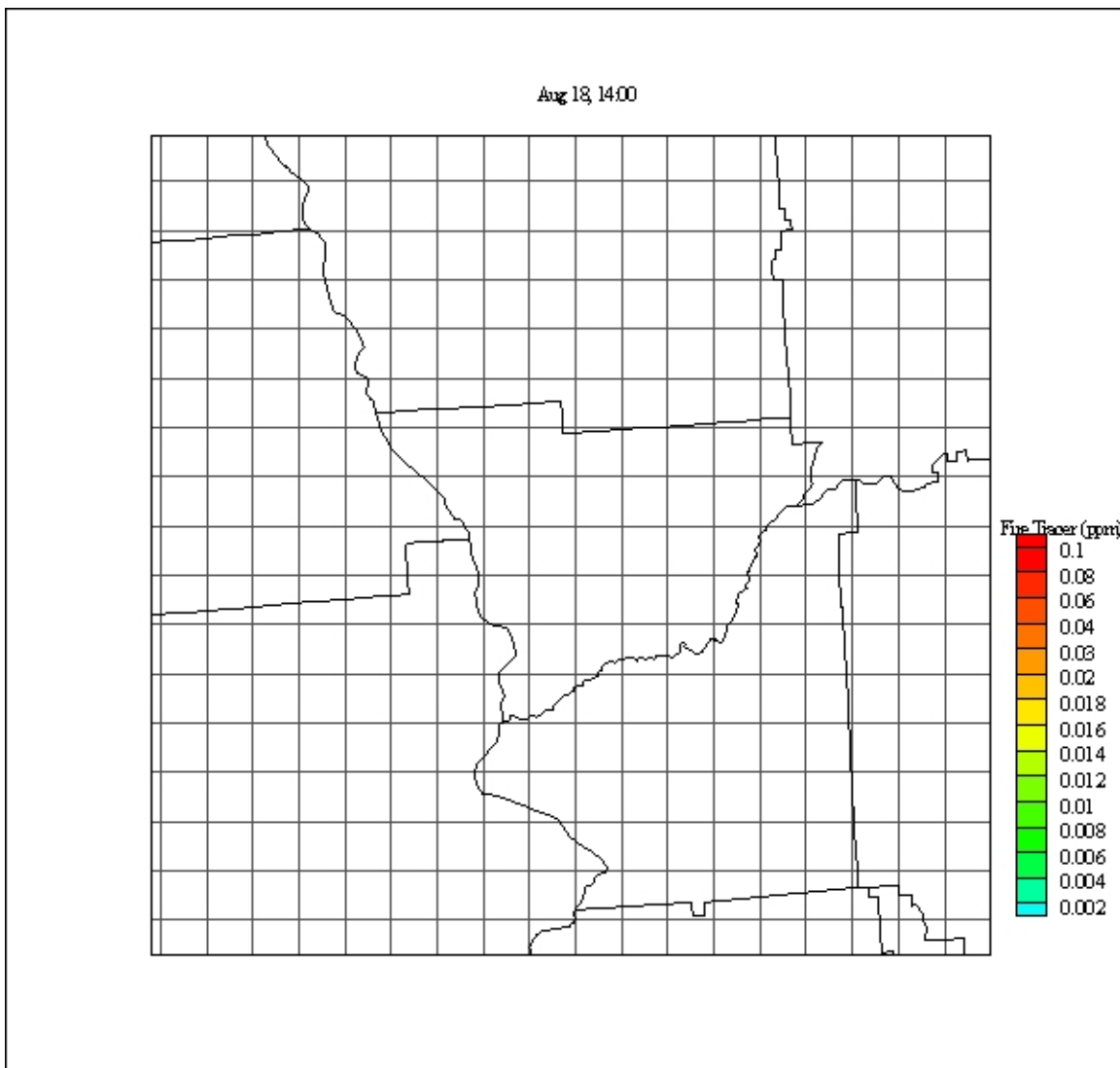
Figure 20 Static Grid Result for Inert Fire Tracer Concentrations (ppm) for August 18, 14:00
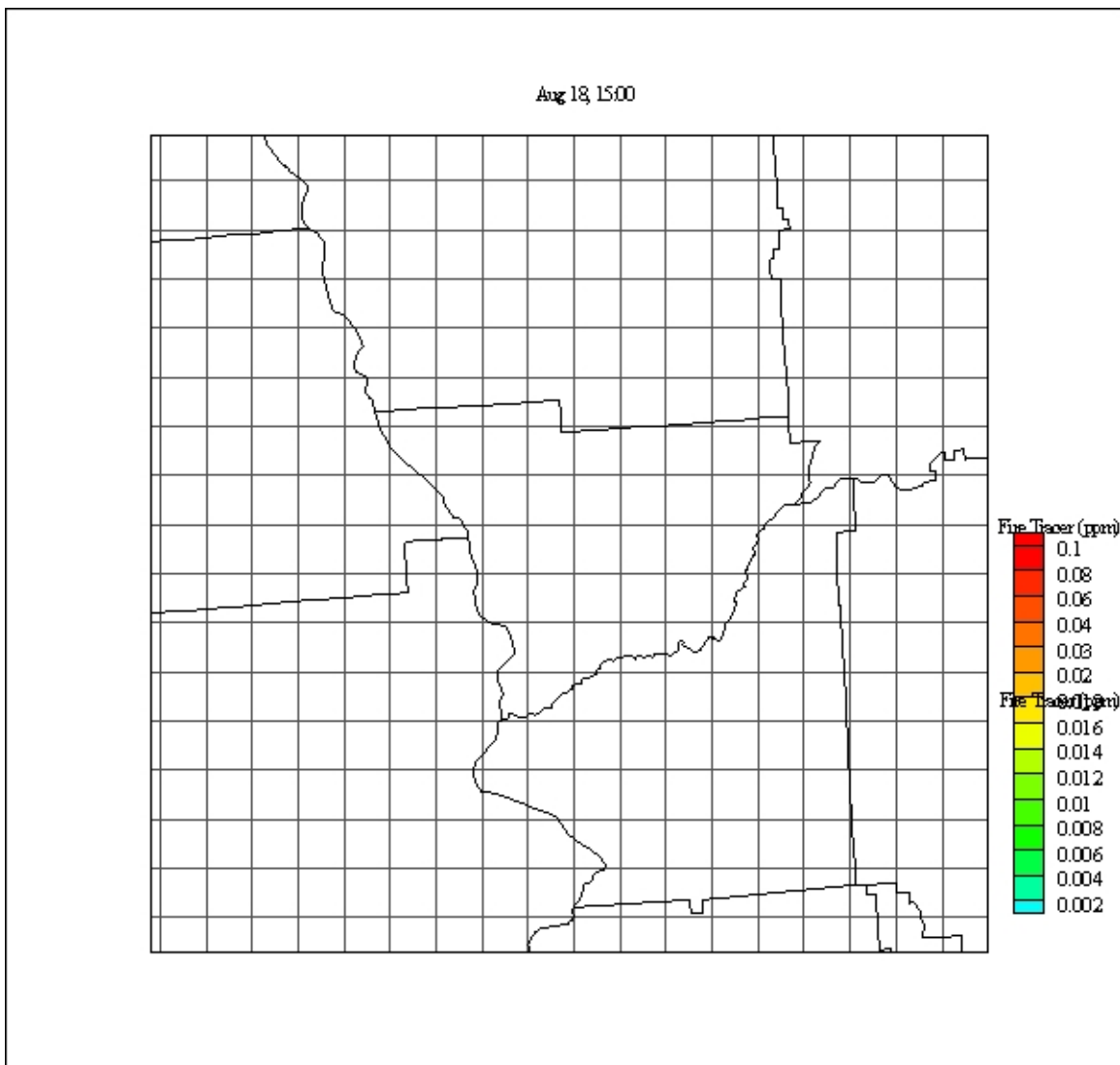
**Figure 21 Static Grid Result for Inert Fire Tracer Concentrations (ppm) for August 18, 15:00**
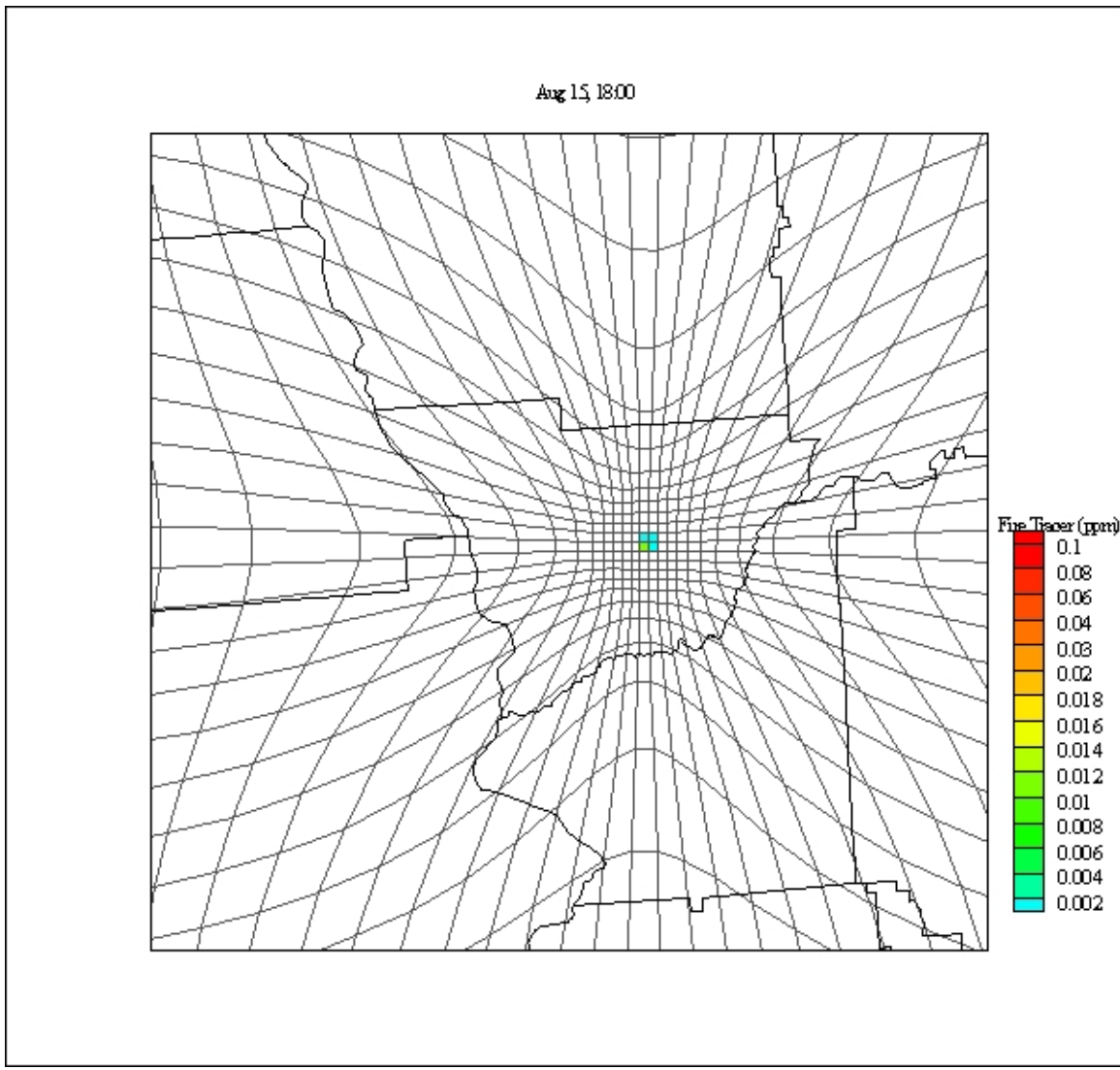
Figure 22 Adaptive Grid Result for Inert Fire Tracer Concentrations (ppm) for August 15, 18:00
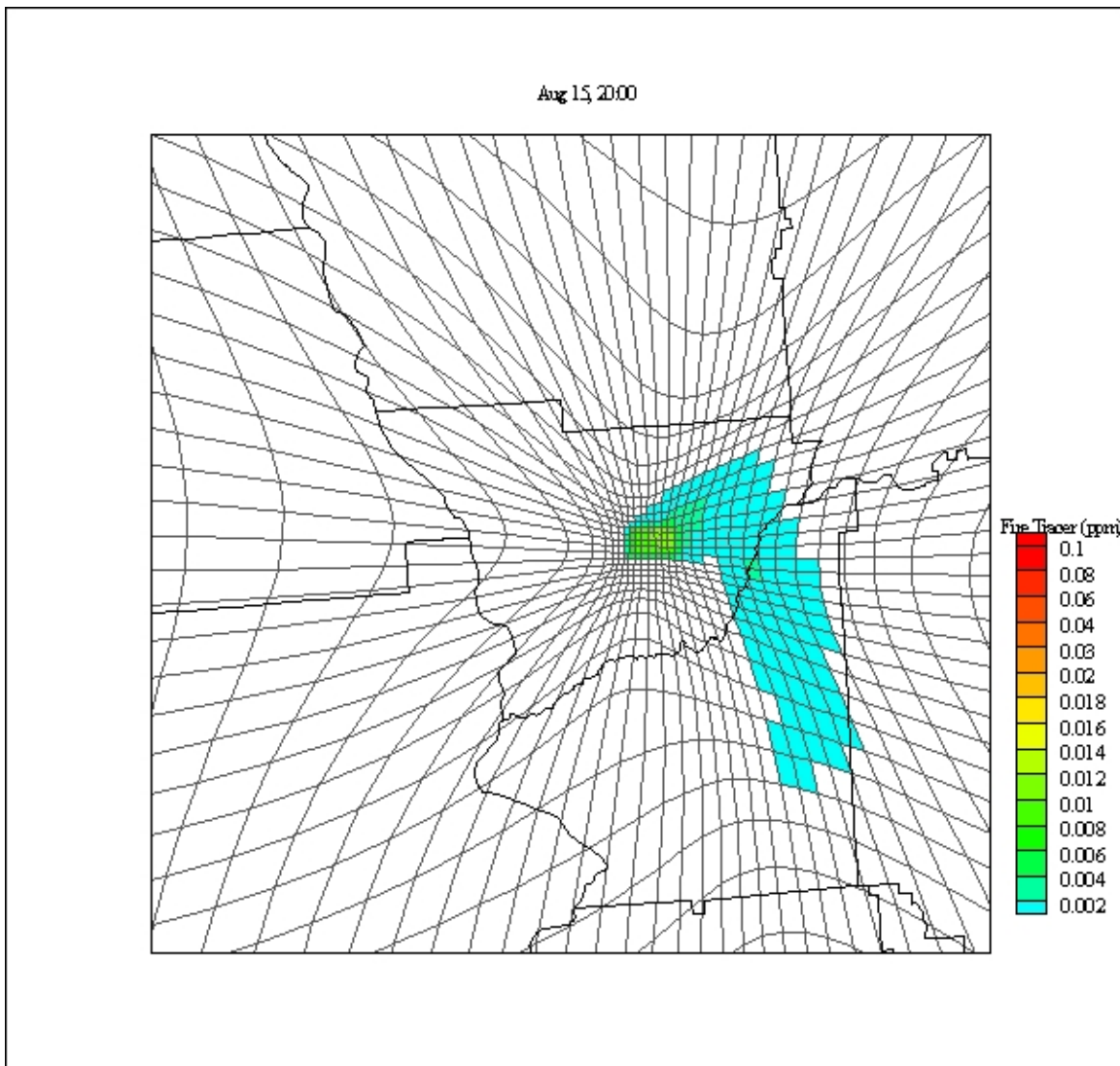
Figure 23 Adaptive Grid Result for Inert Fire Tracer Concentrations (ppm) for August 15, 20:00

Aug 15, 21:00

Fire Tracer (ppm)
0.1
0.08
0.06
0.04
0.03
0.02
0.018
0.016
0.014
0.012
0.01
0.008
0.006
0.004
0.002
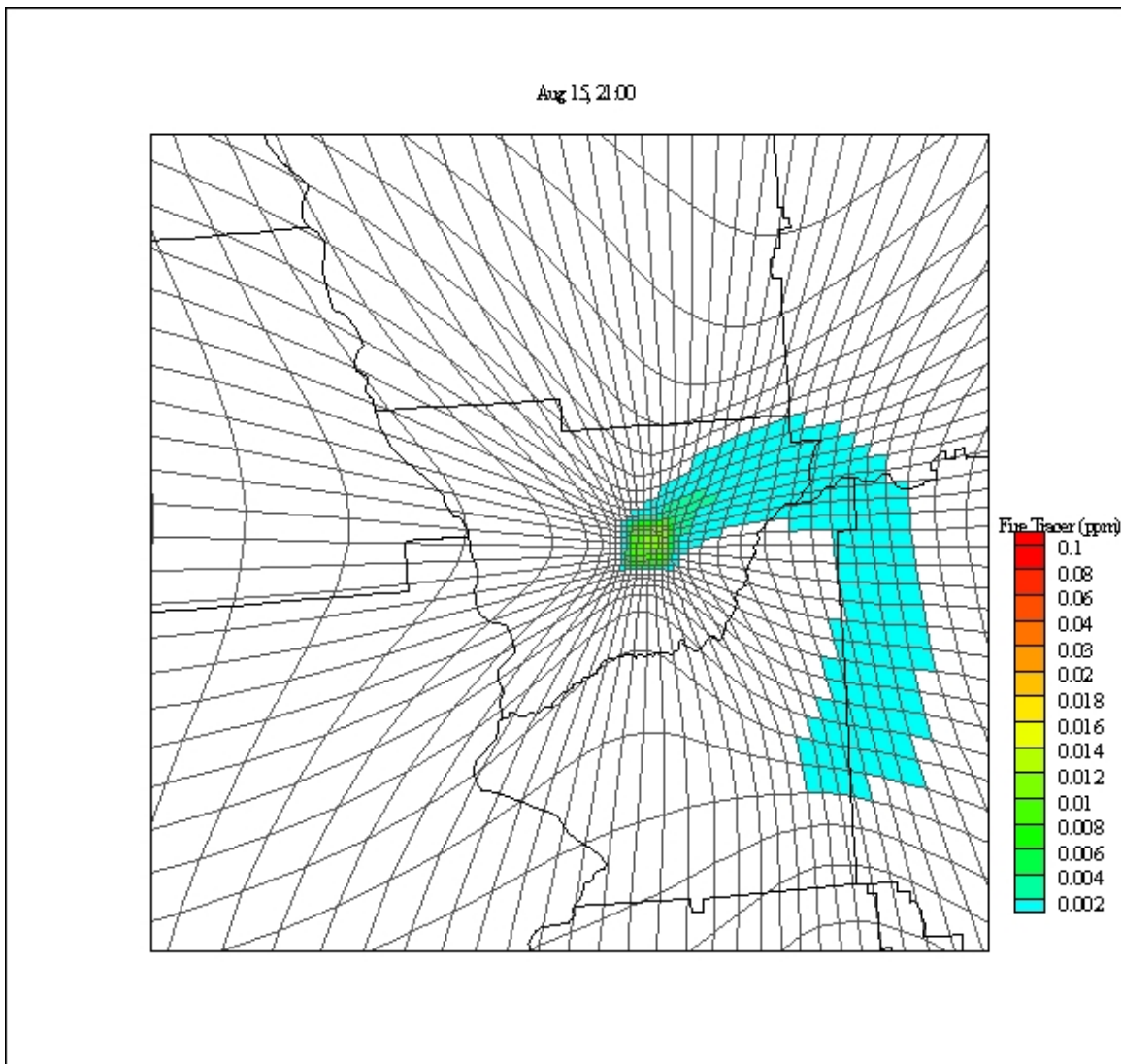
Figure 24 Adaptive Grid Result for Inert Fire Tracer Concentrations (ppm) for August 15, 21:00
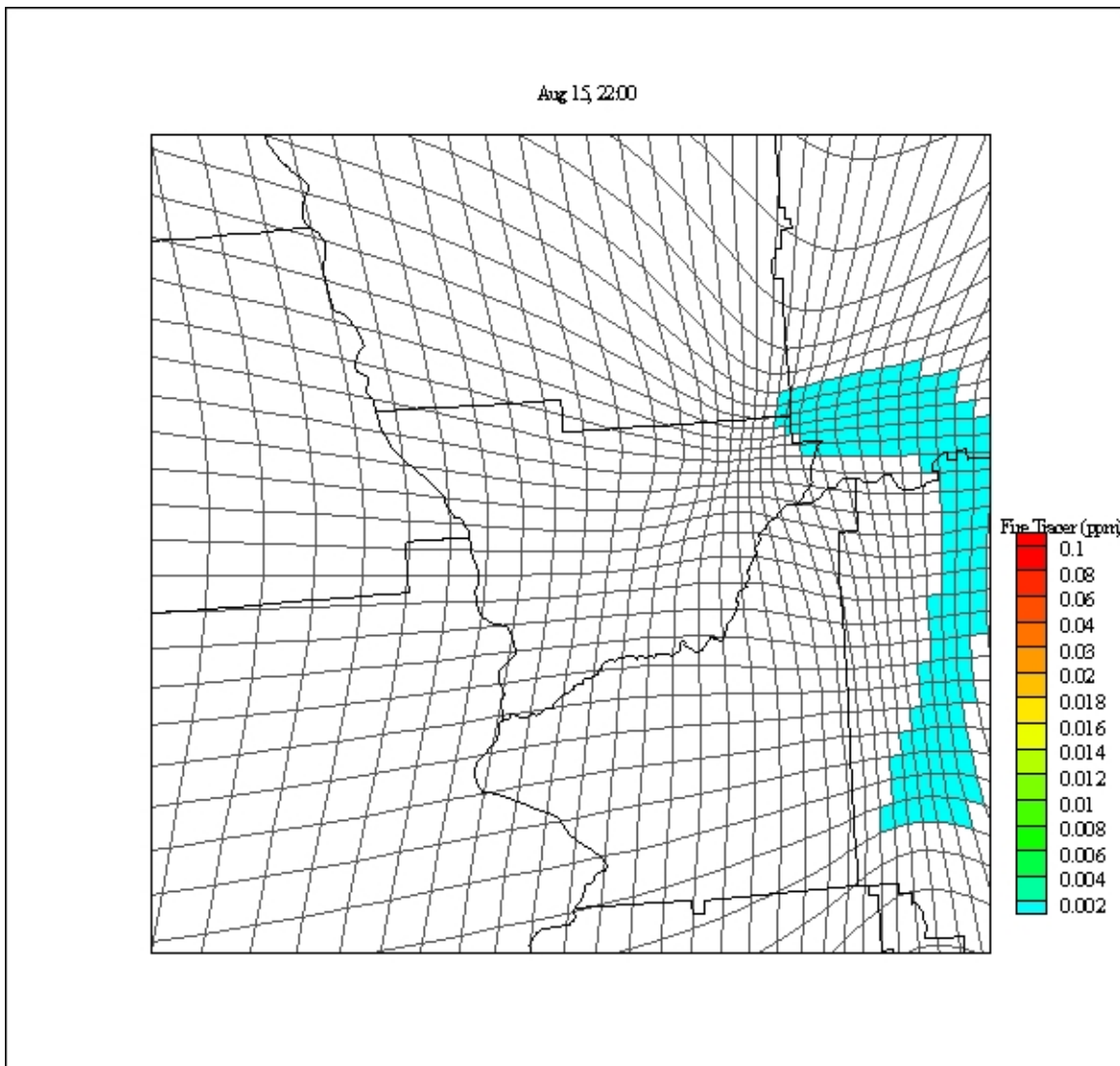
Figure 25 Adaptive Grid Result for Inert Fire Tracer Concentrations (ppm) for August 15, 22:00
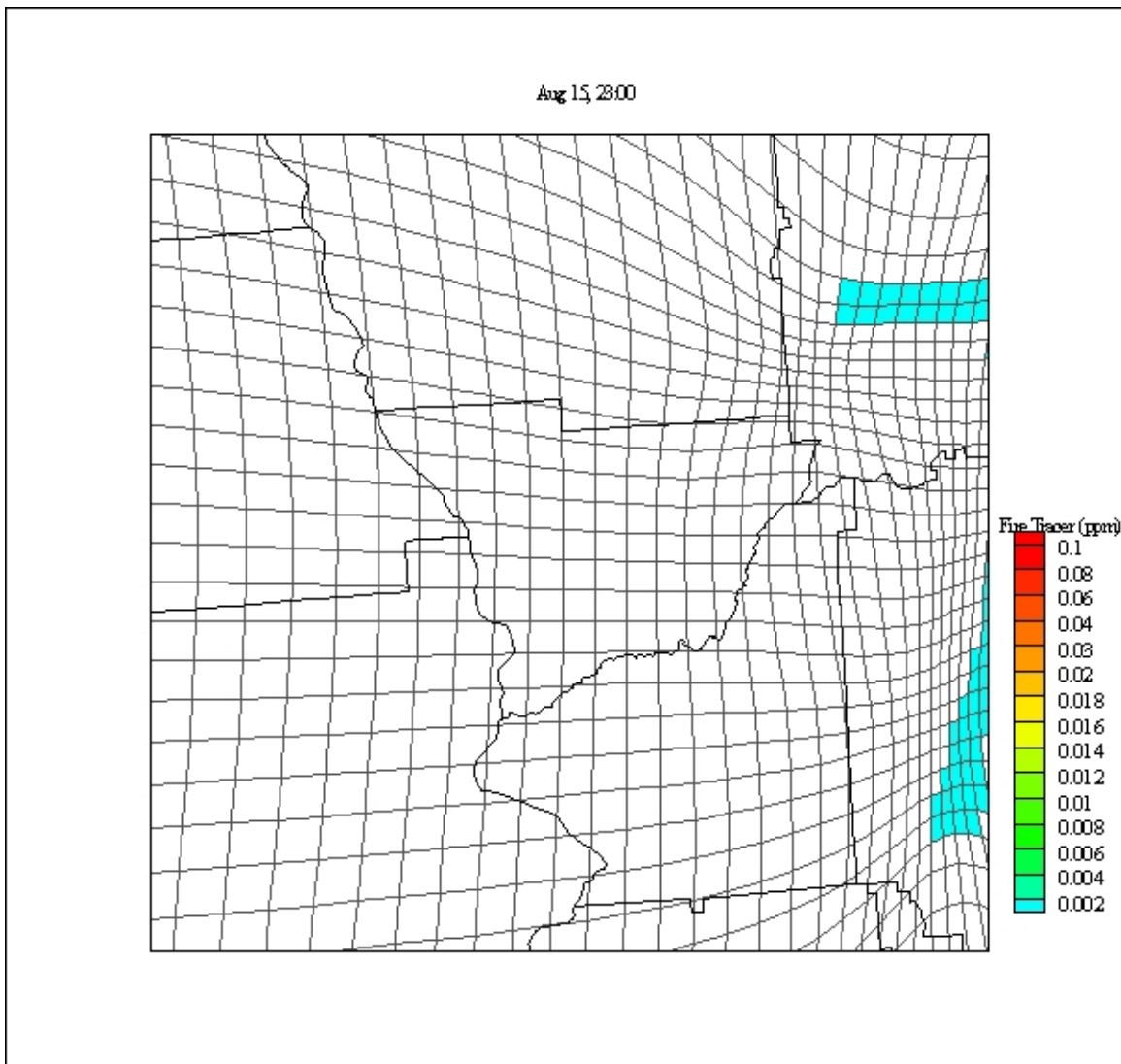
Figure 26 Adaptive Grid Result for Inert Fire Tracer Concentrations (ppm) for August 15, 23:00

Aug 16, 0:00

Fire Tracer (ppm)
0.1
0.08
0.06
0.04
0.03
0.02
0.018
0.016
0.014
0.012
0.01
0.008
0.006
0.004
0.002
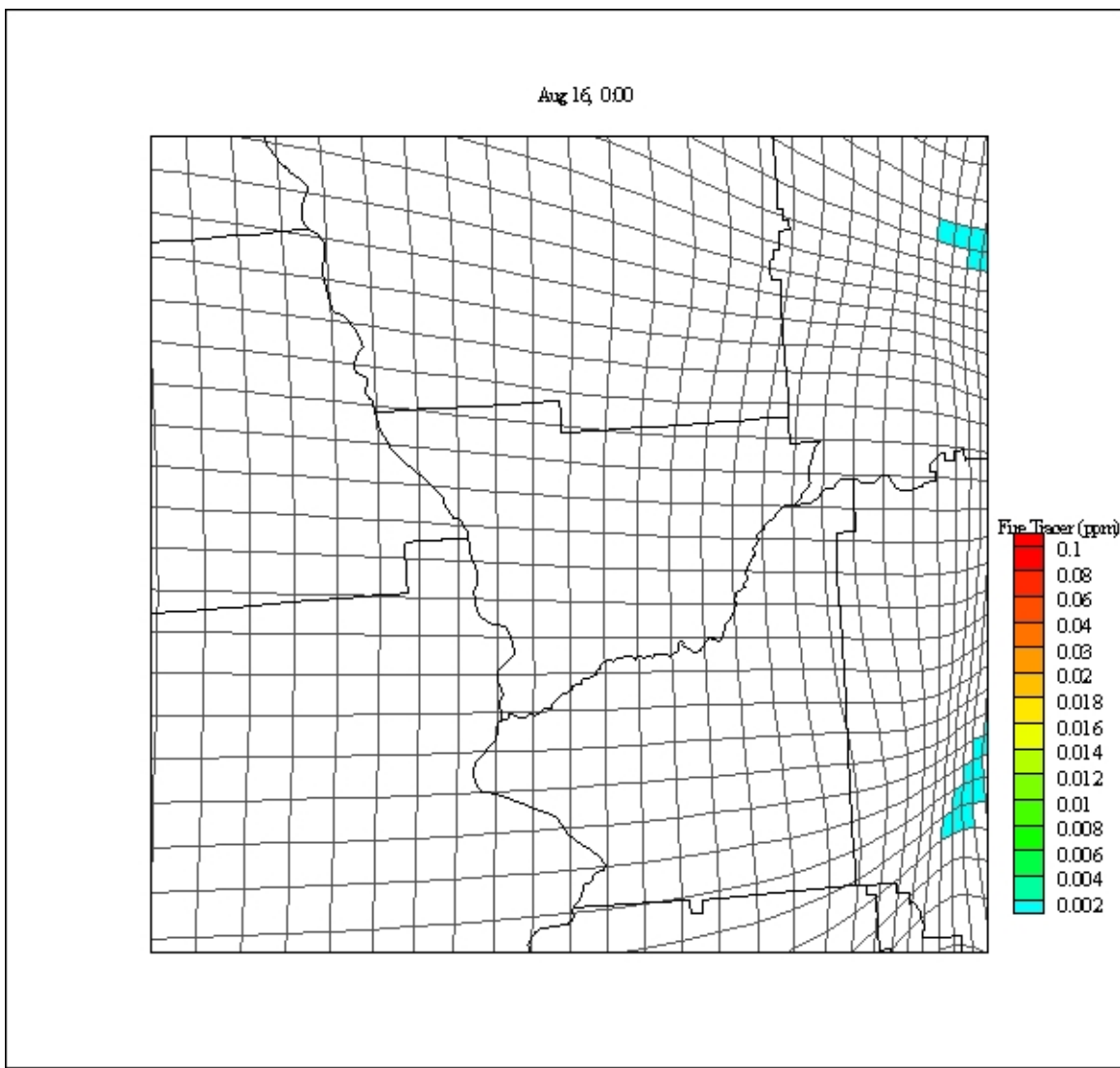
Figure 27 Adaptive Grid Result for Inert Fire Tracer Concentrations (ppm) for August 16, 0:00
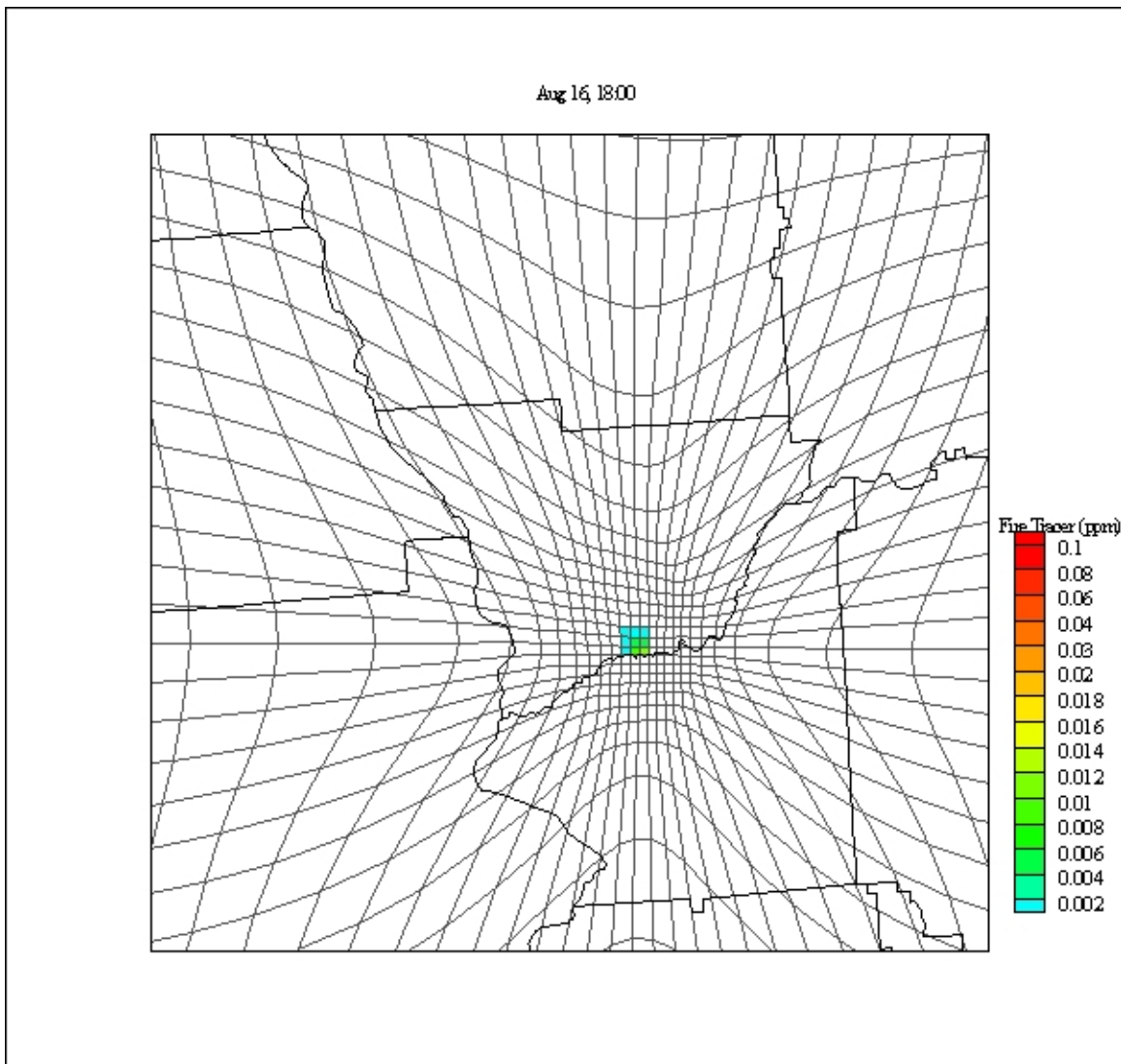
Figure 28 Adaptive Grid Result for Inert Fire Tracer Concentrations (ppm) for August 16, 18:00
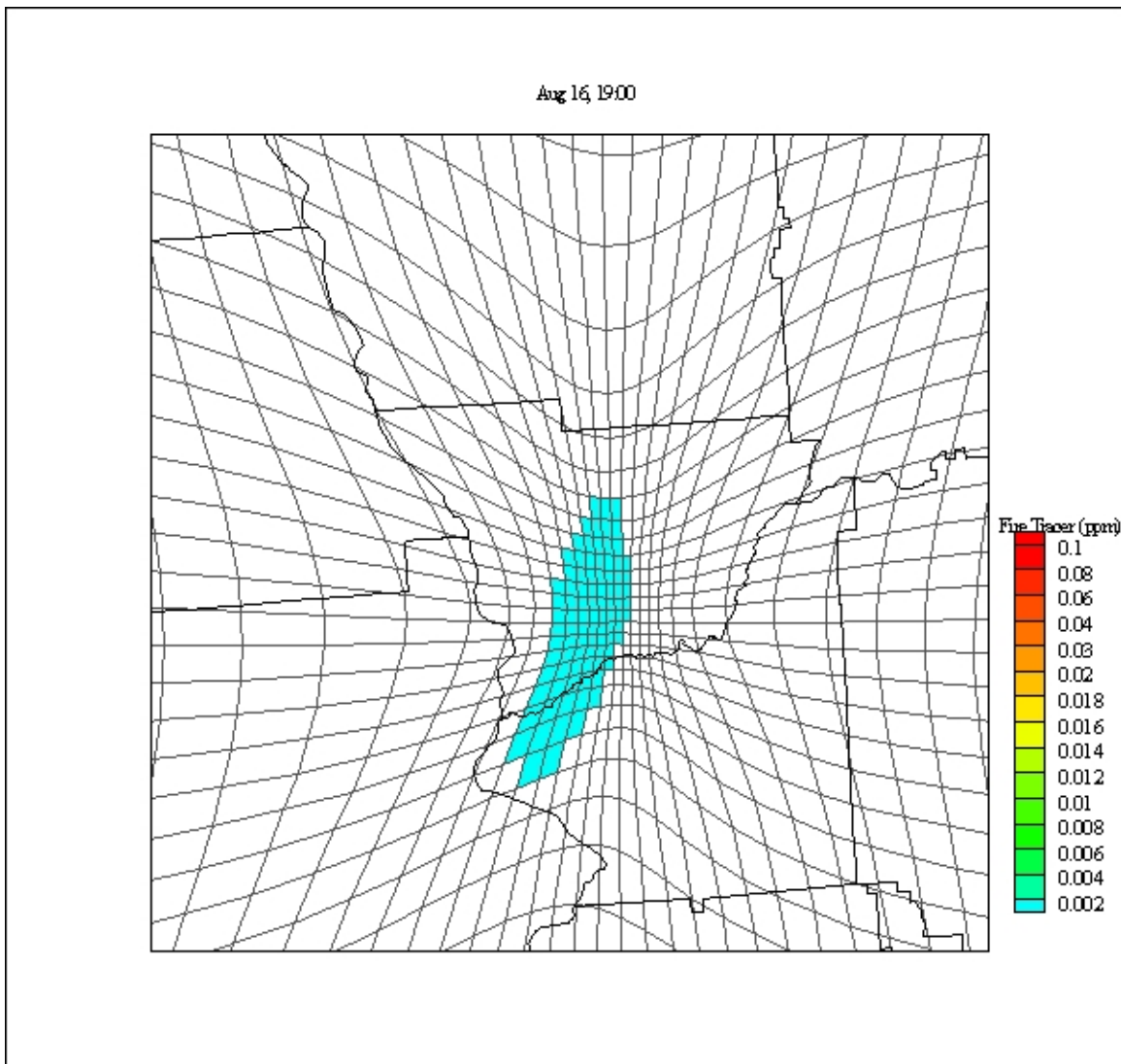
Figure 29 Adaptive Grid Result for Inert Fire Tracer Concentrations (ppm) for August 16, 19:00

Aug 16, 20:00

Fire Tracer (ppm)
0.1
0.08
0.06
0.04
0.03
0.02
0.018
0.016
0.014
0.012
0.01
0.008
0.006
0.004
0.002
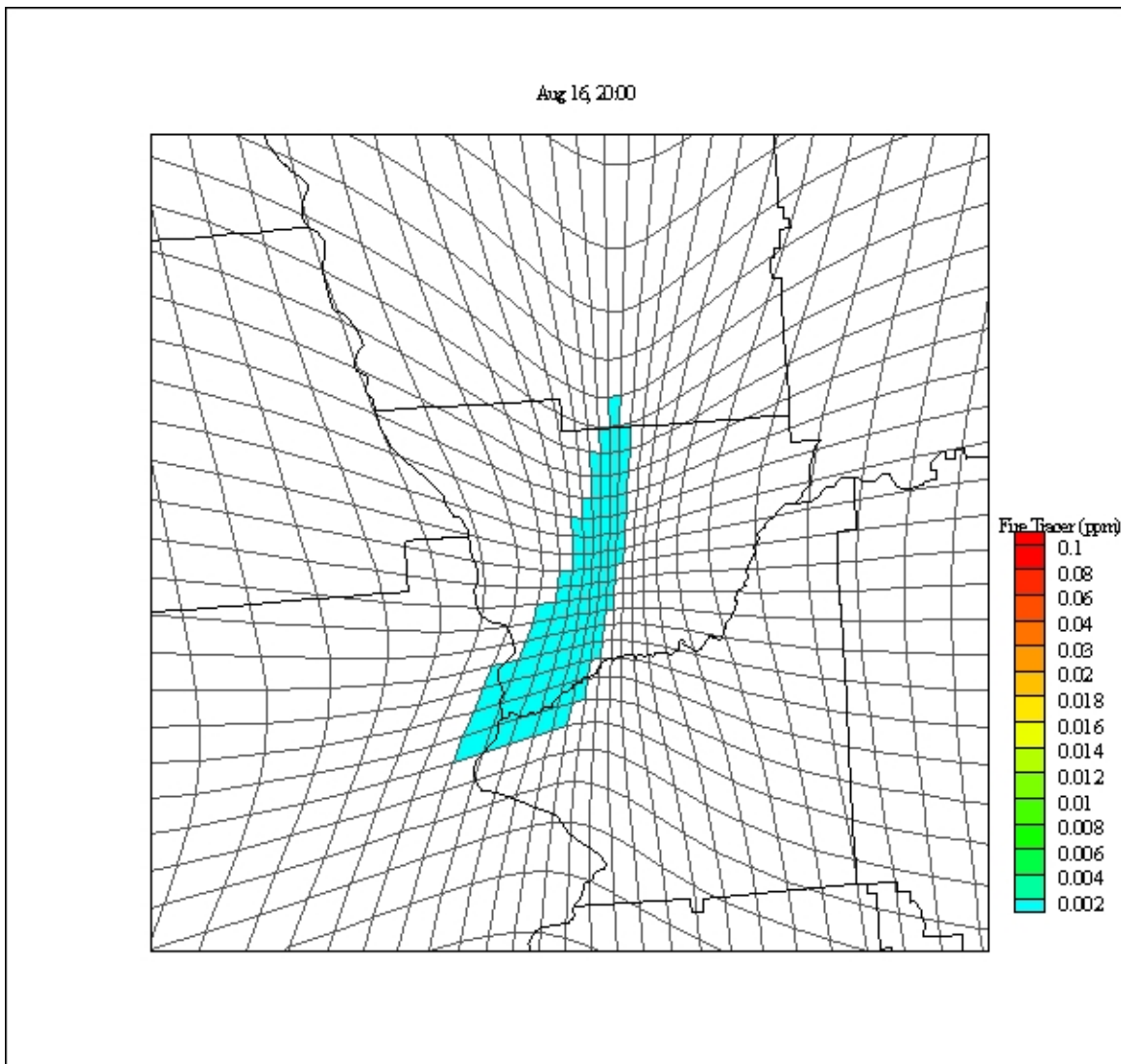
Figure 30 Adaptive Grid Result for Inert Fire Tracer Concentrations (ppm) for August 16, 20:00
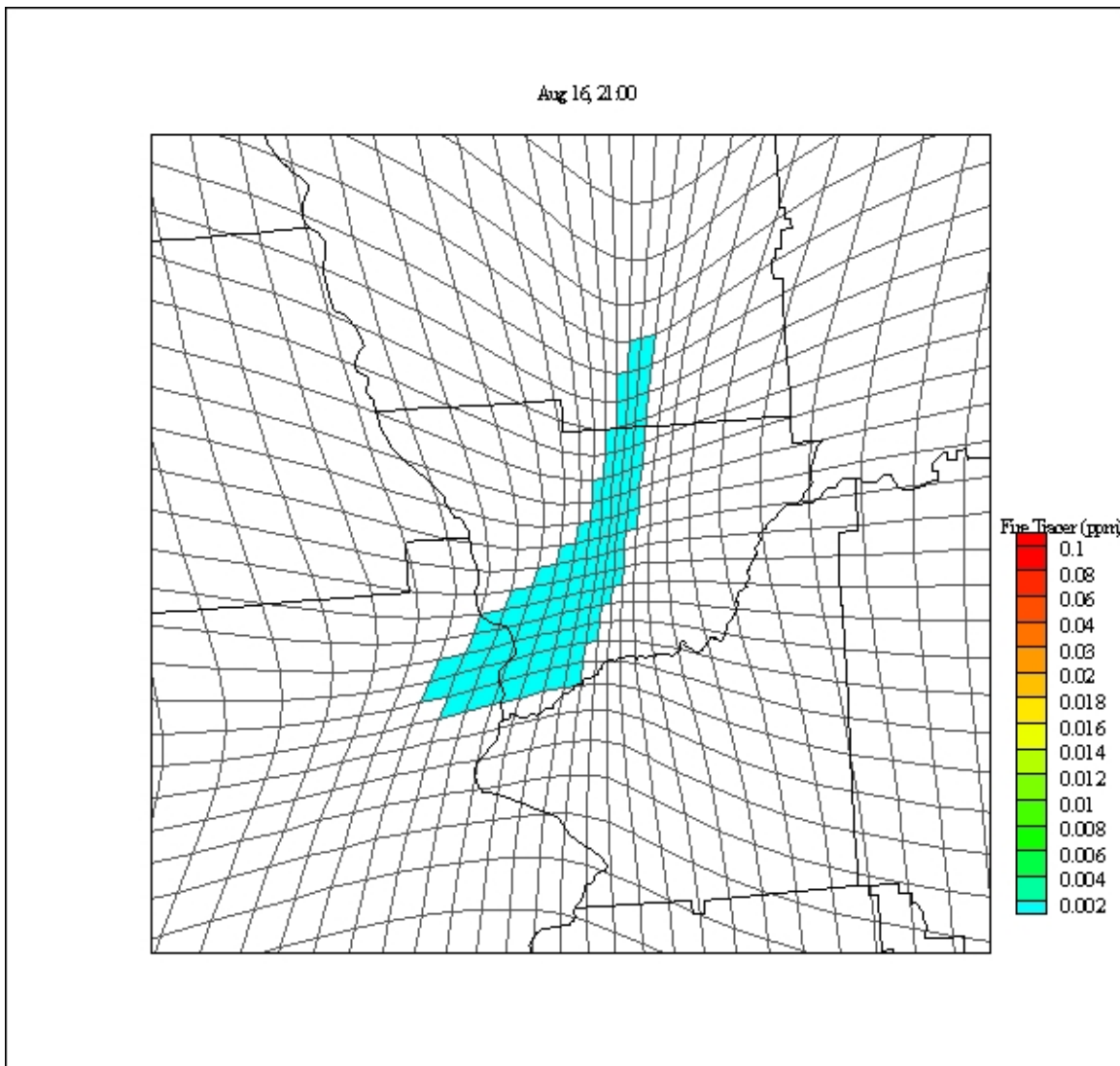
Figure 31 Adaptive Grid Result for Inert Fire Tracer Concentrations (ppm) for August 16, 21:00

Aug 16, 22:00

Fire Tracer (ppm)
0.1
0.08
0.06
0.04
0.03
0.02
0.018
0.016
0.014
0.012
0.01
0.008
0.006
0.004
0.002
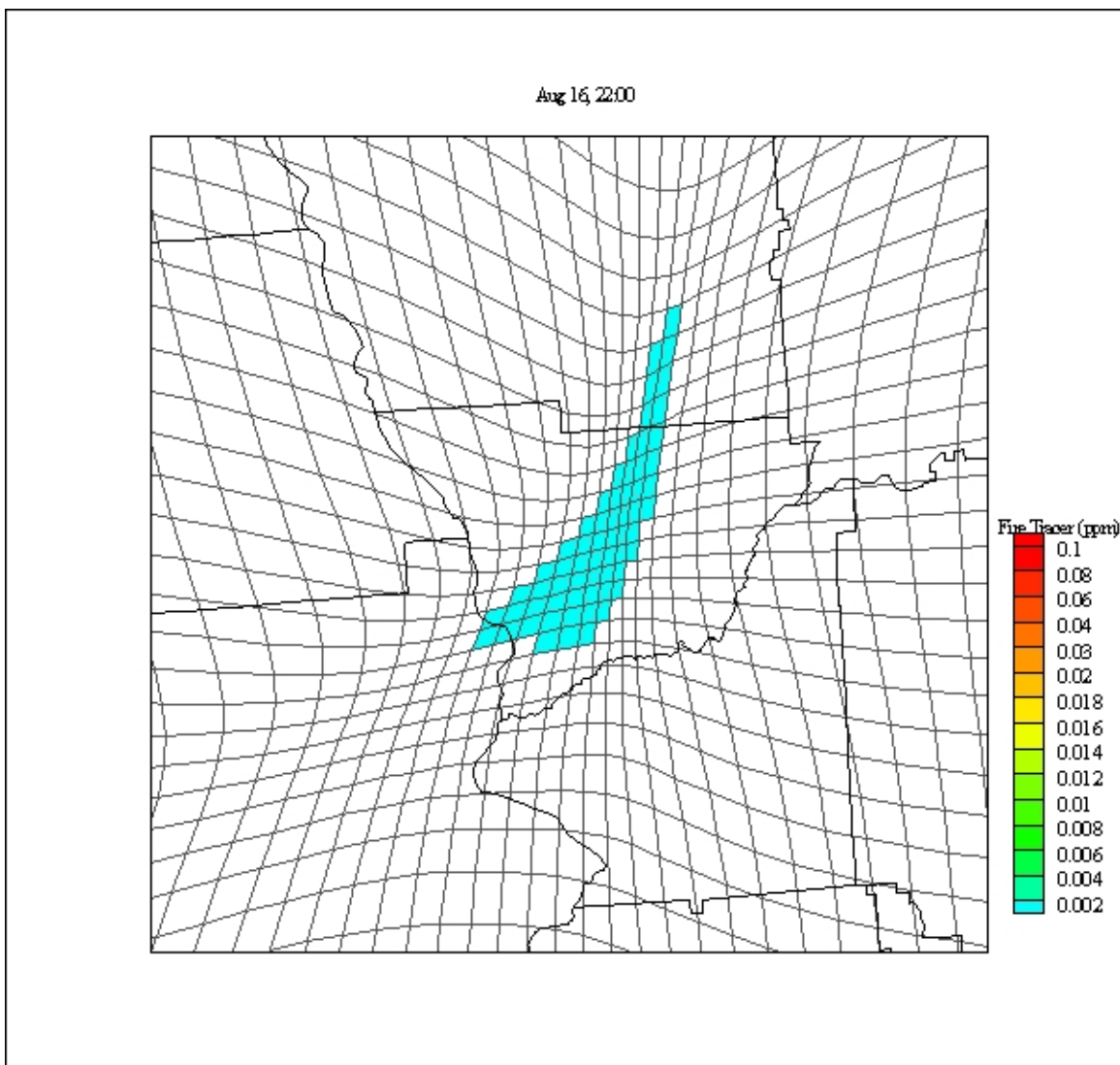
Figure 32 Adaptive Grid Result for Inert Fire Tracer Concentrations (ppm) for August 15, 22:00
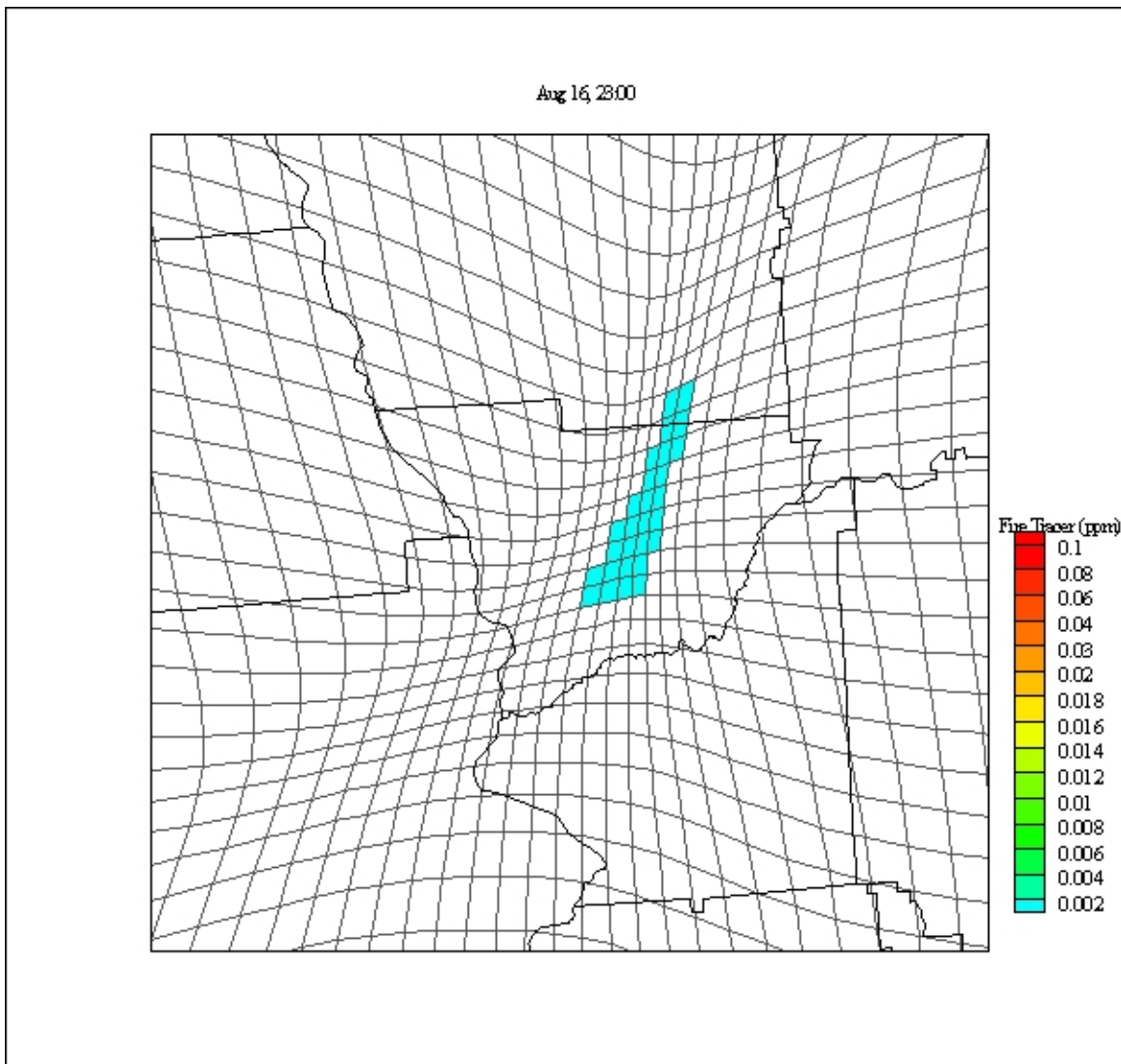
Figure 33 Adaptive Grid Result for Inert Fire Tracer Concentrations (ppm) for August 15, 23:00
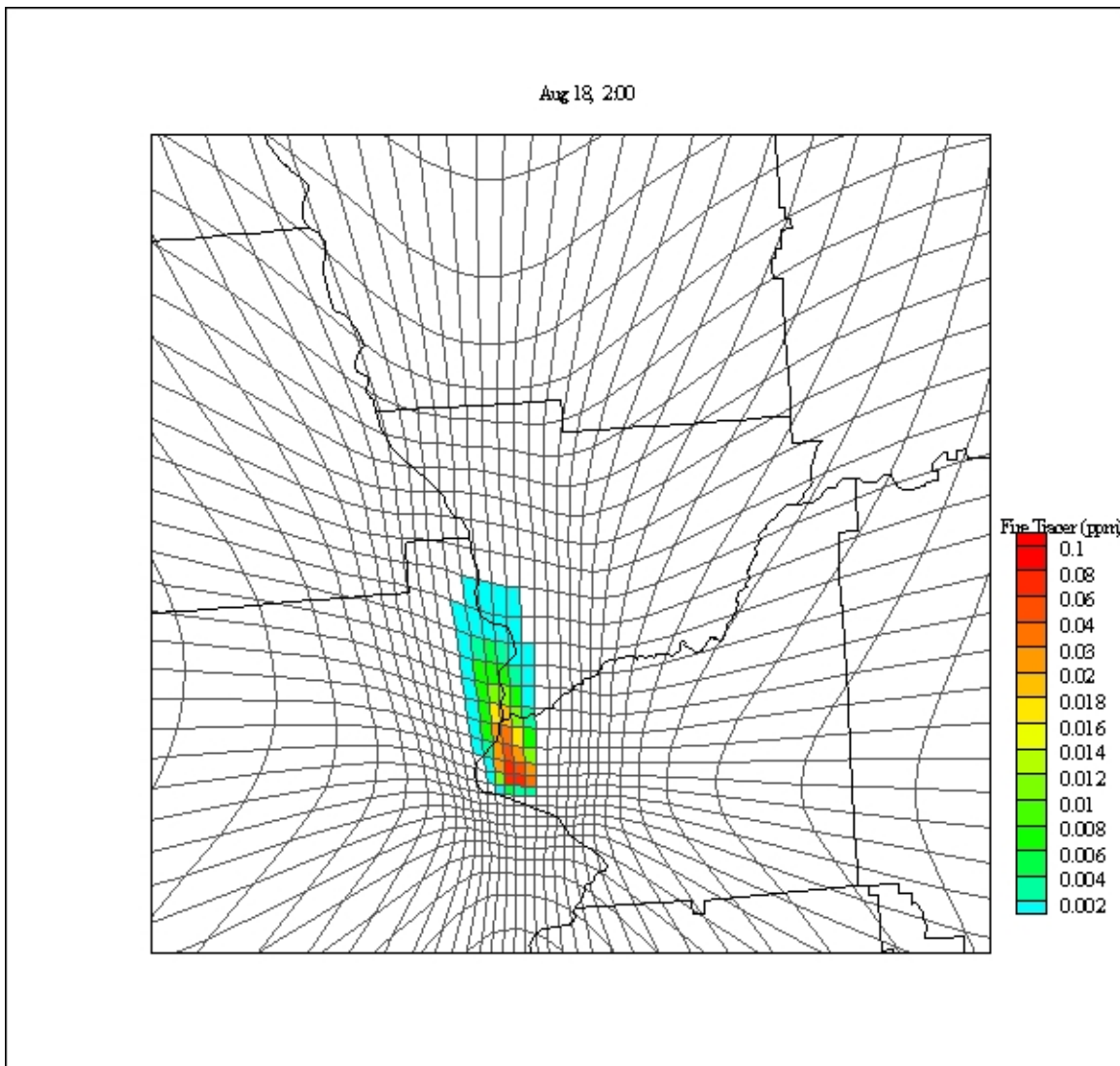
Figure 34 Adaptive Grid Result for Inert Fire Tracer Concentrations (ppm) for August 18, 2:00

Aug 18, 3:00

Fire Tracer (ppm)
0.1
0.08
0.06
0.04
0.03
0.02
0.018
0.016
0.014
0.012
0.01
0.008
0.006
0.004
0.002
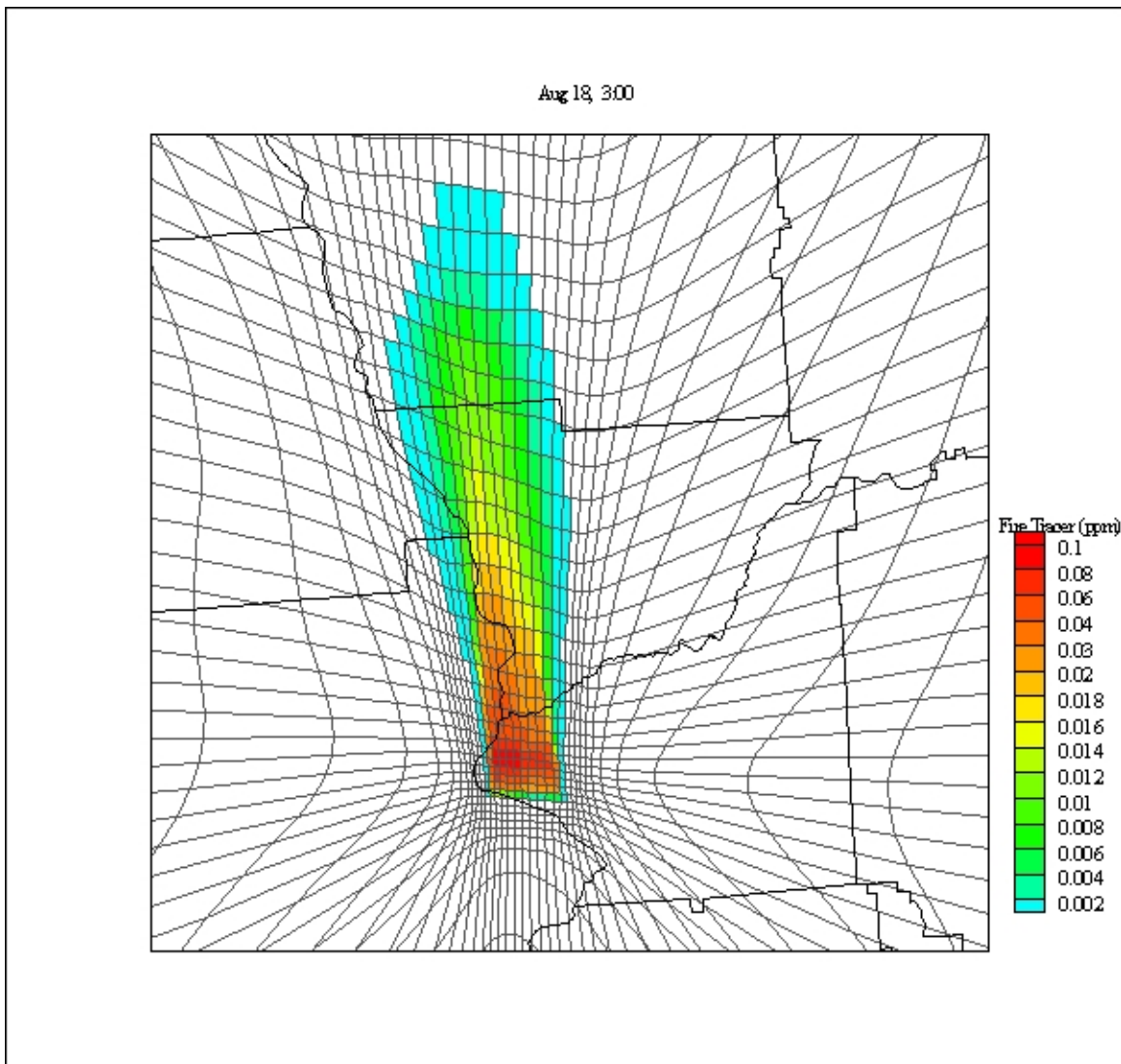
Figure 35 Adaptive Grid Result for Inert Fire Tracer Concentrations (ppm) for August 18, 3:00
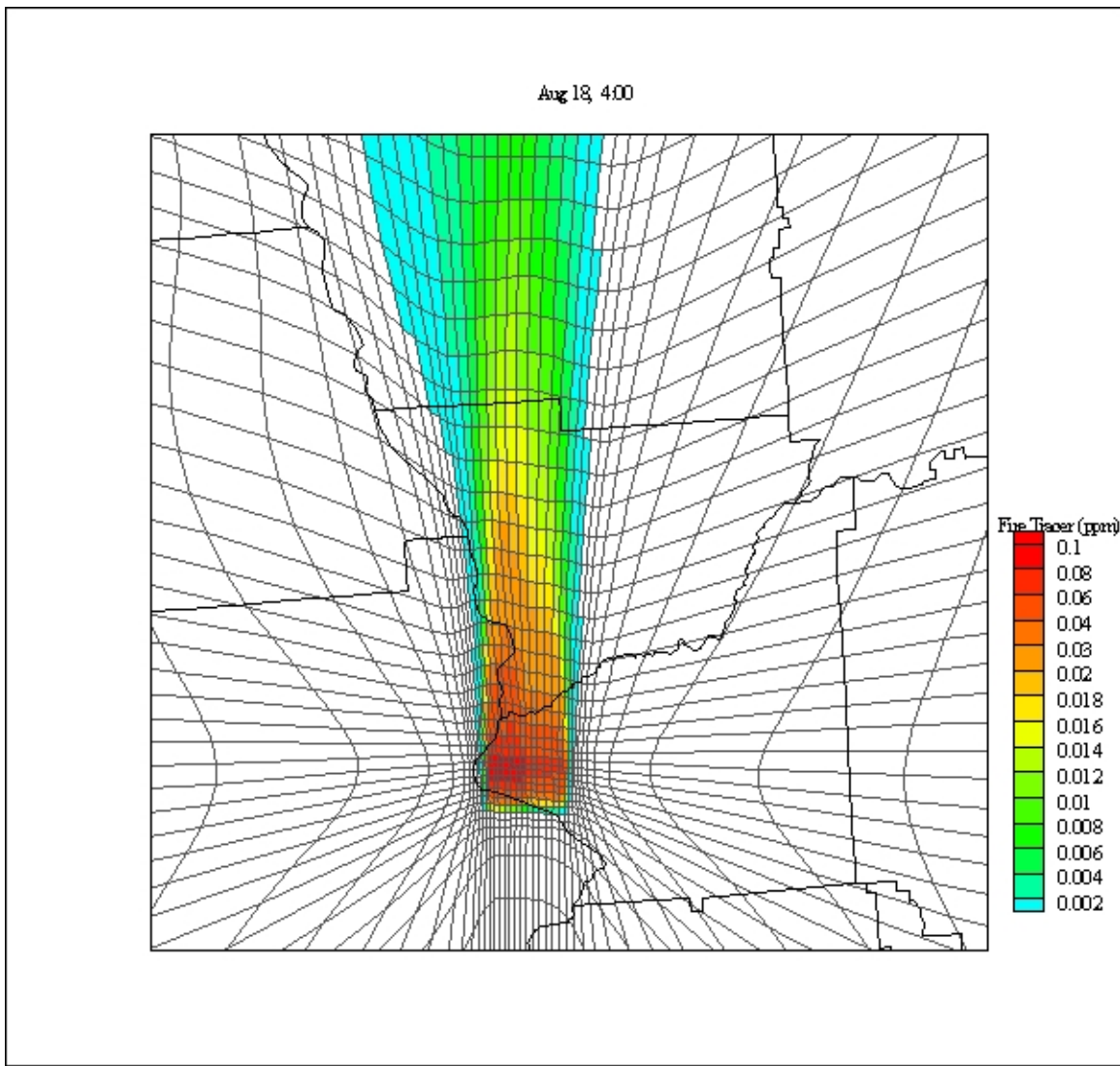
Figure 36 Adaptive Grid Result for Inert Fire Tracer Concentrations (ppm) for August 18, 4:00

Aug 18, 5:00
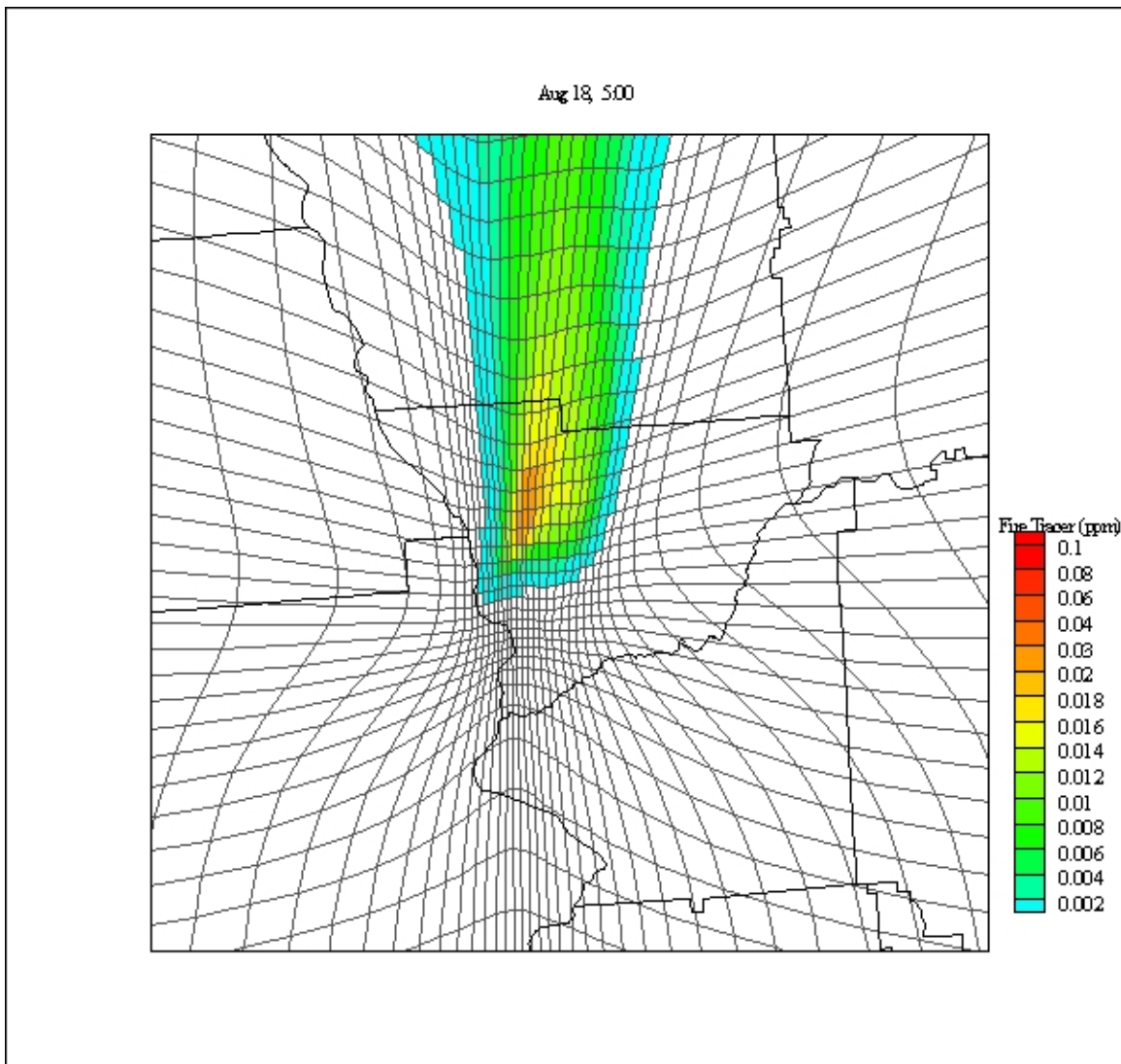
Figure 37 Adaptive Grid Result for Inert Fire Tracer Concentrations (ppm) for August 18, 5:00
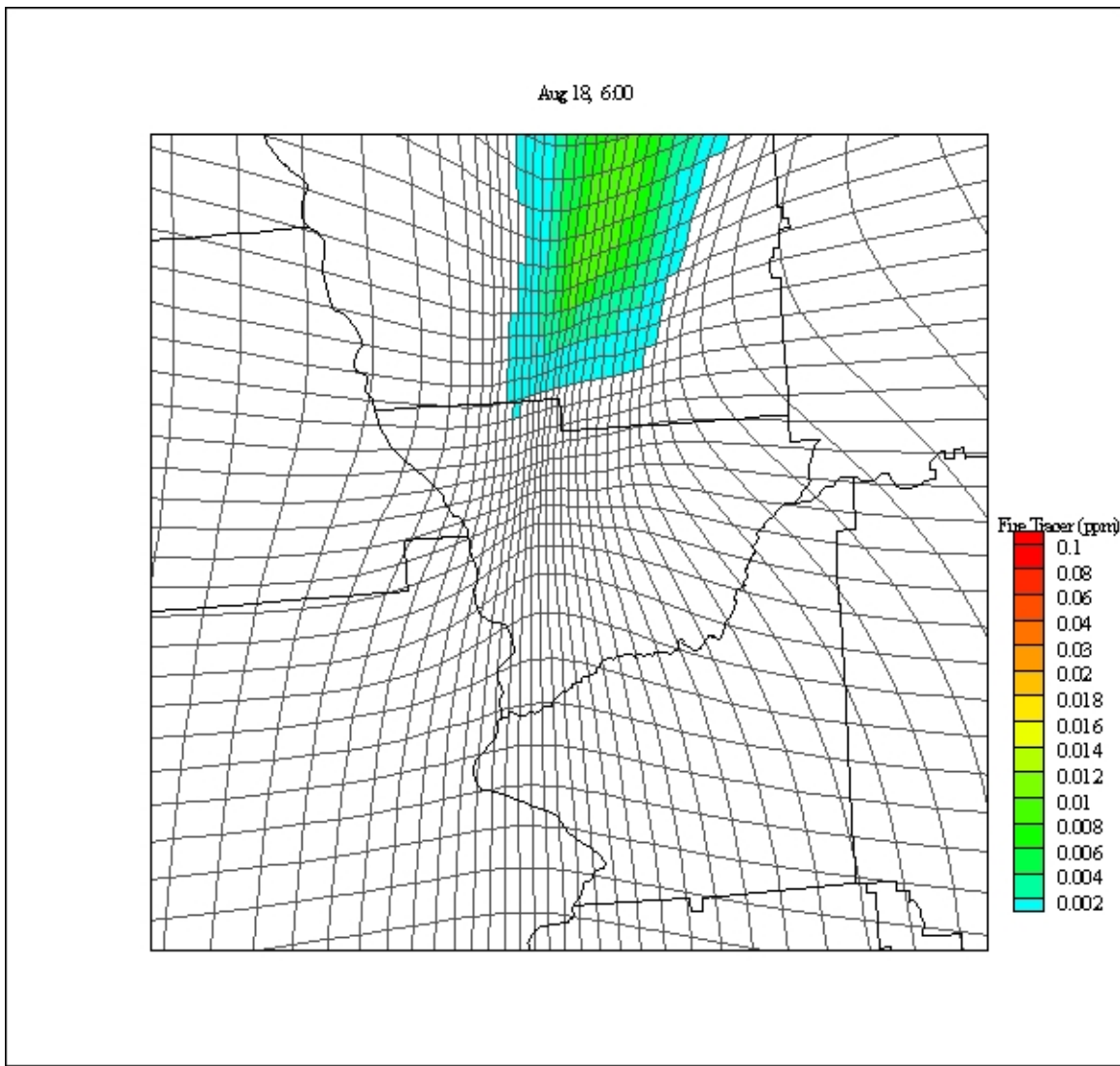
Figure 38 Adaptive Grid Result for Inert Fire Tracer Concentrations (ppm) for August 18, 6:00
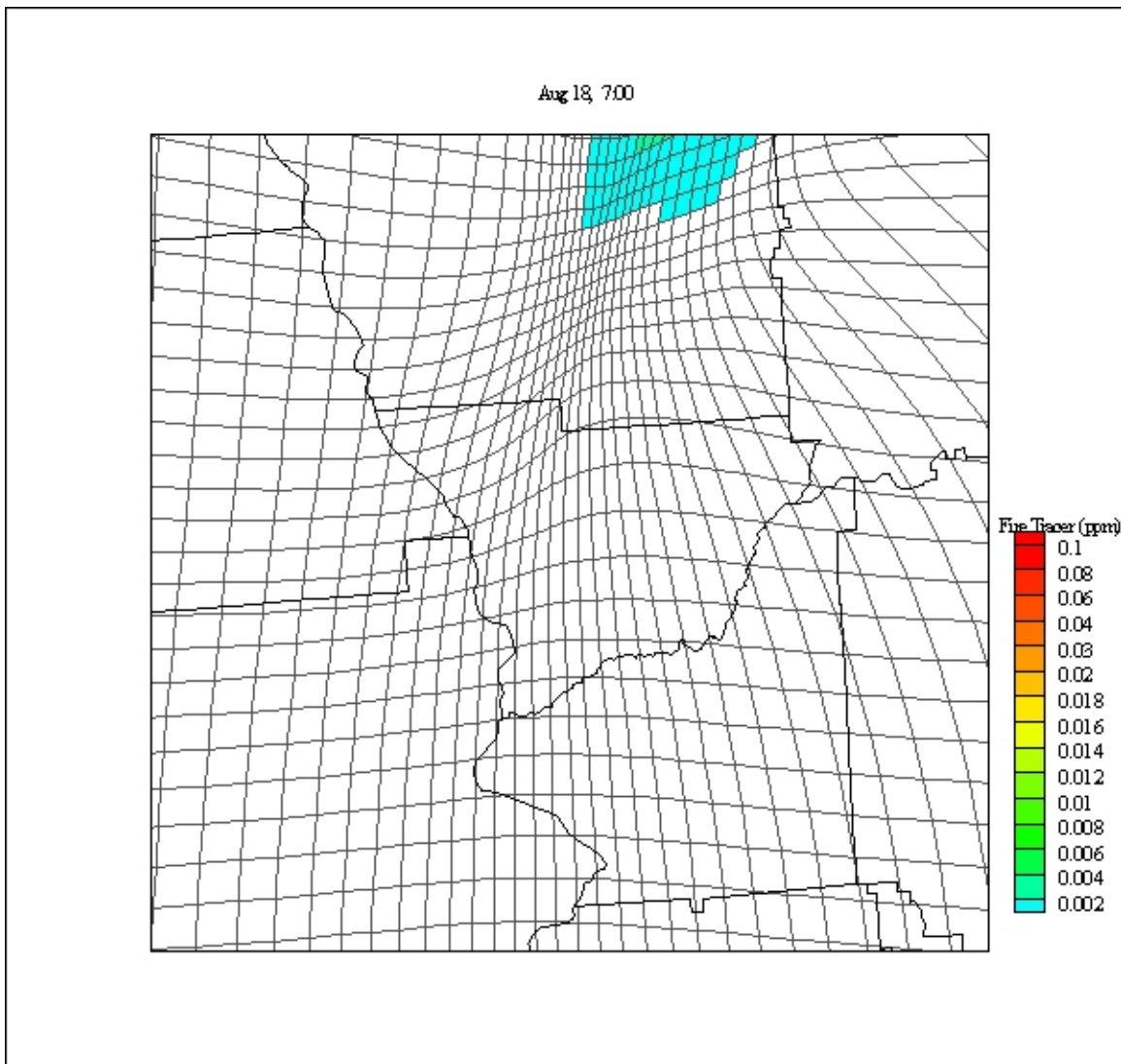
Figure 39 Adaptive Grid Result for Inert Fire Tracer Concentrations (ppm) for August 18, 7:00
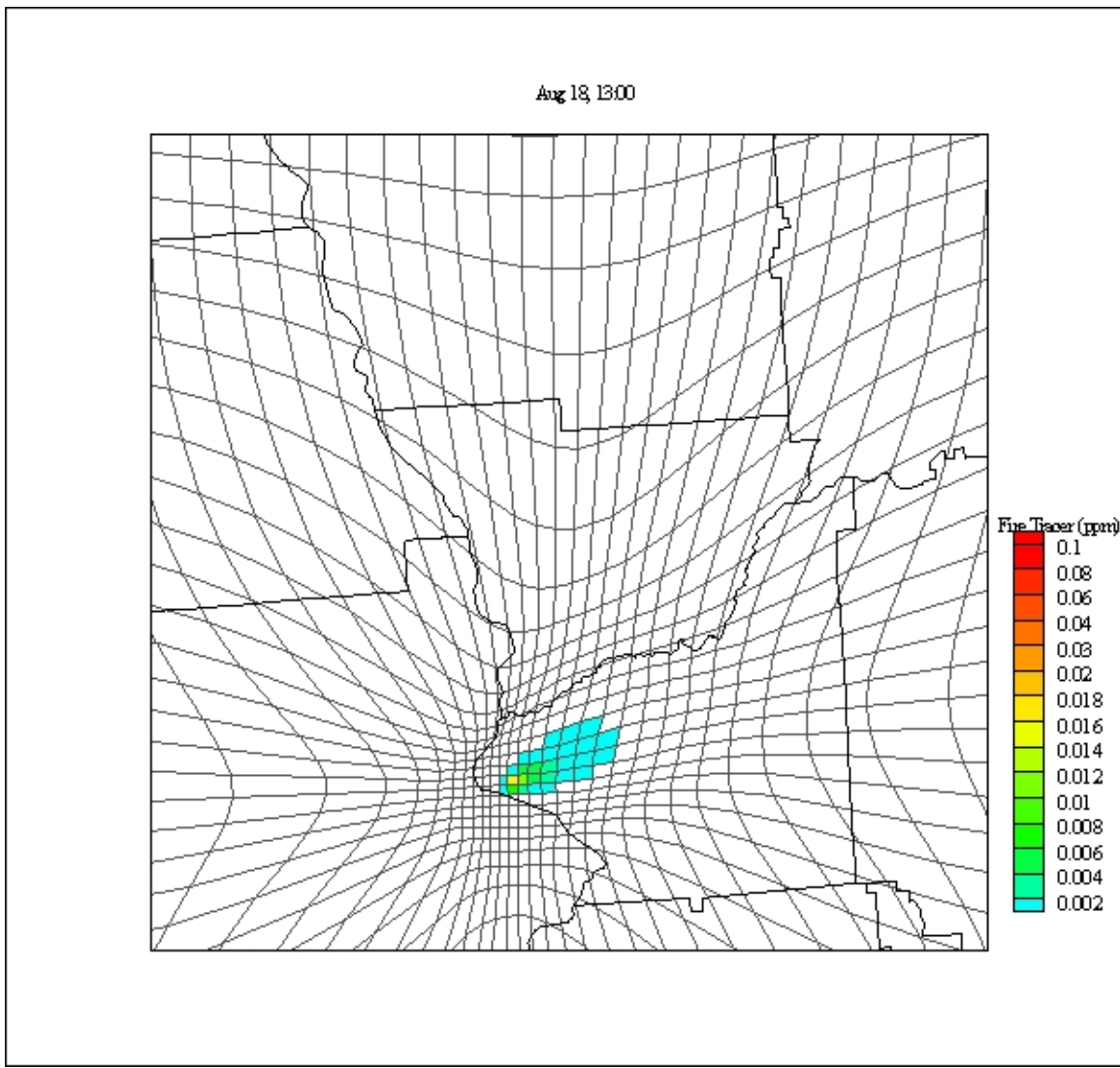
Figure 40 Adaptive Grid Result for Inert Fire Tracer Concentrations (ppm) for August 18, 13:00

Aug 18, 14:00
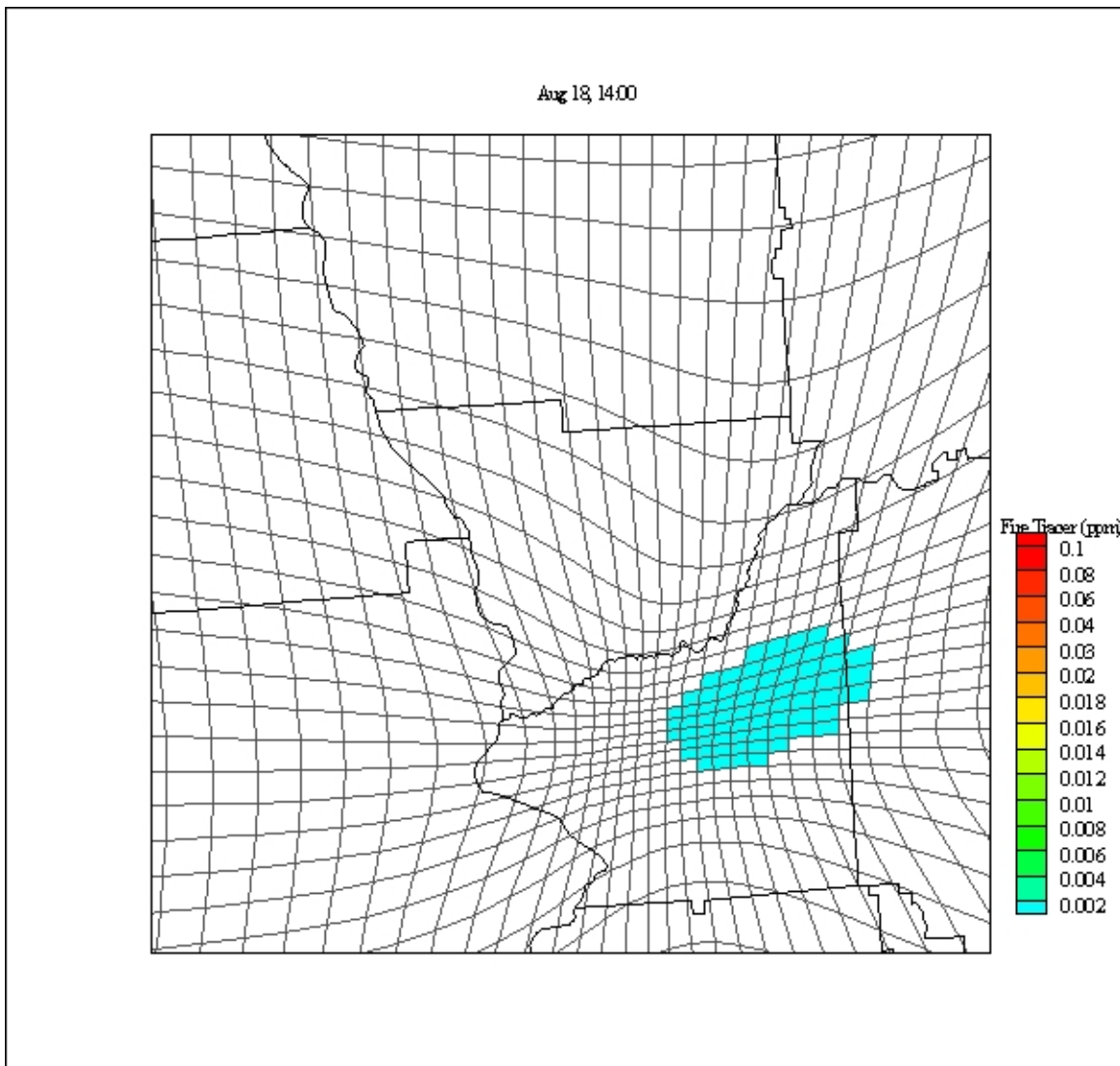
Figure 41 Adaptive Grid Result for Inert Fire Tracer Concentrations (ppm) for August 18, 14:00
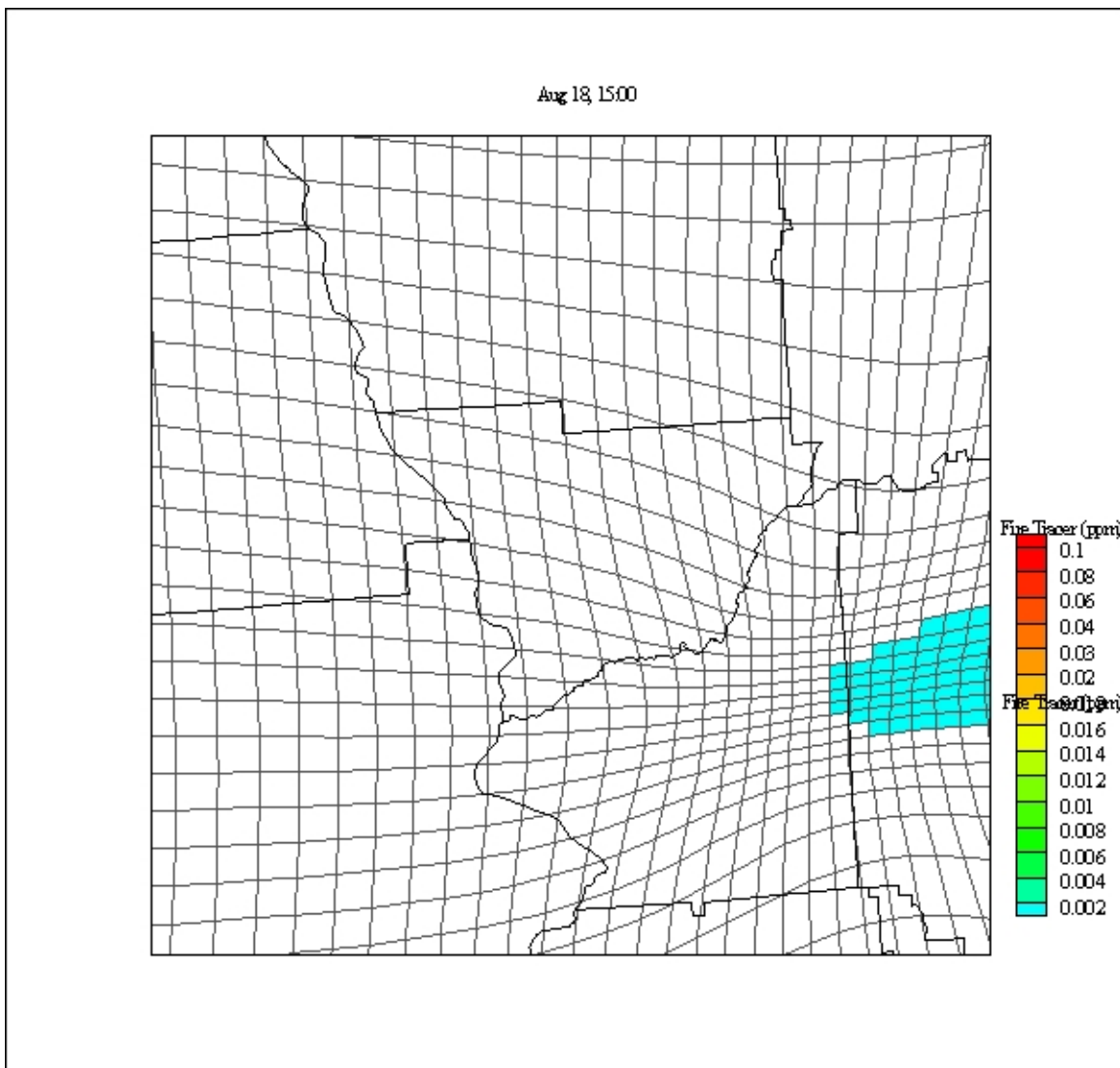
Figure 42 Adaptive Grid Result for Inert Fire Tracer Concentrations (ppm) for August 18, 15:00
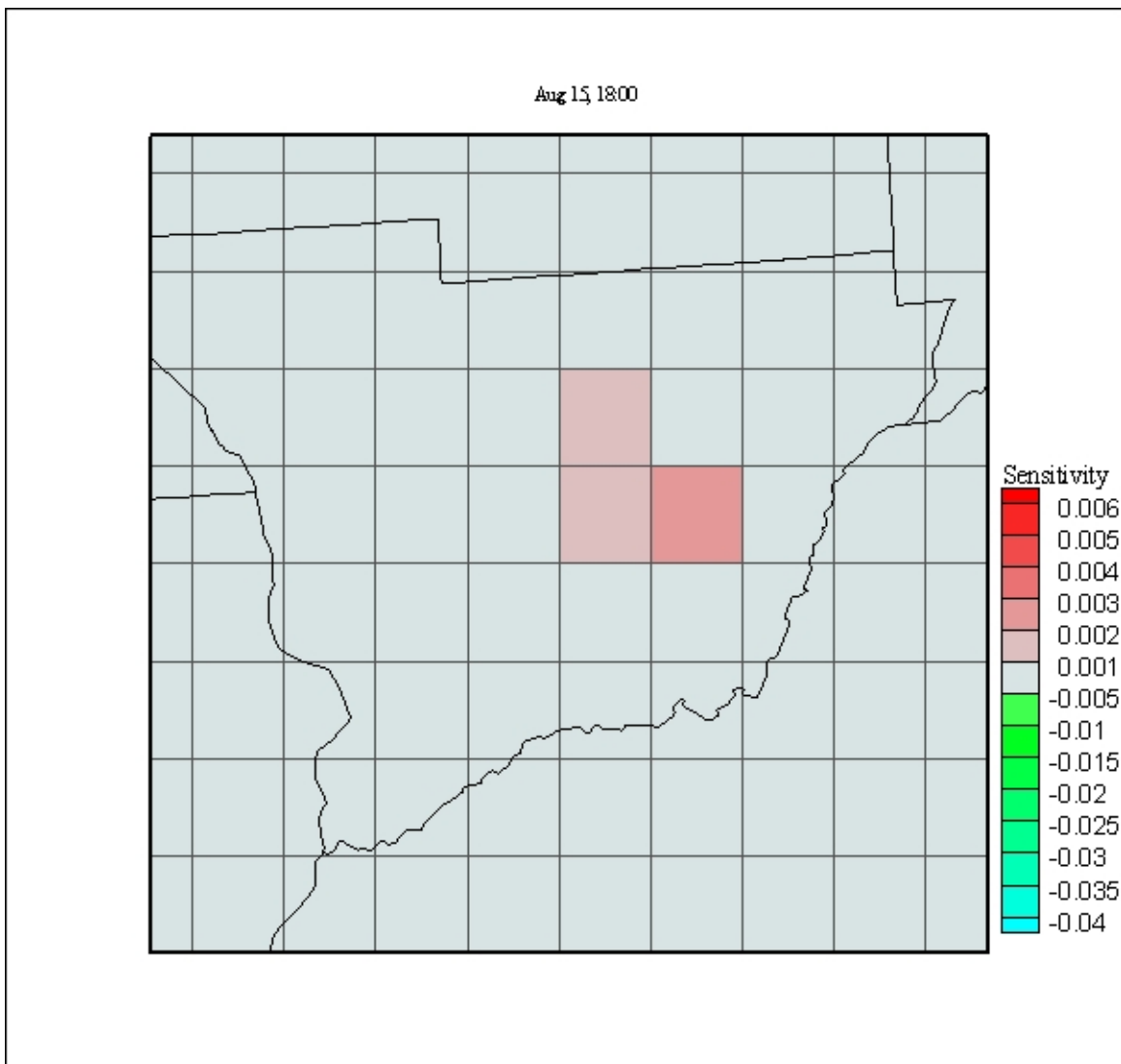
Figure 43 Static Grid Result for Brute-Force Sensitivity of O_3 (ppm) to Fire Emissions, August 15, 18:00
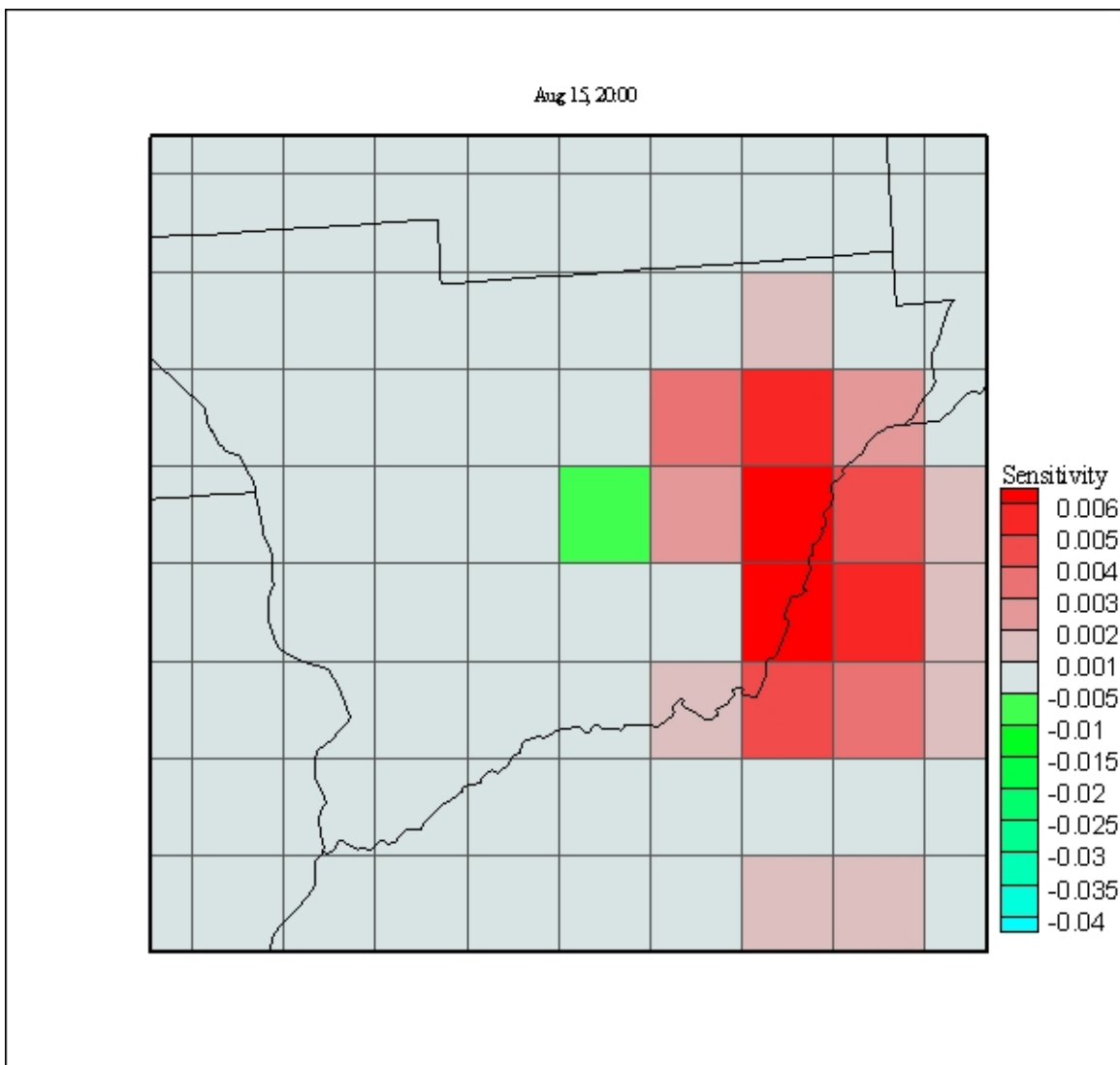
Figure 44 Static Grid Result for Brute-Force Sensitivity of O$_3$ (ppm) to Fire Emissions, August 15, 20:00
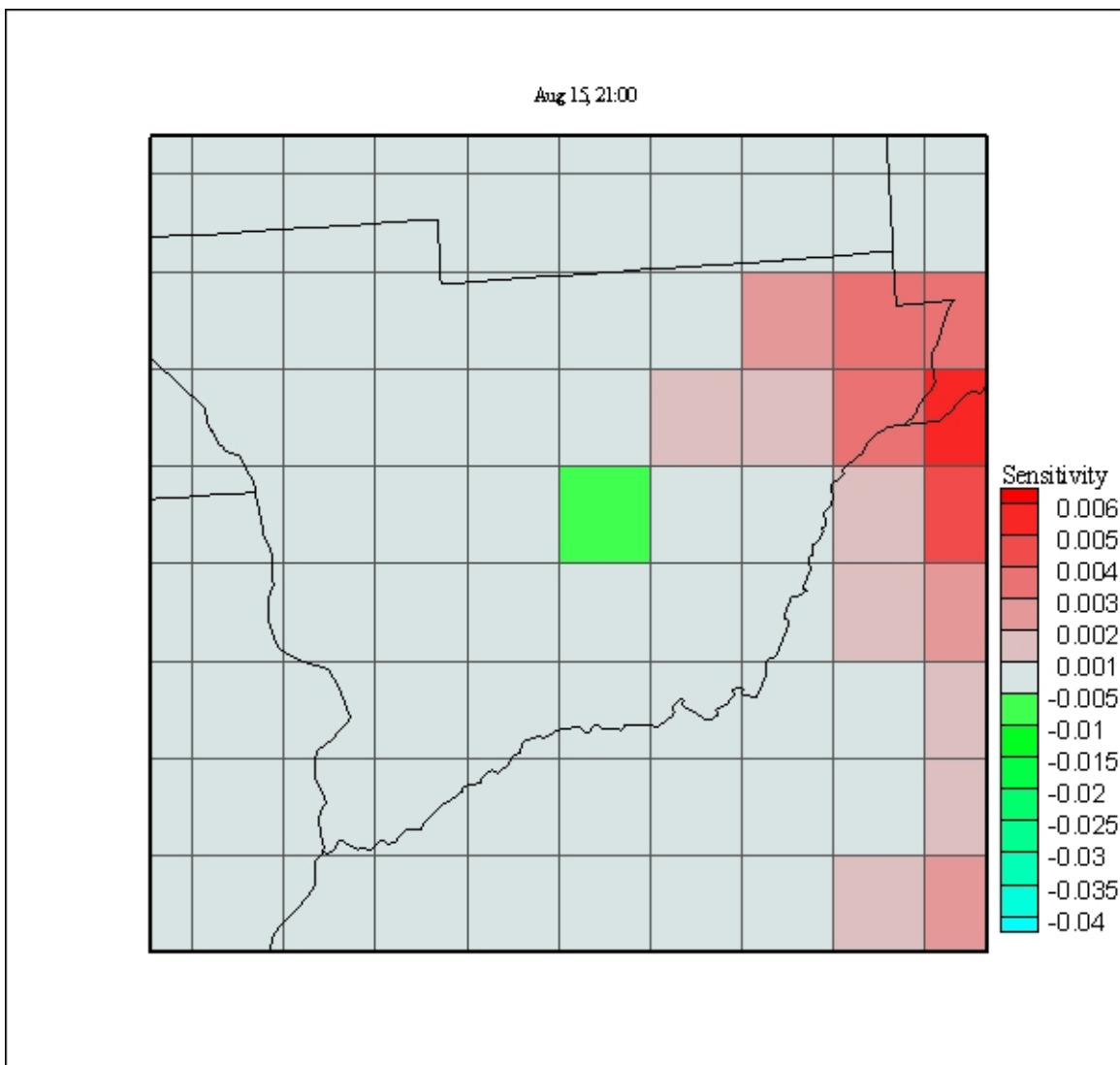
Figure 45 Static Grid Result for Brute-Force Sensitivity of O$_3$ (ppm) to Fire Emissions, August 15, 21:00
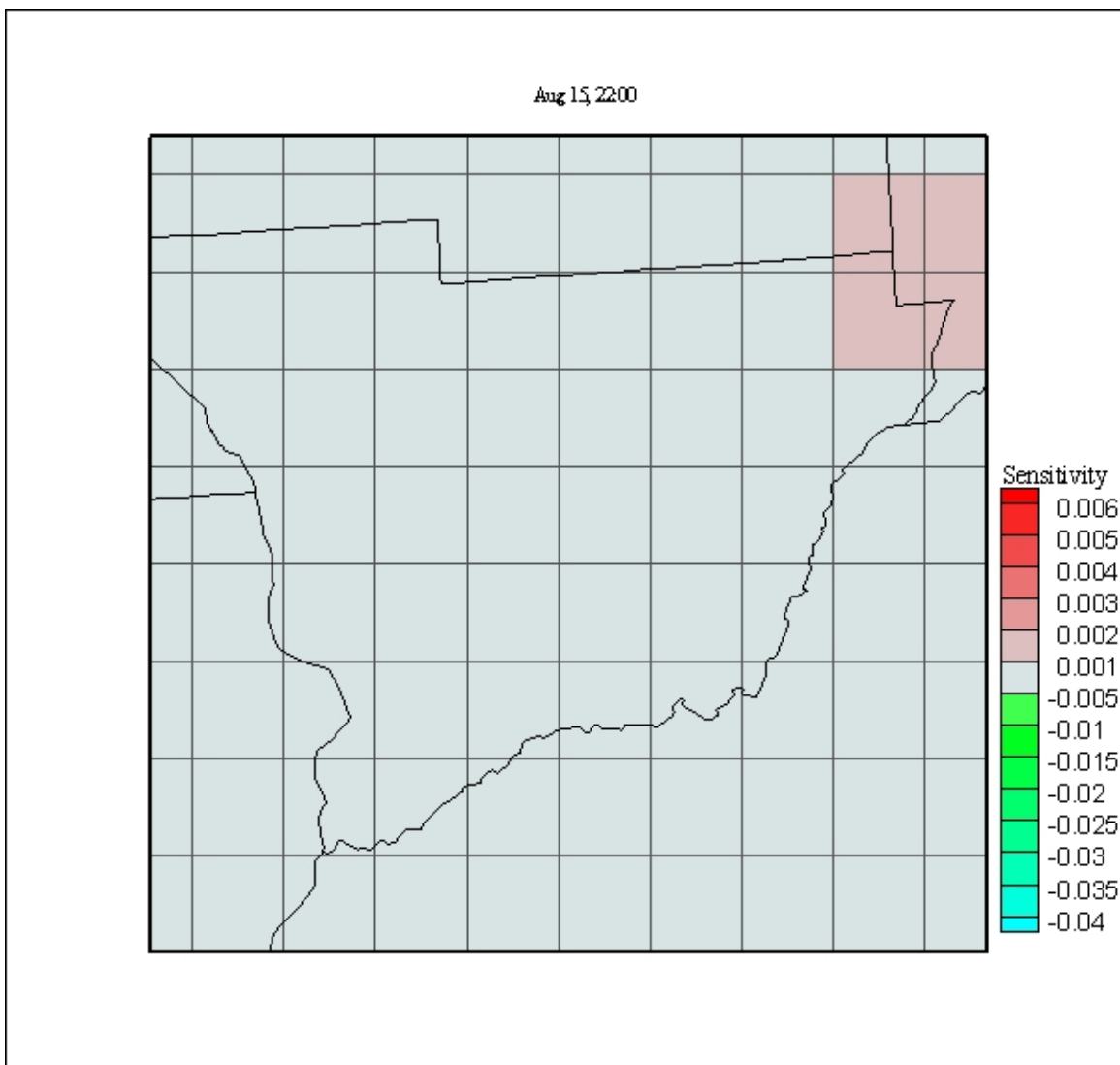
Figure 46 Static Grid Result for Brute-Force Sensitivity of O_3 (ppm) to Fire Emissions, August 15, 22:00
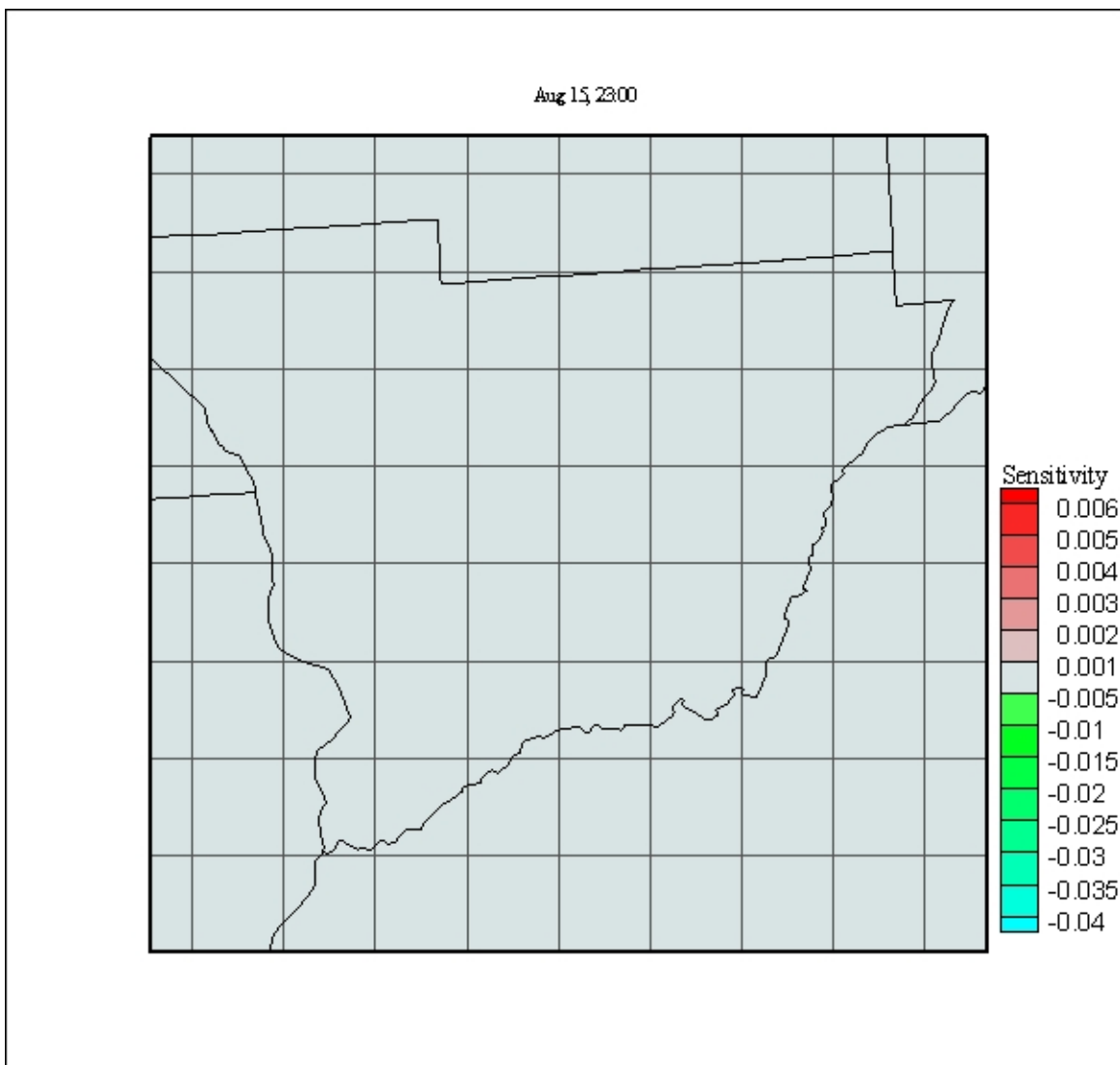
Figure 47 Static Grid Result for Brute-Force Sensitivity of O_3 (ppm) to Fire Emissions, August 15, 23:00
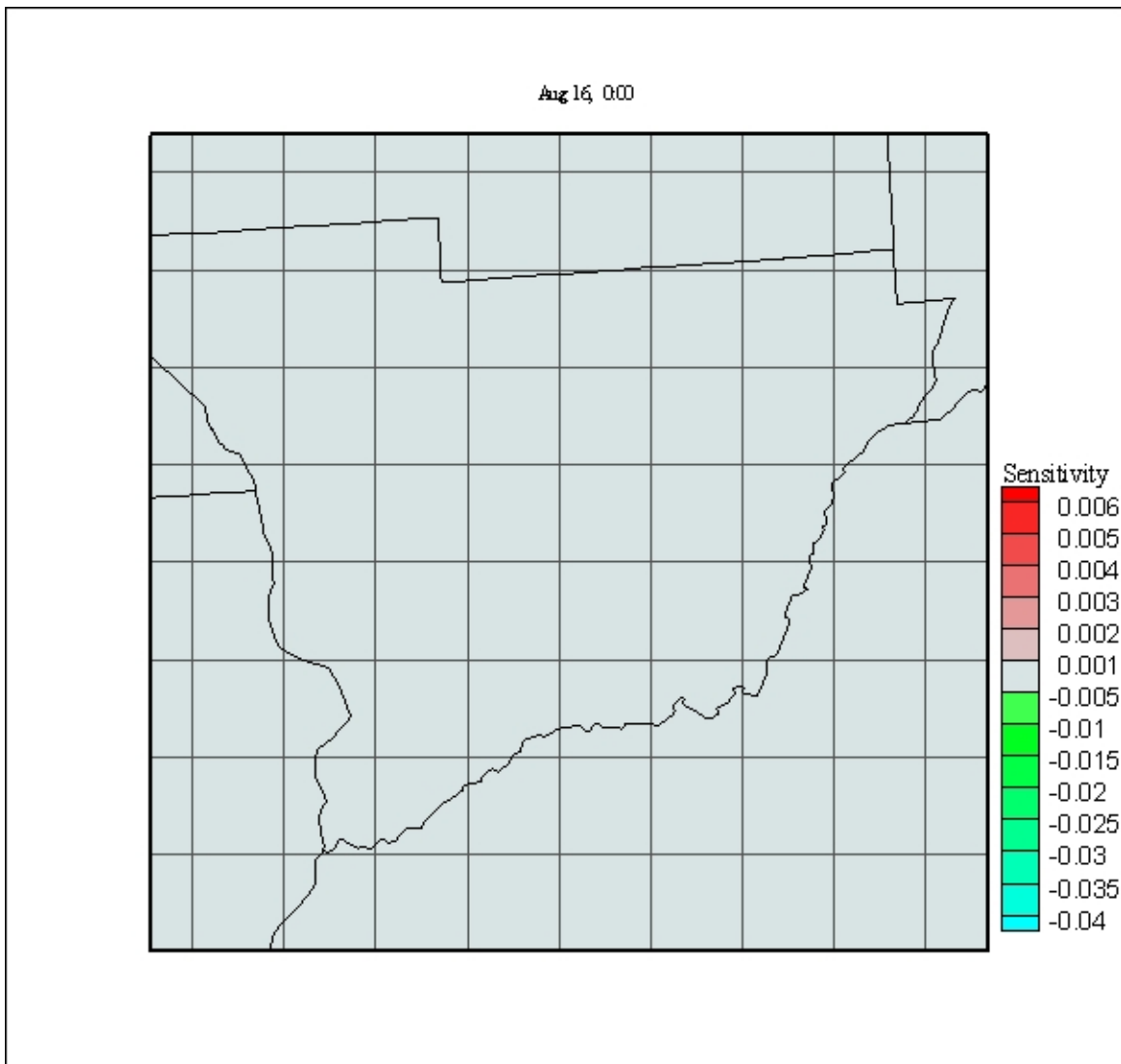
Figure 48 Static Grid Result for Brute-Force Sensitivity of O$_3$ (ppm) to Fire Emissions, August 16, 0:0
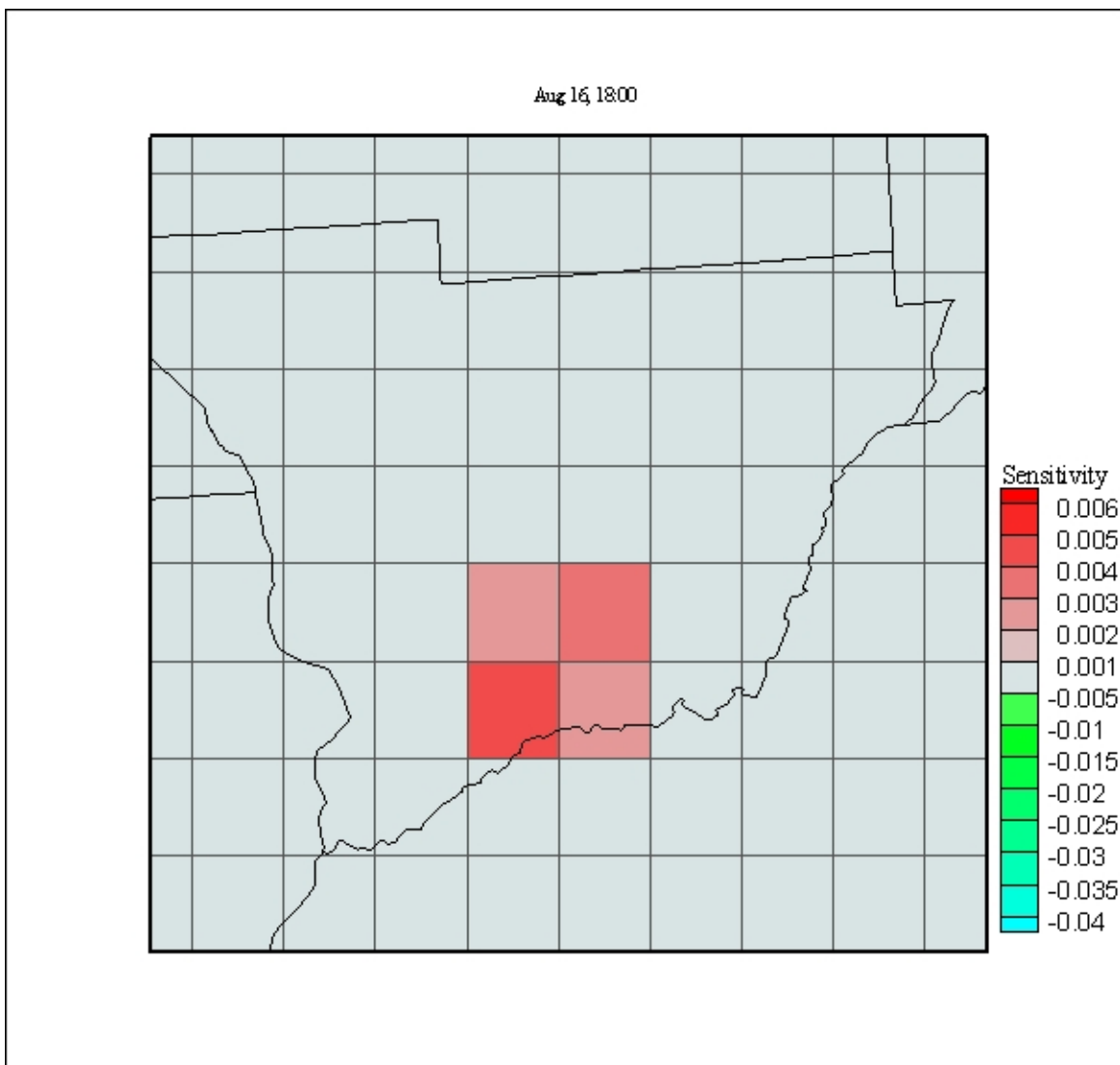
Figure 49 Static Grid Result for Brute-Force Sensitivity of O_3 (ppm) to Fire Emissions, August 16, 18:00
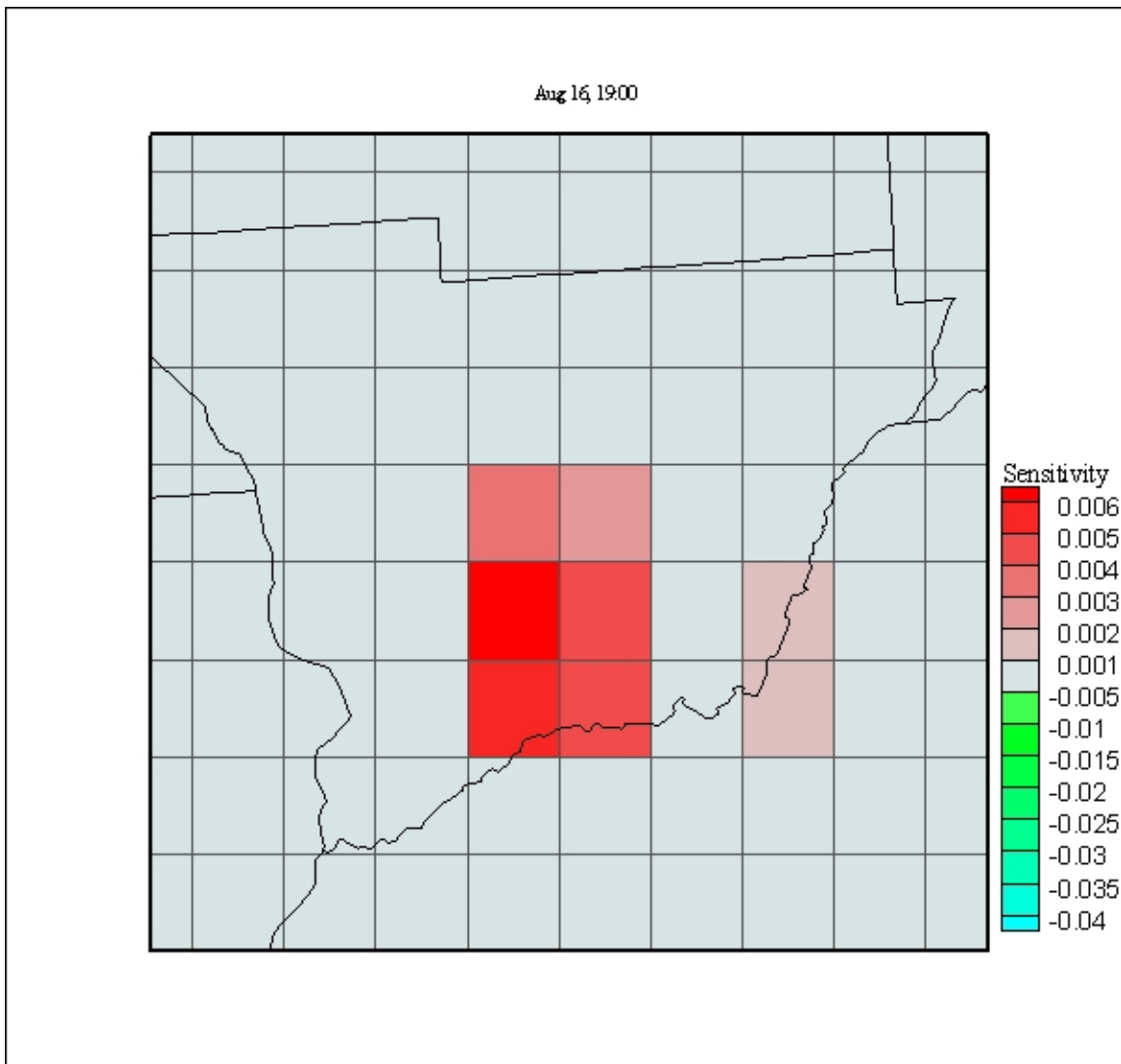
Figure 50 Static Grid Result for Brute-Force Sensitivity of O$_3$ (ppm) to Fire Emissions, August 16, 19:00
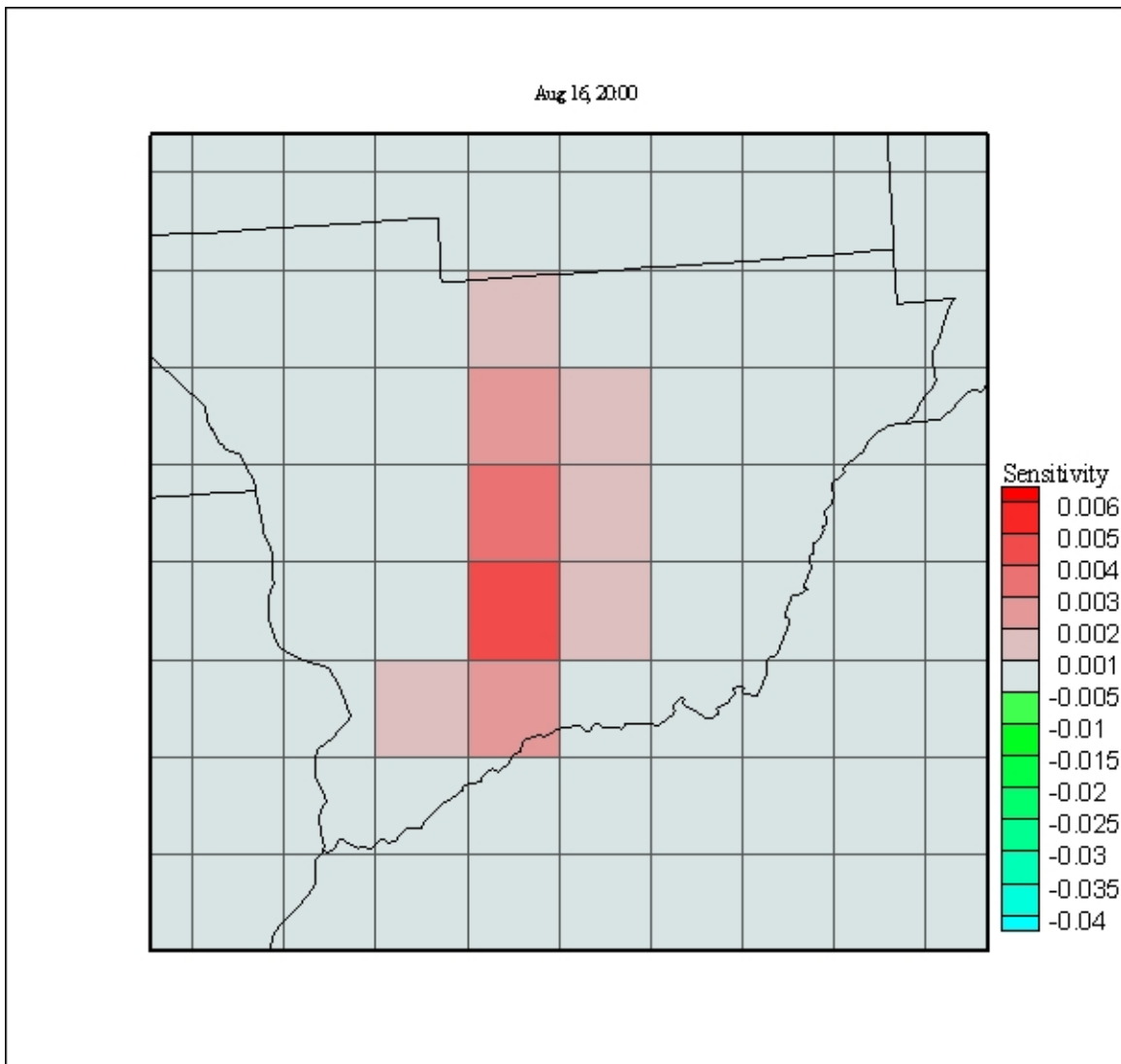
Figure 51 Static Grid Result for Brute-Force Sensitivity of O_3 (ppm) to Fire Emissions, August 16, 20:00
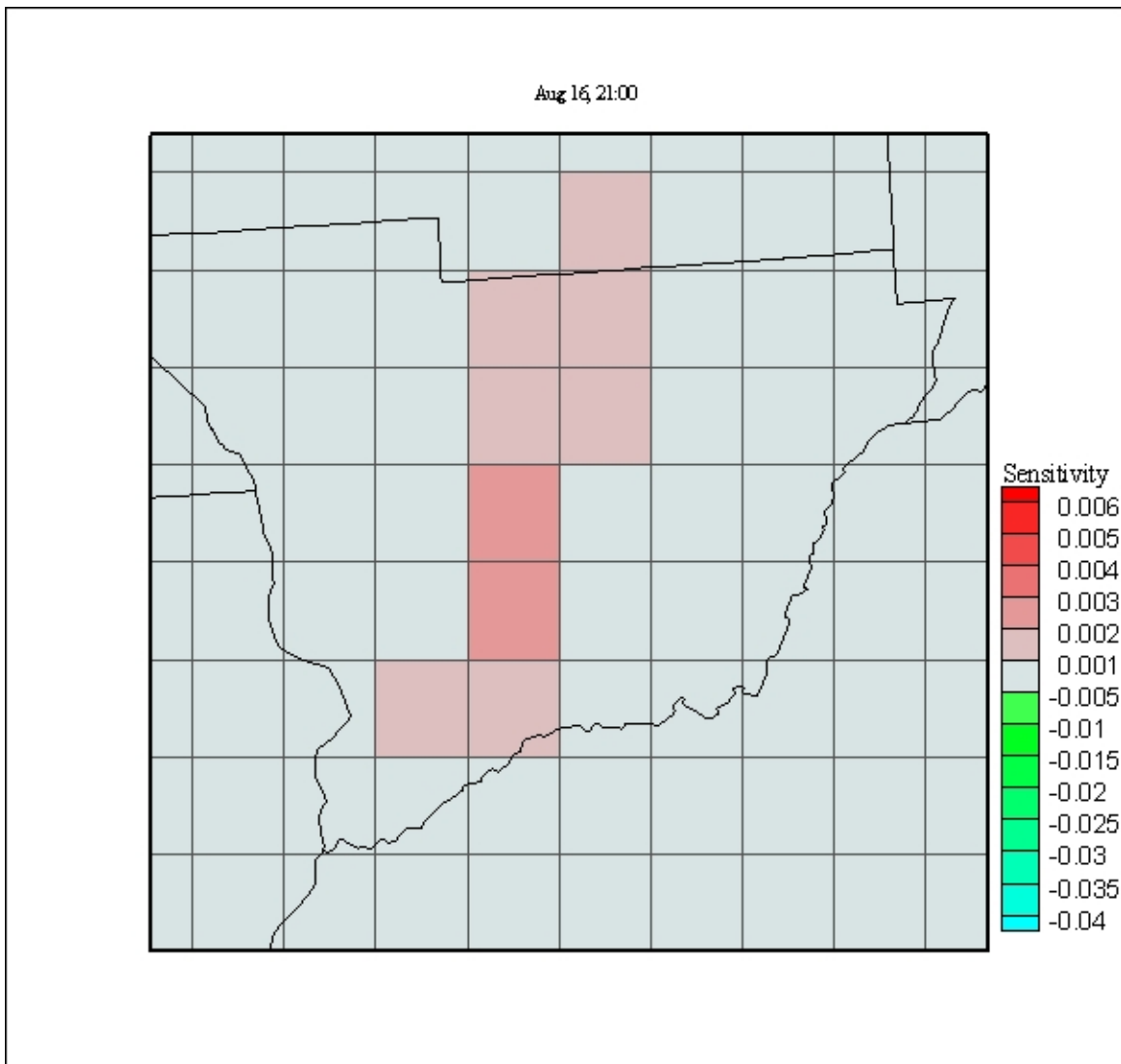
Figure 52 Static Grid Result for Brute-Force Sensitivity of O$_3$ (ppm) to Fire Emissions, August 16, 21:00
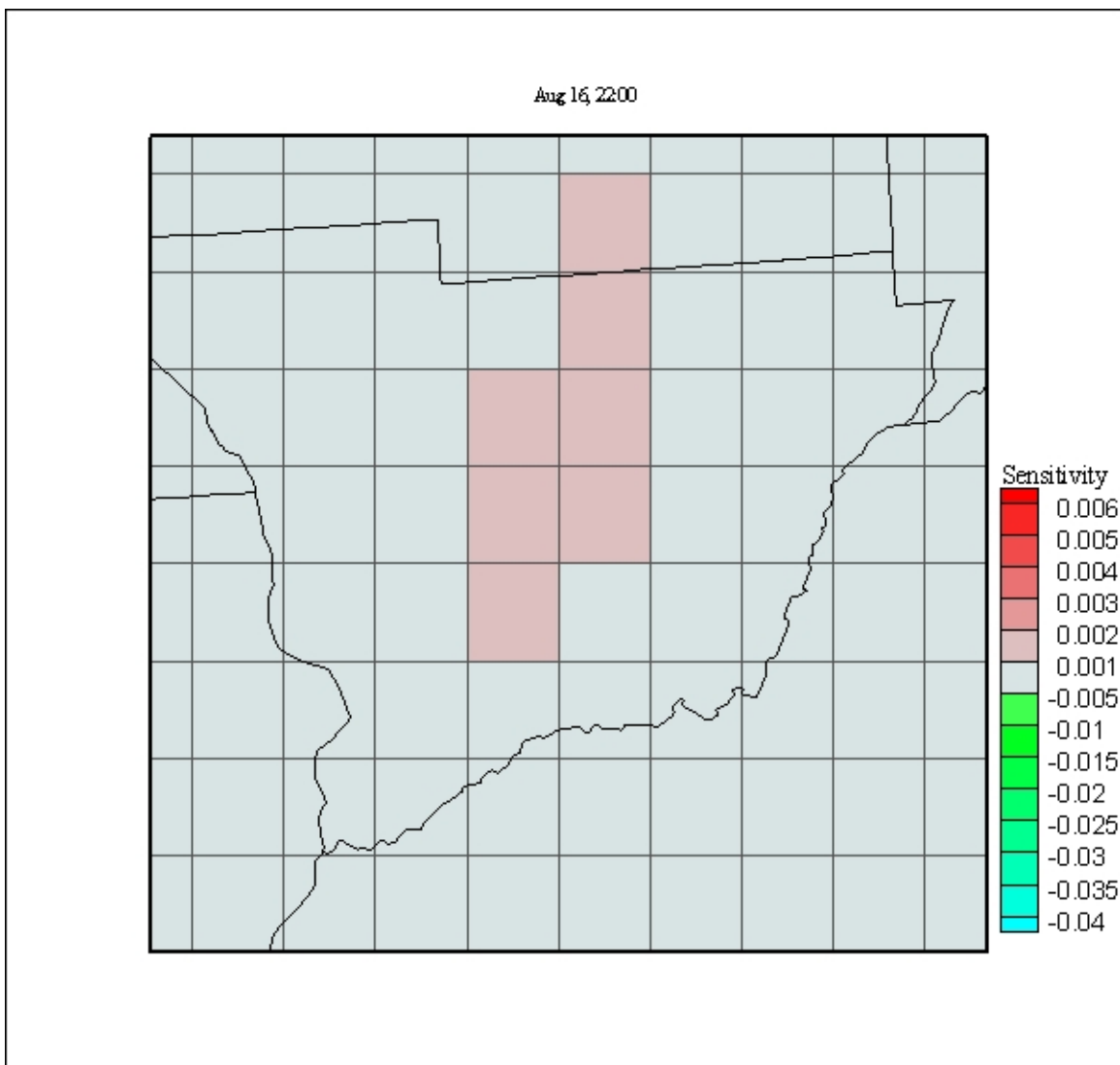
Figure 53 Static Grid Result for Brute-Force Sensitivity of O_3 (ppm) to Fire Emissions, August 16, 22:00
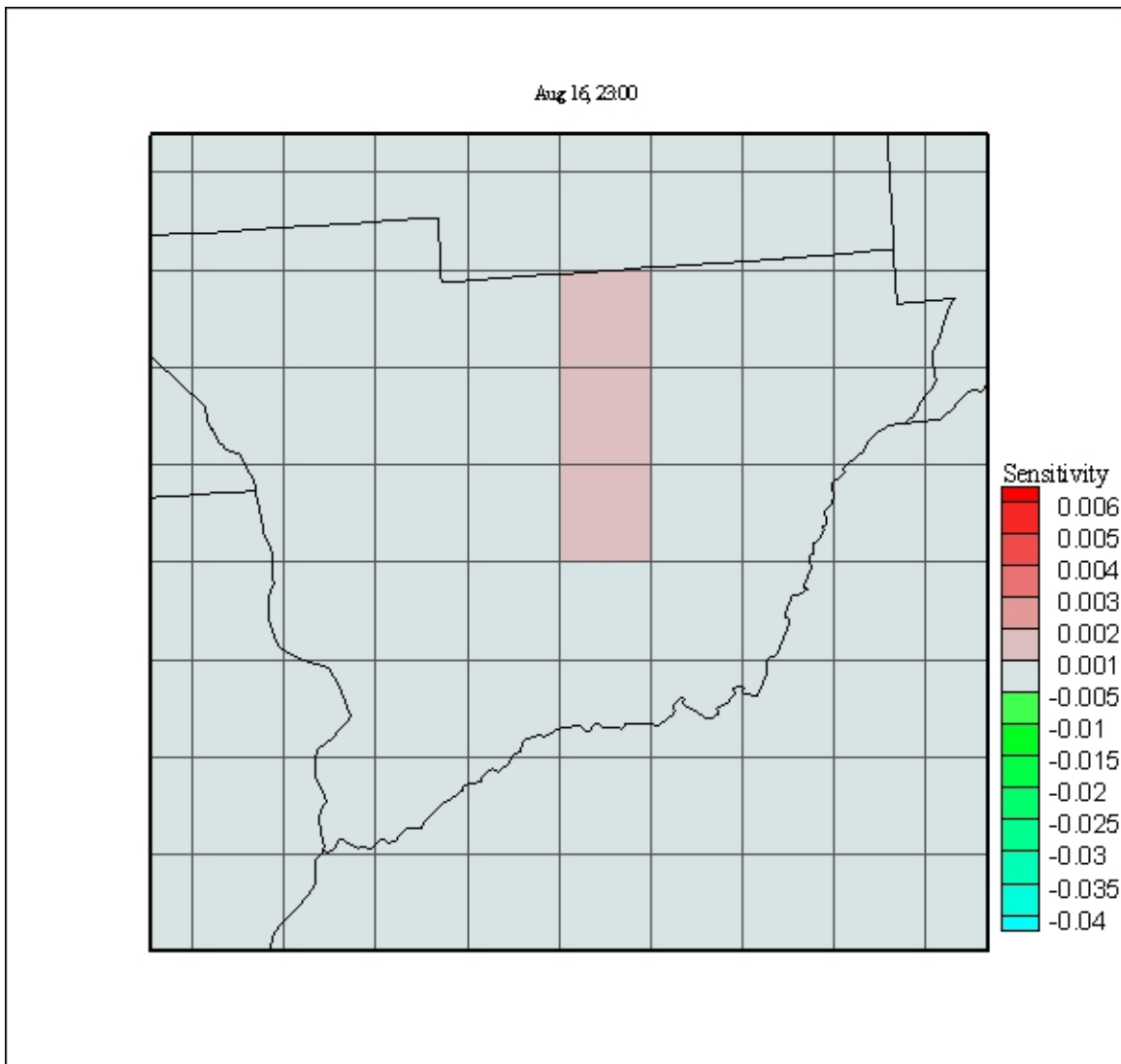
Figure 54 Static Grid Result for Brute-Force Sensitivity of O$_3$ (ppm) to Fire Emissions, August 16, 23:00
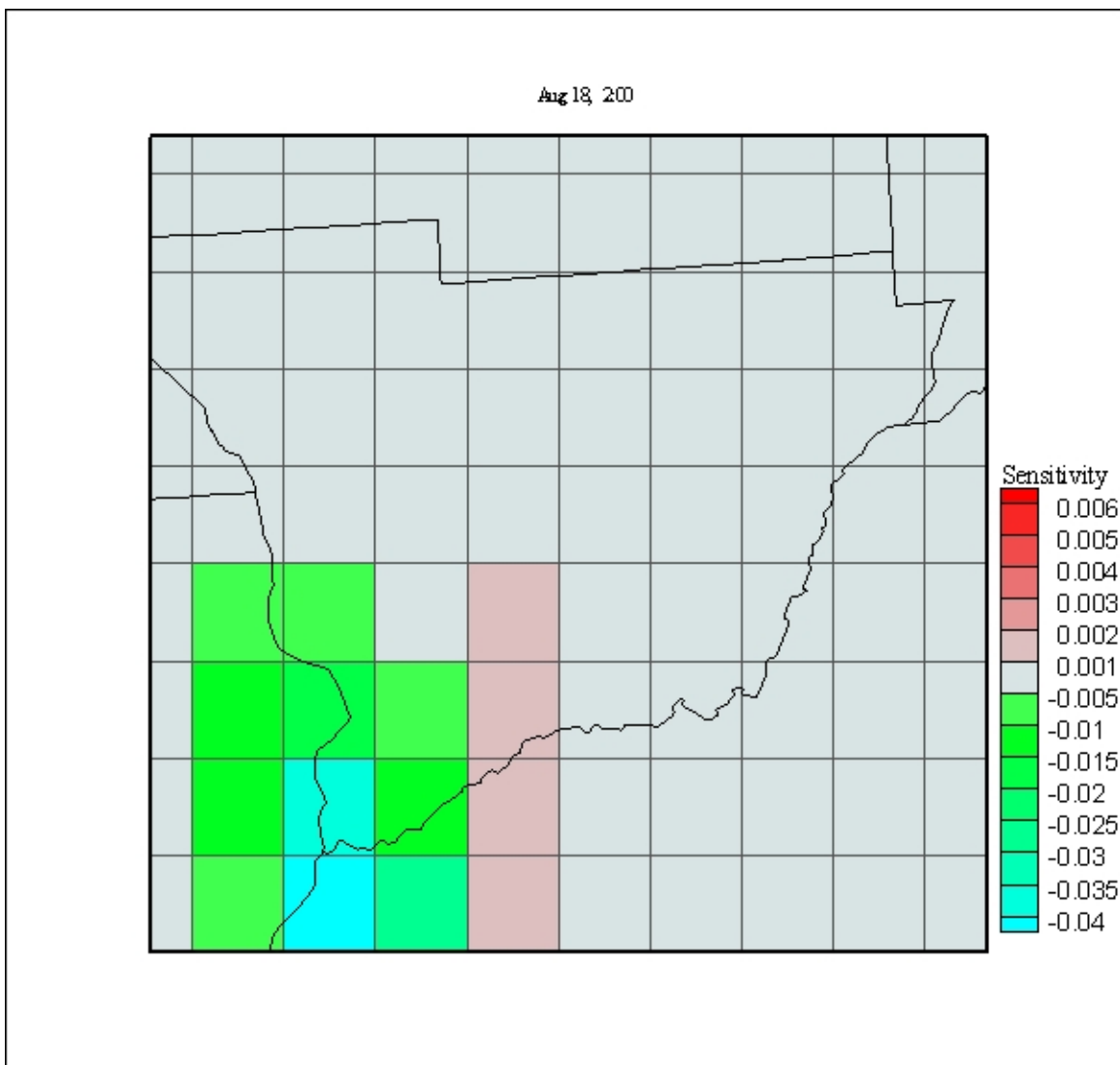
Figure 55 Static Grid Result for Brute-Force Sensitivity of O_3 (ppm) to Fire Emissions, August 18, 2:00
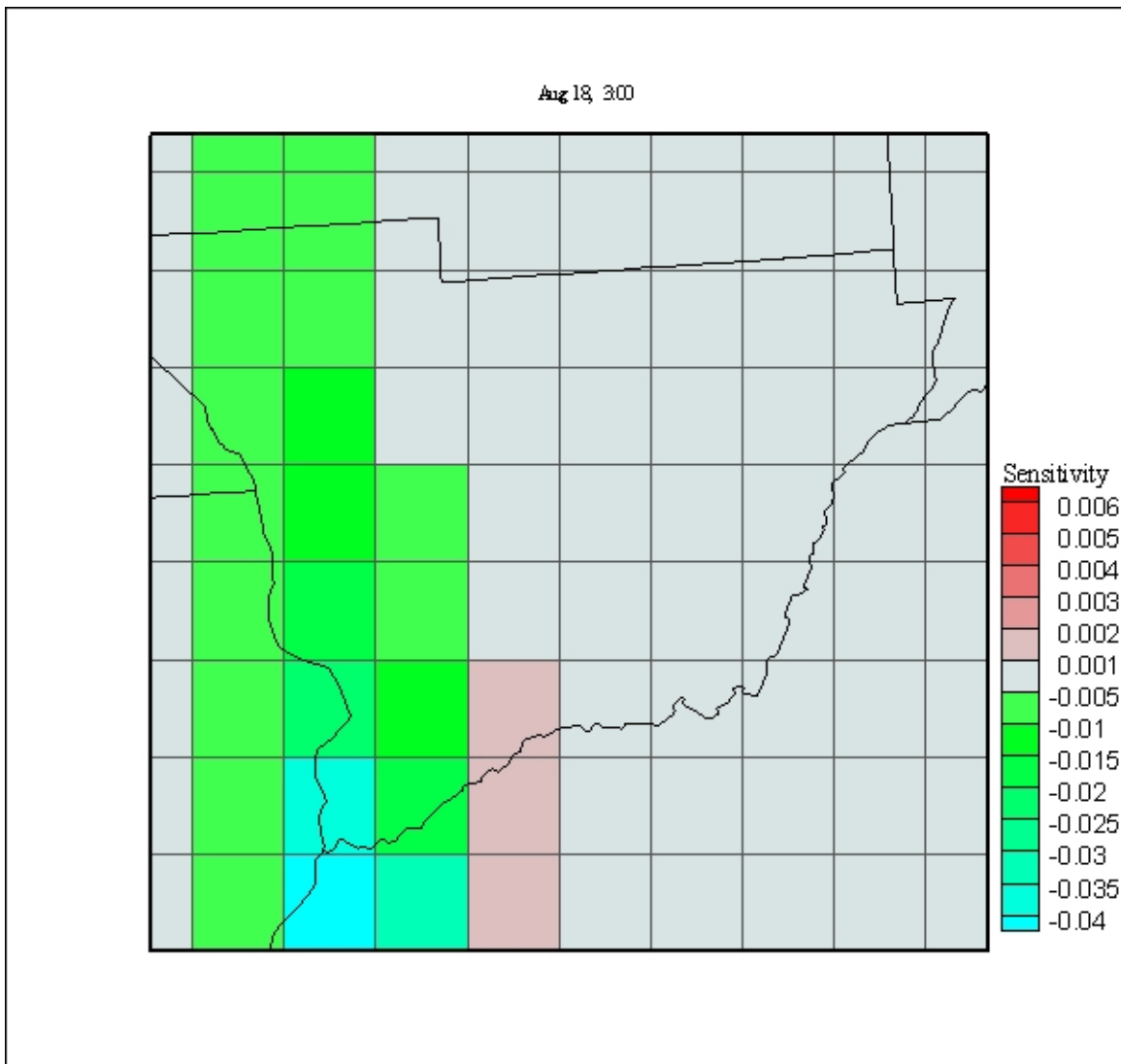
Figure 56 Static Grid Result for Brute-Force Sensitivity of O$_3$ (ppm) to Fire Emissions, August 18, 3:00
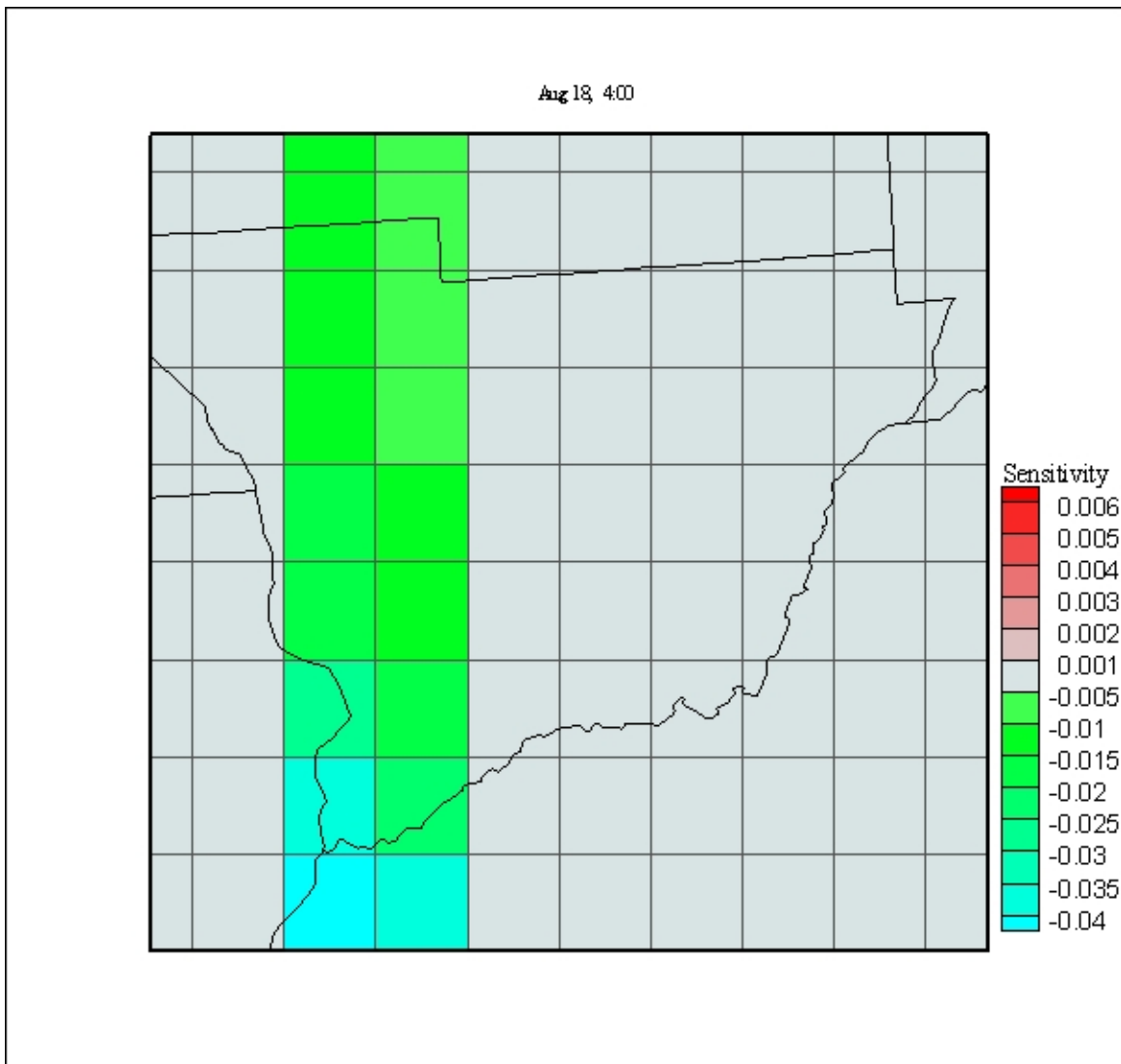
Figure 57 Static Grid Result for Brute-Force Sensitivity of O$_3$ (ppm) to Fire Emissions, August 18, 4:00
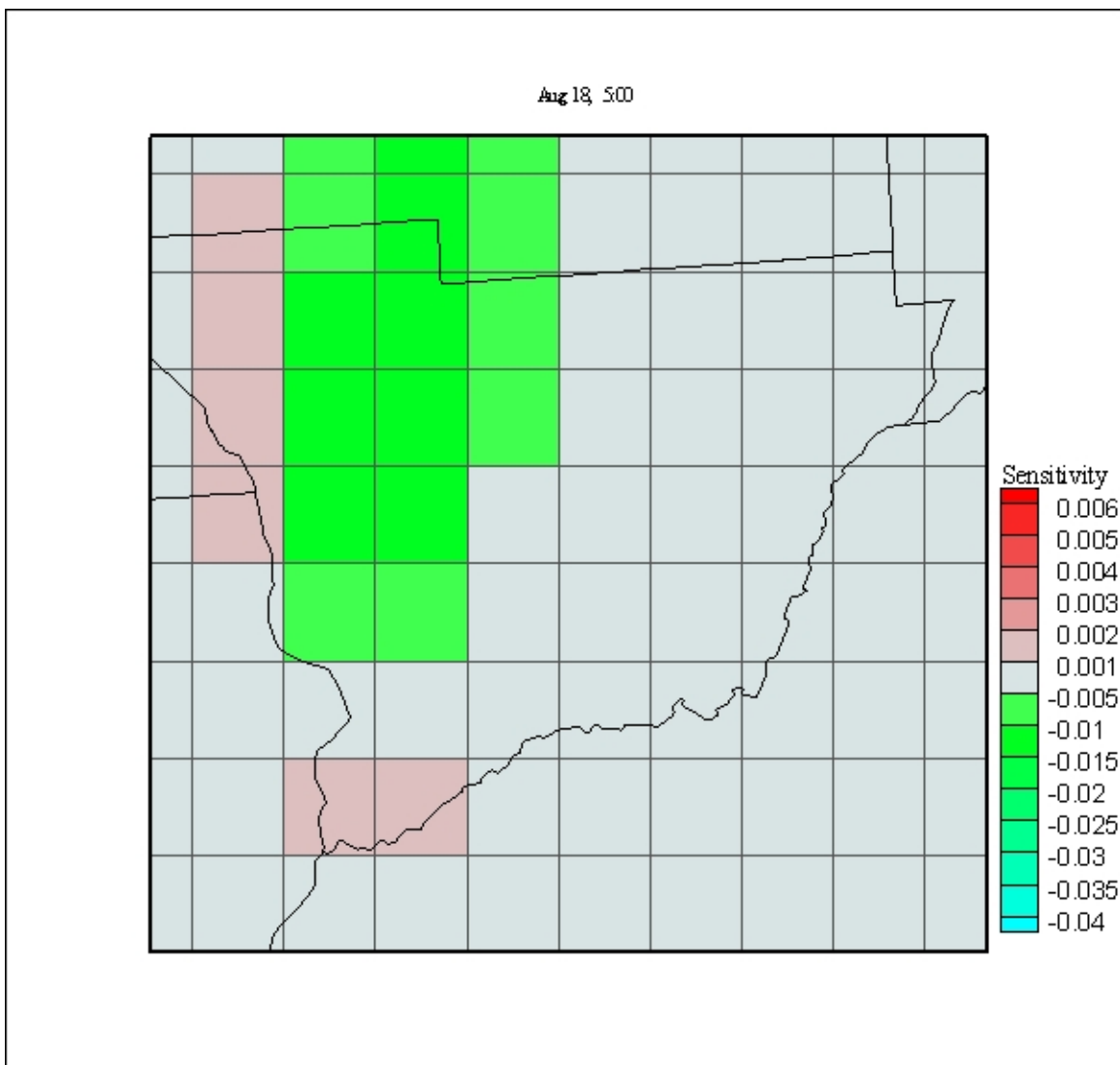
Figure 58 Static Grid Result for Brute-Force Sensitivity of O$_3$ (ppm) to Fire Emissions, August 18, 5:00
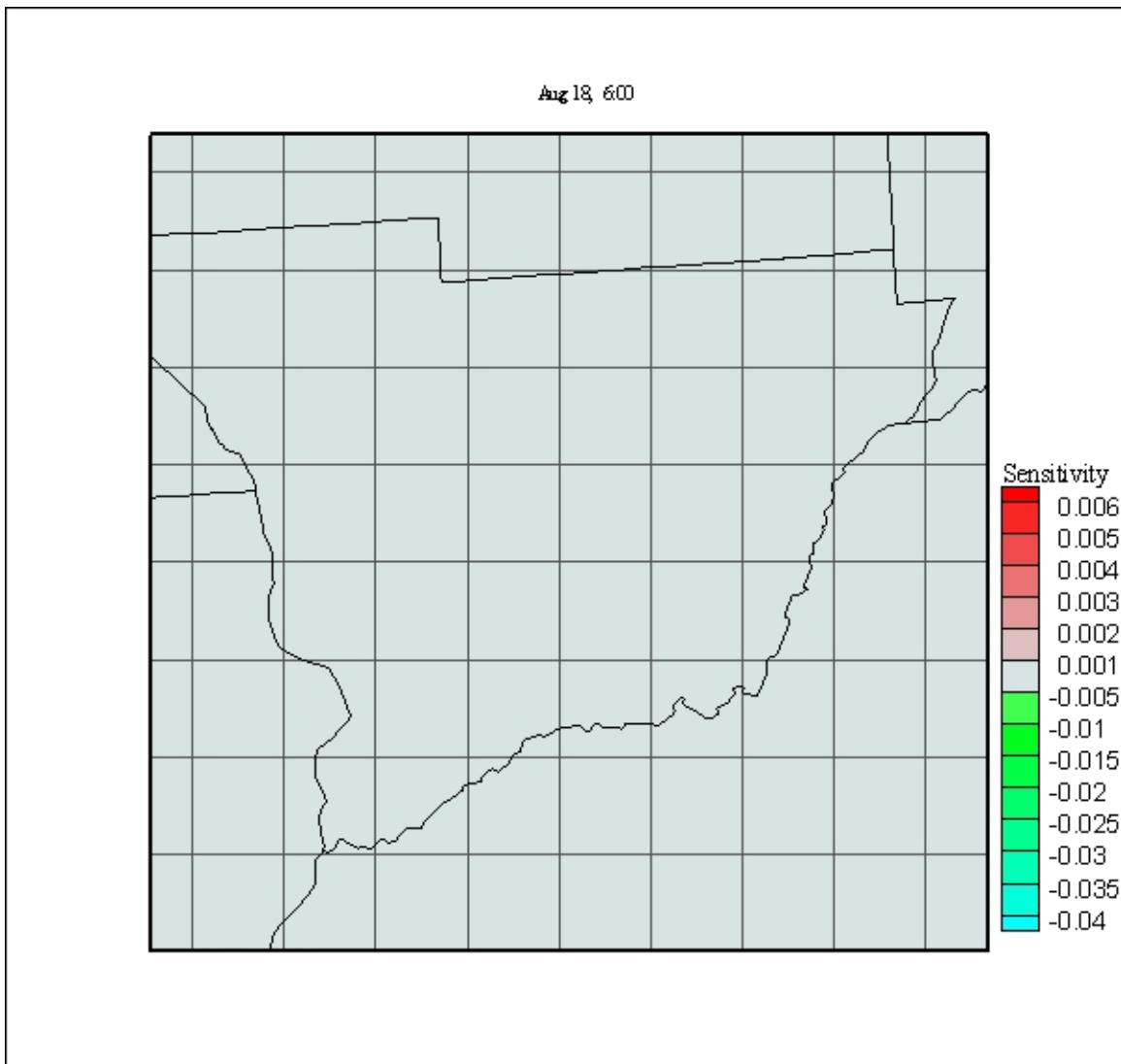
Figure 59 Static Grid Result for Brute-Force Sensitivity of O_3 (ppm) to Fire Emissions, August 18, 6:00
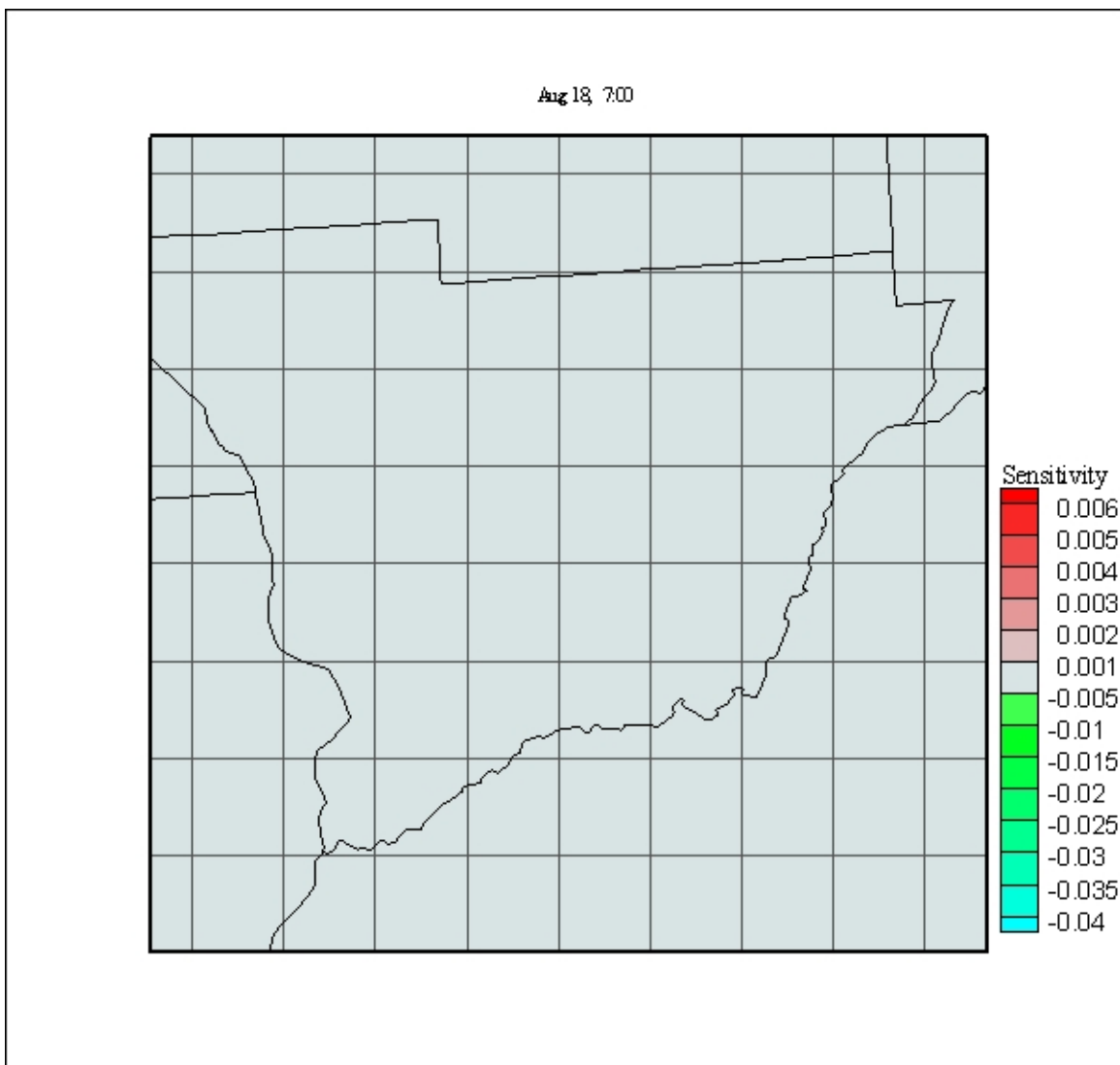
Figure 60 Static Grid Result for Brute-Force Sensitivity of O$_3$ (ppm) to Fire Emissions, August 18, 7:00
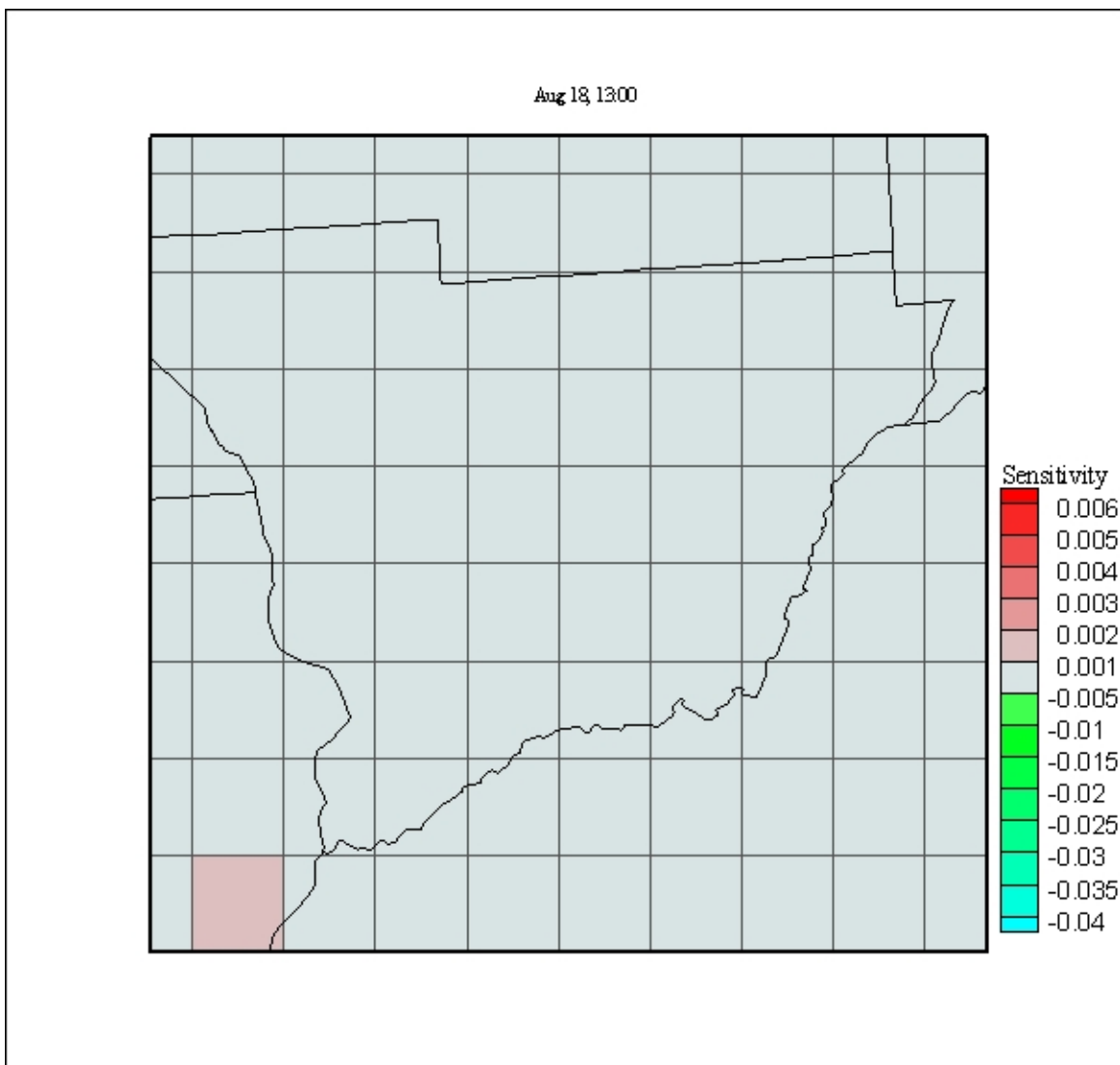
Figure 61 Static Grid Result for Brute-Force Sensitivity of O_3 (ppm) to Fire Emissions, August 18, 13:00
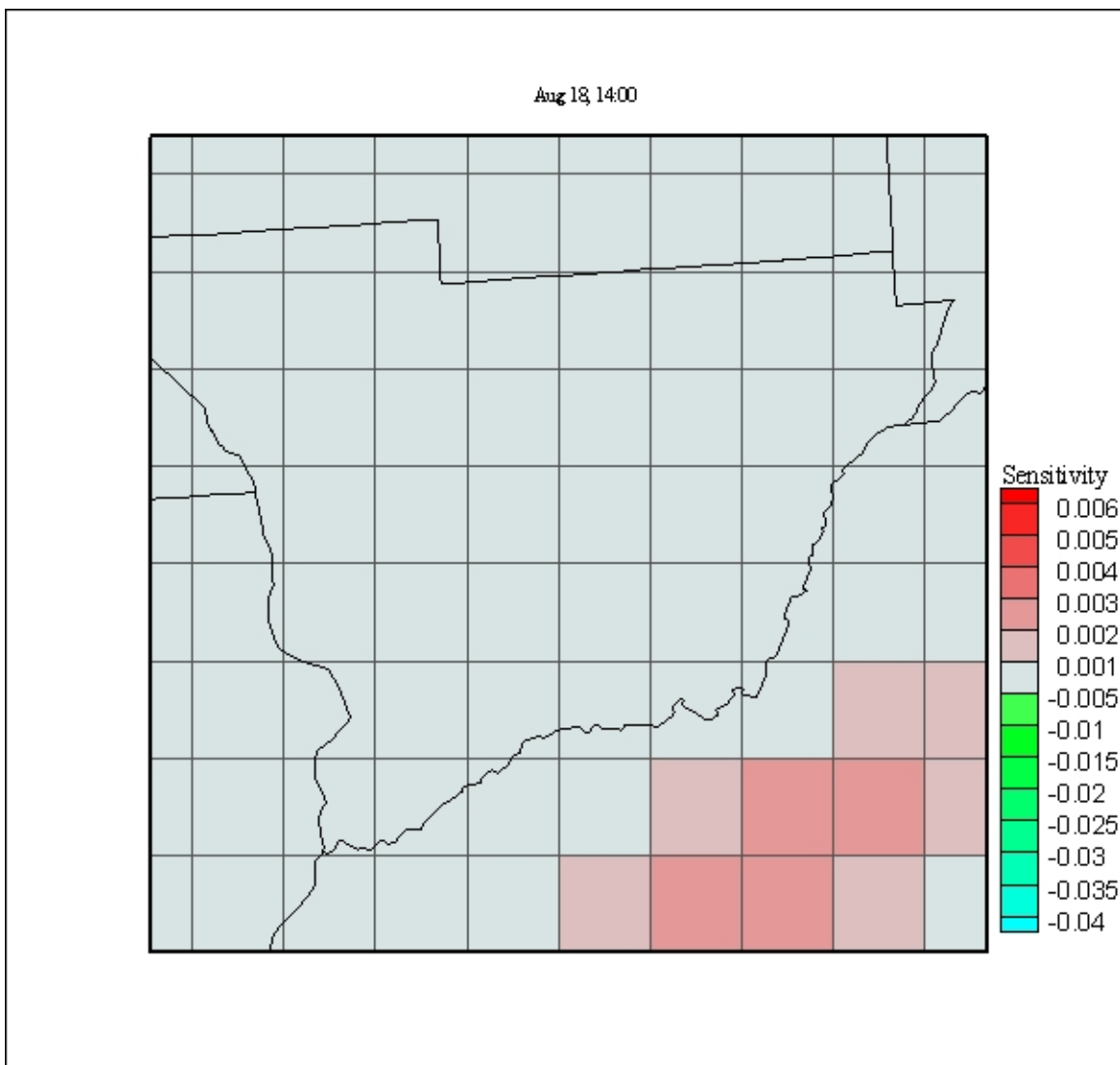
Figure 62 Static Grid Result for Brute-Force Sensitivity of O_3 (ppm) to Fire Emissions, August 18, 14:00
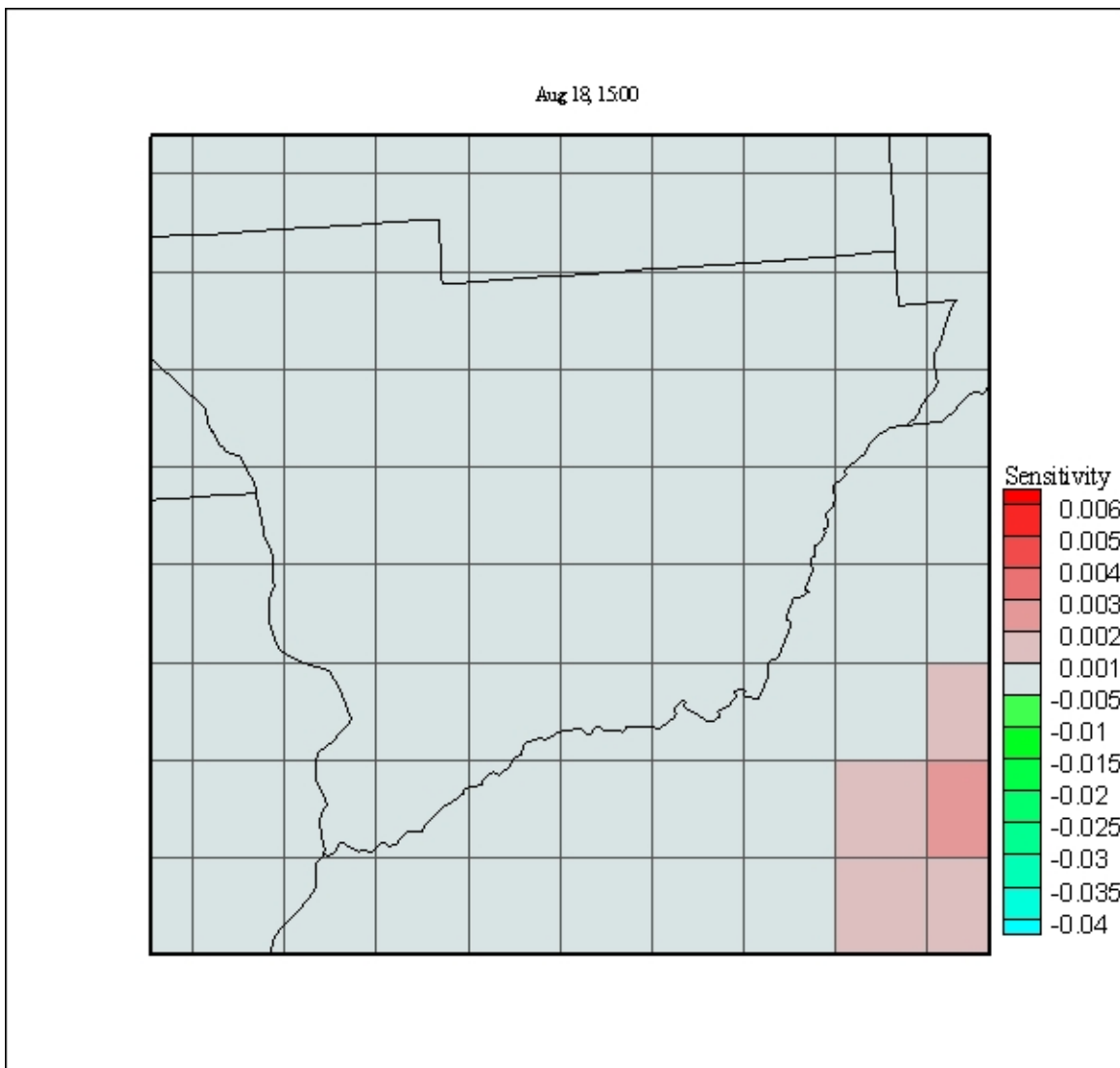
Figure 63 Static Grid Result for Brute-Force Sensitivity of O$_3$ (ppm) to Fire Emissions, August 18, 15:00
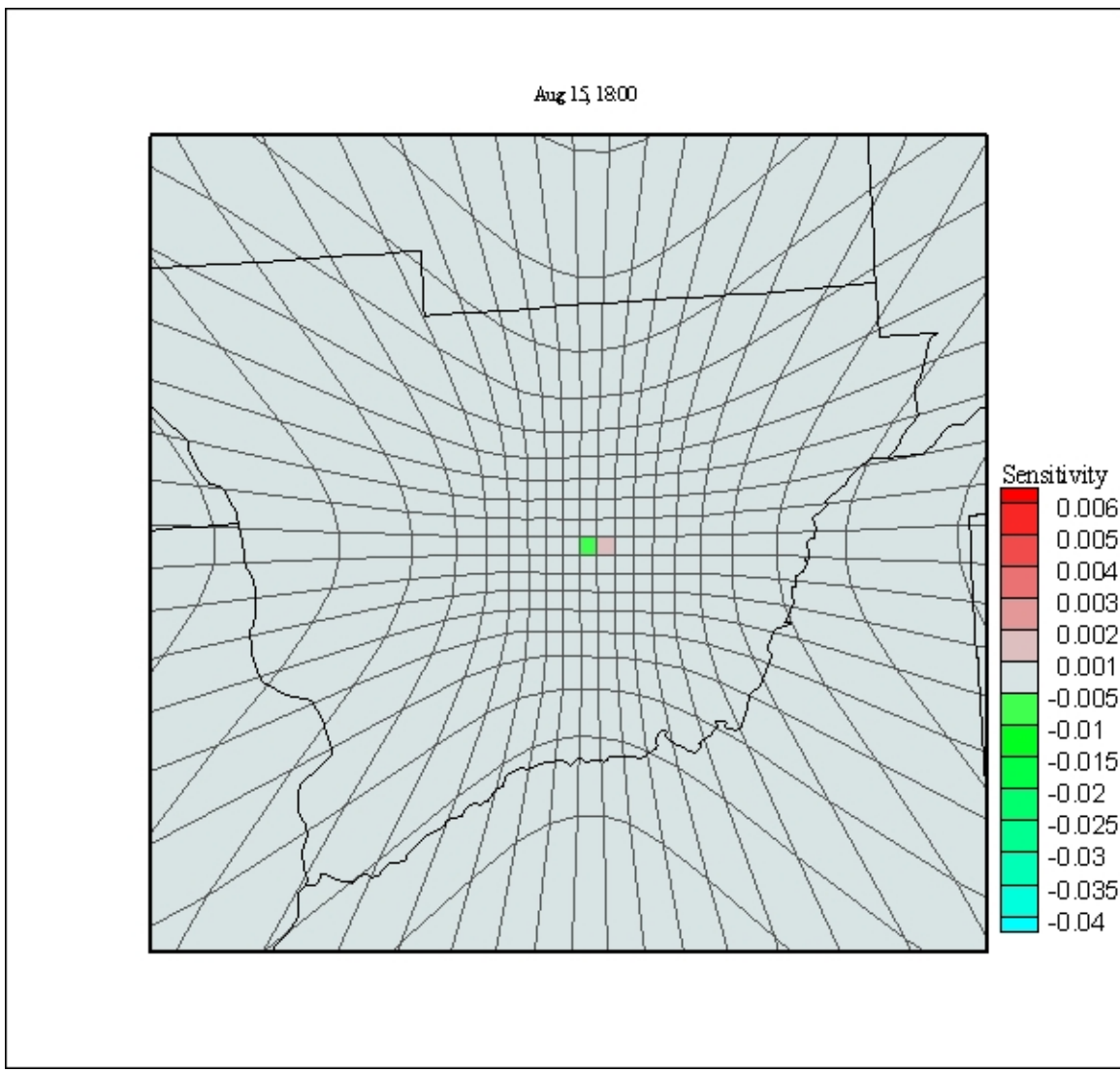
Figure 64 Adaptive Grid Result for Direct Sensitivity of O_3 (ppm) to Fire Emissions, August 15, 18:00
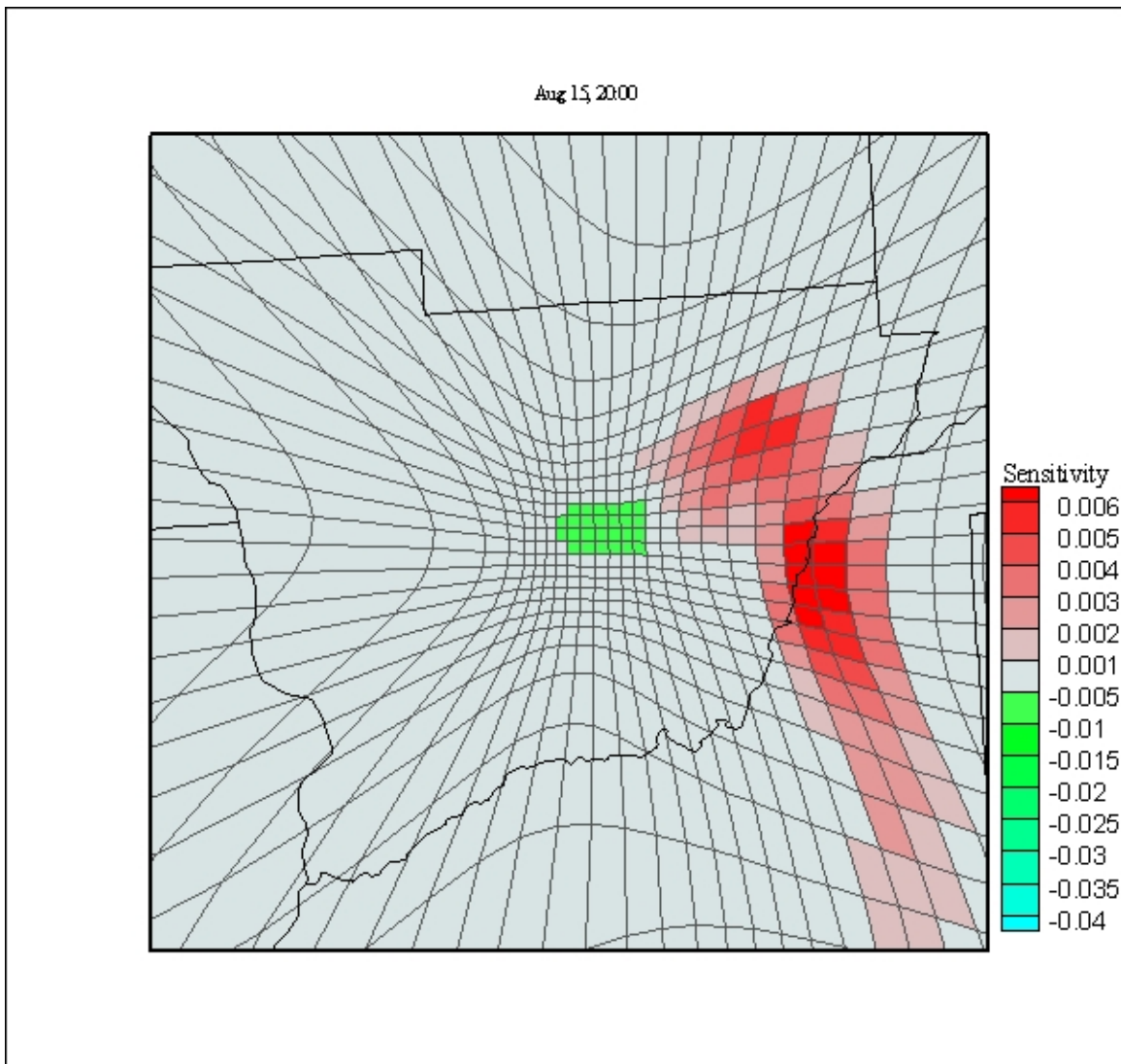
Figure 65 Adaptive Grid Result for Direct Sensitivity of O_3 (ppm) to Fire Emissions, August 15, 20:00
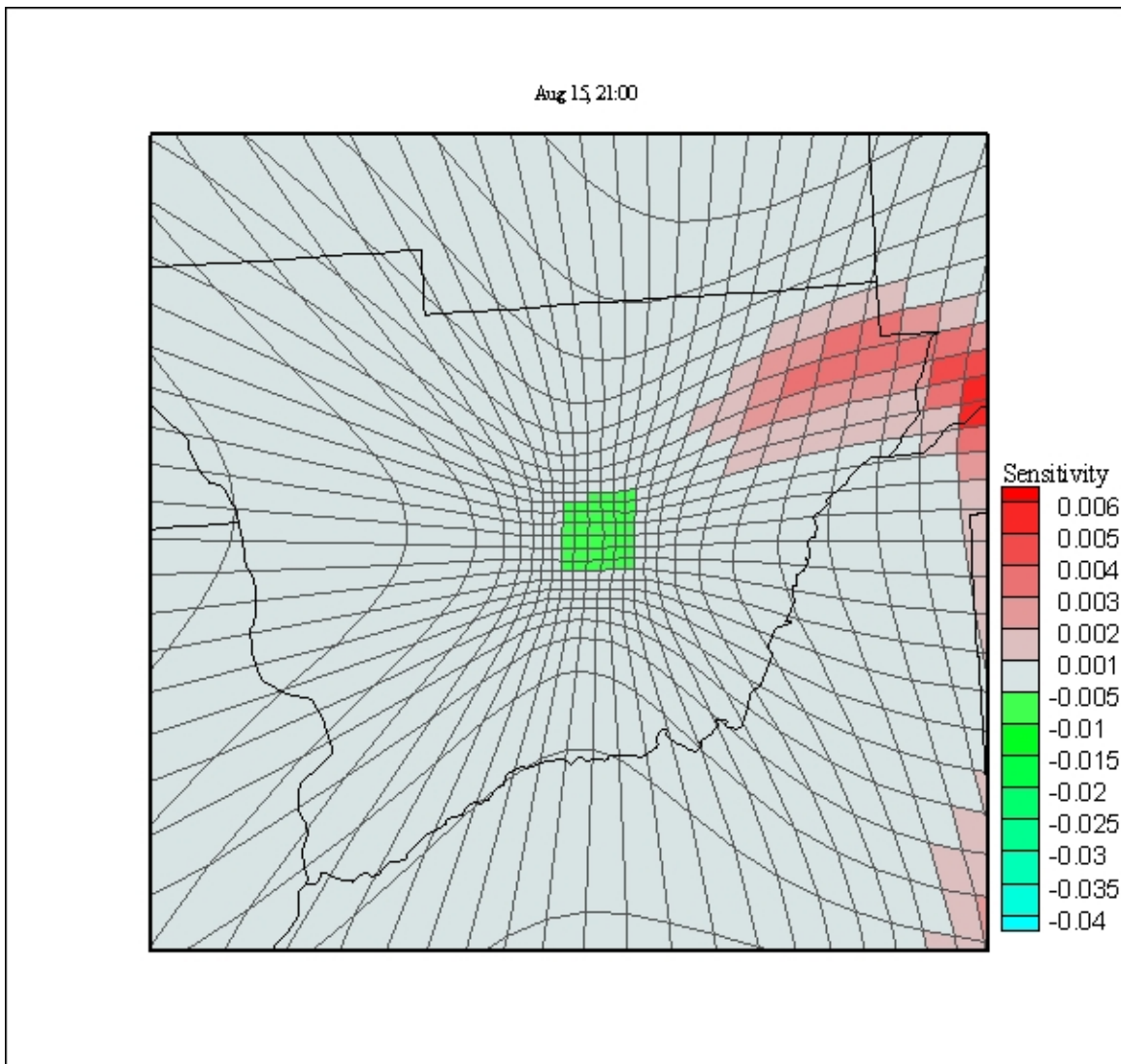
Figure 66 Adaptive Grid Result for Direct Sensitivity of O_3 (ppm) to Fire Emissions, August 15, 21:00
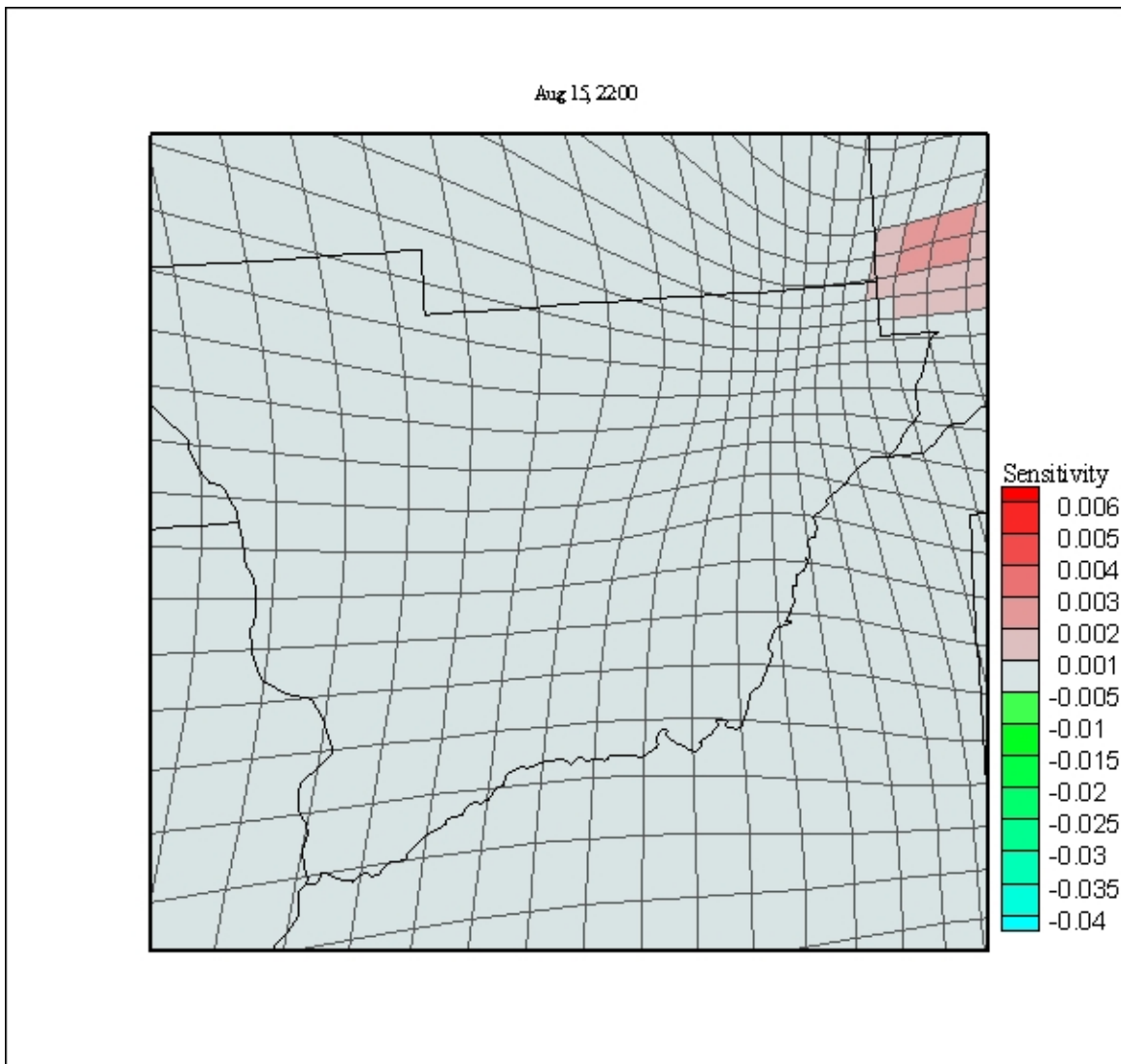
Figure 67 Adaptive Grid Result for Direct Sensitivity of O_3 (ppm) to Fire Emissions, August 15, 22:00
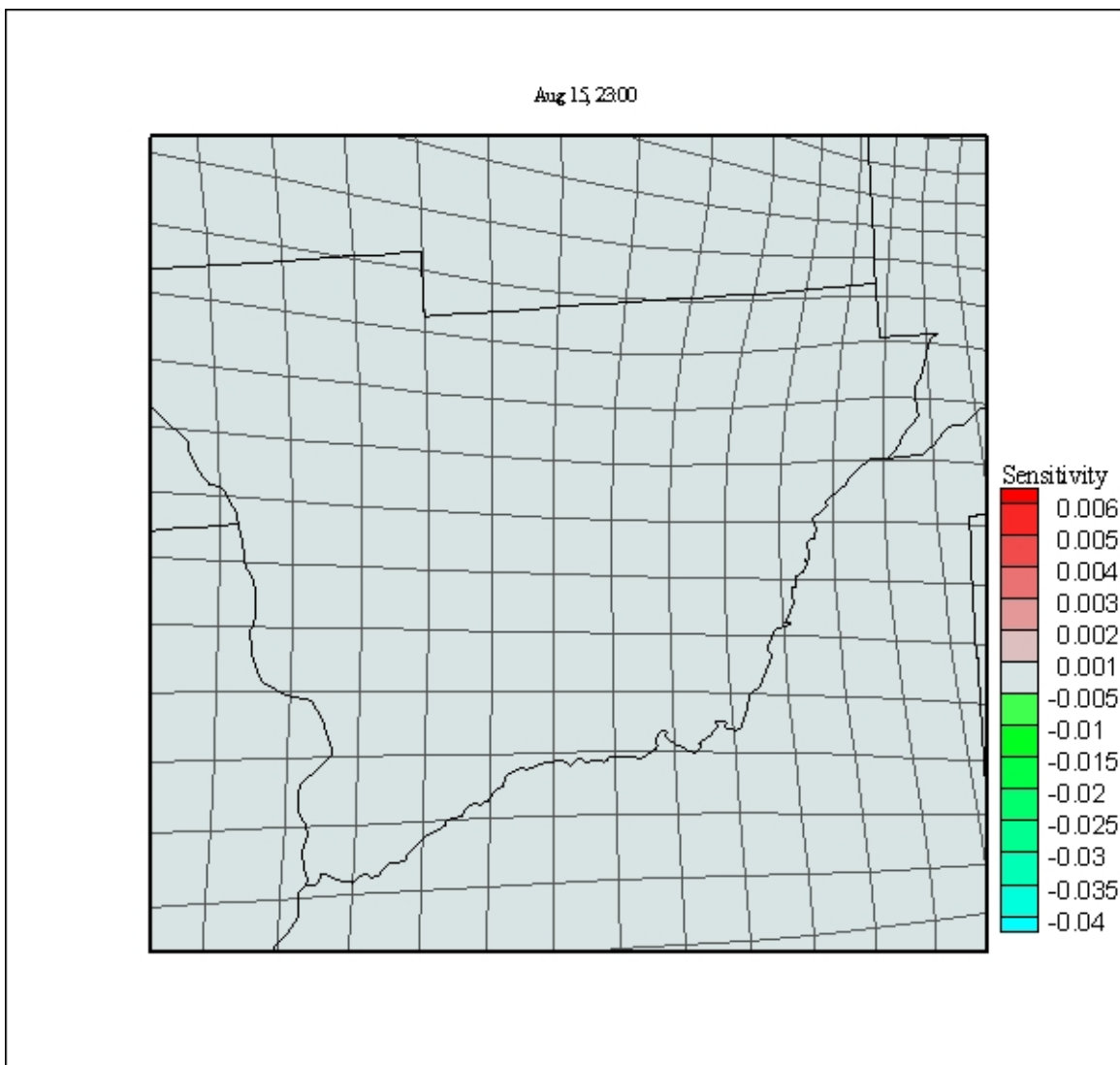
Figure 68 Adaptive Grid Result for Direct Sensitivity of O_3 (ppm) to Fire Emissions, August 15, 23:00
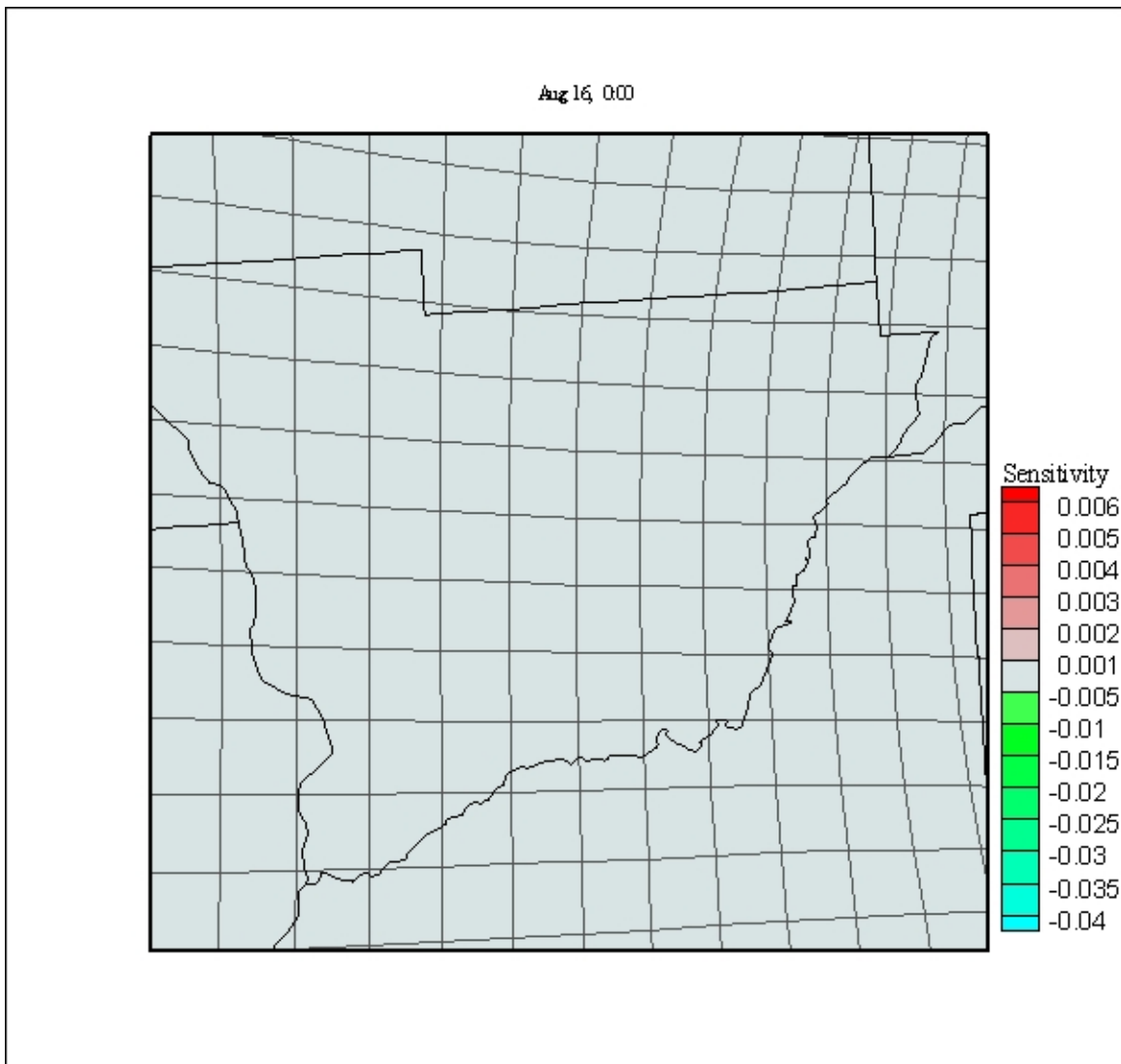
Figure 69 Adaptive Grid Result for Direct Sensitivity of O_3 (ppm) to Fire Emissions, August 16, 0:00
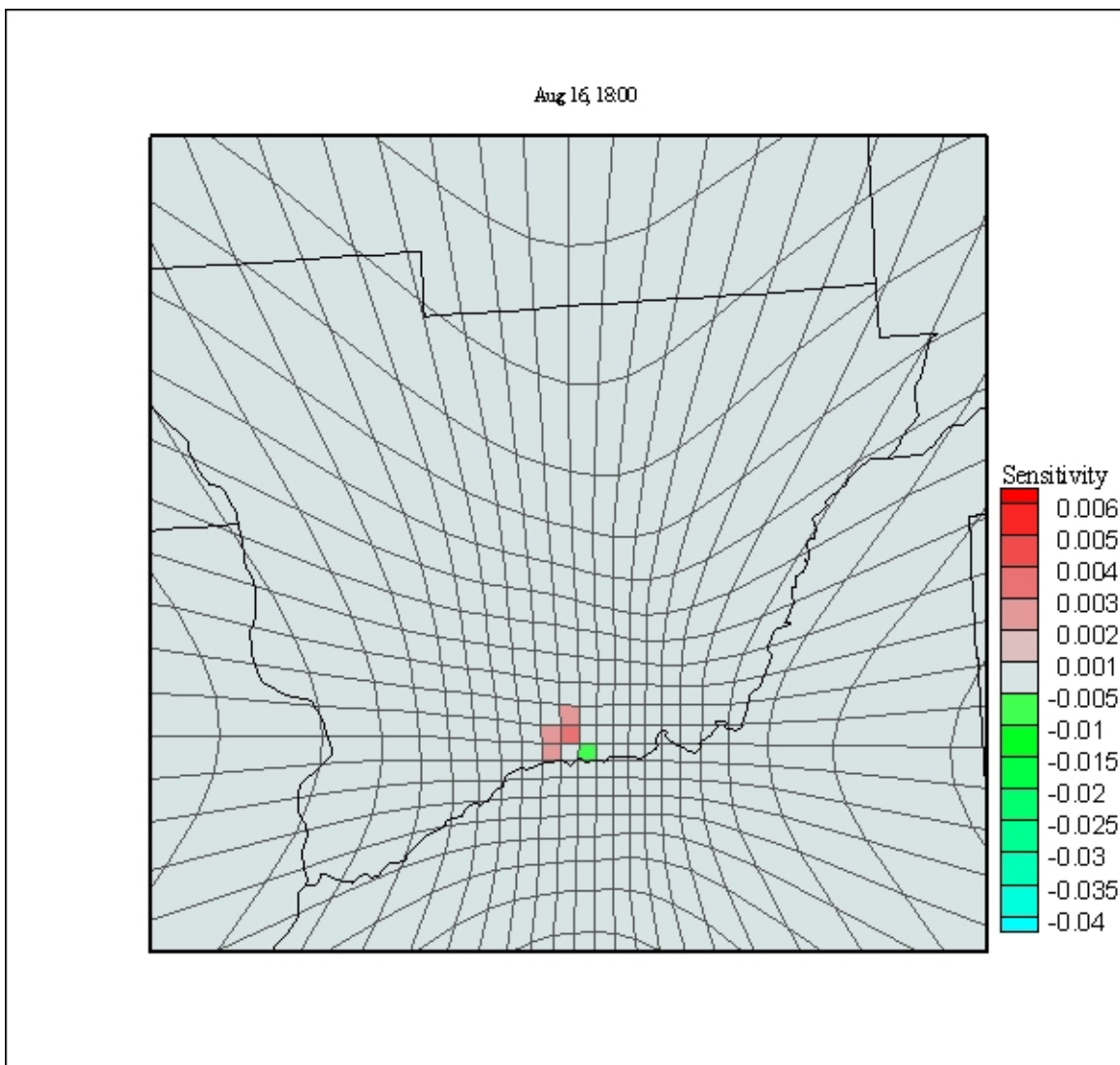
Figure 70 Adaptive Grid Result for Direct Sensitivity of O_3 (ppm) to Fire Emissions, August 16, 18:00
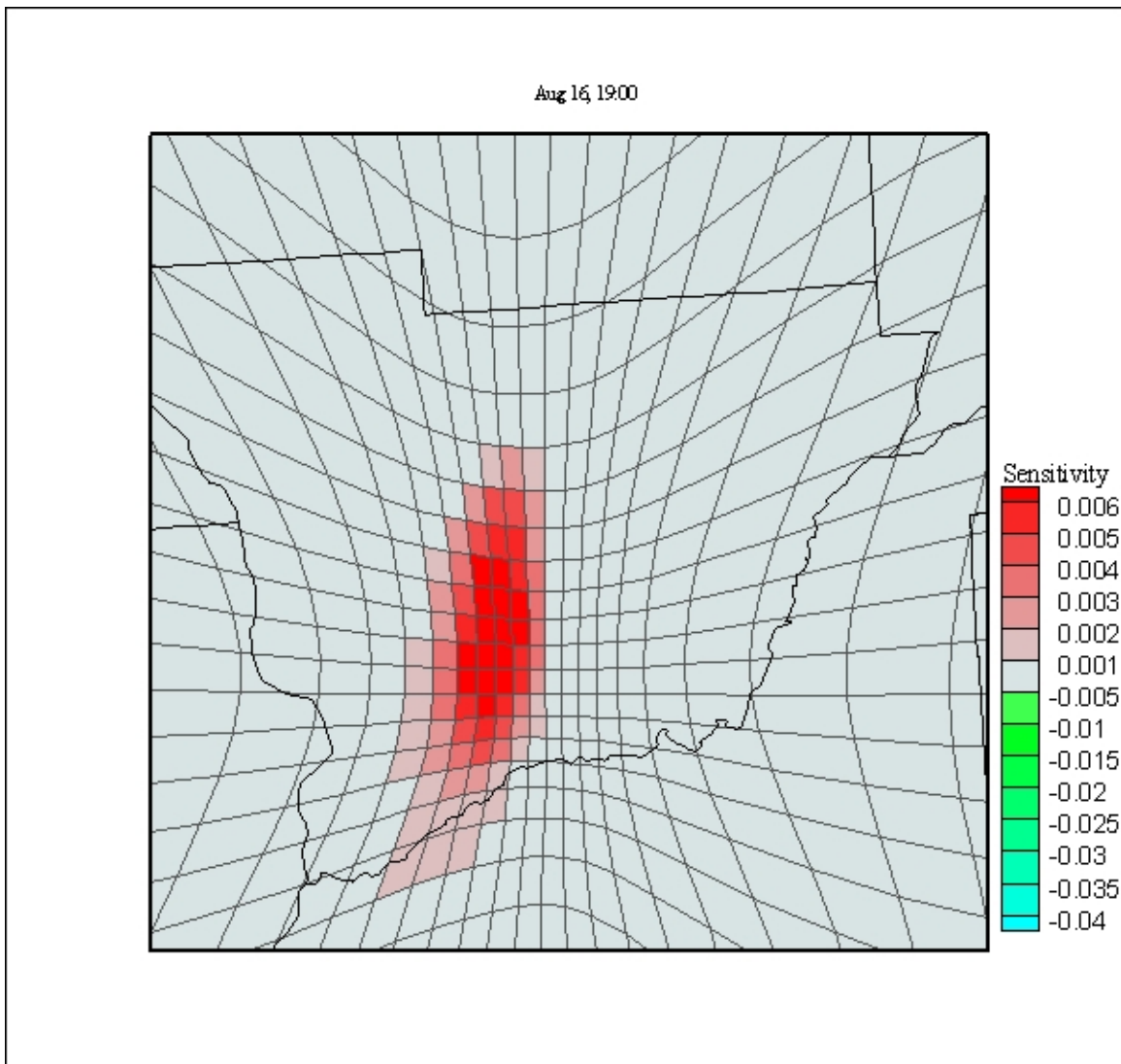
Figure 71 Adaptive Grid Result for Direct Sensitivity of O_3 (ppm) to Fire Emissions, August 16, 19:00
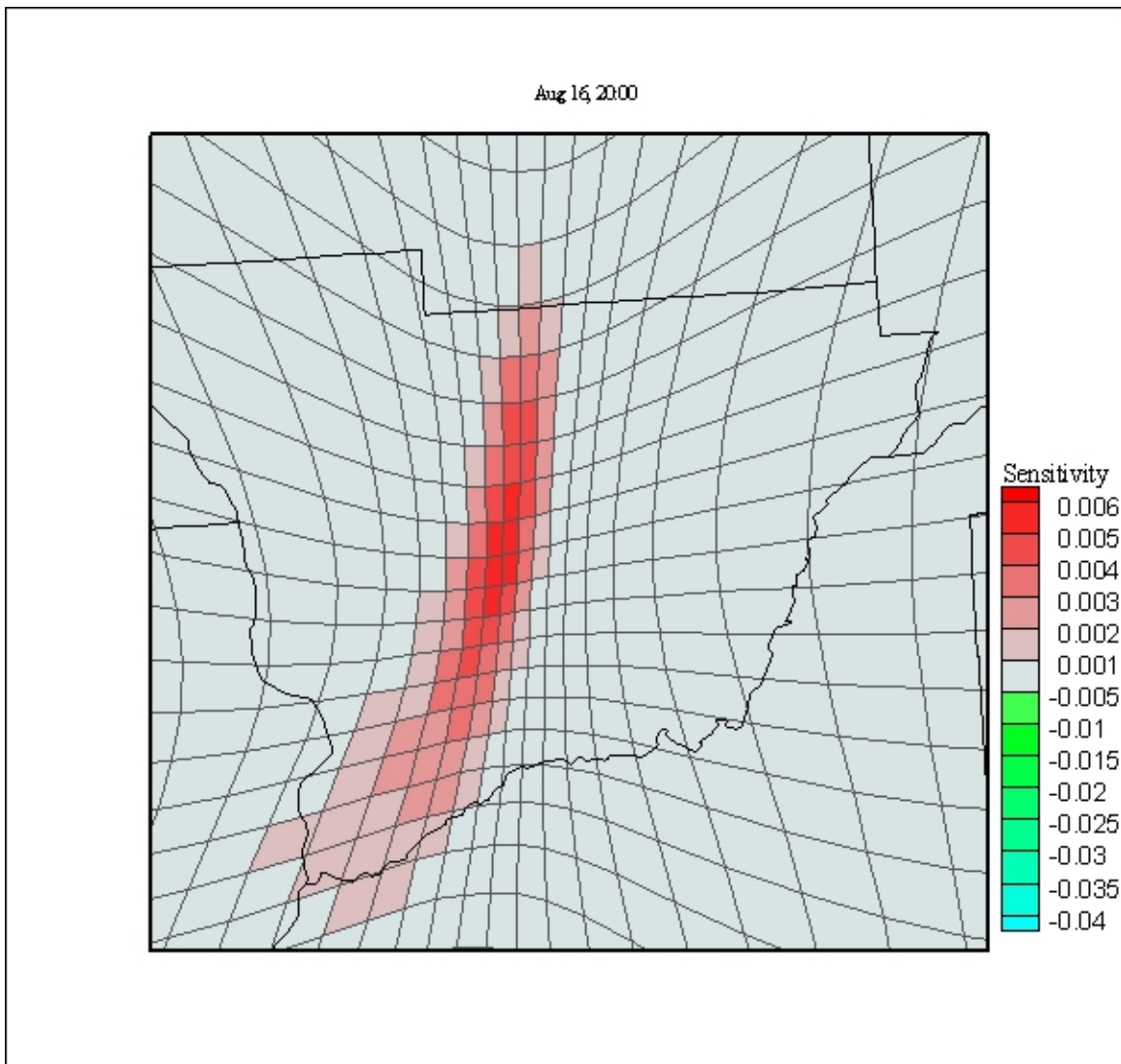
Figure 72 Adaptive Grid Result for Direct Sensitivity of O_3 (ppm) to Fire Emissions, August 16, 20:00
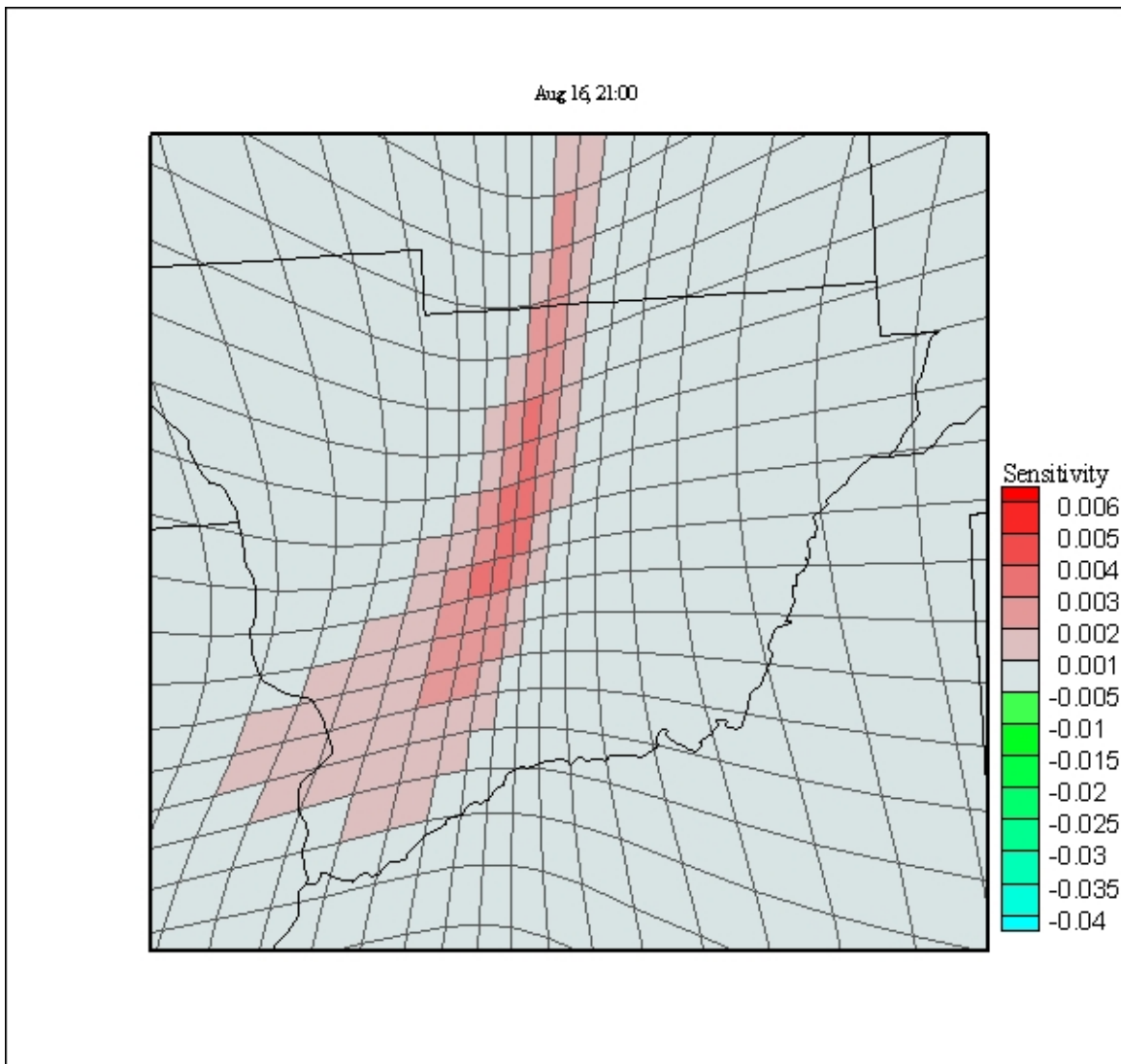
Figure 73 Adaptive Grid Result for Direct Sensitivity of O$_3$ (ppm) to Fire Emissions, August 16, 21:00
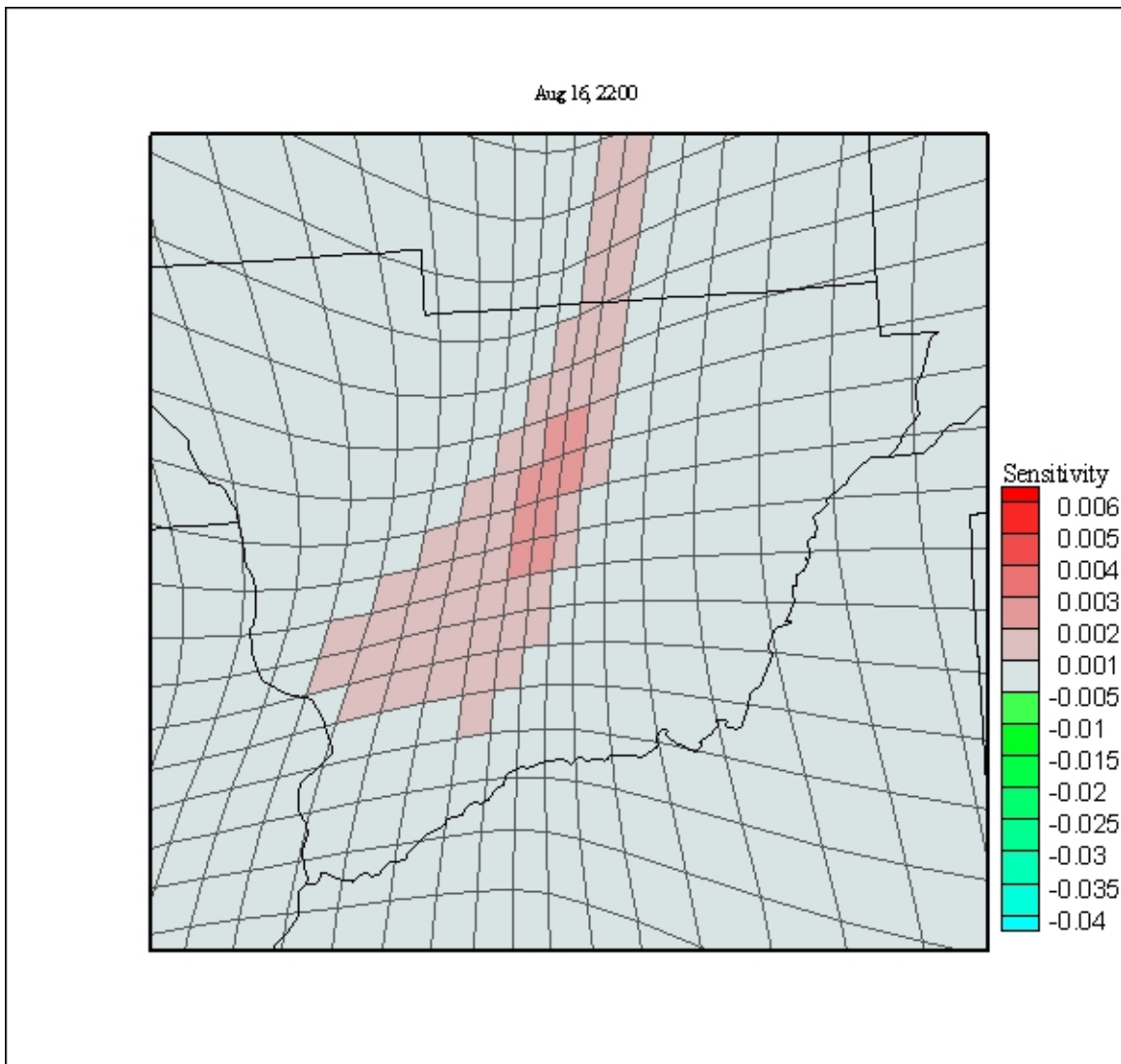
Figure 74 Adaptive Grid Result for Direct Sensitivity of O_3 (ppm) to Fire Emissions, August 16, 22:00
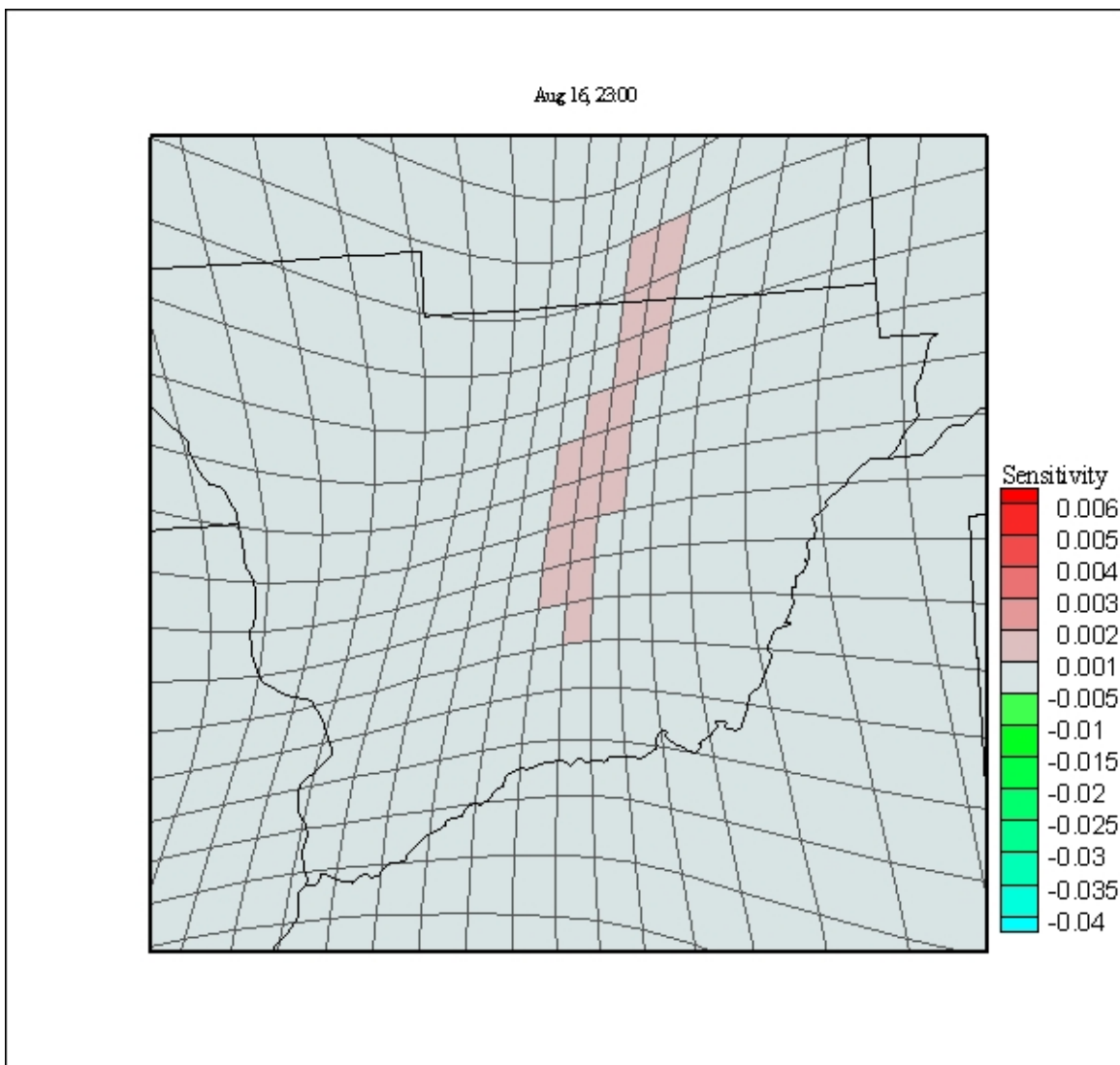
Figure 75 Adaptive Grid Result for Direct Sensitivity of O_3 (ppm) to Fire Emissions, August 16, 23:00
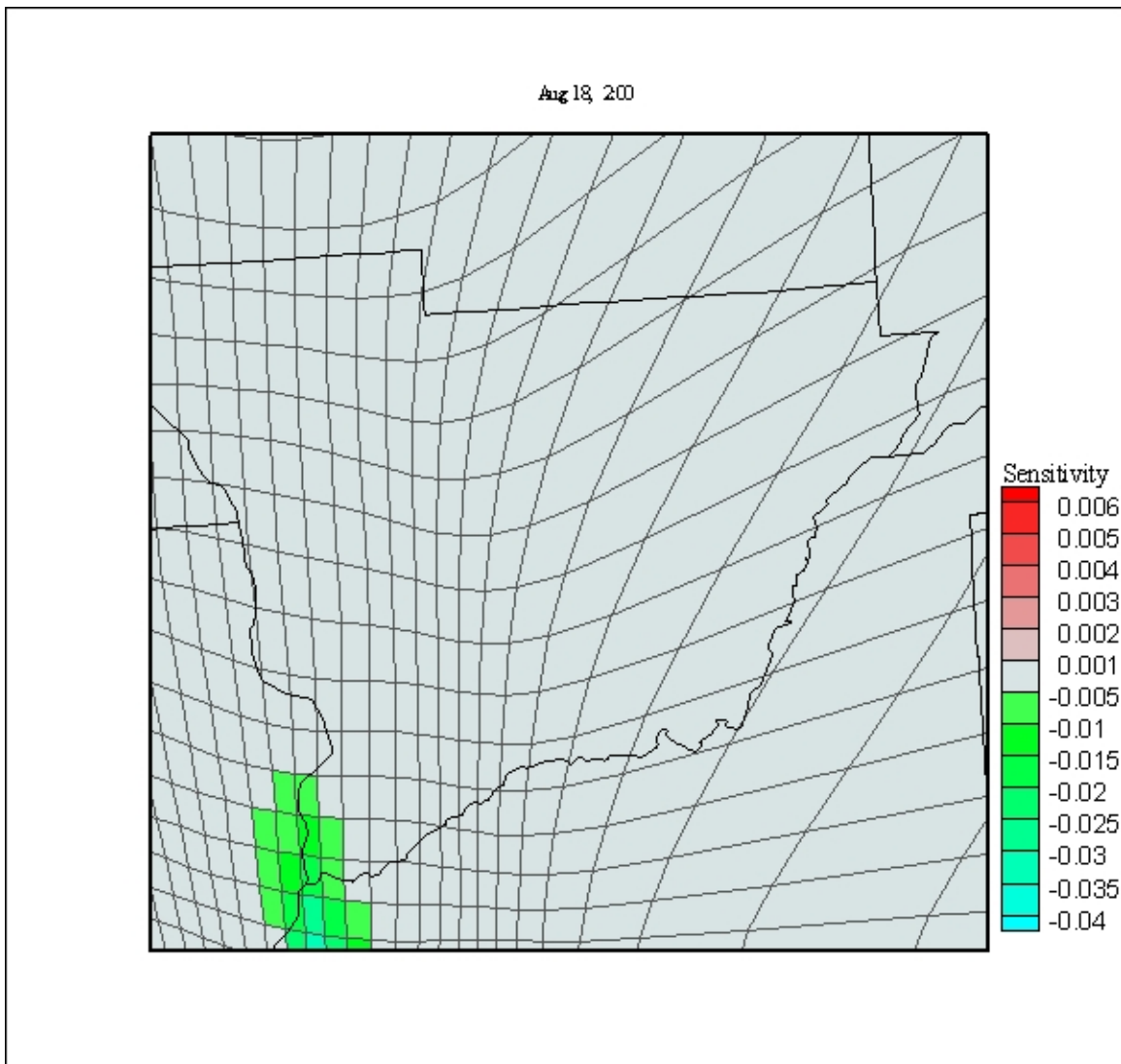
Figure 76 Adaptive Grid Result for Direct Sensitivity of O$_3$ (ppm) to Fire Emissions, August 18, 2:00
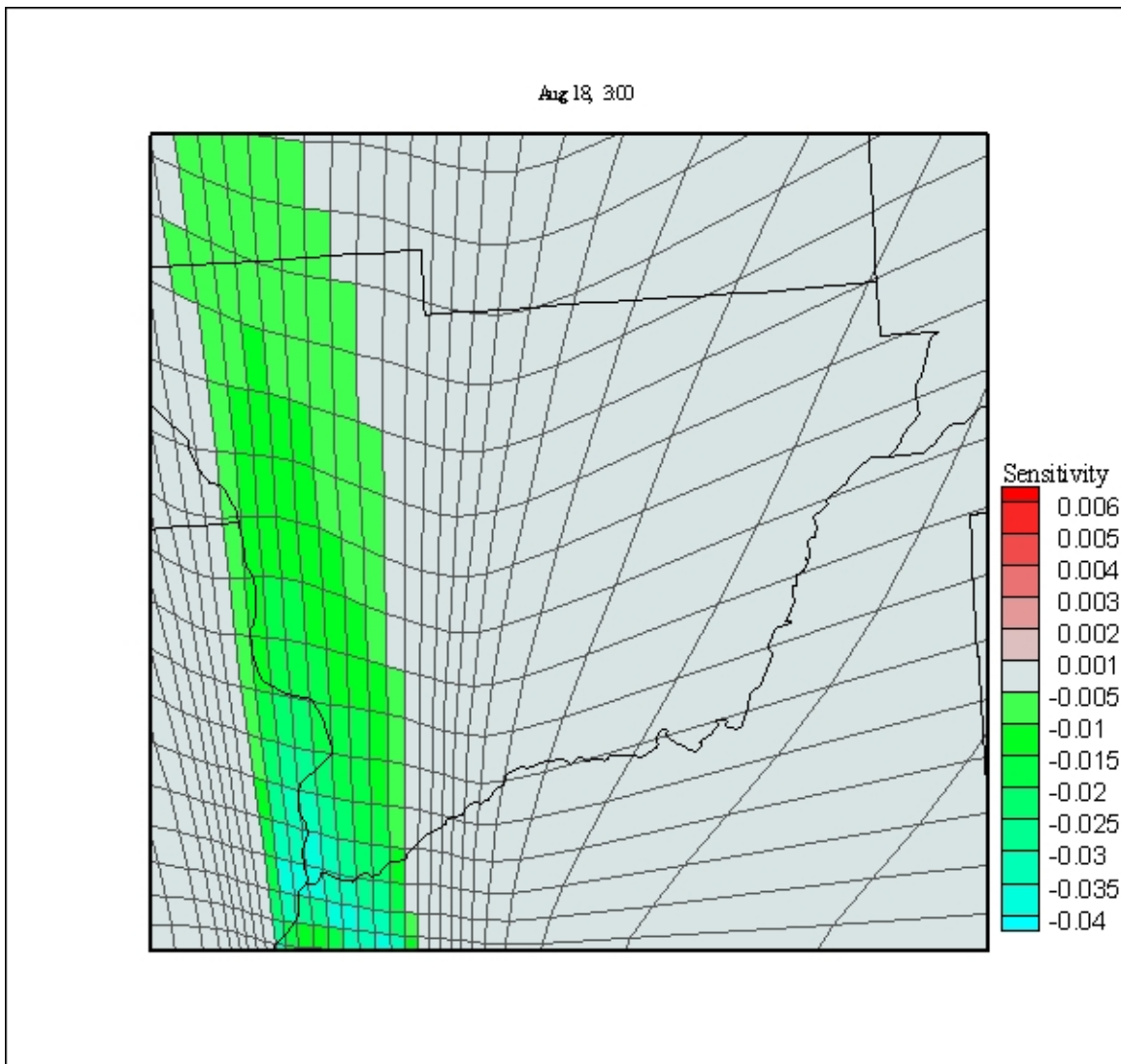
Figure 77 Adaptive Grid Result for Direct Sensitivity of O_3 (ppm) to Fire Emissions, August 18, 3:00
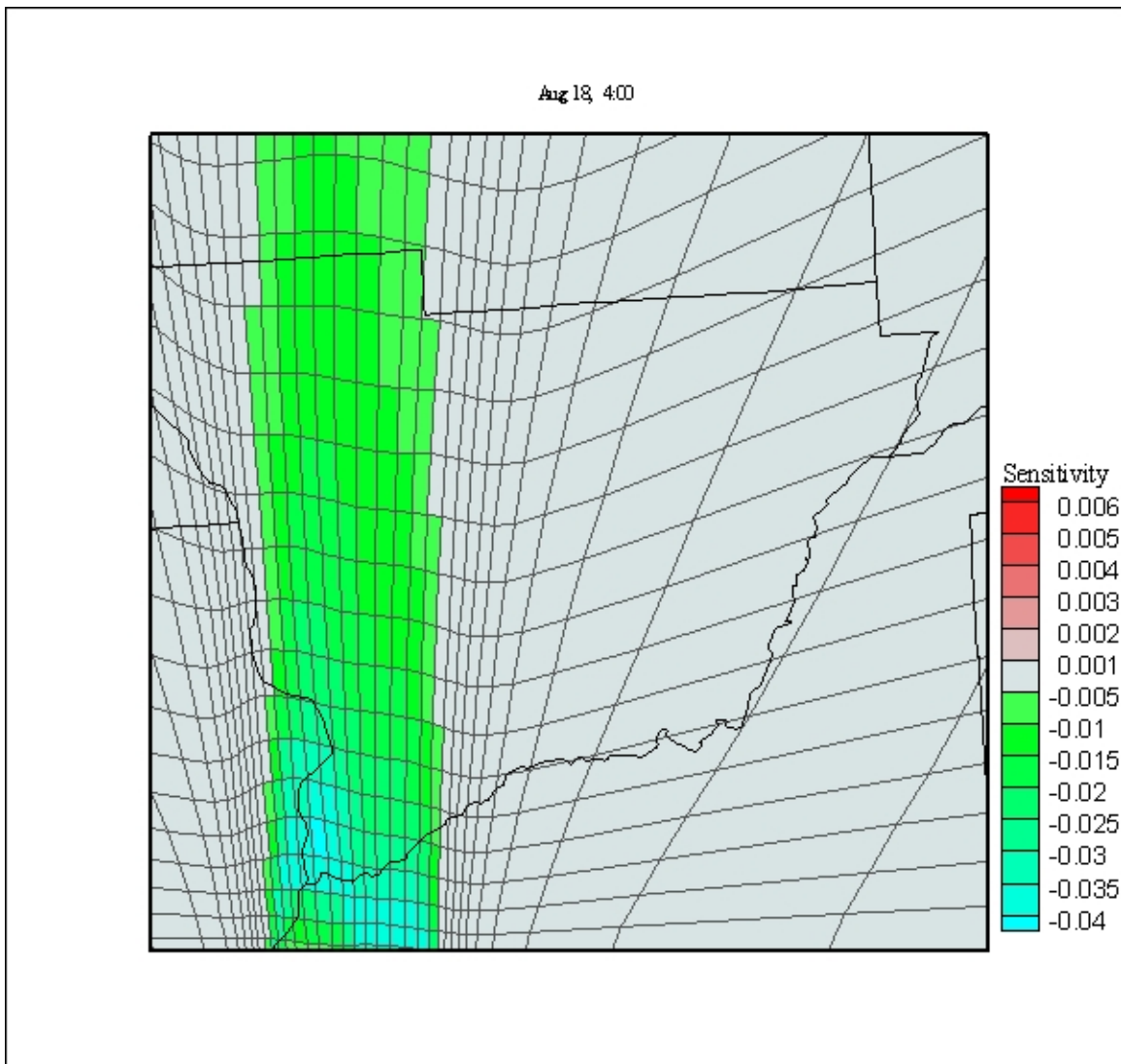
Figure 78 Adaptive Grid Result for Direct Sensitivity of O_3 (ppm) to Fire Emissions, August 18, 4:00
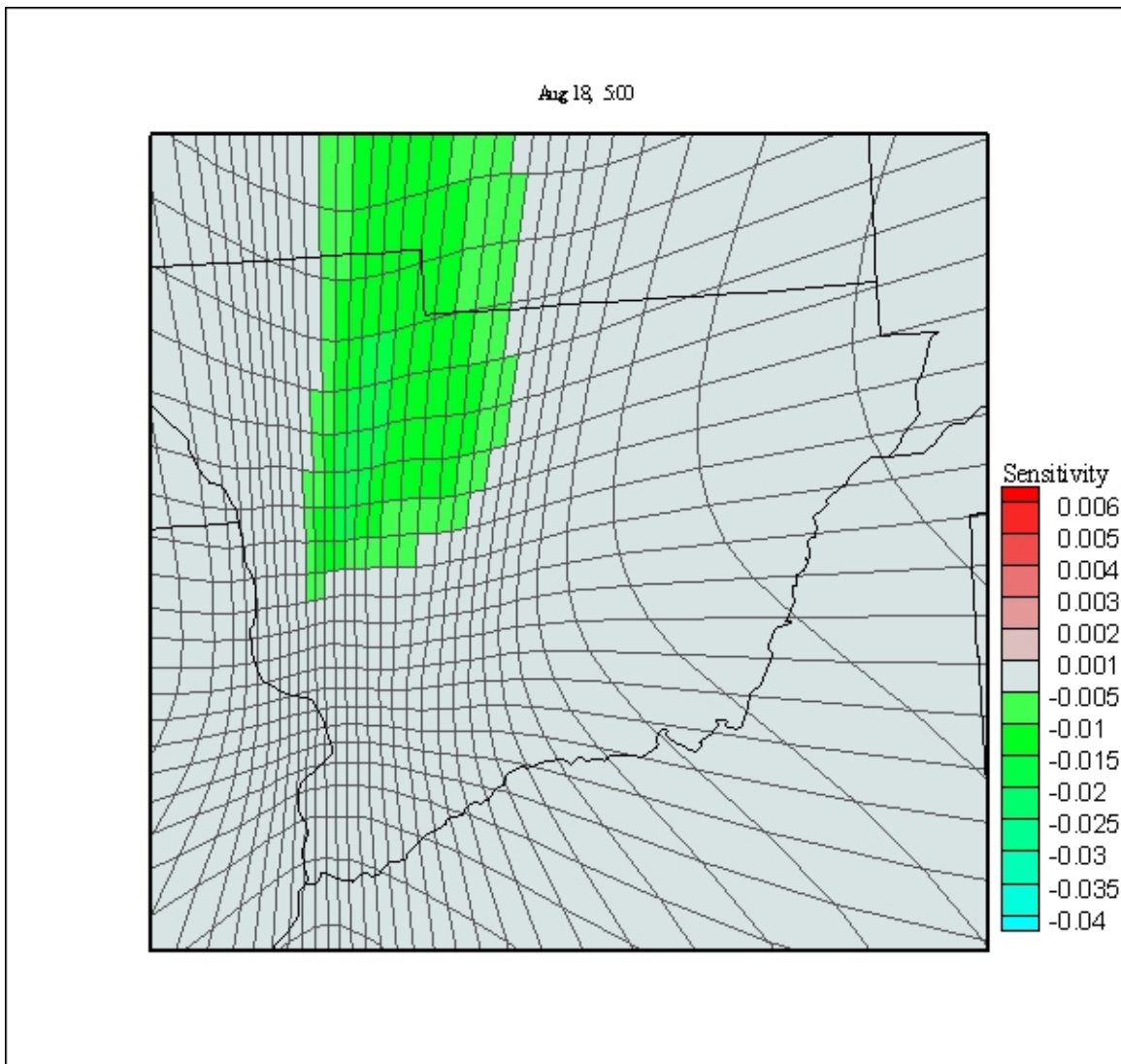
Figure 79 Adaptive Grid Result for Direct Sensitivity of O_3 (ppm) to Fire Emissions, August 18, 5:00
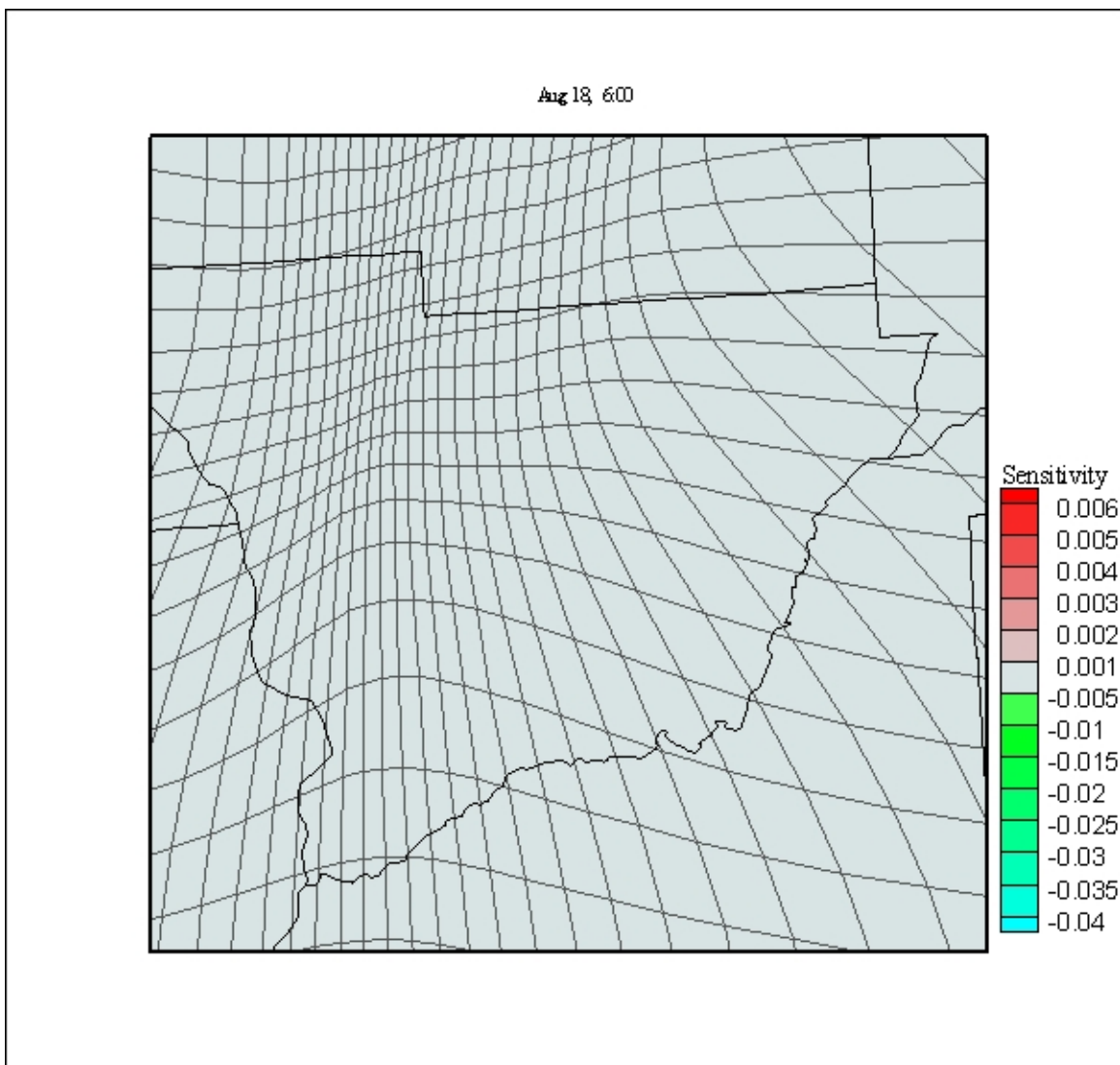
Figure 80 Adaptive Grid Result for Direct Sensitivity of O_3 (ppm) to Fire Emissions, August 18, 6:00
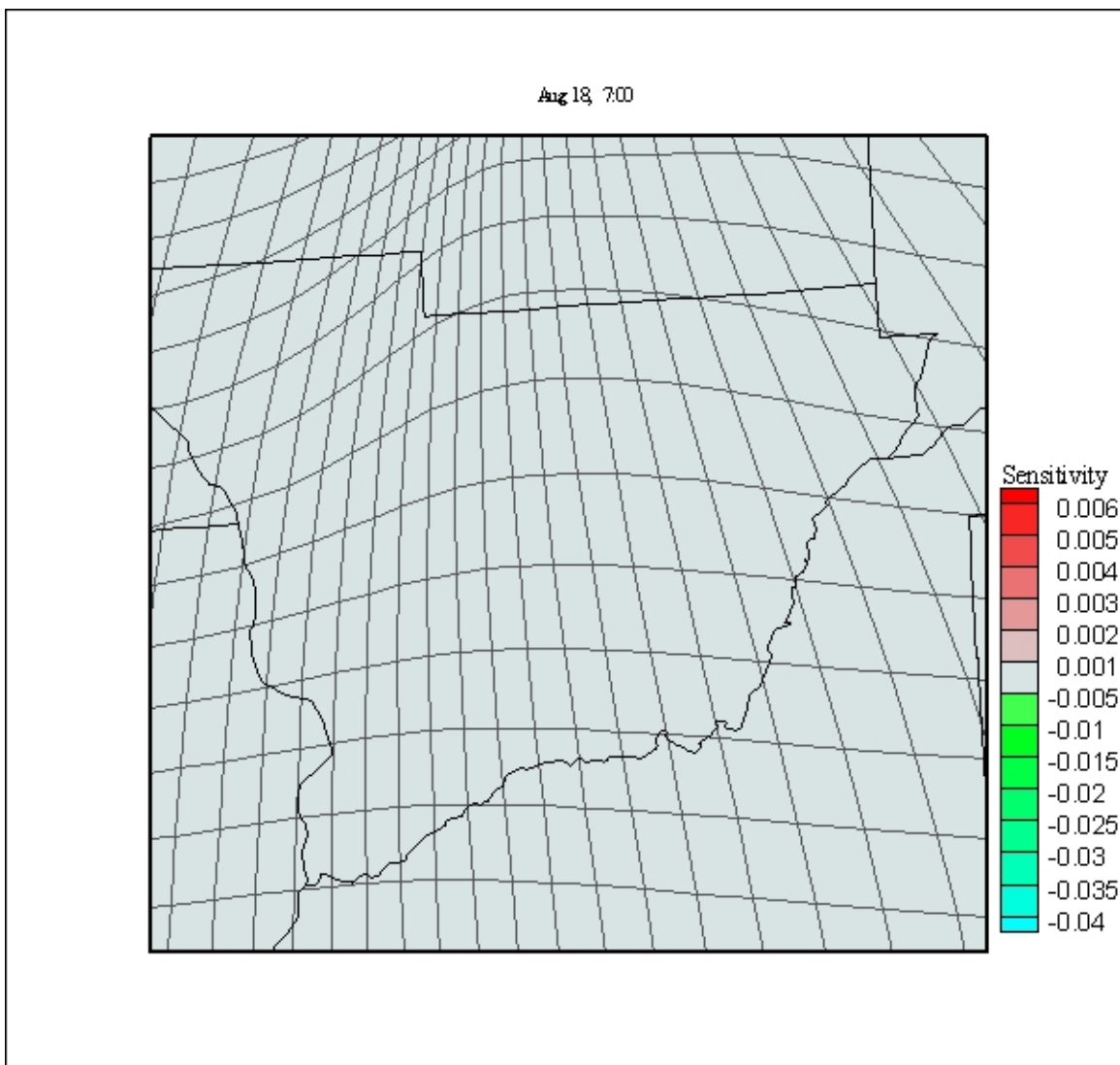
Figure 81 Adaptive Grid Result for Direct Sensitivity of O_3 (ppm) to Fire Emissions, August 18, 7:00
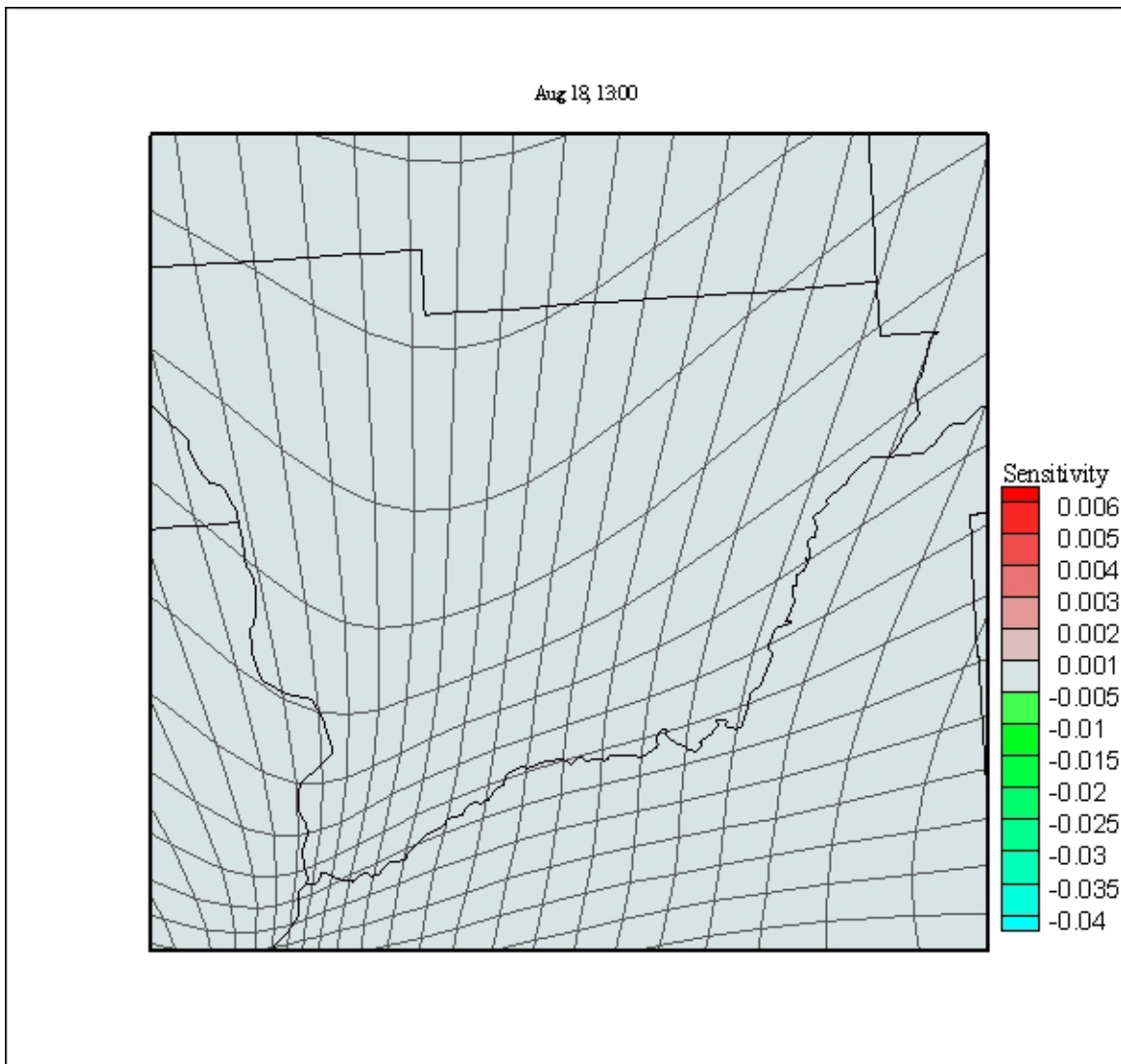
Figure 82 Adaptive Grid Result for Direct Sensitivity of O_3 (ppm) to Fire Emissions, August 18, 13:00
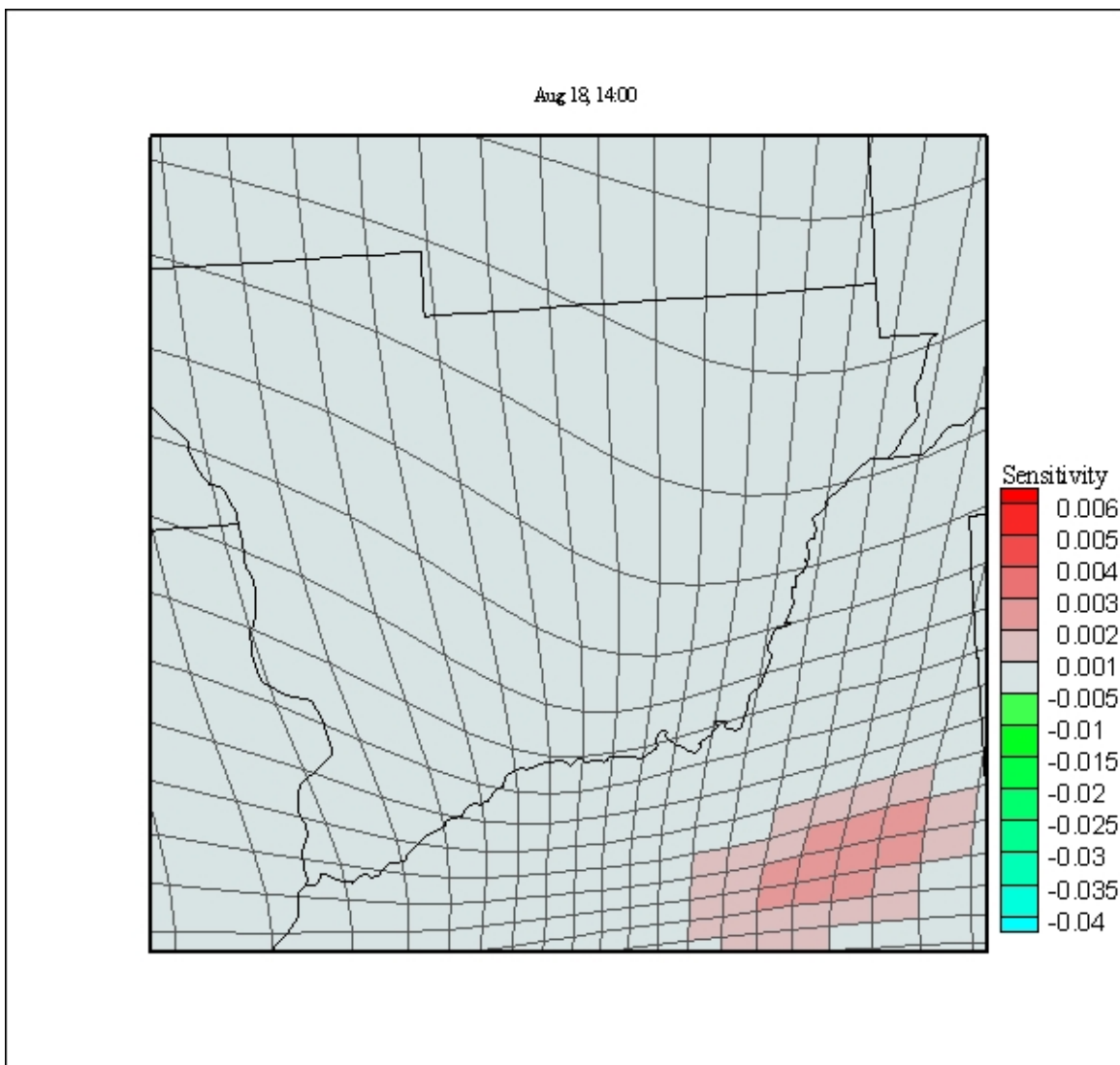
Figure 83 Adaptive Grid Result for Direct Sensitivity of O$_3$ (ppm) to Fire Emissions, August 18, 14:00
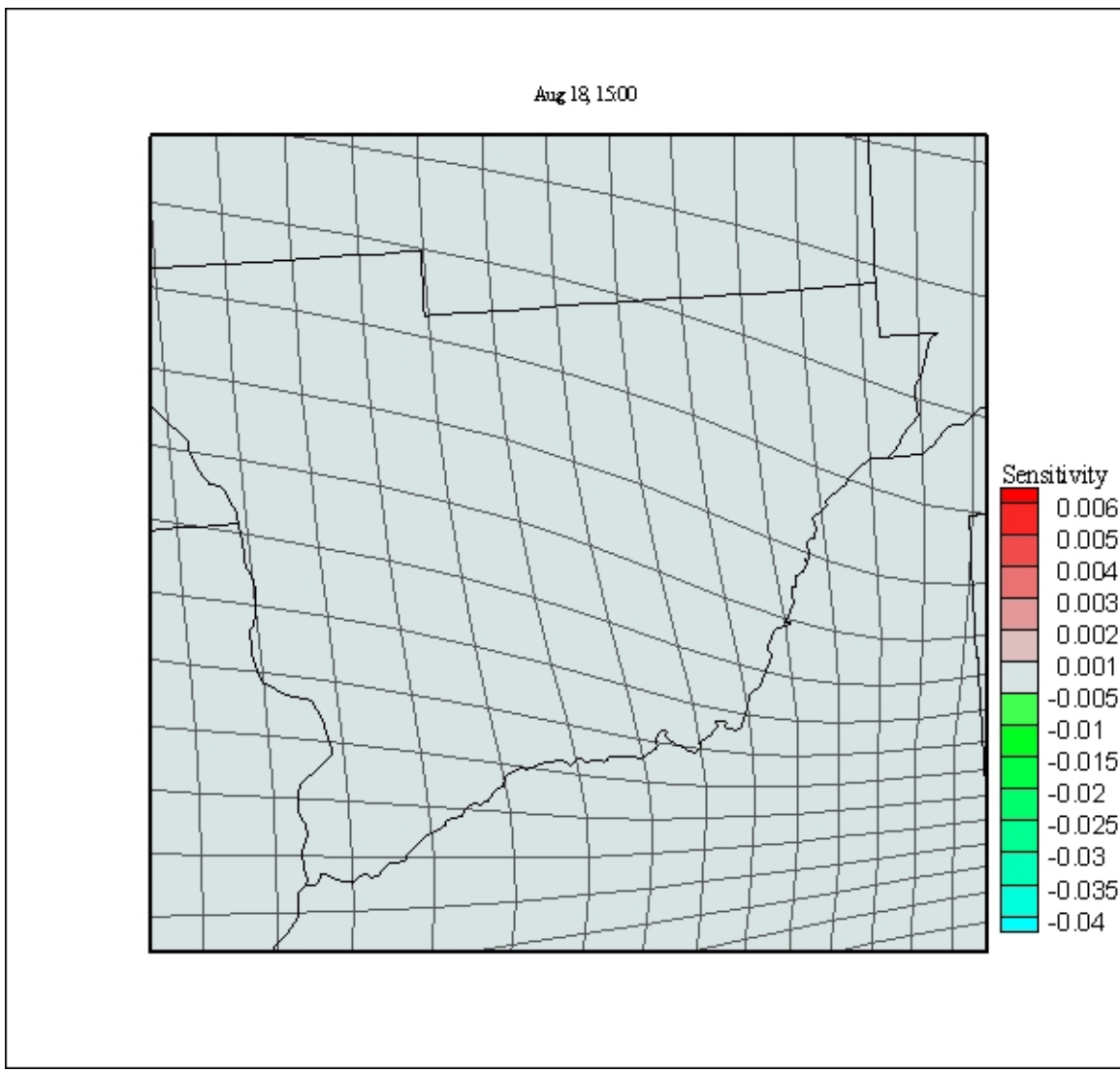
Figure 84 Adaptive Grid Result for Direct Sensitivity of O$_3$ (ppm) to Fire Emissions, August 18, 15:00

8.2 Analysis Results
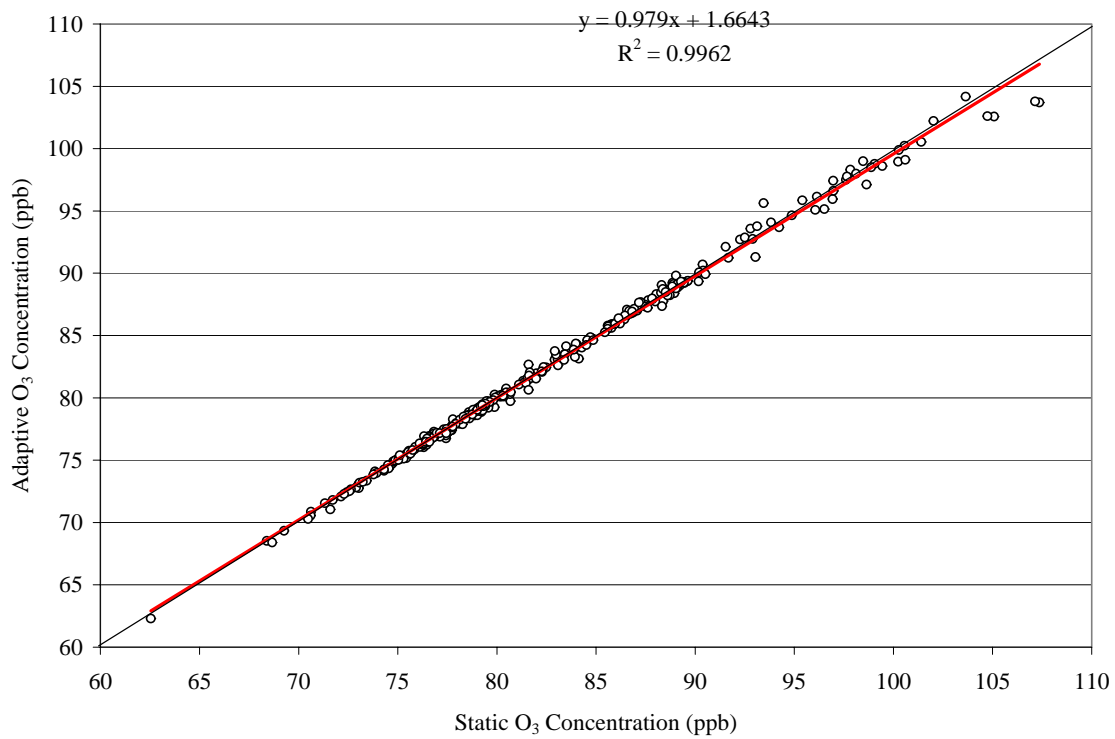
Figure 1. Static versus Adaptive Comparison for O3 Concentration for August 15, 18:00
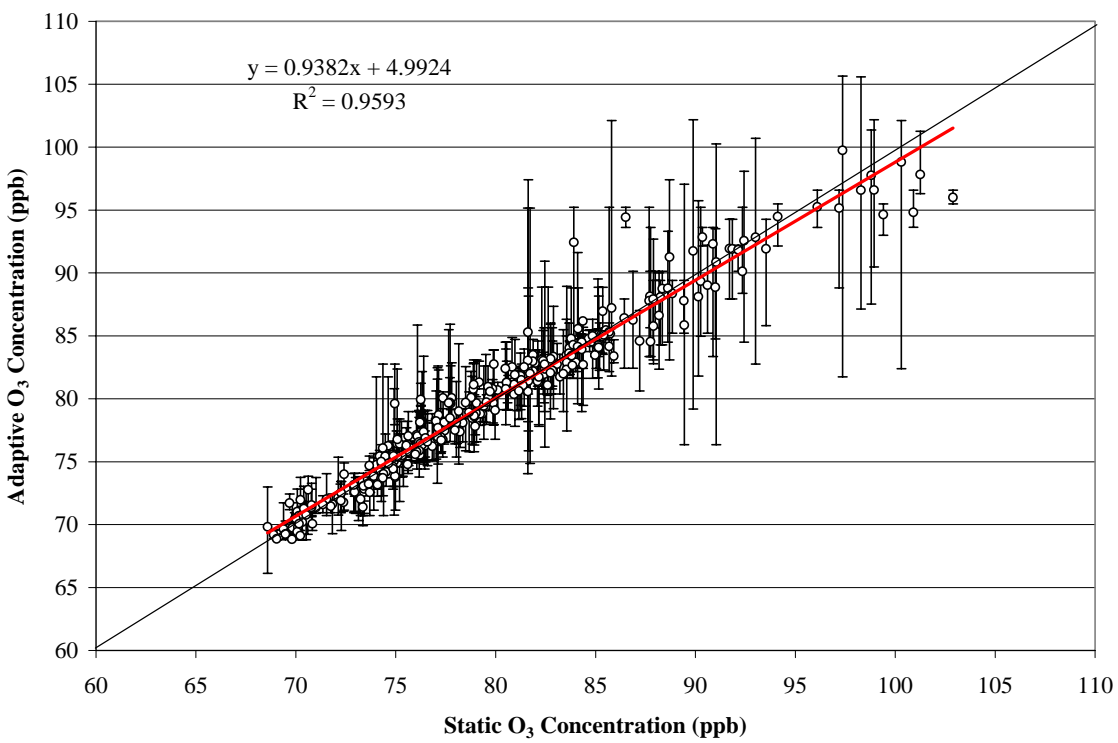
Figure 2. Static versus Adaptive Comparison for O3 Concentration for August 15, 19:00
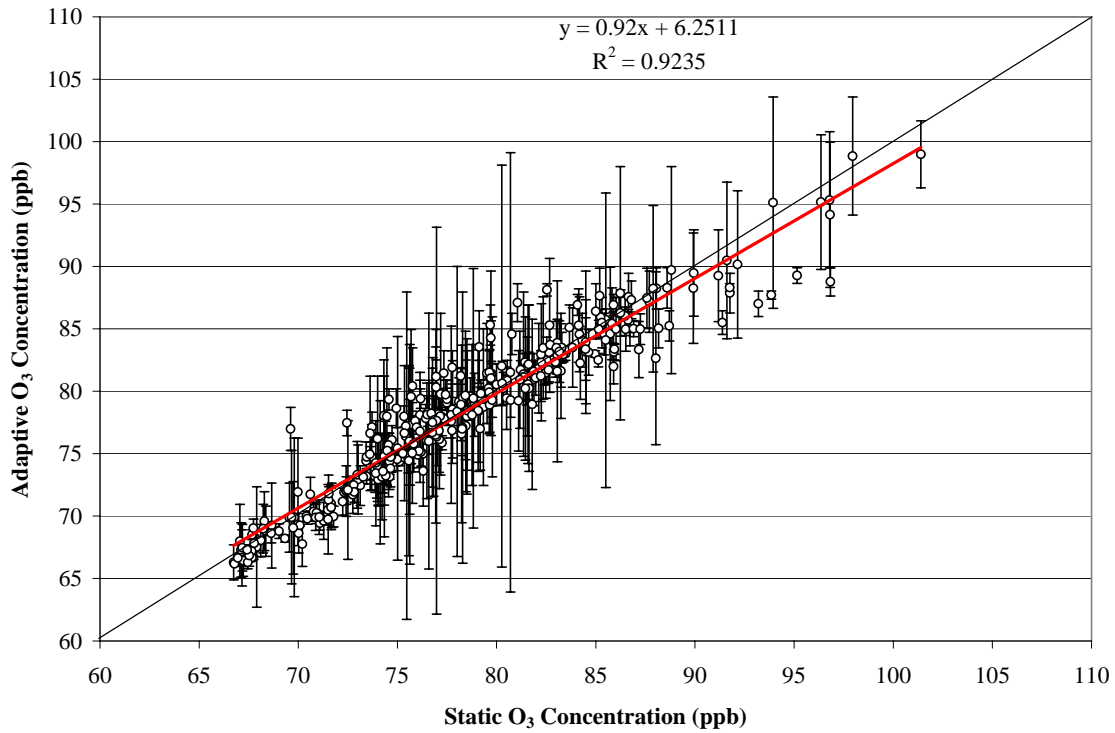
Figure 3. Static versus Adaptive Comparison for O3 Concentration for August 15, 20:00
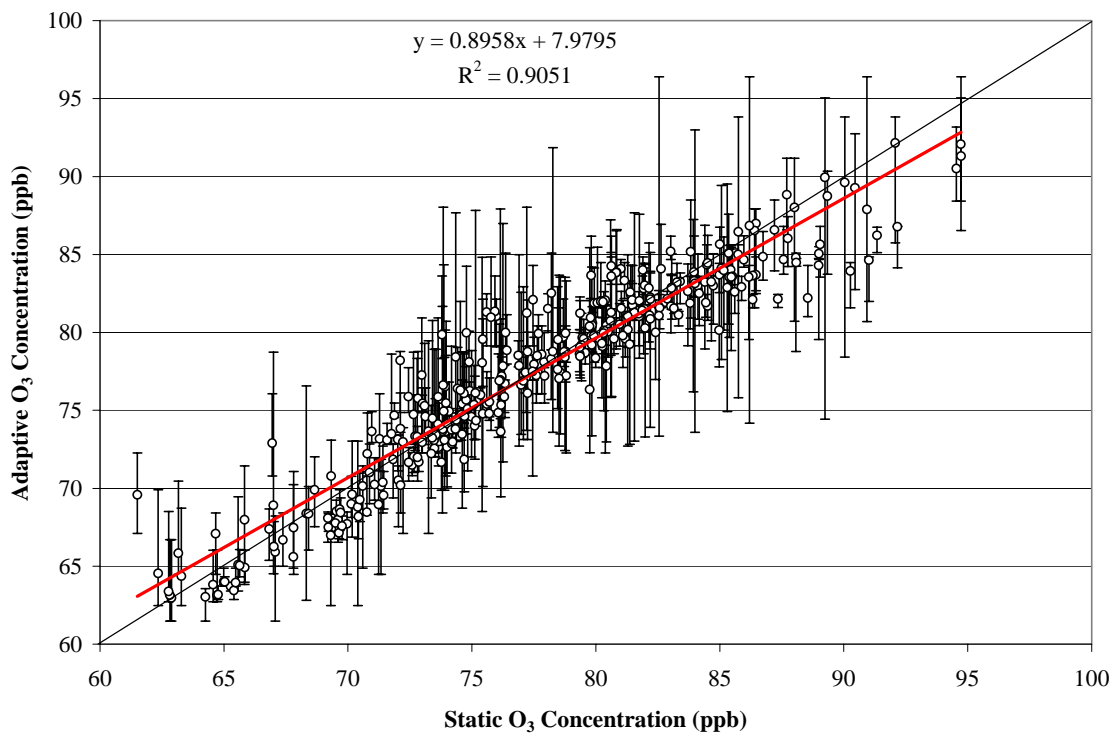
Figure 4. Static versus Adaptive Comparison for O3 Concentration for August 15, 21:00
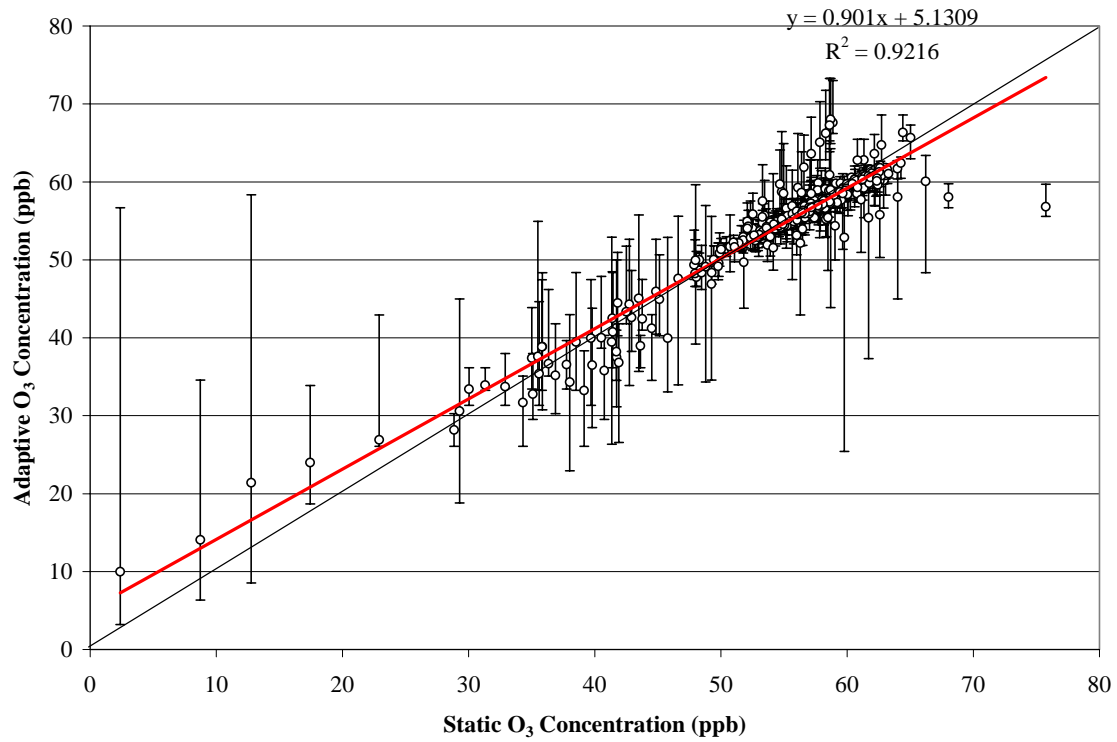
Figure 5. Static versus Adaptive Comparison for O3 Concentration for August 18, 02:00
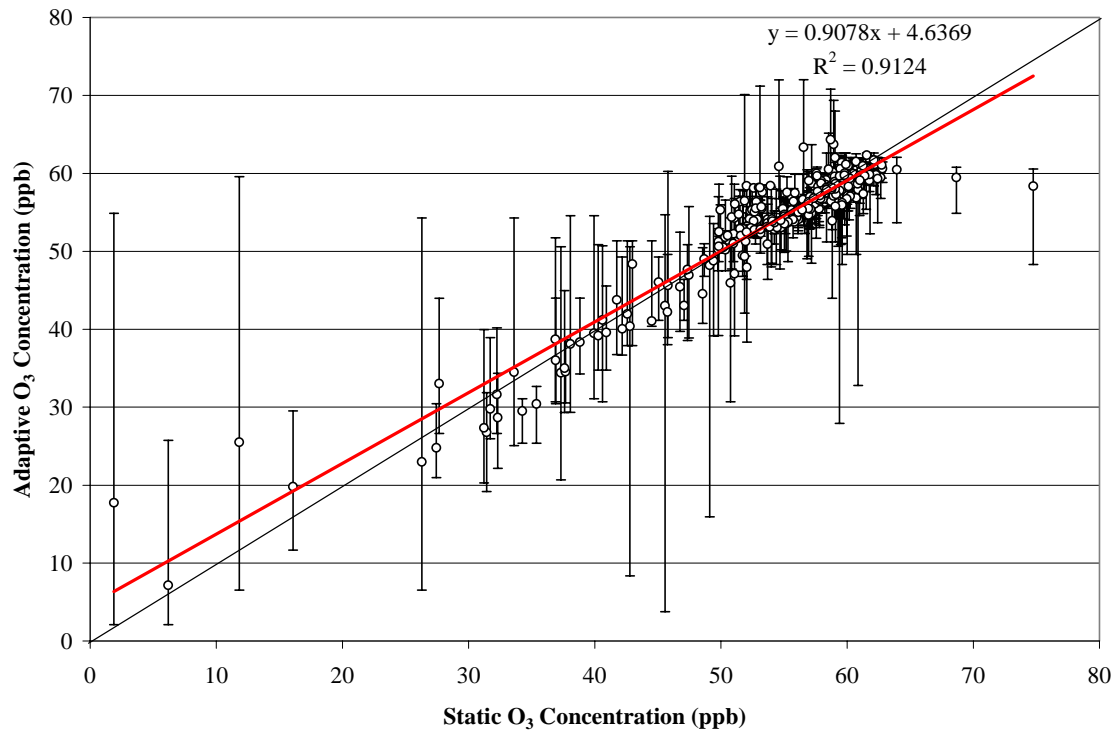
Figure 6. Static versus Adaptive Comparison for O3 Concentration for August 18, 03:00
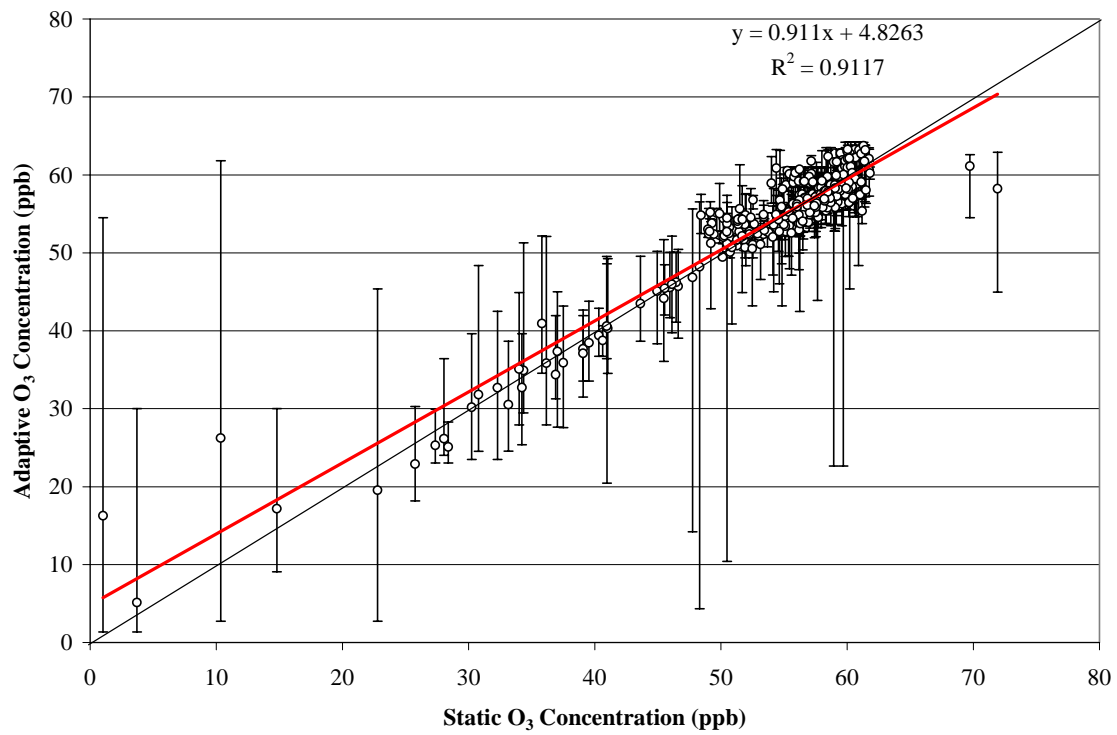
Figure 7. Static versus Adaptive Comparison for O3 Concentration for August 18, 04:00
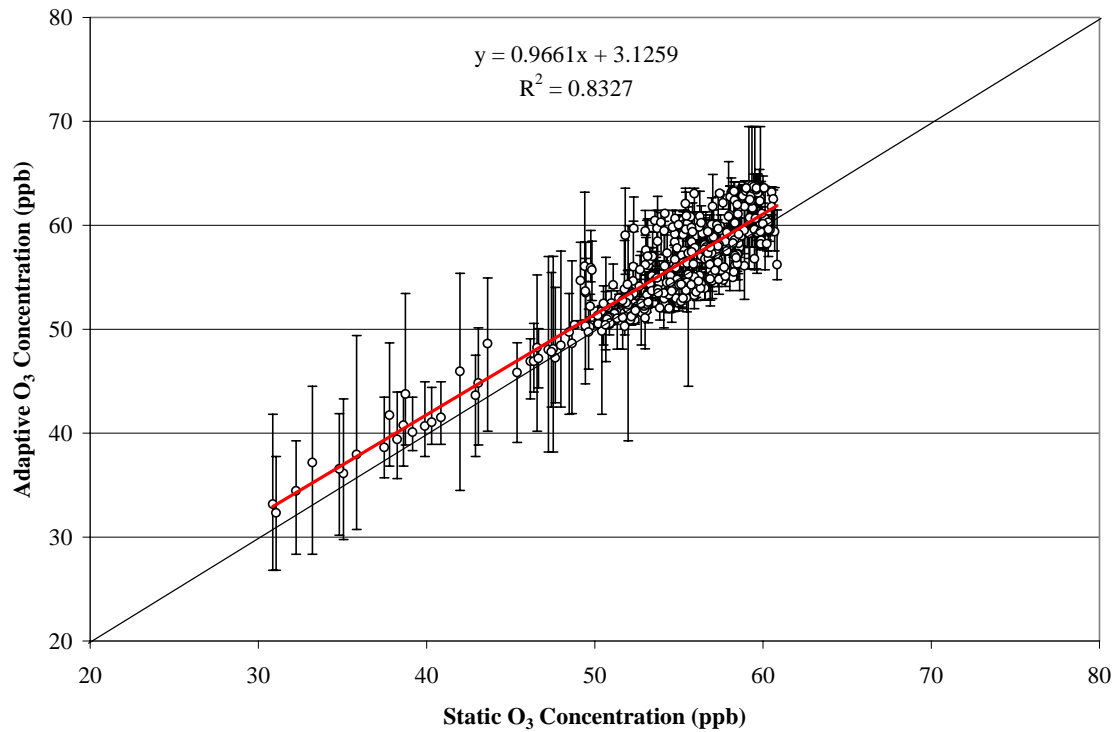
Figure 8. Static versus Adaptive Comparison for O3 Concentration for August 18, 05:00
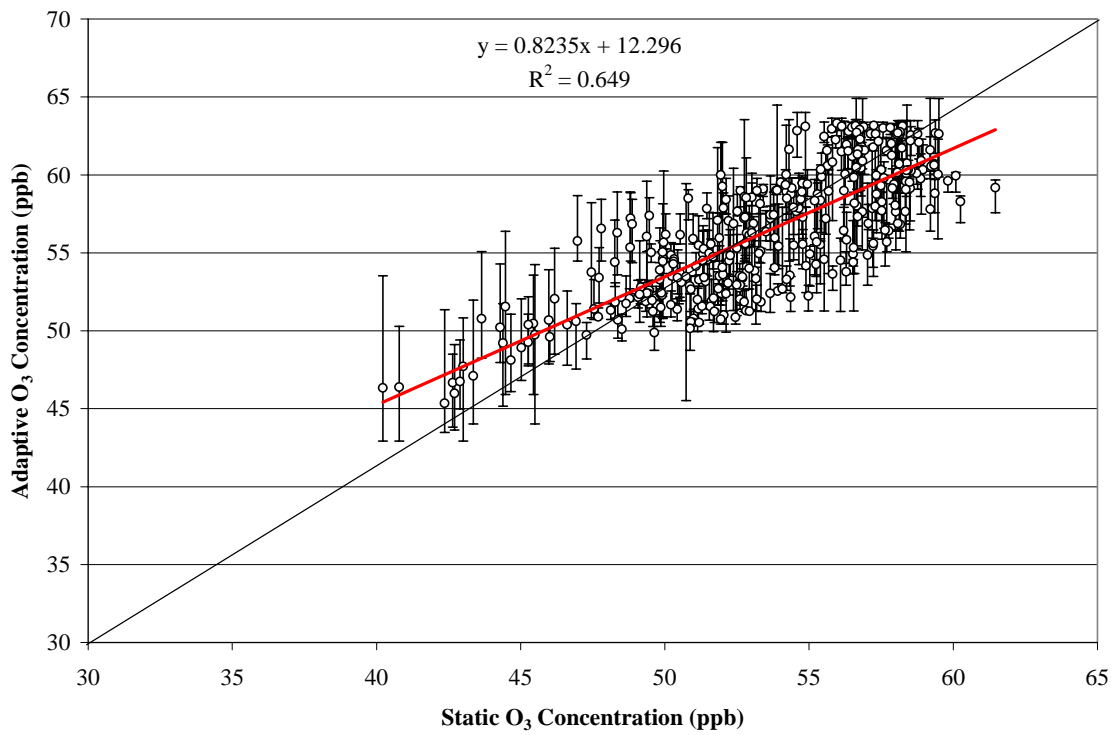
Figure 9. Static versus Adaptive Comparison for O3 Concentration for August 18, 06:00
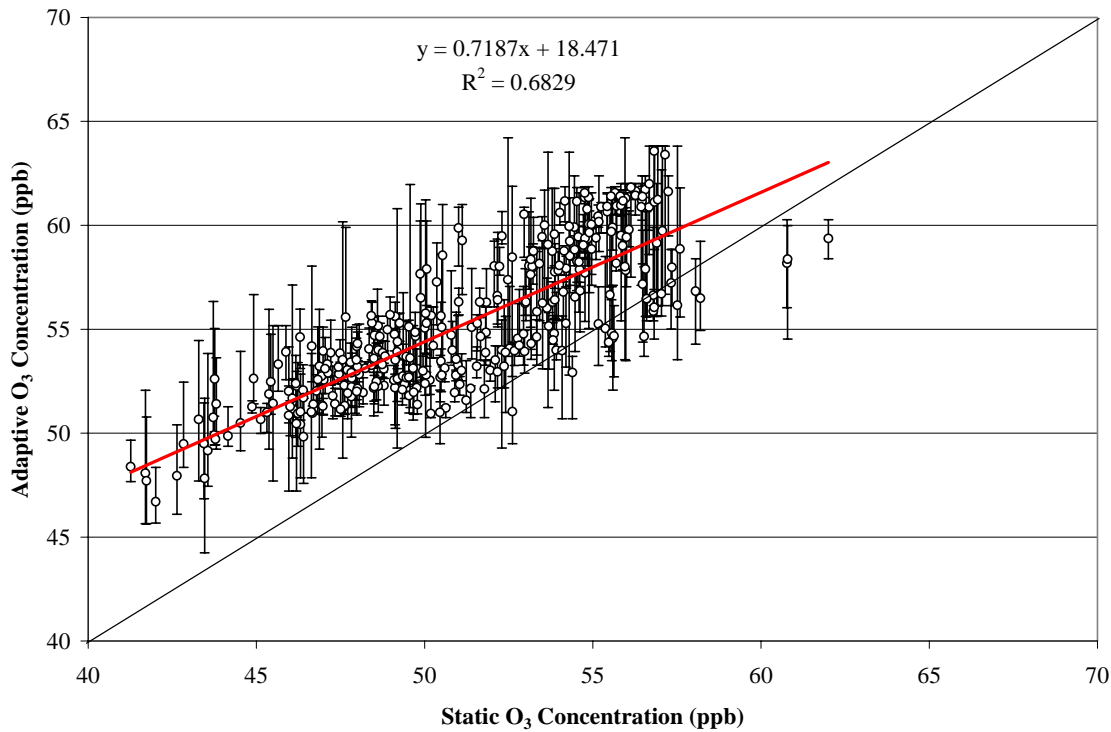
Figure 10. Static versus Adaptive Comparison for O3 Concentration for August 18, 07:00
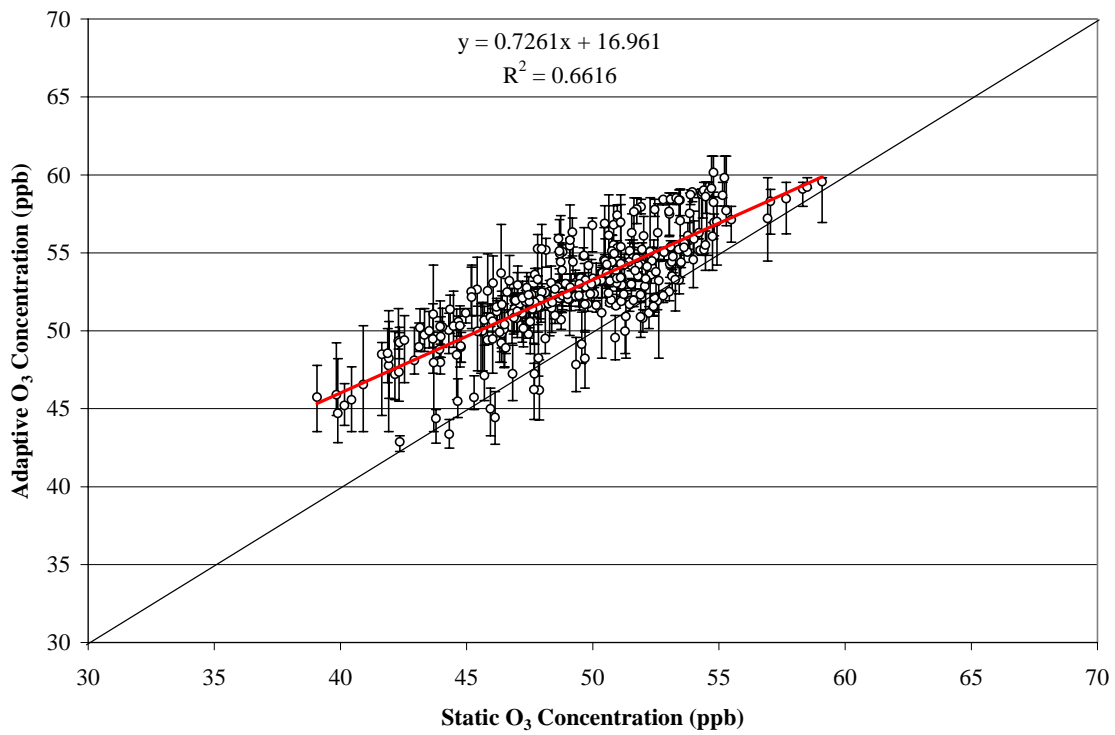
Figure 11. Static versus Adaptive Comparison for O3 Concentration for August 18, 08:00
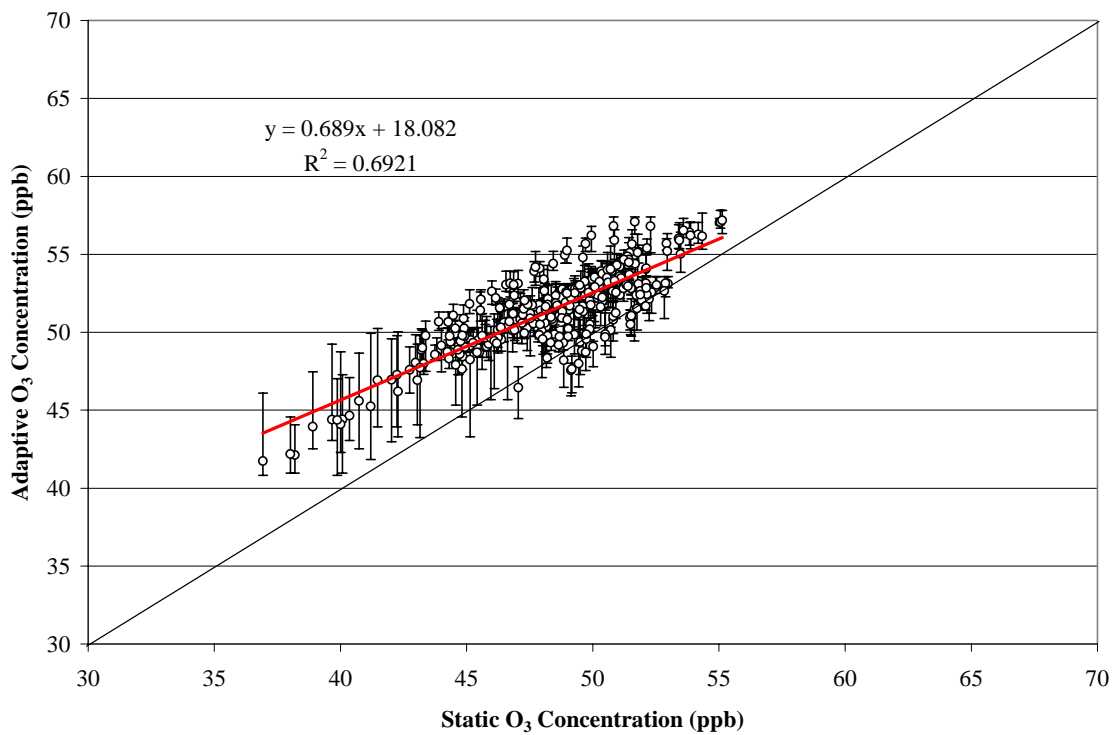
Figure 12. Static versus Adaptive Comparison for O3 Concentration for August 18, 09:00
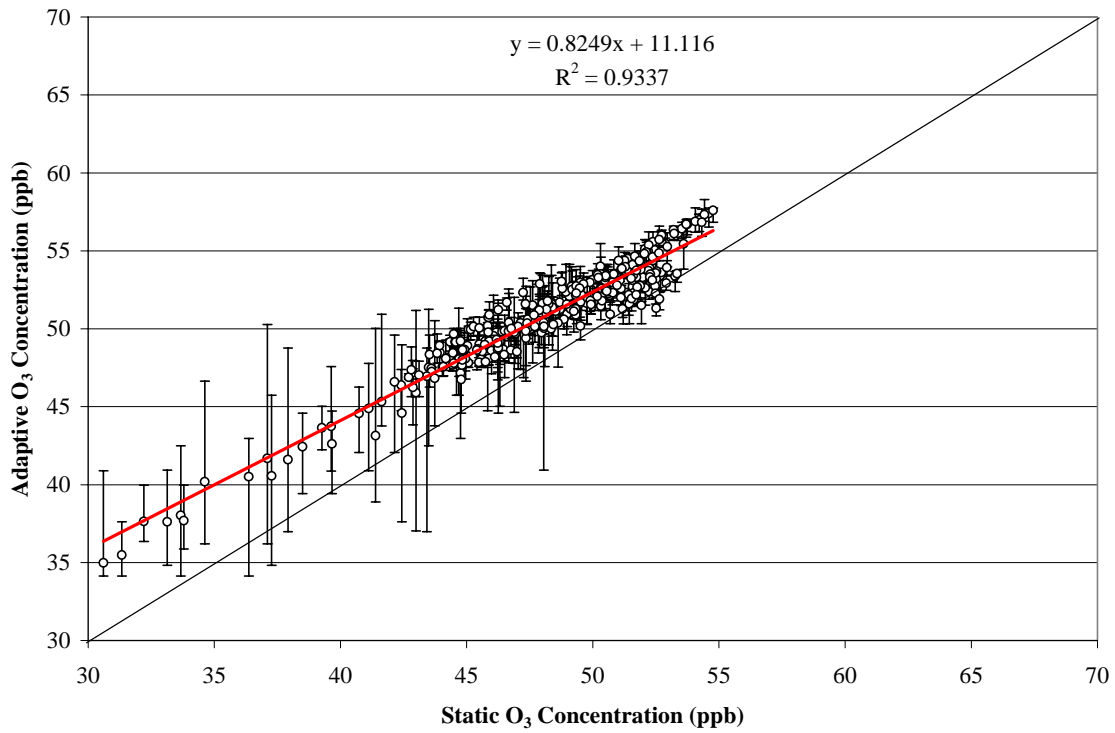
Figure 13. Static versus Adaptive Comparison for O3 Concentration for August 18, 10:00
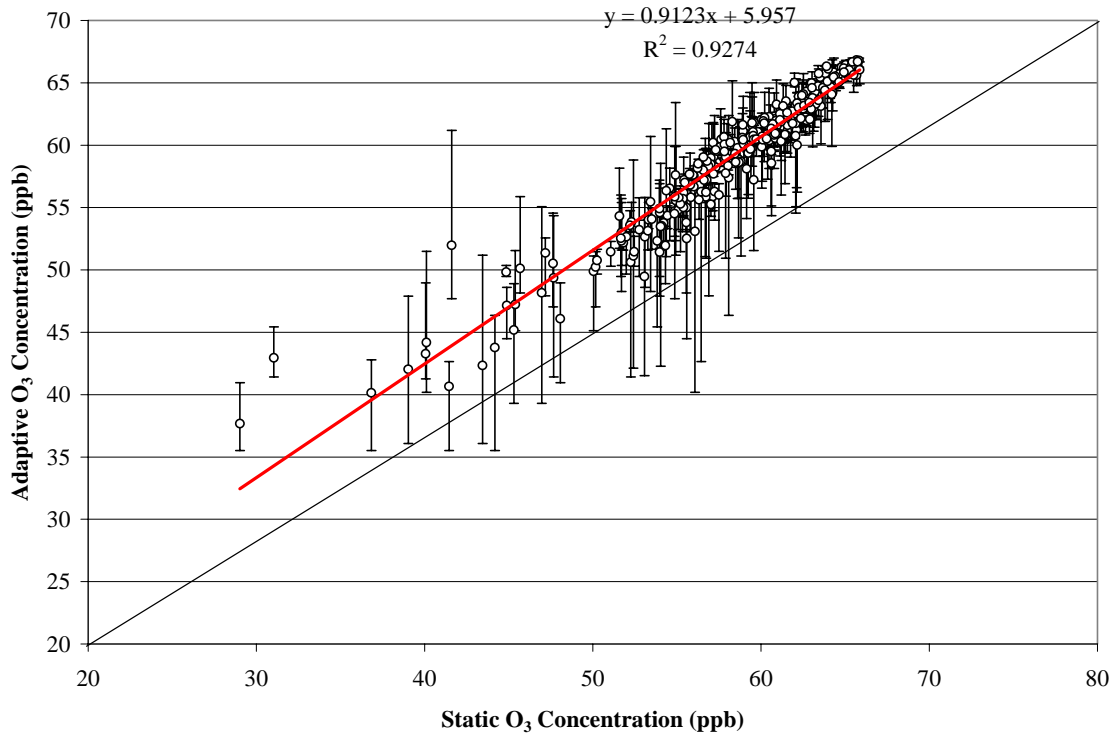
Figure 14. Static versus Adaptive Comparison for O3 Concentration for August 18, 13:00
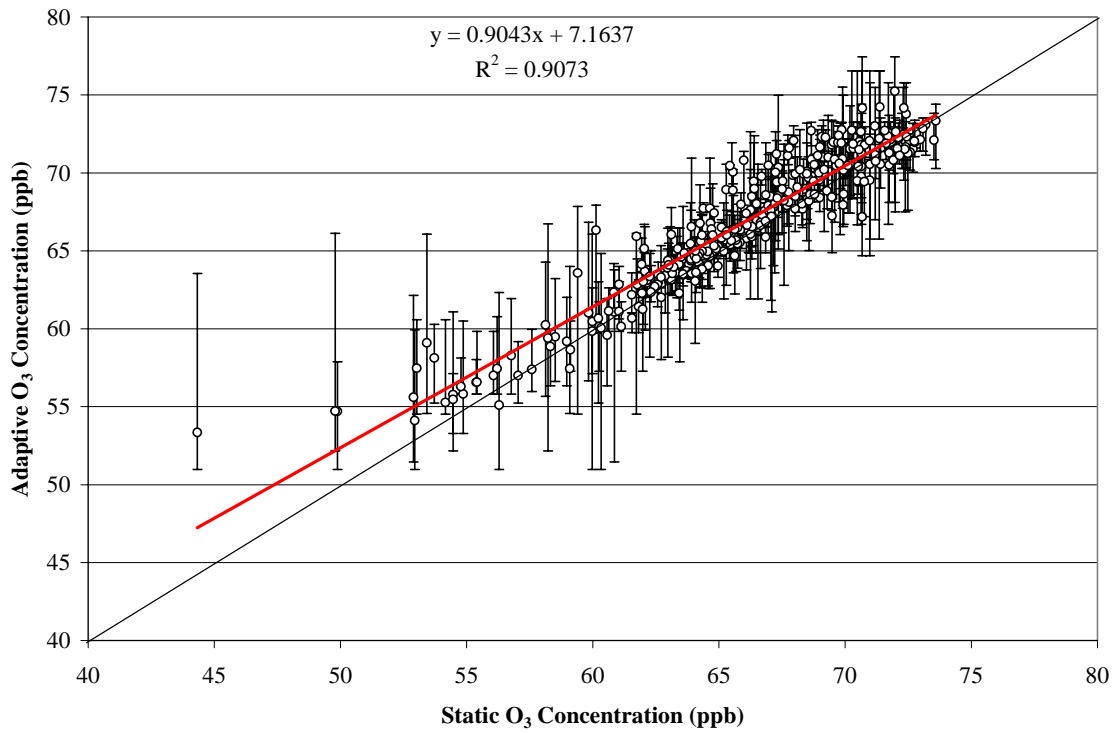
Figure 15. Static versus Adaptive Comparison for O3 Concentration for August 18, 14:00
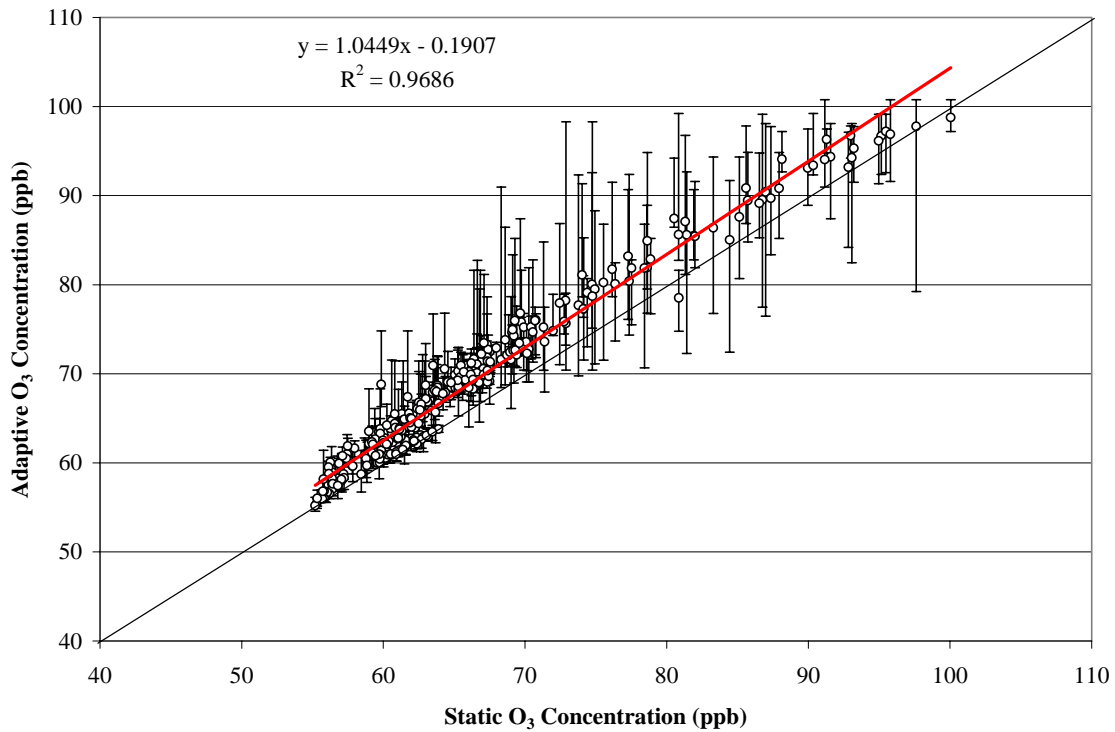
Figure 16. Static versus Adaptive Comparison for O3 Concentration for August 16, 18:00
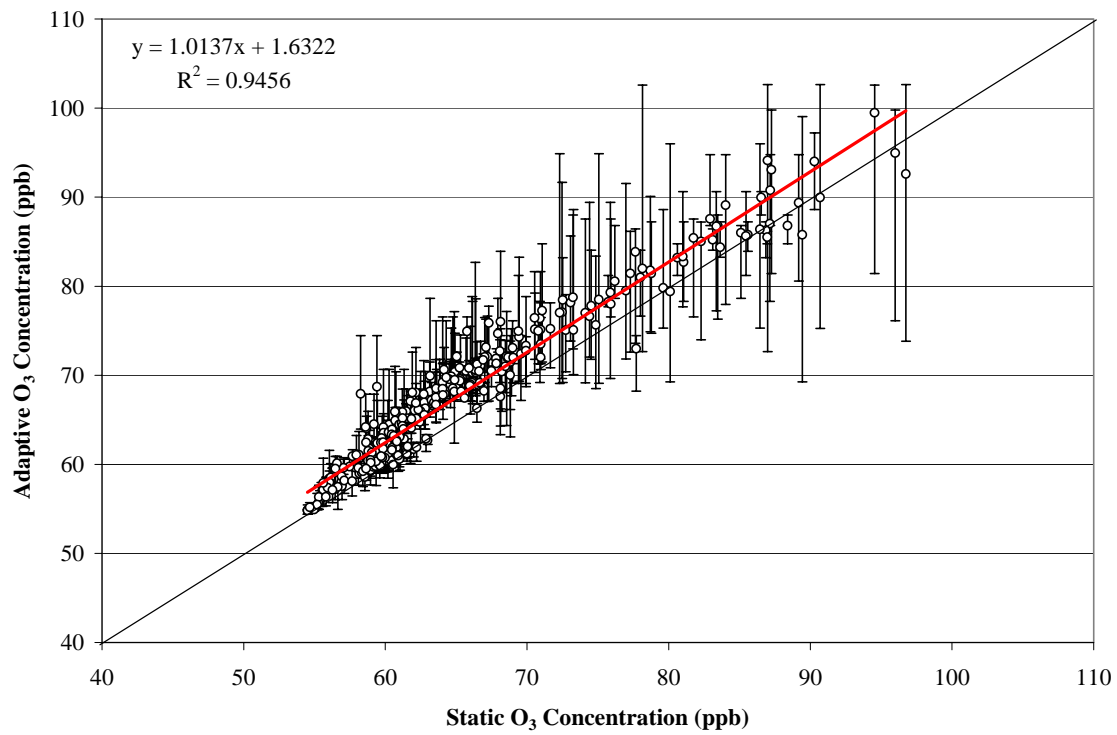
Figure 17. Static versus Adaptive Comparison for O3 Concentration for August 16, 19:00
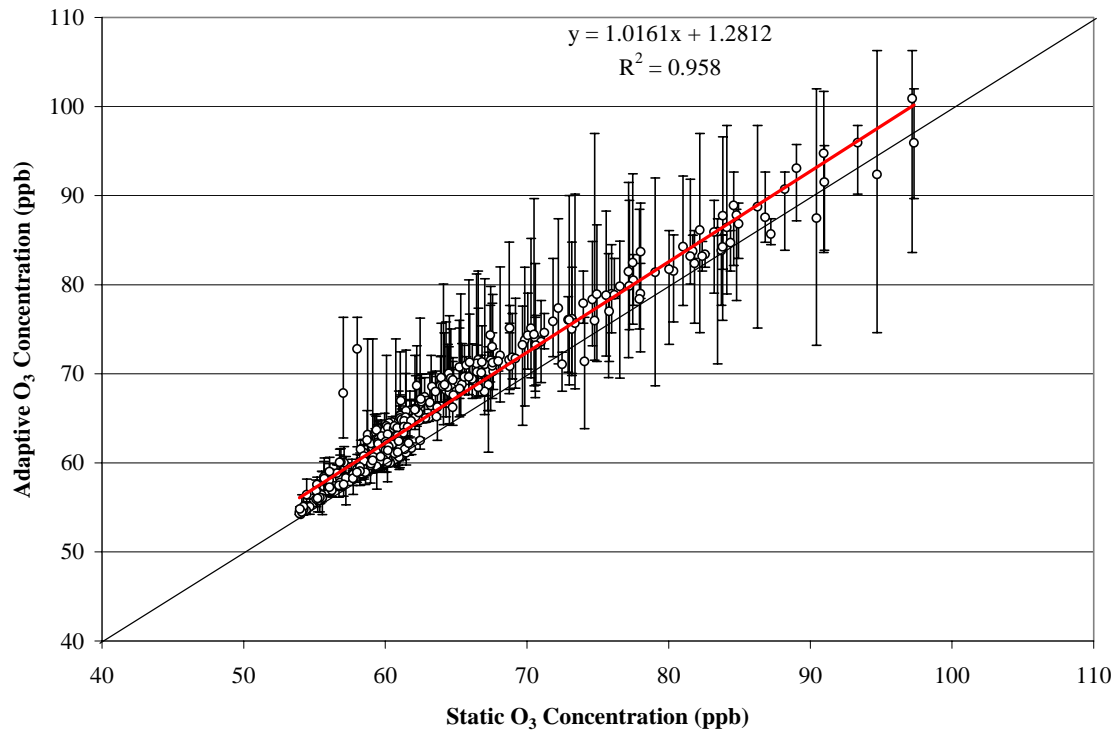
Figure 18. Static versus Adaptive Comparison for O3 Concentration for August 16, 20:00

$$y = 1.0028x + 1.972$$
$$R^2 = 0.9653$$
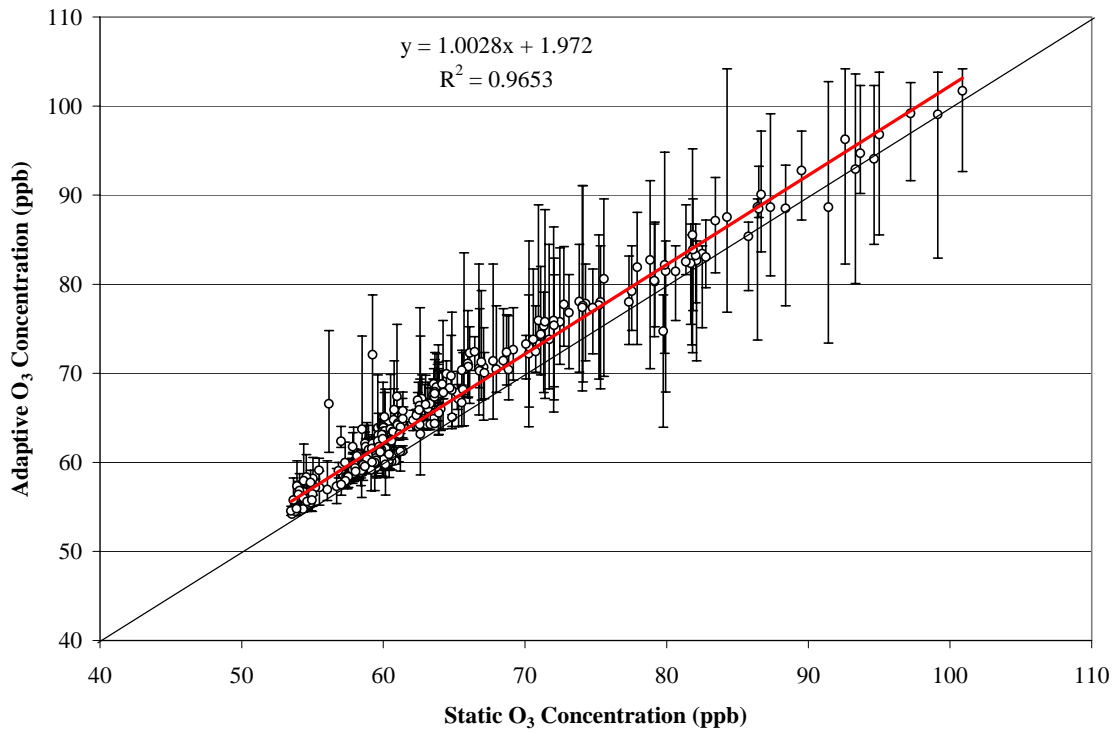
Figure 19. Static versus Adaptive Comparison for O3 Concentration for August 16, 21:00

$$y = 0.9714x + 3.9539$$
$$R^2 = 0.9471$$
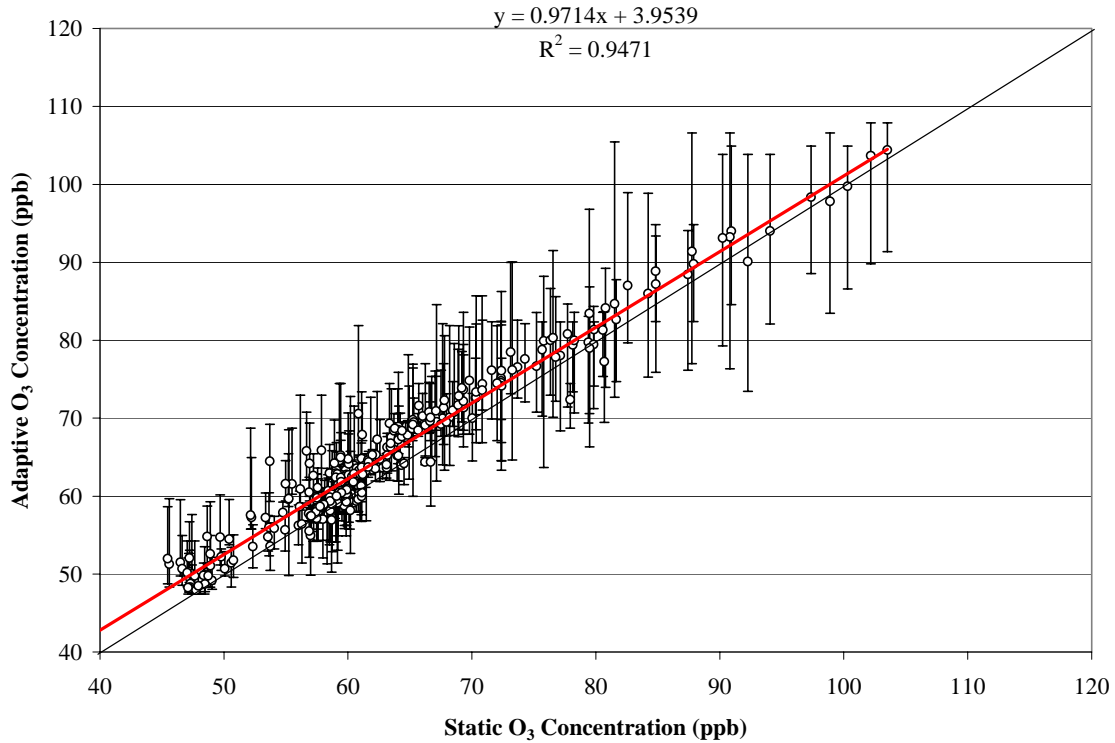
Figure 20. Static versus Adaptive Comparison for O3 Concentration for August 16, 22:00

$$y = 0.9339x + 5.3086$$
$$R^2 = 0.9048$$
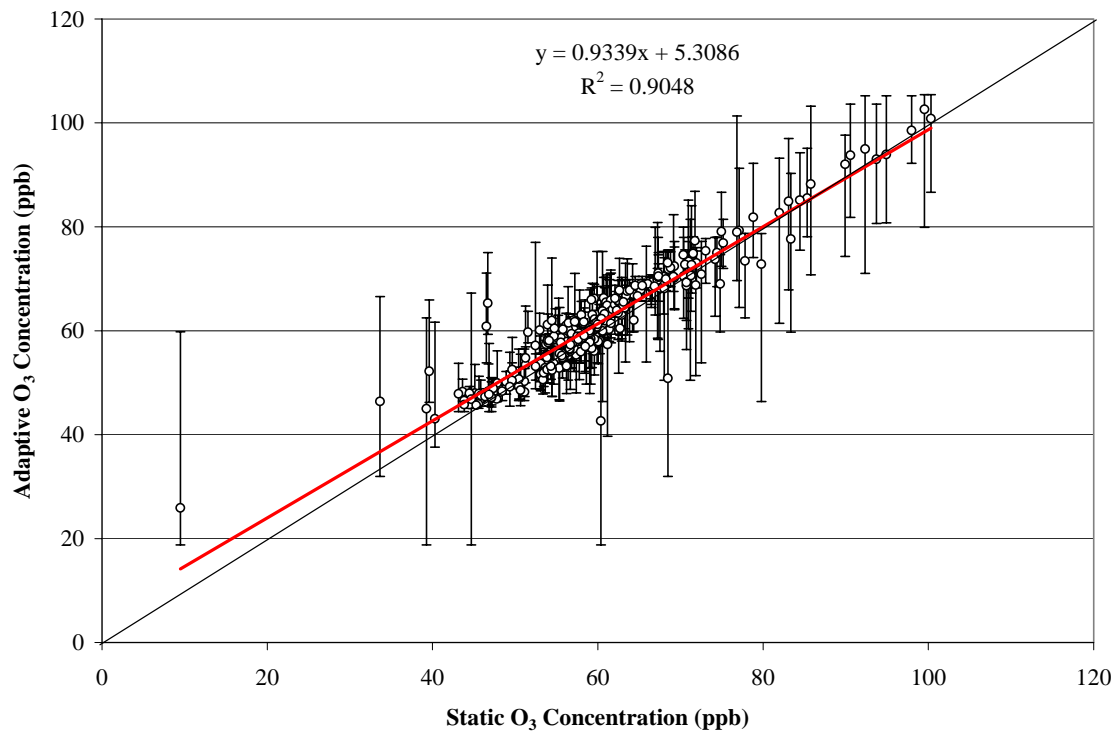
Figure 21. Static versus Adaptive Comparison for O3 Concentration for August 16, 23:00
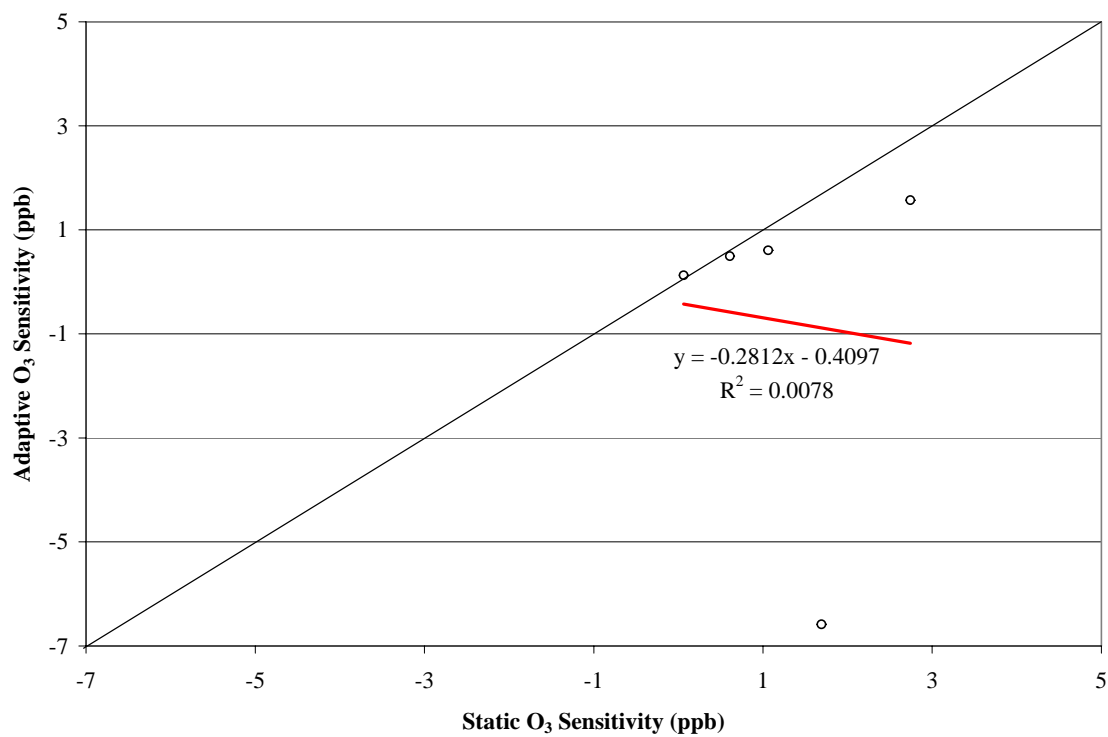
Figure 22. Static versus Adaptive Comparison for O3 Sensitivity for August 15, 18:00
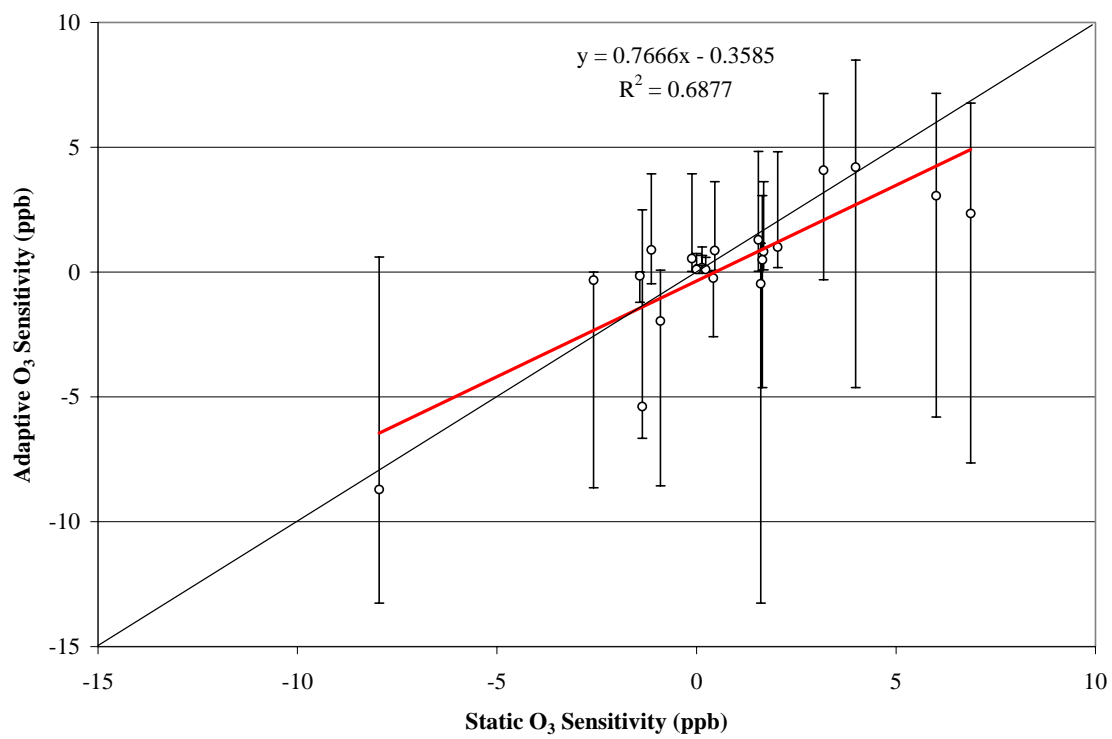
Figure 23. Static versus Adaptive Comparison for O3 Sensitivity for August 15, 19:00
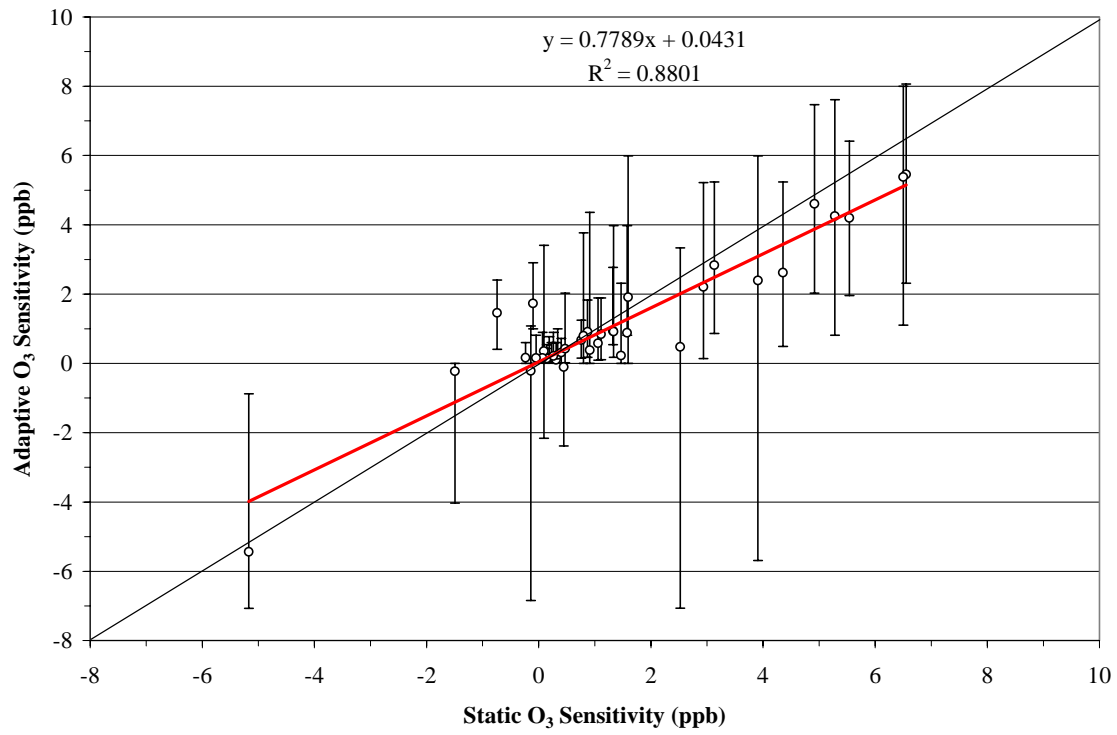
Figure 24. Static versus Adaptive Comparison for O3 Sensitivity for August 15, 20:00
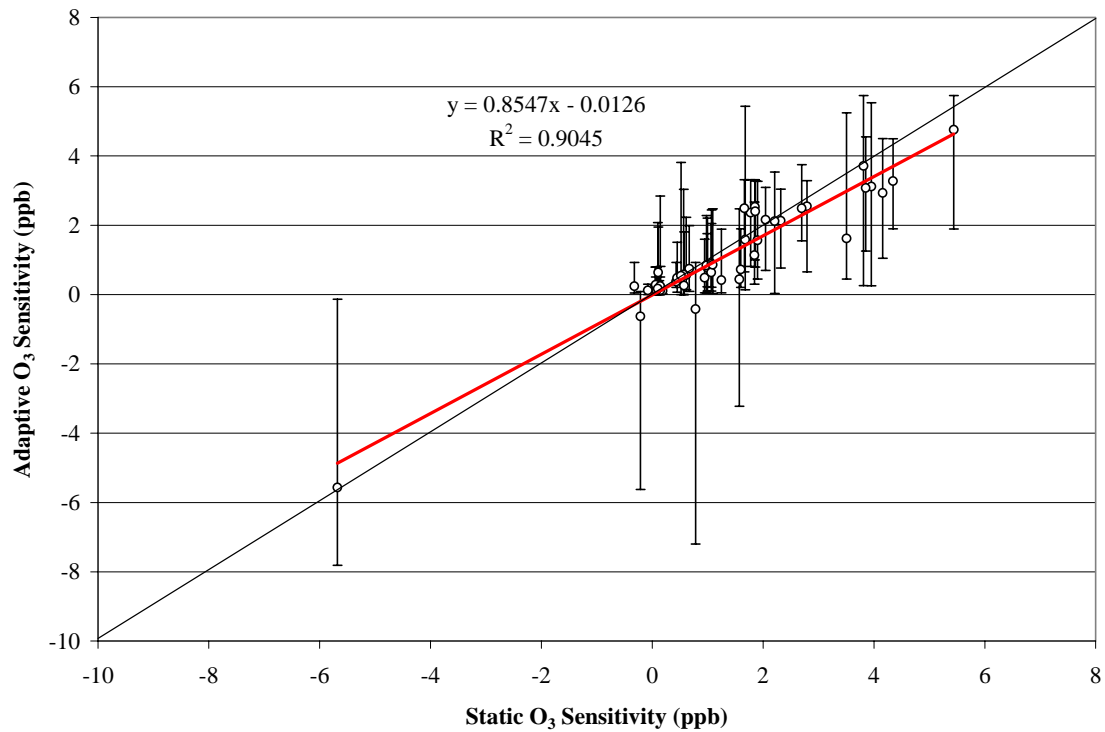
Figure 25. Static versus Adaptive Comparison for O3 Sensitivity for August 15, 21:00
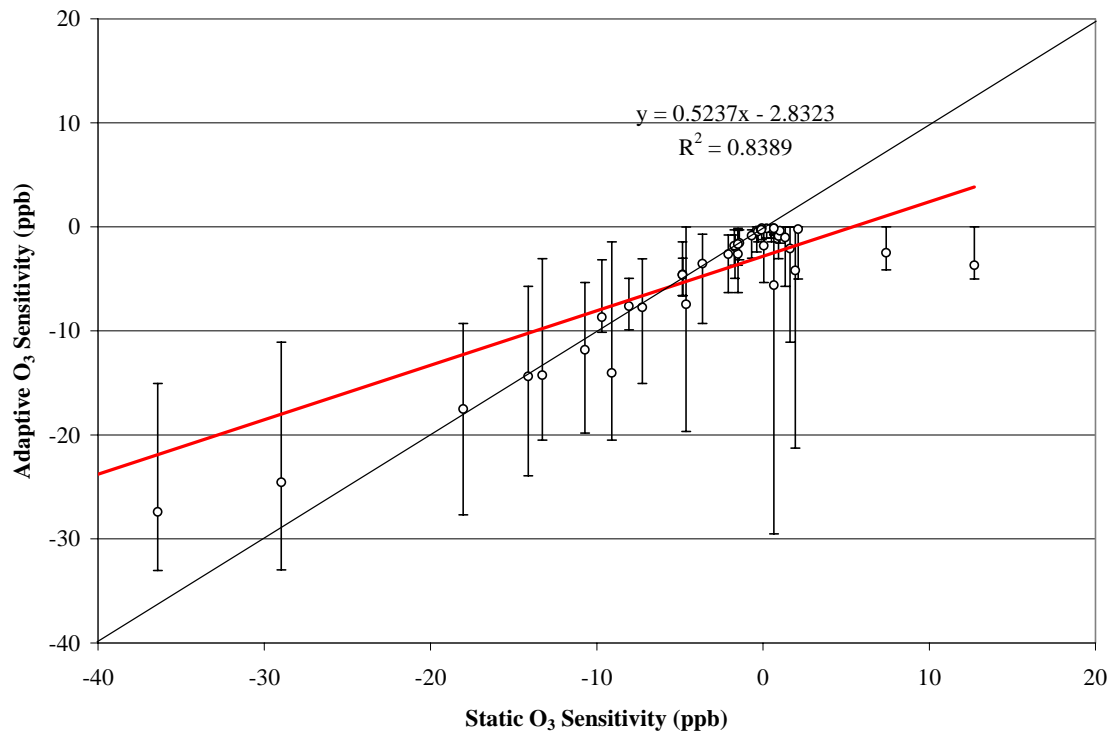
Figure 26. Static versus Adaptive Comparison for O3 Sensitivity for August 18, 02:00

Figure 27. Static versus Adaptive Comparison for O3 Sensitivity for August 18, 03:00

$$y = 0.5792x - 1.5747$$
$$R^2 = 0.7623$$

Figure 28. Static versus Adaptive Comparison for O3 Sensitivity for August 18, 04:00

$$y = 0.9591x - 0.1016$$
$$R^2 = 0.983$$
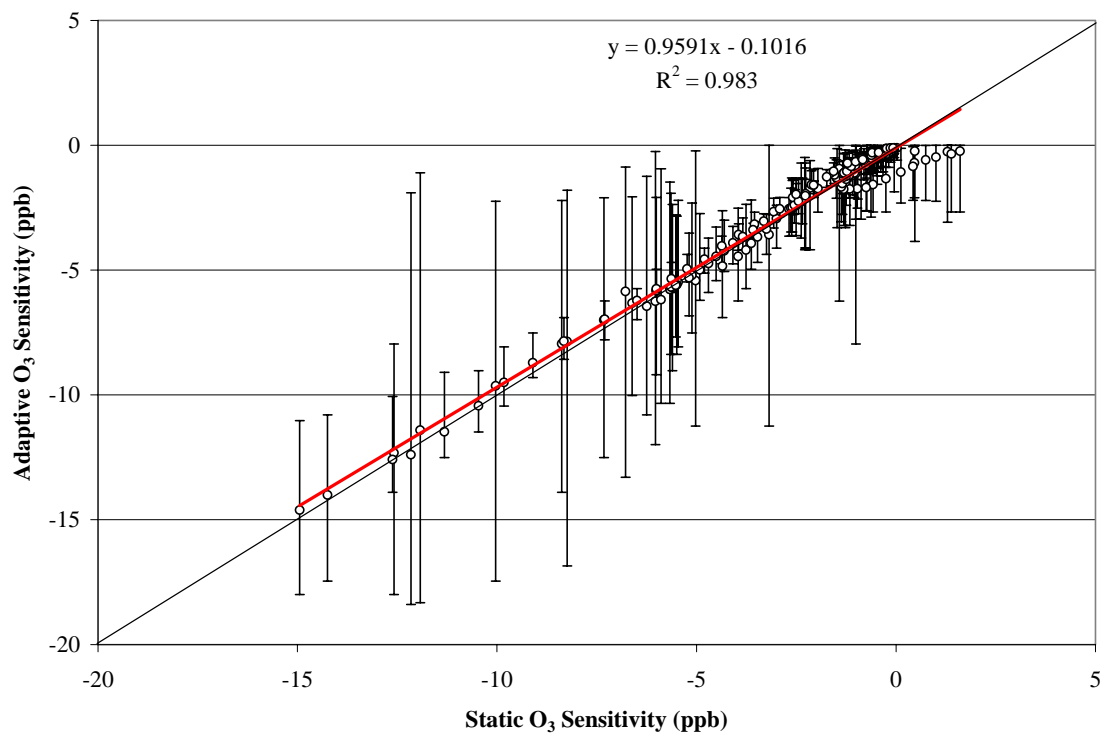
Figure 29. Static versus Adaptive Comparison for O3 Sensitivity for August 18, 05:00

$y = 0.9786x + 0.0307$
$R^2 = 0.9835$
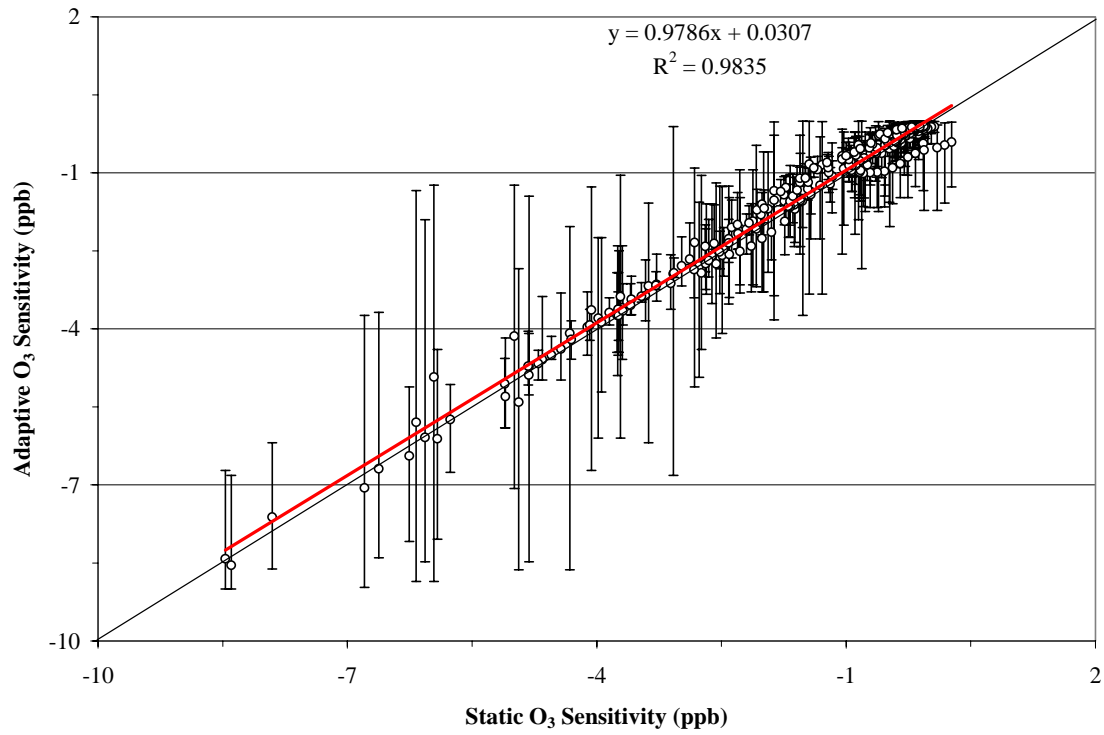
Figure 30. Static versus Adaptive Comparison for O3 Sensitivity for August 18, 06:00

$y = 1.0028x + 0.0687$
$R^2 = 0.9712$
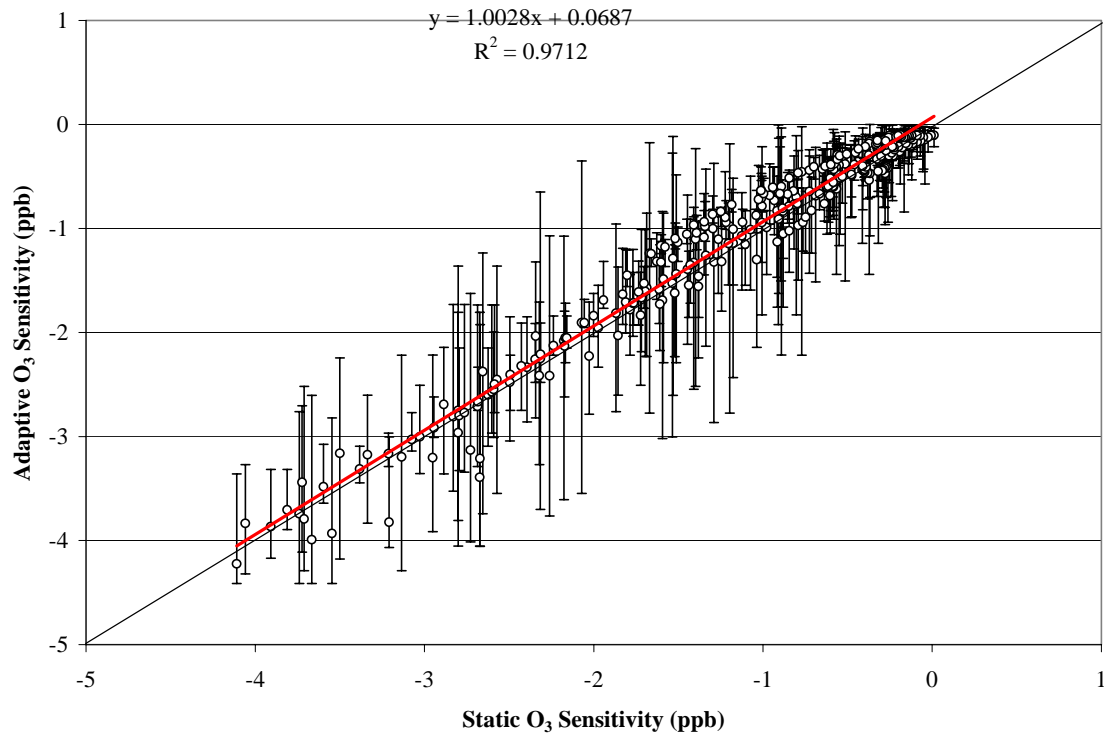
Figure 31. Static versus Adaptive Comparison for O3 Sensitivity for August 18, 07:00

$$y = 0.9668x + 0.0461$$
$$R^2 = 0.9721$$
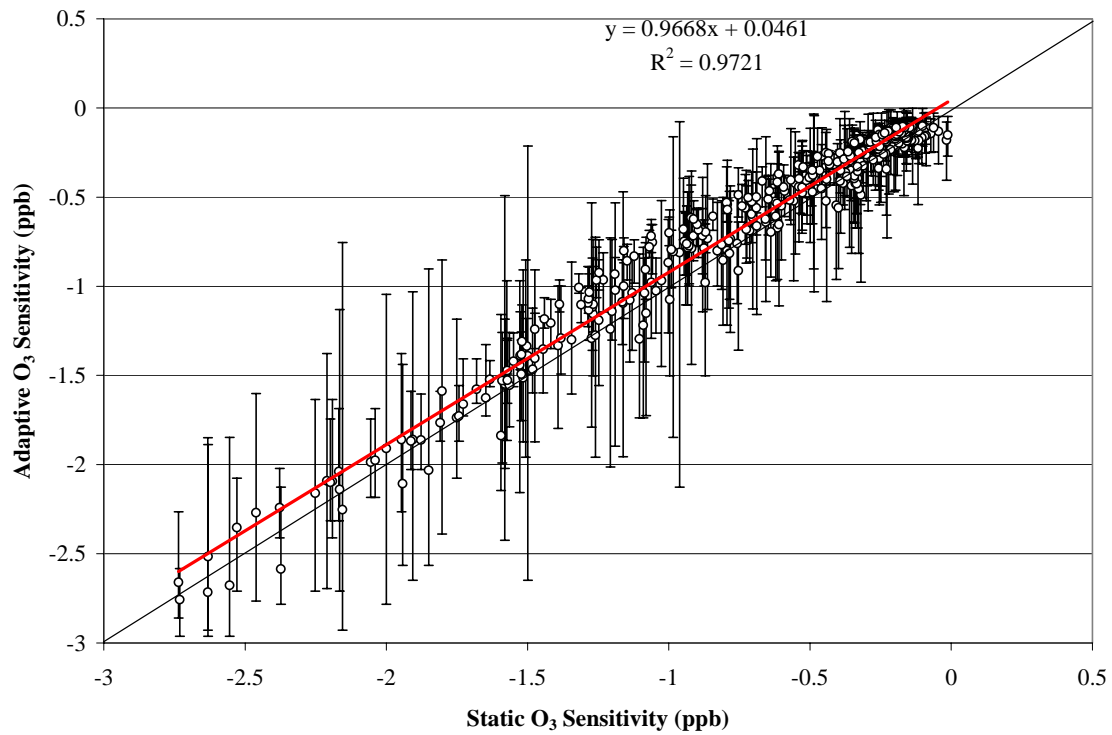
Figure 32. Static versus Adaptive Comparison for O3 Sensitivity for August 18, 08:00

$$y = 0.9522x + 0.0434$$
$$R^2 = 0.963$$
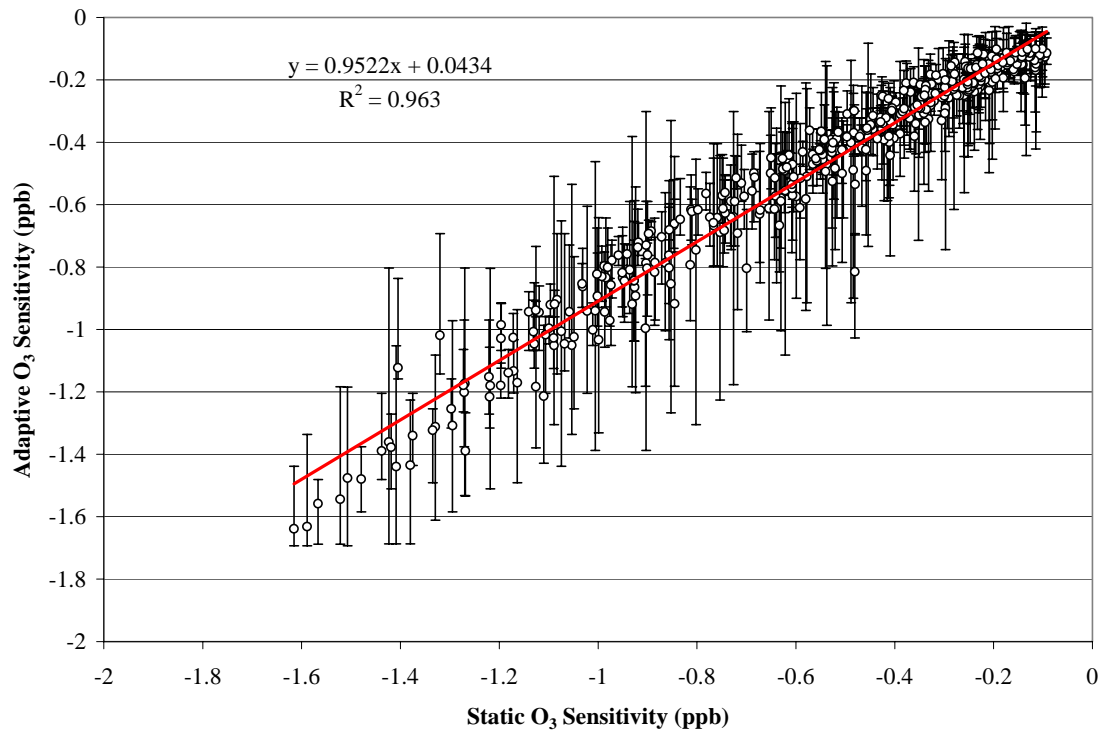
Figure 33. Static versus Adaptive Comparison for O3 Sensitivity for August 18, 09:00

$$y = 0.8899x + 0.0102$$
$$R^2 = 0.9614$$
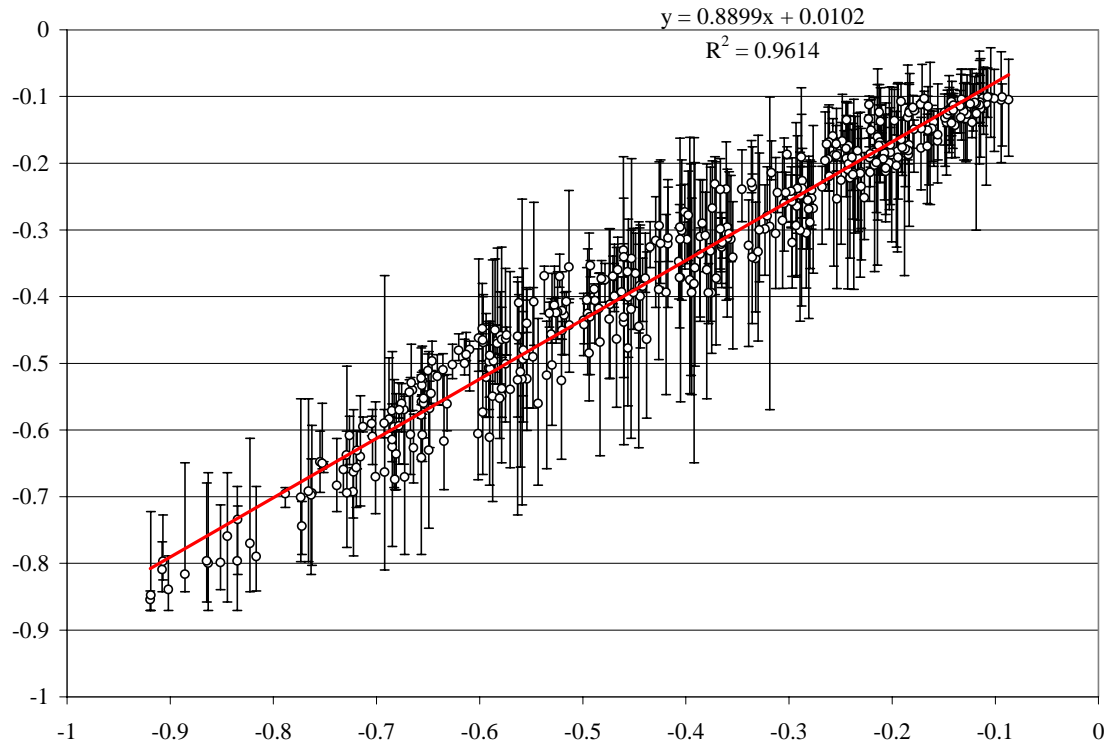
Figure 34. Static versus Adaptive Comparison for O3 Sensitivity for August 18, 10:00

$$y = 0.4908x - 1.1225$$
$$R^2 = 0.869$$

Figure 35. Static versus Adaptive Comparison for O3 Sensitivity for August 18, 13:00

**Figure 36. Static versus Adaptive Comparison for O3 Sensitivity for August 18, 14:00**
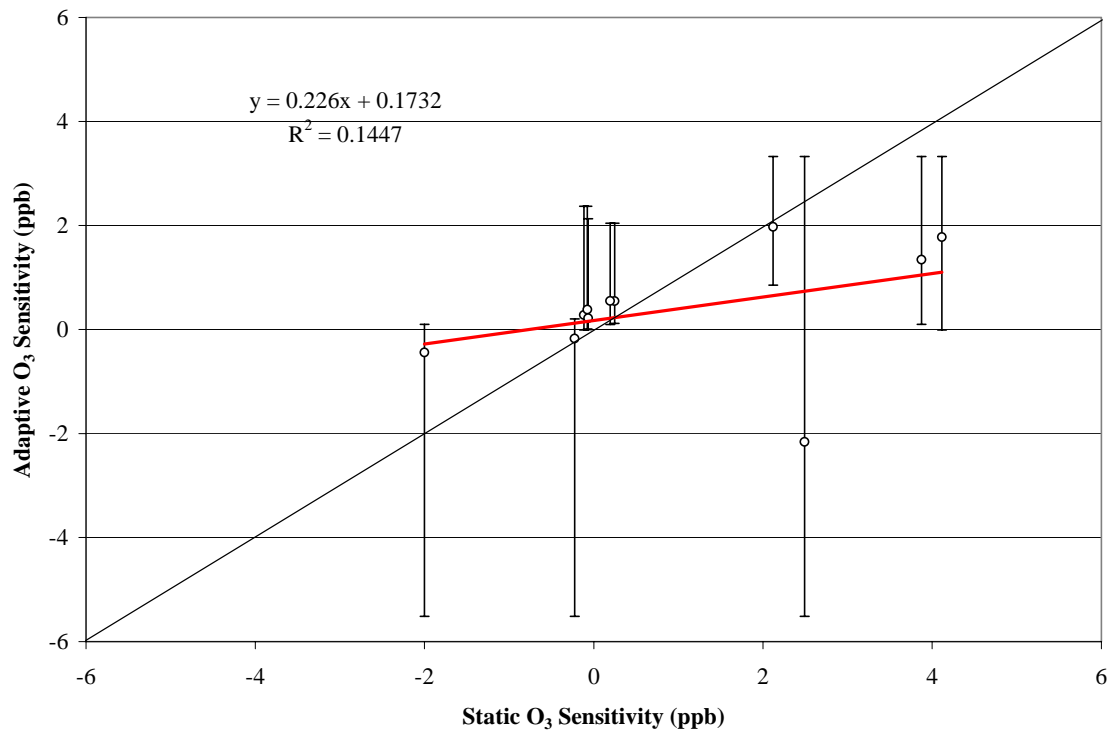
Figure 37. Static versus Adaptive Comparison for O3 Sensitivity for August 16, 18:00
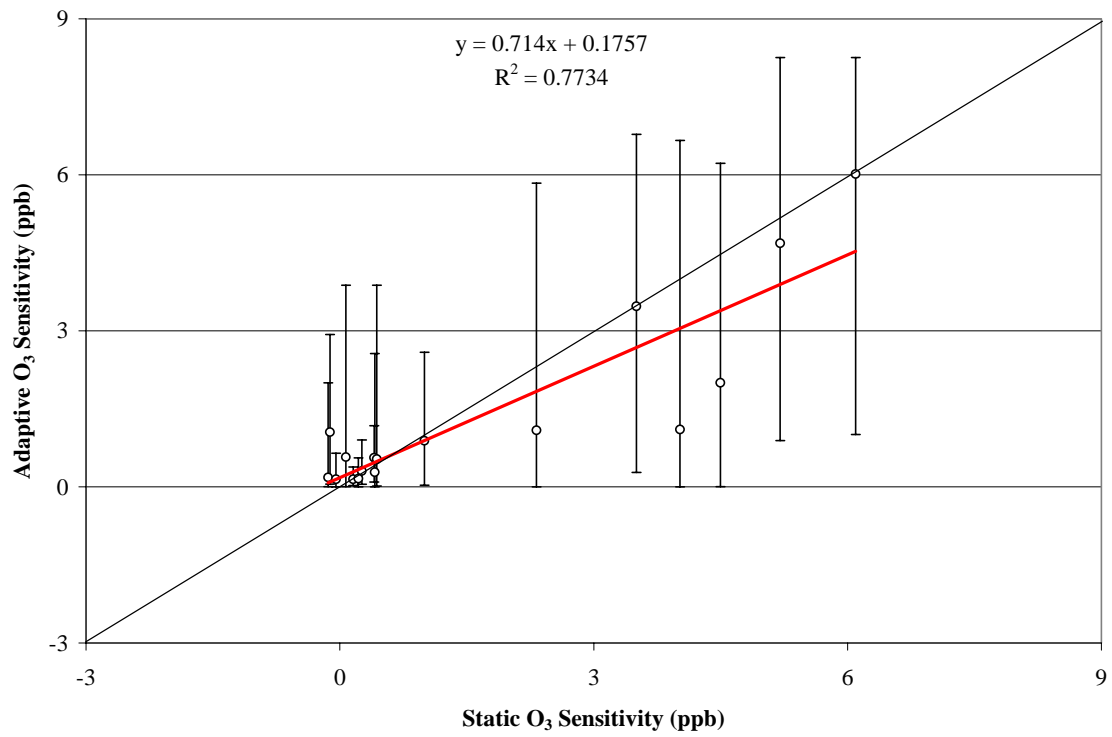
**Figure 38. Static versus Adaptive Comparison for O3 Sensitivity for August 16, 19:00**
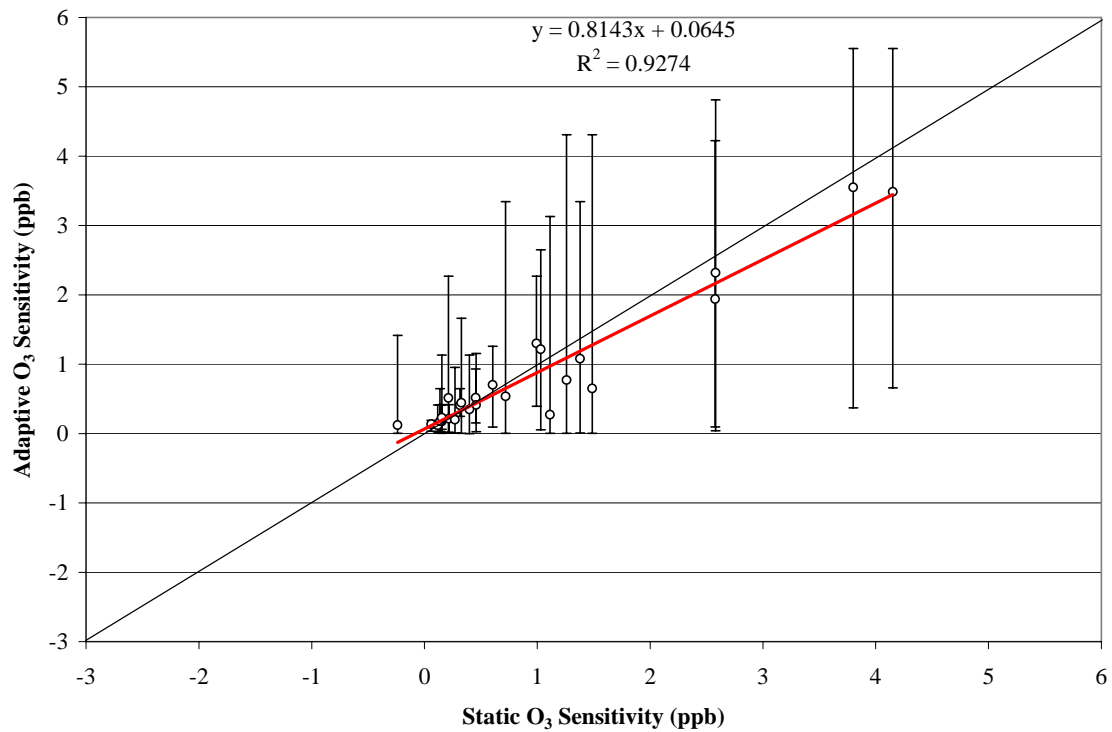
**Figure 39. Static versus Adaptive Comparison for O3 Sensitivity for August 16, 20:00**
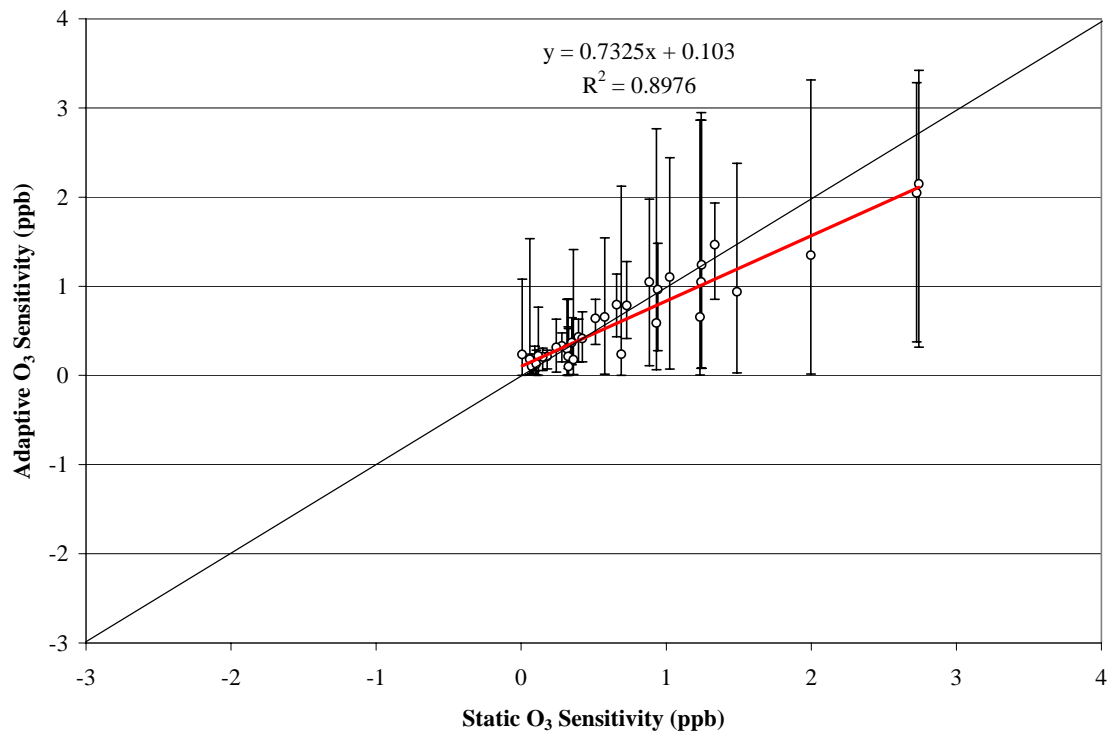
Figure 40. Static versus Adaptive Comparison for O3 Sensitivity for August 16, 21:00
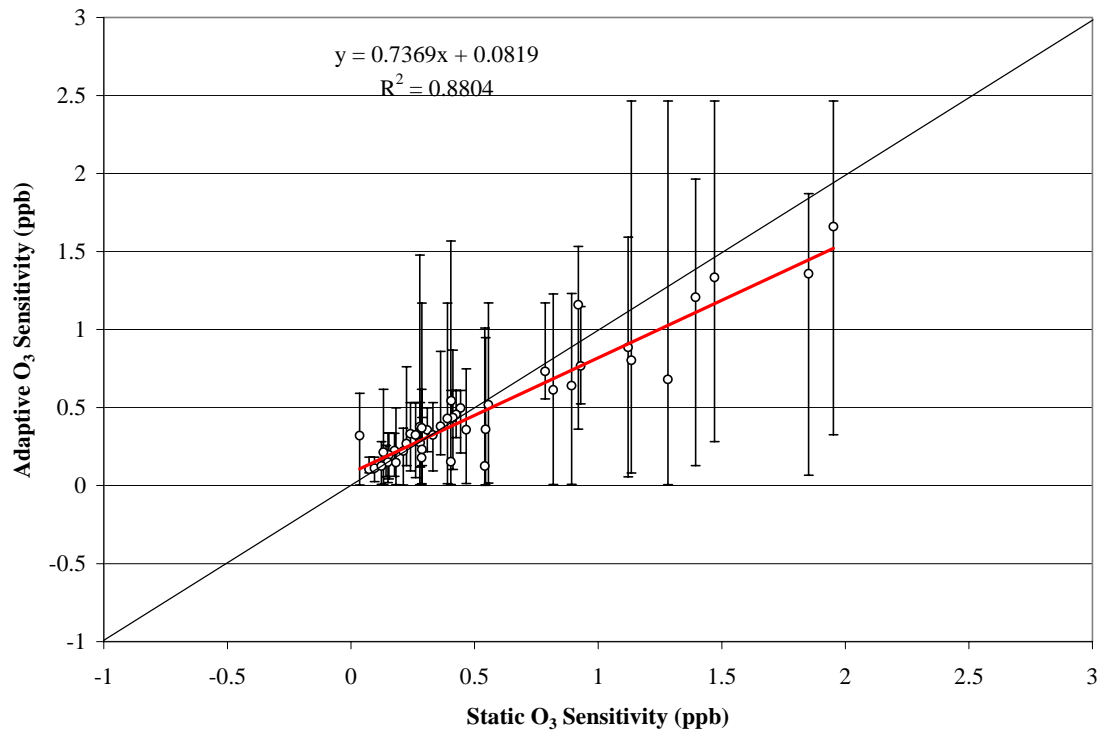
Figure 41. Static versus Adaptive Comparison for O3 Sensitivity for August 16, 22:00
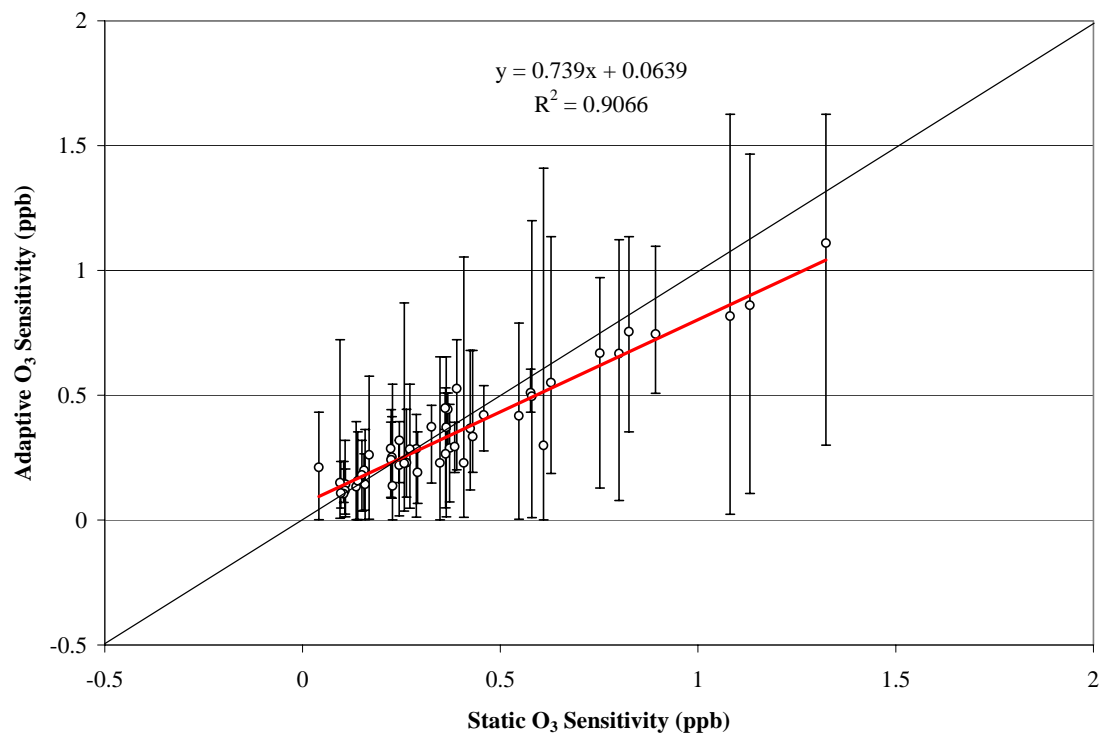
Figure 42. Static versus Adaptive Comparison for O3 Sensitivity for August 16, 23:00
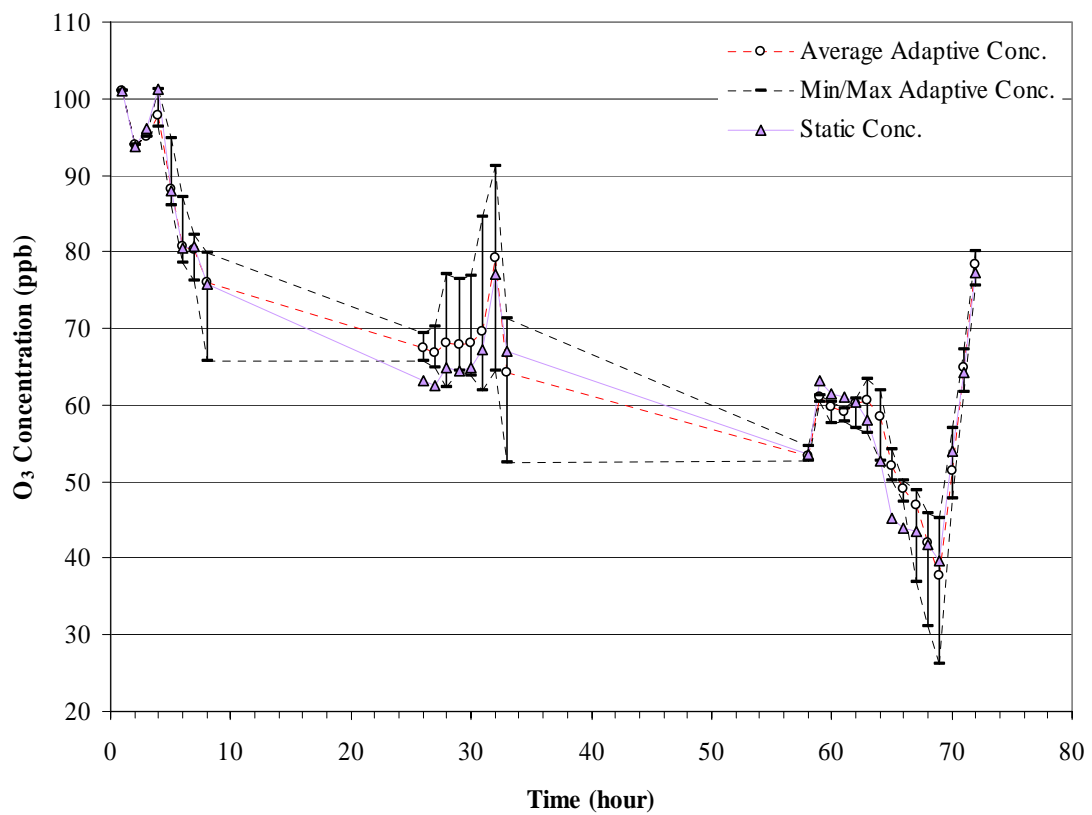
Figure 43 Static versus Adaptive O$_3$ predictions (ppb) for a specific cell near the fires

8.3 Publications

a) Conference Paper (Submitted to 2nd International Wildland Fire Ecology and Fire Management Congress, Orlando, FL 16-20 November 2003)

Adaptive Grid Modeling for Predicting the
Air Quality Impacts of Biomass Burning

Alper Unal and M. Talat Odman

School of Civil and Environmental Engineering, Georgia Institute of Technology, Atlanta, Georgia

1. INTRODUCTION

Wildland fires are essential in creating and maintaining functional ecosystems and achieving other land use objectives (Hardy and Leenhouts, 2001). However, biomass burning produces combustion byproducts that are harmful to human health and welfare (Hardy and Leenhouts, 2001; Battye and Battye, 2002). Guided by the Endangered Species Act (ESA), the Department of Interior (DoI) through the Fish and Wildlife Service (FWS) mandates that some military installations and air force bases in the South-Eastern United States use prescribed burning to recreate the natural fire regimes needed to maintain the health of its native long leaf pine forestland thus protecting the habitat of the endangered Red Cockaded Woodpecker (RCW). Proper management may require as much as 1/3 of the forest to undergo treatment by fire each year. These activities, however, can contribute significantly to already burdened local and regional air pollutant loads. In recognition of the conflicting requirements between the ESA and Clean Air Act (CAA) statutes, the Strategic Environmental Research and Development Program (SERDP), supported by Department of Defense (DoD), initiated a program to determine the effects of biomass burning from military installations. As part of this effort, we focused on determining the effects of biomass burning from military reservation, Fort Benning in Georgia, to the local and regional air quality, specifically, in Columbus metropolitan area.

Fort Benning, which covers an area of approximately 182,000 acres, is located in the lower part of central Georgia and Alabama, six miles southeast of Columbus, Georgia, as shown in Figure 1. Thus

emissions from this facility may be affecting the air quality in Columbus, which is reported to violate air quality standards for Ozone (EPD, 2003). The Columbus Environmental Committee is viewing the prescribed burning operation as a potential contributor to the ozone problem. This became a public relations concern for Fort Benning (Larimore, 2000).

Approximately 30,000 acres must be prescribed burned each year at Fort Benning, during the growing season (i.e., March through August). This period falls within the "ozone season." In order to restore the RCW habitat, longleaf seedlings are planted. Prescribed burnings continue from August through October for site preparation purposes, which also overlaps with the ozone season. These fires reduce unwanted vegetation that would compete with longleaf seedlings. Operational and safety constraints limit the burnings to an average of 300 acres per day (Environmental Management Division, 2000). For example, although an attempt is made to burn all RCW clusters during the growing season it is logistically impossible due to the number of clusters (75-80 annually) and scheduling conflicts with training. Natural firebreaks, such as roads, trails, drains, and creeks dictate the size of burn areas. All these limitations make it necessary to continue the burnings throughout the year. In realization of the Columbus ozone problem, the majority of the burnings (70-75%) were shifted to the January-April period, which is outside the "ozone season."

Currently, the only external constraint on prescribed burning arises as a result of smoke management concerns. Smoke complaints and the threat of litigation from smoke-related incidents / accidents

Figure 1   Location of Study Area

are the primary concerns. Fort Benning follows voluntary (not mandated by state or federal government) smoke management guidelines in an effort to minimize the adverse impacts from smoke. An additional concern is the effect of prescribed burning on ozone levels in Columbus. Forest fires produce nitrogen oxide and hydrocarbon emissions that form ozone (Cheng *et al.,* 1998; Battye and Battye, 2002; Ottmar, 2001). These pollutants may be transported downwind, mix with emissions from other sources and contribute to the poor air quality in urban areas. Sulfur dioxide and particulate matter emissions from forest fires are also of concern but, in general, they do not have a direct influence on the urban ozone problem. The ozone alert season is from 1 May through 30 September in Georgia. It is during this season that emissions from prescribed burning operations could affect smog levels in Columbus. In collaboration with the Partnership for a Smog-Free Georgia (PSG), Fort Benning is avoiding prescribed burns when meteorological conditions are conducive to ozone buildup. However, more complex methods are required to identify the real effects of biomass burning from Fort Benning on ozone problem in Columbus region.

Main objective in this study is to improve the ability to model the air quality impacts of biomass burning on the surrounding environment. For this purpose we equipped an advanced air quality model, Multiscale Air Quality Simulation Platform (MAQSIP) (Odman and Ingram, 1996), with two newly developed techniques; Adaptive Grid Modeling, and Direct Sensitivity Analysis to accurately isolate and determine the effects of biomass burning on ozone formation. In this paper we first describe the methods utilized and then discuss the important findings of the study.

2. METHODOLOGY

The atmospheric and chemical modeling systems currently used by various agencies tend to focus on a single scale that seems to be the most relevant to a particular air pollution problem. Global scale models address climate issues while regional scale models are used for the tropospheric ozone, regional haze or acid deposition studies. Urban scale smog models are being replaced with urban-to-regional scale models in most places where transport from other upwind sources play an

2

important role. On the local scale, models are used to deal with problems such as accidental releases. The domains of local scale models are limited by design; therefore, they cannot be used for regional scale impact studies.

One of the most advanced urban-to-regional scale models is the MAQSIP. Urban-to-regional scale models are used in developing emission control strategies for problems such as urban and regional ozone, acid deposition, or regional haze which is attributed to primary (emitted) and secondary (formed in the atmosphere) fine particulate matter. While these models are equipped with special tools to treat emissions from large power plants (Karamchandani et al, 2000), they lack the ability to resolve emissions from relatively small area sources such as those from prescribed burnings. To account for such area sources, the models rely on grid resolution. Prescribed burnings are performed over areas as small as one square kilometer (approximately 200 acres). This scale is too small for typical regional applications. Therefore, emissions from prescribed fires are blended with emissions from many other sources within the same grid cell of regional scale models. This would make it impossible to conduct an impact study that would target emissions from biomass burnings.

Another limitation of current air quality models is related to numerical errors involved during the simulations. Let us suppose that the grid cell size could be reduced to one square kilometer by using nested-grid techniques (Odman et al, 1997). In that case, a typical prescribed burning unit would cover a single grid cell. The effect of having or not having prescribed burning emissions from a single grid cell would be a small perturbation for air quality models. As the perturbation gets smaller in size, numerical errors that affect the simulation results become more important. The results of an impact study such as the one proposed here would be highly uncertain if the models were used as is. Therefore, urban-to-regional scale models, in their current state, are not very reliable tools for determining the impact of prescribed burning emissions to the surrounding environment.

The study of the impact of biomass burning from DoD facilities requires investigation of the interaction between various scales due to the fact that both the location of the facilities and the lifetimes of emitted pollutants are conducive to long-range transport. Below, we describe a methodology to improve current urban-to-regional scale air quality models with two modeling techniques. These techniques improve representation of the transport and transformation processes over a wide range of scales and provide more reliable source-receptor relationships. The product is a more reliable tool that can predict accurately the ultimate fate of pollutants emitted from specific sources such as DoD facilities.

2.1. Adaptive Grid Modeling

We developed an adaptive grid modeling approach to reduce the uncertainty in air quality predictions. By clustering the grid nodes in regions that would potentially have large errors in pollutant concentrations, the model is expected to generate much more accurate results than the traditional fixed, uniform grid counterparts. The repositioning of grid nodes is performed automatically through the use of a weight function that assumes large values when the curvature (change of slope) of the pollutant fields is large. The nodes are clustered around regions where the weight function bears large values, thereby increasing the resolution where it is needed. Since the number of nodes is fixed, refinement of grid scales in regions of interest is accompanied by coarsening in other regions where the weight function has smaller values. This yields a continuous multiscale grid where the scales change gradually. Unlike nested grids, there are no grid interfaces, which may introduce numerous difficulties due to the discontinuity of grid scales. The availability of computational resources determines the number of grid nodes that can be afforded in any model application. By clustering grid nodes automatically in regions of interest, the adaptive grid technique uses computational resources in an optimal fashion throughout the simulation.

A detailed description of the technique can be found in Srivastava et al. (2000). Here we will not repeat that information; instead, we will try to illustrate the technique and its potential with relevant applications. The adaptive technique was applied to problems with increasing complexity and relevance to air quality modeling. First, it was applied to pure advection tests (Srivastava et al., 2000). In a rotating cone test, the adaptive grid solution was more

accurate than the fixed uniform grid with the same number of grid nodes. The error in maintaining the peak of the cone was only 13% compared to 39% with the fixed grid: an accuracy that could only be achieved by using 22 times more grid nodes with a fixed uniform grid. Srivastava et al. (2001a) conducted a third test with concentric conical puffs of NO$_x$ and VOCs reacting in a rotational wind field. The parameters of this problem are such that, after a certain time, ozone levels drop below the background near the base of the conical puffs but they peak near the vertex of the cones. This feature was resolved by the adaptive grid solution while it was completely missed by the uniform fixed grid solution. When nine times more grid nodes were used, the fixed grid was finally able to reveal this feature but not as accurately as the adaptive grid technique.

Next, the adaptive grid technique was applied to the simulation of a power plant plume (Srivastava et al., 2001b). A two dimensional plume with a VOC/NO$_x$ emission ratio of 14% was advected with uniform winds and diffused over a background with a VOC/NO$_x$ ratio of 35. Other parameters were chosen to make the dispersion as realistic as possible. After about 12 hours of simulation, the composition of the plume was analyzed taking cross sections at various downwind distances. At 10 km downwind, the adaptive grid solution showed a NO$_x$ rich, but ozone deficient core. This feature, which is also observed in actual power plant plumes, was completely missing in the uniform grid solution, which artificially diffused the NO$_x$ and displayed highest ozone levels at the core of the plume. The adaptive grid, on the other hand, had ozone bulges developing near the plume edges. At a downwind distance of 30 km, these bulges continued to grow as NO$_x$ diffused slowly from the core to the edges (at a rate more in line with physical diffusion) and radicals were entrained into the plume. This plume structure started disappearing after about 80 km. At a downwind distance of 135 km, the plume was fully *matured* with an ozone peak at the center. The peak ozone concentration was larger than one predicted by the fixed uniform grid. A similar evolution of the plume was observed in the fixed uniform grid solution when the number of grid nodes was increased by a factor of nine. However, this solution was about five times more expensive than the adaptive grid solution.

After these and other testing of the algorithm (Odman et al., 2001; Khan et al, 2003), finally an adaptive grid AQM was developed (Odman et al., 2002). The model was applied to an ozone simulation in the Tennessee Valley (Khan and Odman 2003). Ozone results from this application were evaluated and showed significant improvement over those from fixed grid models, even those employing up to four times more grid cells. In several cases the agreement with observations was better compared to fixed grid models. When the reasons were investigated it was found that the complex source-receptor relationships, especially the long-range ones were much better resolved with the adaptive grid.

2.2. *Direct Sensitivity Analysis*

Sensitivity analysis is essential in determining source-receptor relationships and designing emission control strategies. The traditional "brute-force" method involves running the model several times, each time perturbing one type of emission (e.g., NO$_x$ or VOC) from a different source. If the perturbation is small, the brute-force method may not yield accurate sensitivities due to numerical errors propagating in the model. Our group has developed a new and powerful direct sensitivity analysis technique to study the response of air quality to various types of emissions (Yang et al, 1997). Unlike the brute force approach, this technique is not limited by the magnitude of the perturbation and, in theory, it can be used for even infinitesimal changes in emissions. Therefore, the technique has the potential of improving current models to a level where they can be used for impact analysis of relatively small sources such as military installations.

Air quality models are based on the atmospheric diffusion equation:

$$\frac{\partial c_i}{\partial t} + \nabla \cdot \left(\mathbf{u} \, c_i \right) = \nabla \cdot \left(\mathbf{K} \, \nabla c_i \right) + R_i + S_i \qquad (1)$$

Here, c_i is the concentration of the *i*th pollutant species, $\mathbf{u}$ describes the velocity field, $\mathbf{K}$ is the diffusivity tensor, $R_i(c_1, c_2, ...)$ is the chemical reaction term and S_i is a source term for certain types of emissions. The local sensitivity of the

concentration of a species (e.g., ozone) to a certain emission type (e.g., NO$_x$ or VOC) from a particular source can be defined as:

$$s_{ij}(t) = \frac{\partial c_i(t)}{\partial E_j} \qquad (2)$$

Here, s_{ij} is the sensitivity of c_i to emission E_j. Since the sensitivities to different emissions can vary by many orders of magnitude, it is necessary to define semi-normalized sensitivity coefficients, s^*_{ij}.

$$s^*_{ij}(t) = \widetilde{E}_j \frac{\partial c_i(t)}{\partial E_j} \qquad (3)$$

where $\widetilde{E}_j$ is the unperturbed emission field (i.e., without fire). Using direct derivatives of Equation (1) the following equation can be obtained for sensitivities.

$$\frac{\partial s^*_{ij}}{\partial t} = -\nabla(\mathbf{u}s^*_{ij}) + \nabla(\mathbf{K}\nabla s^*_{ij}) + J_{ik}s^*_{kj} + \frac{\partial R_i}{\partial \varepsilon_j}$$
$$+ \frac{\partial S_i}{\partial \varepsilon_j} - \nabla(\mathbf{u}c_i)\delta_{ij} + \nabla(\mathbf{K}\nabla c_i)\delta_{ij} \qquad (4)$$

Here, s^*_{ij} is the semi-normalized sensitivity coefficient, J_{ik} is the Jacobian matrix, ε_j is a scaling variable with a nominal value of 1, and δ_{ij} is a binary variable (either 1 or 0).

The similarity between Equations (1) and (4) allows us to use the same or very similar numerical solution techniques and calculate local sensitivities to emission sources simultaneously along with the species concentrations. This also makes the implementation of the technique in any model relatively straightforward. The technique is also computationally efficient because several of these sensitivities (the number being limited by available core memory) can be calculated simultaneously with a fractional increase in CPU time. The emission sources can be discerned by type as point, area, mobile, or biogenic, and by composition such as SO$_2$, NO$_x$, or VOC. Also, the location of the emission source can be specified, for example, as the boundaries of a DoD facility (to the grid scale resolution). The technique would predict the

sensitivity of air quality at any desired location in the modeling domain (e.g., sensitivity of ozone concentrations at a downwind urban center) to a fractional change in the emissions from the source of interest.

The technique has been evaluated in an application to the Southern California where the sensitivities of ozone concentrations to the domain wide reductions of mobile and area sources of NO$_x$ were compared to a brute-force method (Yang et al., 1997). This technique was used in an integrated modeling system focusing, simultaneously, on ozone, particulate matter and acid deposition (Boylan, et al., 2001). We investigated the sensitivity of particulate matter concentrations to the reductions of SO$_2$ and NO$_x$ emissions in the Southern Appalachian Mountains region. We also investigated the sensitivity of ozone concentrations to NO$_x$ and VOC emissions from different states, using state boundaries as sub-regions. As part of that project, we compared our method to the brute-force approach for ozone sensitivities to domain wide NO$_x$ and VOC emissions. The general agreement between the direct sensitivity and the brute-force method shows that the former is a reliable tool. Whenever we observed differences, we were able to relate the difference to the numerical errors associated with the brute force technique and show that the direct sensitivity method yields results that are more accurate.

3. AIR QUALITY SIMULATIONS

3.1. Episode Selection

The episode selection is based primarily on the availability and quality of meteorological and emissions data and the impact potential of prescribed burns at Fort Benning on regional air quality. As part of Fall Line Air Quality Study (FAQS), we have already simulated several episodes during summer of 1999 and 2000 in Georgia using MM5 meteorological model and SMOKE emissions model. The ideal scenario for our case study is one with southeasterly winds, biomass burning performed at Fort Benning and high ozone levels observed at Columbus. Based upon contacts with Land Management Brach at Fort Benning we obtained the locations, date, and time of biomass burning efforts (Westbury, 2002). There were

biomass burnings at Fort Benning between August 15 and August 18 2000. Also ozone levels in Columbus region were over the standards at least four times and prevailing winds were southeasterly during the same period. Therefore, we decided to simulate the period from August 15 through August 18, 2000.

3.2. Data Preparation

Data preparation efforts included meteorological and emissions data preparation as well as post-processing. Meteorological data were obtained from FAQS. Detailed information on meteorological data preparation is given elsewhere (Hu *et al.*, 2003). Similarly emissions data were obtained from FAQS study. More information on emissions data can be obtained elsewhere (Unal et al., 2003; Hu et al., 2003). For biomass burning emissions First Order Fire Effects Model (FOFEM) Version 5, developed by Intermountain Fire Sciences Laboratory was utilized. In this model fuel type was assumed as natural fuel with long leaf pine trees. For some of the pollutants, such as speciated VOCs and NOx, emission factors provided by Battye and Battye (2002) were utilized.

3.3. Static Grid Simulation

To verify model efforts, a 4×4 km Static Grid version of the MAQSIP model was used in simulation for the selected episode. Lambert Conformal projection with parameters of 30^0N, 60^0N, and 90^0W, centered at 40^0N and 90^0W, was utilized for the domain. The 4×4 grid has 102 columns and 78 rows with 13 vertical layers. The results of the Static Grid run were compared with outputs from the FAQS project for the same location and time period. The comparison showed that Static Grid results were similar to FAQS results.
A separate run was made with emissions including fire as well. The difference between the concentrations of these two simulations yields an static grid "brute-force".

3.4. Adaptive Grid Simulation

The adaptive grid also used the same domain definitions as for the static grid. In adaptive runs inert fire tracer concentrations are used to calculate the weight function that drives the adaption. The tracer is assumed to be a product of the fires at Fort Benning emitted at the same rate as NO emissions from fire. The tracer is transported and deposited the same way as other fire species but it is non reactive. Two different runs were made with the Adaptive Grid model. These runs include: one run with base emissions; and one run with base emissions plus fire emissions, which also has the direct sensitivity calculations. In both runs the grid adapted to the same fire tracer, therefore the grids are identical in both simulations. The difference between the concentrations of these two simulations yields an adaptive grid "brute-force".

4. RESULTS AND DISCUSSIONS

First we compared the Adaptive Grid model with the Static Grid version. The tracer concentrations predicted by the two models as a result of fires at Fort Benning are shown in Figures 2 and 3. On August 15, 2000 at 19:00 UTM, two different fires happened at two different cells of the Static Grid, which is clearly observed in Figure 2. The fire to the south is emitting at a higher rate than the northern one, since the area burned is almost 1.5 times bigger. It should be noted that Static Grid distributes emissions uniformly to the whole cell area where the fire takes place.

Figure 3 presents concentrations of the inert fire tracer as well as the grid orientation around Fort Benning at 19:00. From Figure 3 it is clear that Adaptive model increases the grid resolution around the fire at Fort Benning. Figure 3 also gives an enlargement of the figure where adaption occurs. At the points where fires occur, adaptive grid size reduces almost to 400m by 400 m, one tenth of the Static grid size. As seen in Figure 3, two distinct plumes from fires at Fort Benning are clearly visible during the simulation. Note that concentration gradients are much better resolved by the Adaptive Grid model than by the Static Grid model.

Another way of evaluating the results of an air quality simulation is to compare them to air quality observations from the existing monitoring network. Unfortunately, there are no measurements along the trajectory of the fire plumes during the simulated period. Special air quality measurements are required for this purpose.
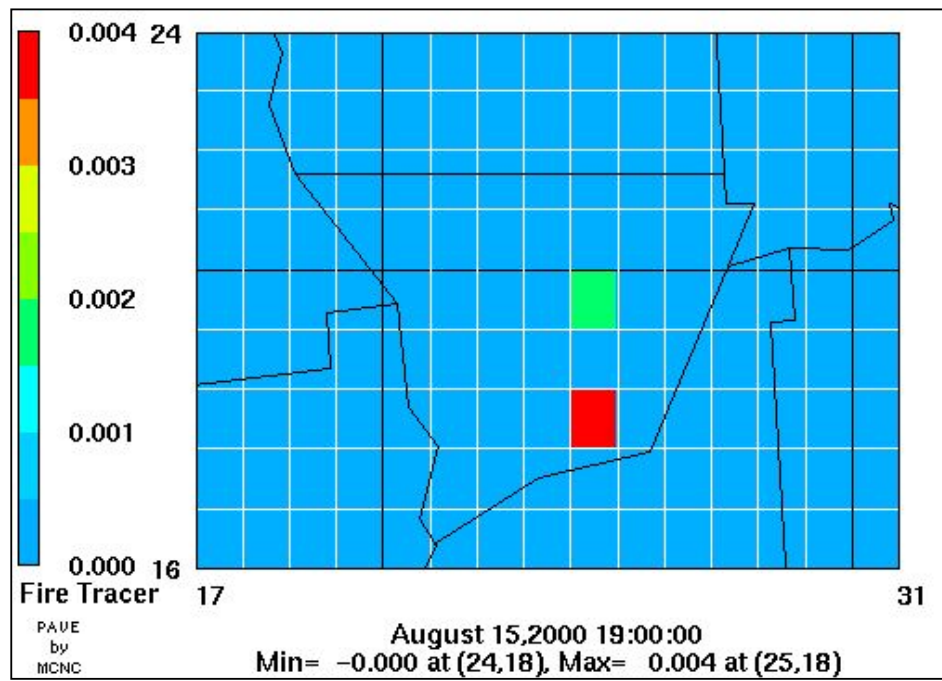
Figure 2 Static Grid Result for Inert Fire Tracer Concentrations (ppm)
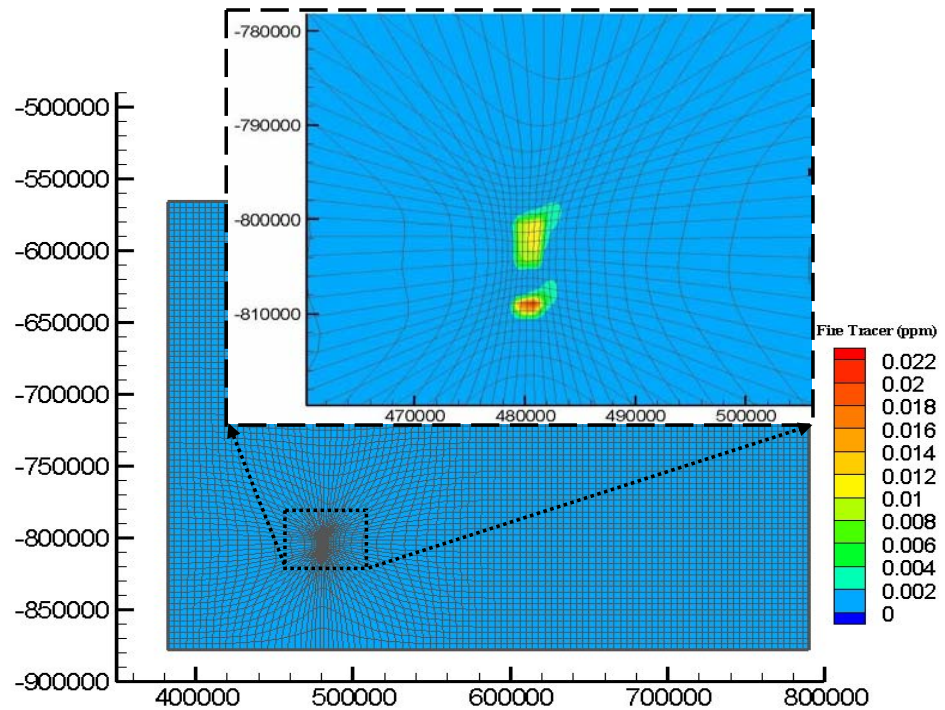
Figure 3 Adaptive Grid Result for Inert Fire Tracer Concentrations (ppm)

7

Researchers at Georgia Tech are currently collecting air quality data in the vicinity of Fort Benning as part of a study supported by SERDP to characterize pollutants emitted from prescribed burning (Baumann *et al.*, 2003). Data from this study were not available for the selected episode. However, as part of our future work we are planning to utilize these data for evaluation of our model.

Recall that another objective of this study was to utilize direct sensitivity method to estimate sensitivity of ozone to NO emissions from fires. For this purpose, we equipped our Adaptive Grid model with direct sensitivity technique. Figure 4 presents this sensitivity in the afternoon of August 15. While the fires reduce the ozone concentrations near the source by as much as 16 ppb, they result in an increase by as much as 7 pbb further downwind. Such a distinction between the near and the far field impacts is not so clear in the "brute-force" sensitivities calculated by the Static Grid model, as shown in Figure 5. The impacts of the fires on the air quality in Columbus are minimal on this particular day.

5. CONCLUSIONS AND FUTURE WORK

The objective of this study is to determine the air quality impacts of biomass burning on the surrounding environment. Fort Benning military reservation, Georgia, was utilized as a case study.

Current air quality models lack the capability of dealing with multi-scale air quality problems. In this study we utilized an Adaptive Grid model which inherently has the ability of continuous multiscale gridding. This method also reduces uncertainty in air quality predictions by clustering the grid nodes in regions that would potentially have large errors in pollutant concentrations.

We successfully implemented the Adaptive Grid model in our study and observed that concentration gradients are much better resolved by the Adaptive Grid model than the Static Grid version. This is due to the fact that Adaptive Grid model has 400m by 400m grid cells at locations where fires occur compared to 4km by 4km Static Grid cells.

It should be noted that we did not have the air quality observations data to compare our simulation

results for the selected episode. However, we are going to compare our results to a database that is being developed by researchers at Georgia Tech.

Another important aspect of this study is to implement direct sensitivity technique to our Adaptive Grid model. We successfully achieved this task and showed that our results are superior to the results of "brute-force" technique that we utilized with the Static Grid version. The Static Grid can not resolve the difference between the near and far field impacts as Adaptive Grid does. It was found that the impact of the fires ranged from 16 ppb reduction to 7 ppb increase in ozone concentrations. The impact of the fires on the air quality in Columbus area was minimal during the selected period.

Overall, we successfully incorporated two new techniques into a regional-scale air quality model. This study showed that Adaptive Grid model equipped with direct sensitivity method can accurately determine the impact of small-scale emission events on the air quality in larger scales. We showed that these techniques can be utilized to determine the impact of biomass burning.

6. REFERENCES

Battye, W. and Battye, R. (2002) "*Development of Emissions Inventory Methods for Wildland Fires*", Report Prepared for U.S. Environmental Protection Agency, Durham, NC.

Boylan, J., Wilkinson, J., Odman, T., Russell, A., Imhoff, R. (2001) Response and sensitivity of $PM_{2.5}$ in the southern Appalachian mountains. *A&WMA Annual Conference and Exhibition*, Orlando, Florida, June 24-28, 2001.

Cheng L., McDonald K.M., Angle R.P. and Sandhu H.S. (1998) Forest fire enhanced photochemical air pollution: A case study. *Atmospheric Environment* **32**, 673-681.

EPD (2003) "*Exceedances of Federal Air Quality Standards in Georgia, 2000*" Georgia Environmental Protection Division, http://www.air.dnr.state.ga.us/tmp/00exceedances/ ,Located: 08/22/2003.

Hardy, C. C. and Leenhouts, B. (2001) "Introduction Section", *2001 Smoke Management Guide for Prescribed and Wildland Fire*, Prepared by National Wildfire Coordinating Group, NFES-1279.

Hu, Y., Odman, M. T., and Russell, A. (2003a) "*Air Quality Modeling of the First Base Case Episode for the Fall Line Air Quality Study*," Prepared for Georgia Department of Natural Resources, Environmental Protection Division, June 2003.

Hu, Y., Odman, M. T., and Russell, A. (2003b) "*Meteorological Modeling of the First Base Case Episode for the Fall Line Air Quality Study*," Prepared for Georgia Department of Natural Resources, Environmental Protection Division, February 2003.

Karamchandani, P., Santos, I., Sykes, I., Zhang, Y., Tonne, C. and Seigneur, C. (2000) Development and evaluation of a state-of-the-science reactive plume model*. Environmental Science and Technology* **34**, 870-880.

Karsten, B., Zheng, M., Chang, M., and Russell, A. (2003) "Study of Air Quality Impacts Resulting from Prescribed Burning on Military Facilities" Presentation given at Georgia Institute of Technology.

Khan, M. N. and Odman, M. T. (2003) Application and performance evaluation of an adaptive grid air quality model, in preparation.

Khan, N. K., Odman, M. T. and Karimi, H. (2003) Evaluation of algorithms developed for adaptive grid air quality modeling using surface elevation data," *Computers, Environment and Urban Systems*, in press.

Larimore, R. (2000) *Prescribed Burning on the Fort Benning Military Reservation*. Presentation to the Columbus Environmental Committee, August 8, 2000

Odman, M. T. and Ingram, C. L. (1996), *Multiscale Air Quality Simulation Platform (MAQSIP): Source Code Documentation and Validation*. Technical Report, ENV-96TR002, MCNC—North Carolina Supercomputing Center, Research Triangle Park, NC, 83 pp.

Odman, M. T., Khan M. N., and McRae, D. S. (2000b) Adaptive grids in air pollution modeling: Towards an operational model. *Millennium NATO/CCMS International Technical Meeting on Air Pollution Modelling and Its Application*, Boulder, Colorado, May 15-19, 2000.

Odman, M. T., Khan M. N., and McRae, D. S. (2001) Adaptive grids in air pollution modeling: Towards an operational model," in Air Pollution Modeling and Its Application XIV, pp. 541-549, (S.-E. Gryning and F. A. Schiermeier, Eds.), New York: Kluwer Academic/Plenum Publishers.

Odman, M. T., Khan, M. N., Srivastava, R. K. and McRae, D. S. (2002a) Initial application of the adaptive grid air pollution model," in Air Pollution Modeling and its Application XV, pp. 319-328 (C. Borrego and G. Schayes, Eds.), New York: Kluwer Academic/Plenum Publishers

Odman, M. T., Mathur, R., Alapaty, K., Srivastava, R. K., McRae, D. S. and Yamartino, R. J. (1997) Nested and adaptive grids for multiscale air quality modeling. *Next Generation Environmental Models Computational Methods*, G. Delic and M. F. Wheeler, SIAM, Philadelphia, p. 59-68.

Ottmar, R. D. (2001) "Smoke Source Characteristics" *2001 Smoke Management Guide for Prescribed and Wildland Fire*, Prepared by National Wildfire Coordinating Group, NFES-1279.

Srivastava, R. K., McRae, D. S. and Odman, M. T. (2000) An adaptive grid algorithm for air quality modeling. *Journal of Computational Physics* **165**, 437-472.

Srivastava, R. K., McRae, D. S. and Odman, M. T. (2001a) Simulation of a reacting pollutant puff using an adaptive grid algorithm. *Journal of Geophysical Research*, in press.

Srivastava, R. K., McRae, D. S. and Odman, M. T. (2001b) Simulation of dispersion of a power plant plume using an adaptive grid algorithm. *Atmospheric Environment*, revisions submitted.

Unal, A., Tian, D., Hu, Y., Russell, T. "*2000 Emissions Inventory for Fall Line Air Quality Study (FAQS),*" Prepared for Georgia Department of

Natural Resources, Environmental Protection Division, April 2003.

Westbury, H. (2002) Personal communication on 10-21-2002.

Yang, Y.-J., J. G. Wilkinson and A. G. Russell, Fast direct sensitivity analysis of multidimensional photochemical models, *Environ. Sci. Technol*. **31**, 2859-68, 1997.
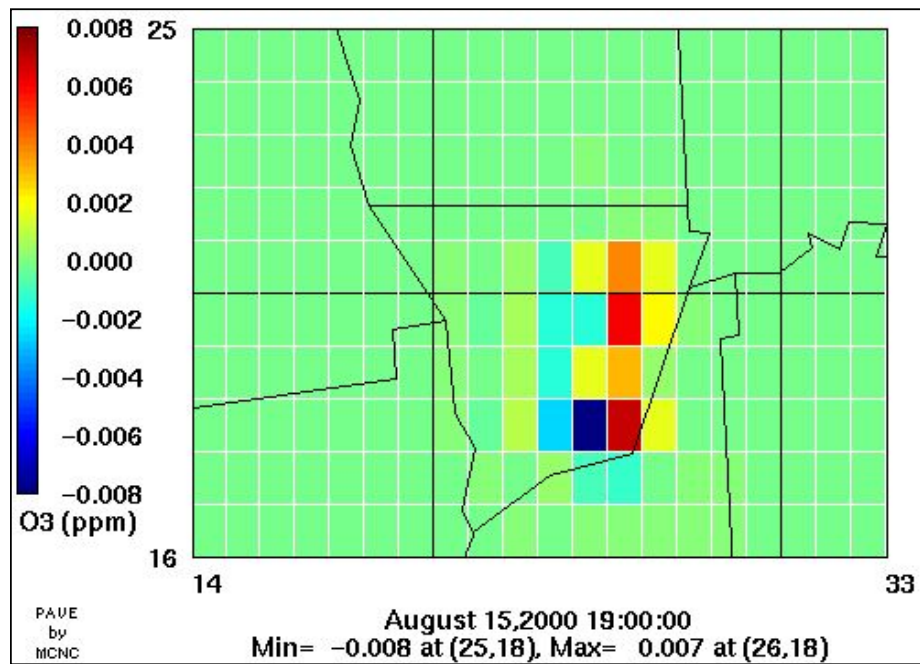
Figure 4 Static Grid Result for Brute Force Sensitivity of O_3 (ppm) to Fire Emissions
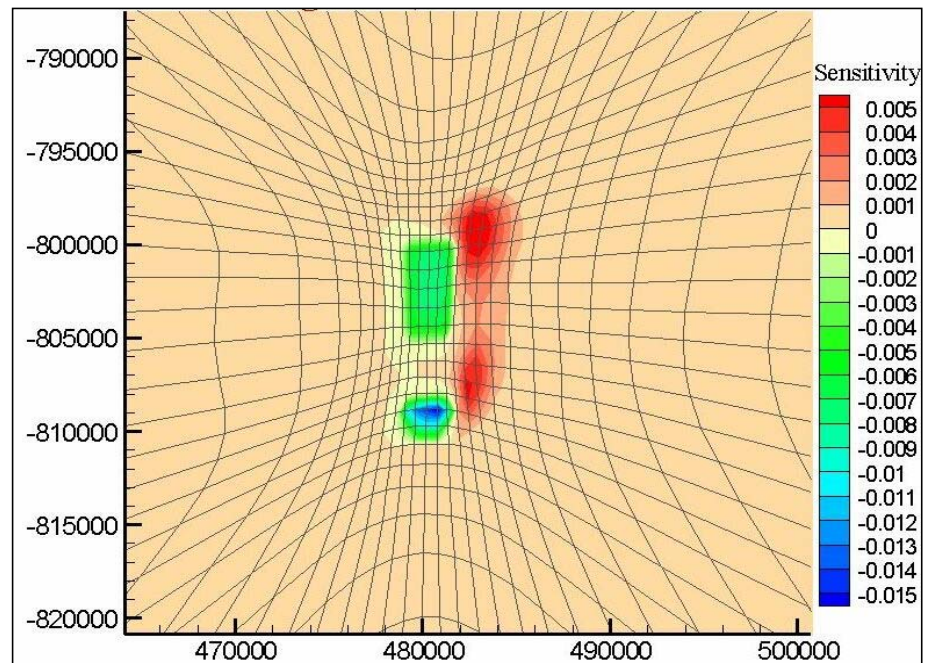
Figure 5 Adaptive Grid Result for Direct Sensitivity of O3 (ppm) to Fire Emissions

11

b) Conference Presentation (Presented at 2nd International Wildland Fire Ecology and Fire Management Congress, Orlando, FL 16-20 November 2003)

Adaptive Grid Modeling for Predicting the Air Quality Impacts of Biomass Burning

Alper Unal, Talat Odman

School of Civil & Environmental Engineering
Georgia Institute of Technology

2nd International Wildland Fire Ecology and
Fire Management Congress, Orlando, FL

16-20 November 2003

Georgia Institute of Technology

Motivation

Endangered Species Act

Clean Air Act

Motivation

- The endangered Red Cockaded Woodpecker (RCW) resides **only** in the mature long-leaf pine forests.

- Most of the forests are on federal and **military** lands.

- These ecosystems **require** periodic burning to maintain health.

- Prescribed burning is a safe and effective alternative to natural fire regimes.

Motivation
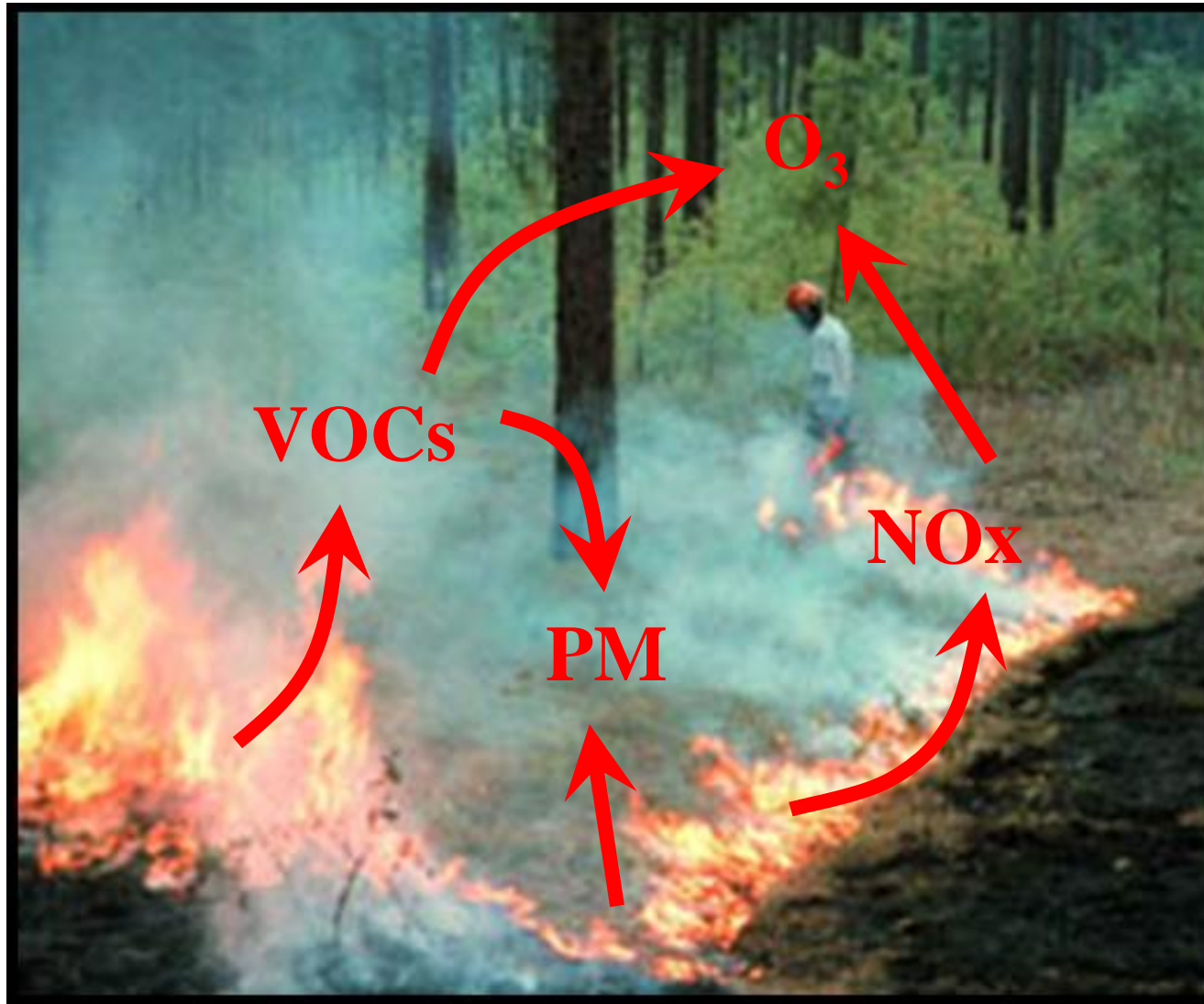
Motivation
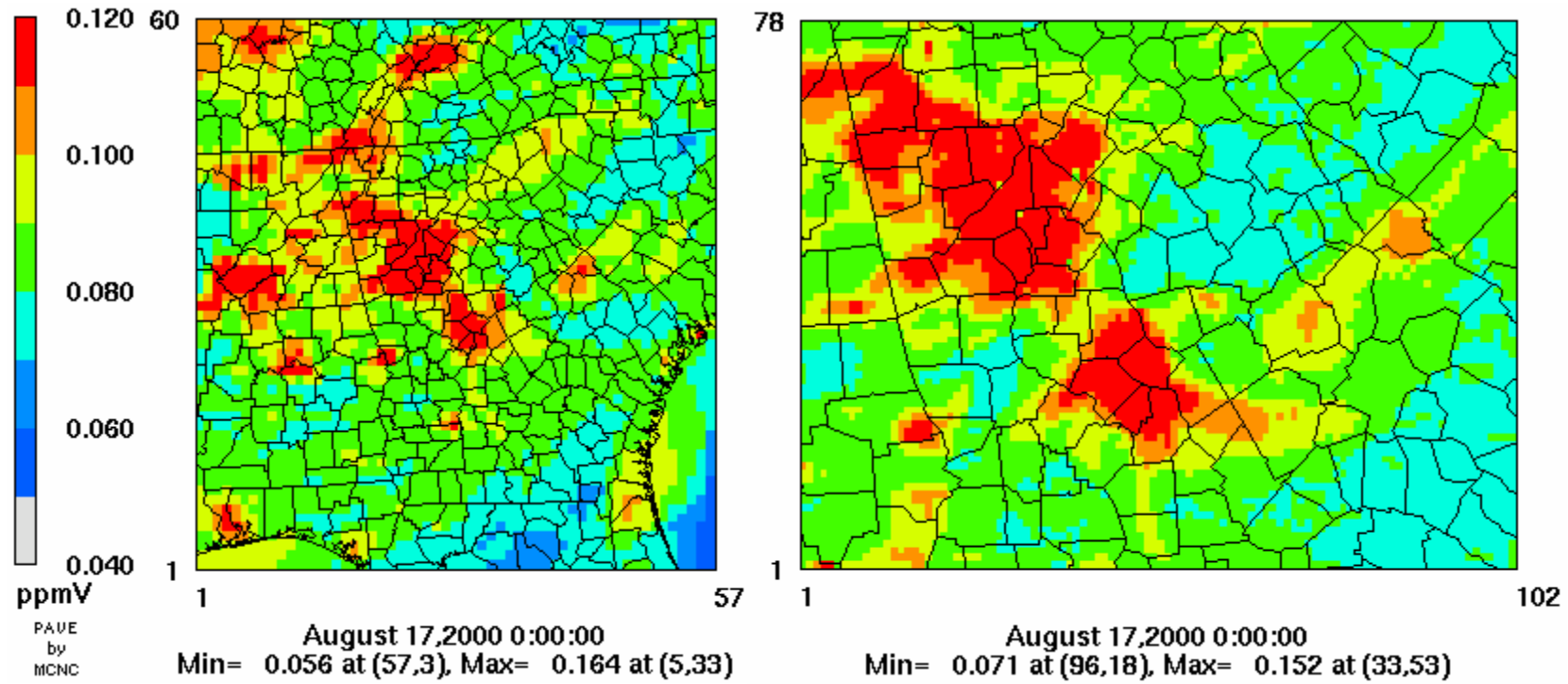
**Gridded Daily Maximum Hourly Averaged Surface Ozone Concentrations
for 12-km grid (left) and 4-km grid (right).**

Objectives

$$s_{ij} = \frac{\partial c_i}{\partial E_j}$$

Adaptive Grid

Sensitivity Analysis

Computer Simulation with Air Quality Model

Strategy Design

Controlled Burning at Military Base

Impact to Downwind City
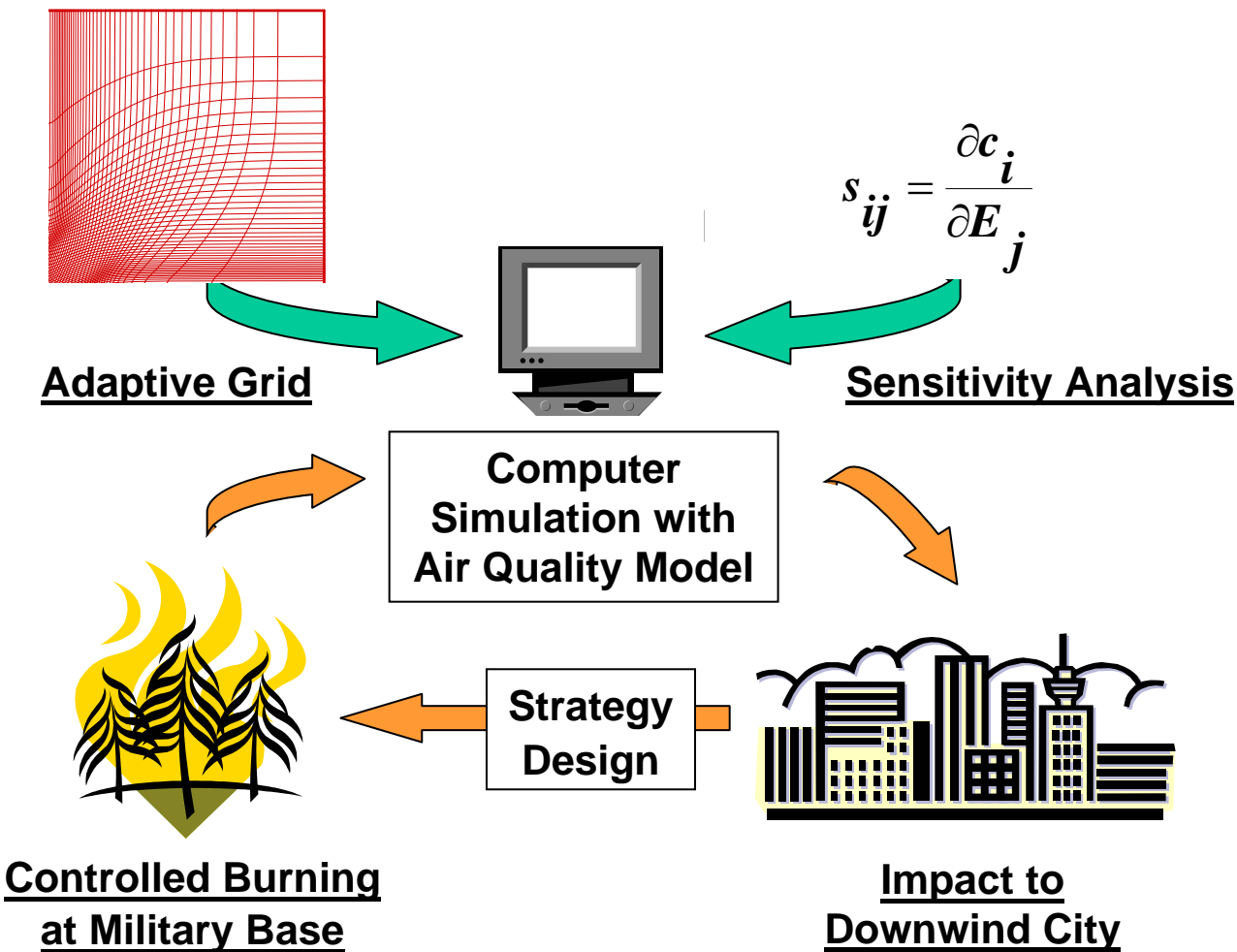
Study Area: Fort Benning, GA
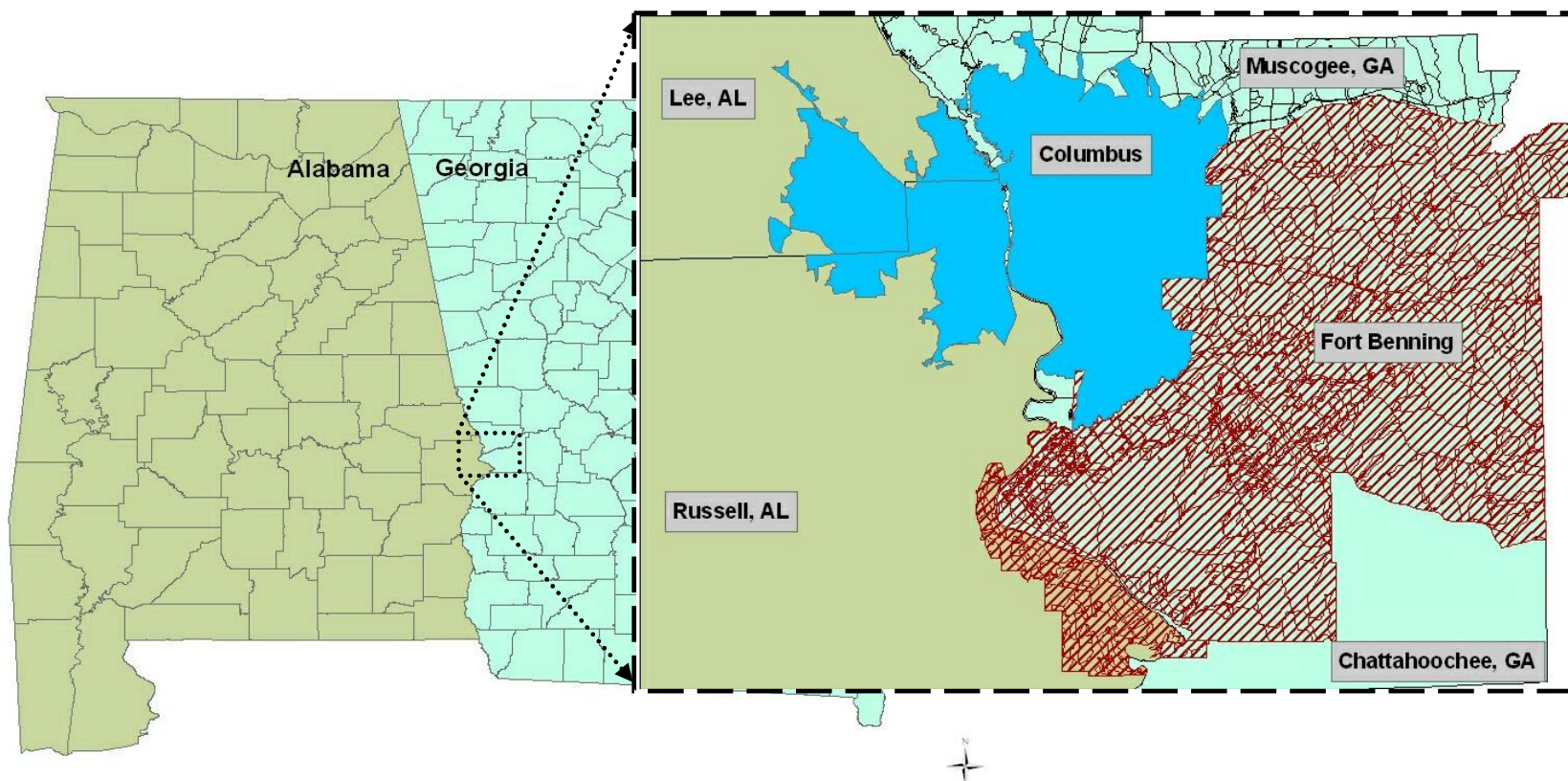
Methodology

- Adaptive Grid Modeling

- Direct Sensitivity Analysis

Adaptive Grid Modeling

- Inadequate grid resolution -- Important source of uncertainty in air quality models. Adaptive grids offer an effective and efficient solution.

- Our adaptive grid technique is a *mesh refinement* algorithm where the number of grid cells remains constant and the structure (topology) of the grid is preserved.

- A weight function controls the movement of the grid nodes according to user-defined criteria. It automatically clusters the nodes where resolution is most needed.

- Grid nodes move continuously during the simulation. Grid cells are automatically refined/coarsened to reduce the solution error.

Adaptive Grid Modeling
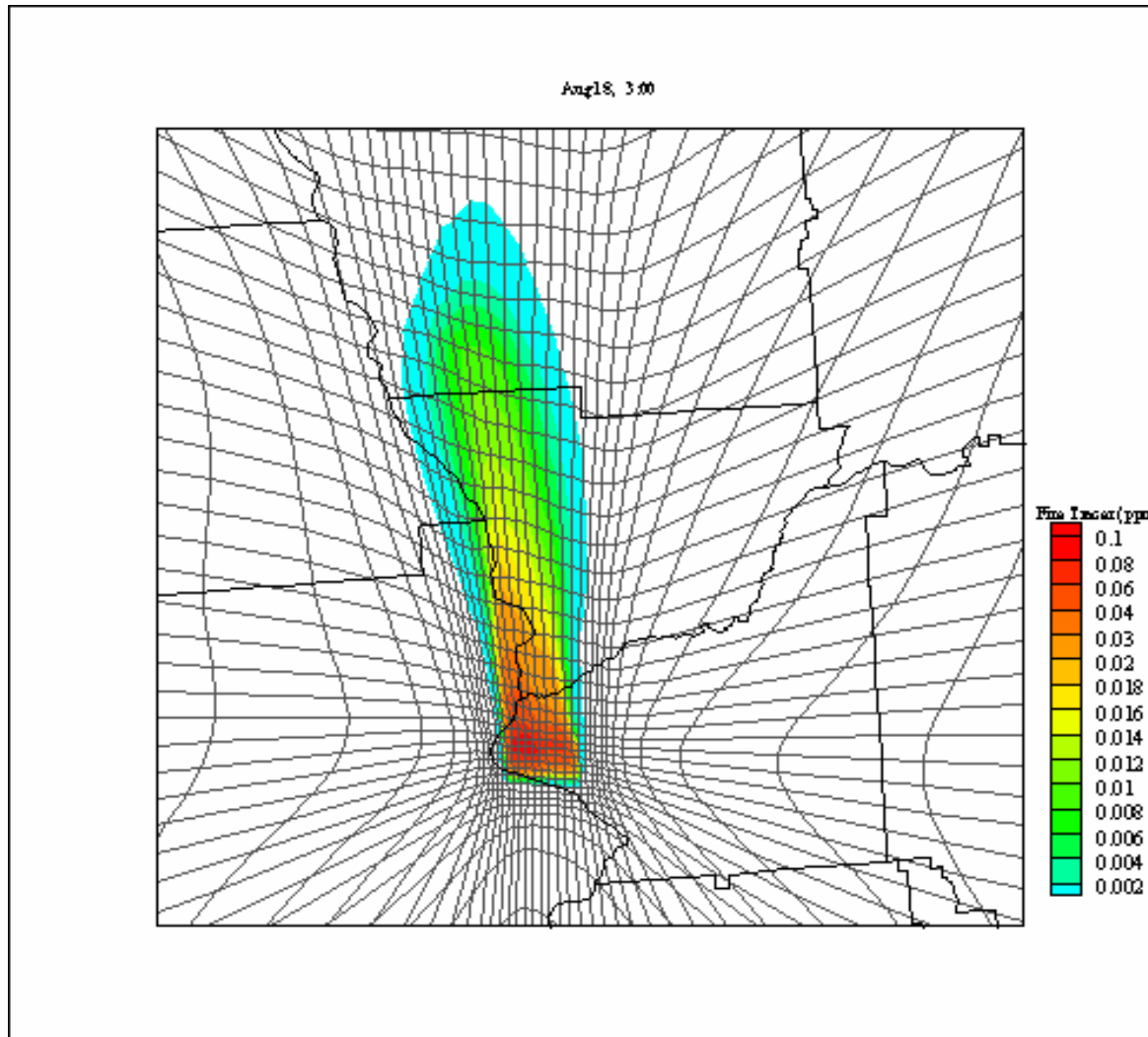
Sensitivity Analysis with Decoupled Direct Method (DDM)

- Define first order sensitivities as $\quad S_{ij}^{(1)} = \partial C_i / \partial E_j$

- Take derivatives of $\quad \dfrac{\partial C_i}{\partial t} = -\nabla(\mathbf{u}C_i) + \nabla(\mathbf{K}\nabla C_i) + R_i + E_i$

- Solve sensitivity equations simultaneously

$$\frac{\partial S_{ij}^{(1)}}{\partial t} = -\nabla(\mathbf{u}S_{ij}^{(1)}) + \nabla(\mathbf{K}\nabla S_{ij}^{(1)}) + \mathbf{J}_i \mathbf{S}_j^{(1)} + \frac{\partial R_i}{\partial \varepsilon_j}\delta_{5j_1} + \tilde{E}_i \delta_{1j_1}\delta_{ij_2}$$

$$-\nabla(\tilde{\mathbf{u}}C_i)\delta_{3j_1} + \nabla(\tilde{\mathbf{K}}\nabla C_i)\delta_{4j_1}$$

- Approximate response as $\quad \Delta C_i = S_{ij}^{(1)}\Delta E_j$

Data Preparation

- <u>Episode</u>: August 15-18, 2000 (Hugh Westburry @ Fort Benning provided the fire data)

- <u>Meteorology Data</u>: MM5 (FAQS)

- <u>Base Emissions</u>: FAQS-2000 Inventory

- <u>Biomass Burning Emissions</u>: FOFEM V5 + Battye and Battye (2002)

Fire Tracer: Adaptive Grid

Aug 15, 16:00

Fire Tracer (ppm)
- 0.1
- 0.0875
- 0.075
- 0.0625
- 0.05
- 0.0375
- 0.025
- 0.0125
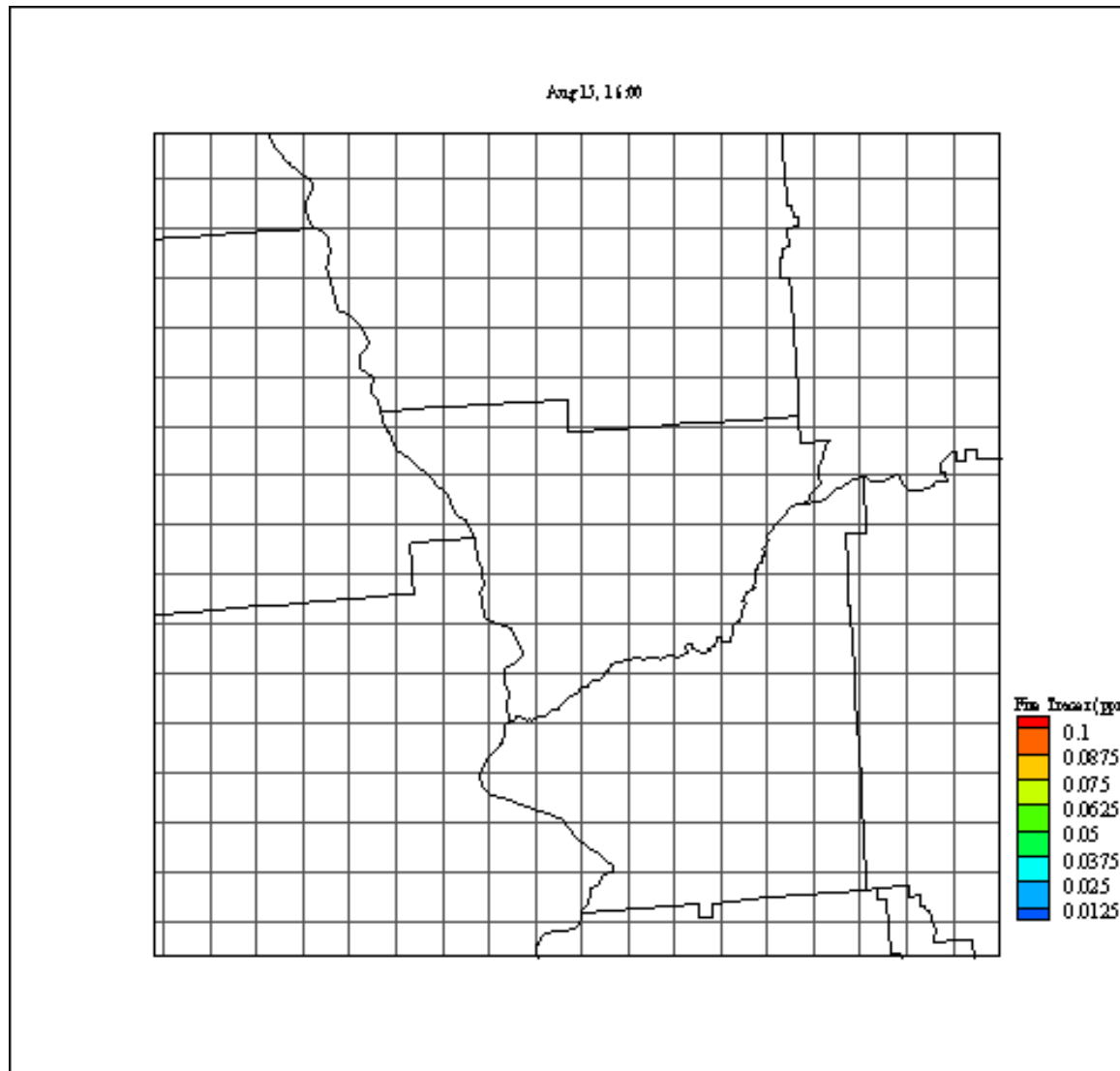
O₃ Sensitivity to FIRE
Static + Brute Force
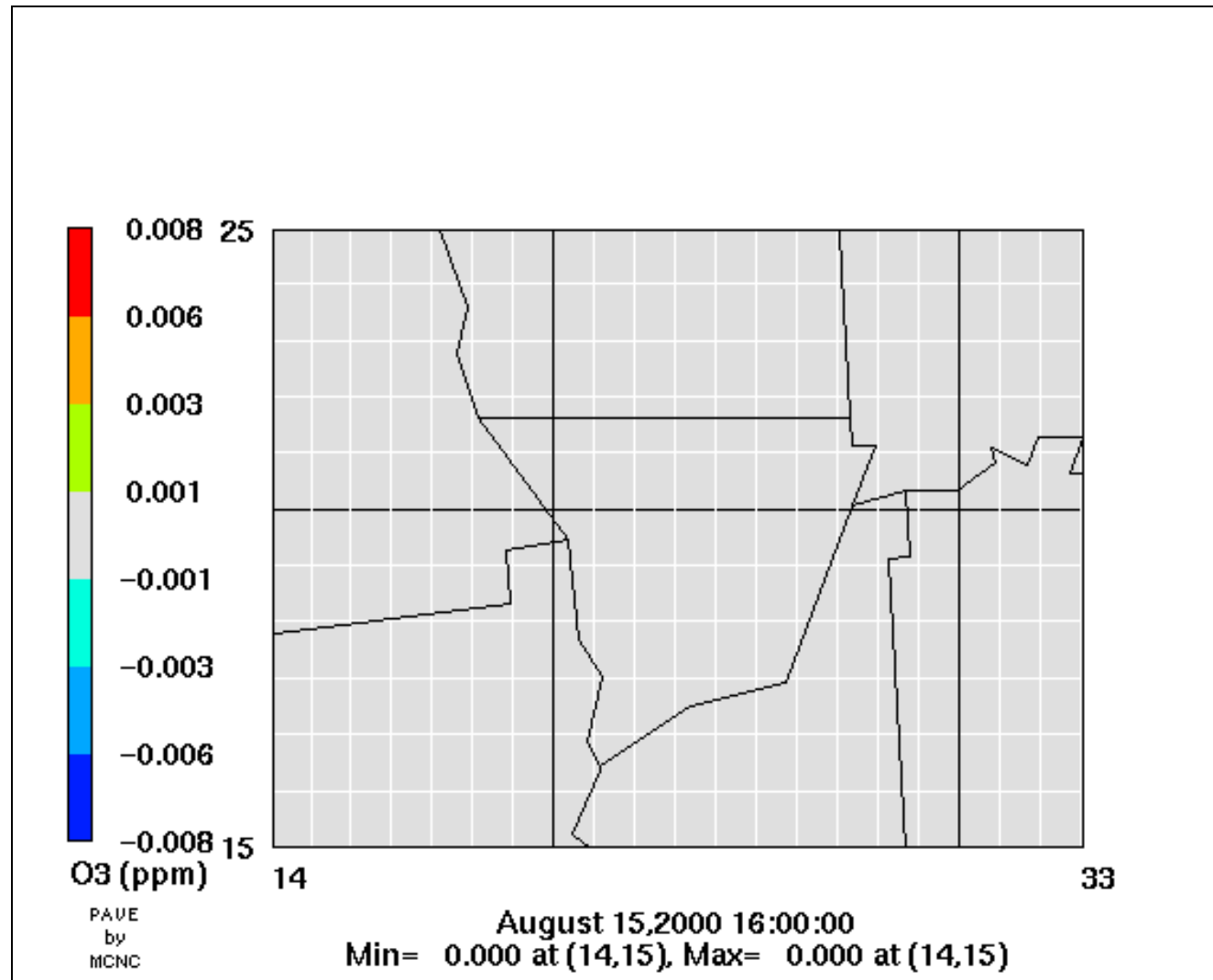
O$_3$ Sensitivity to FIRE
Adaptive + Direct Sensitivity

Aug 15, 16:00

Sensitivity

	0.01
	0.005
	0.001
	-0.005
	-0.01
	-0.015
	-0.02
	-0.025
	-0.03
	-0.035
	-0.04

Georgia Institute of Technology
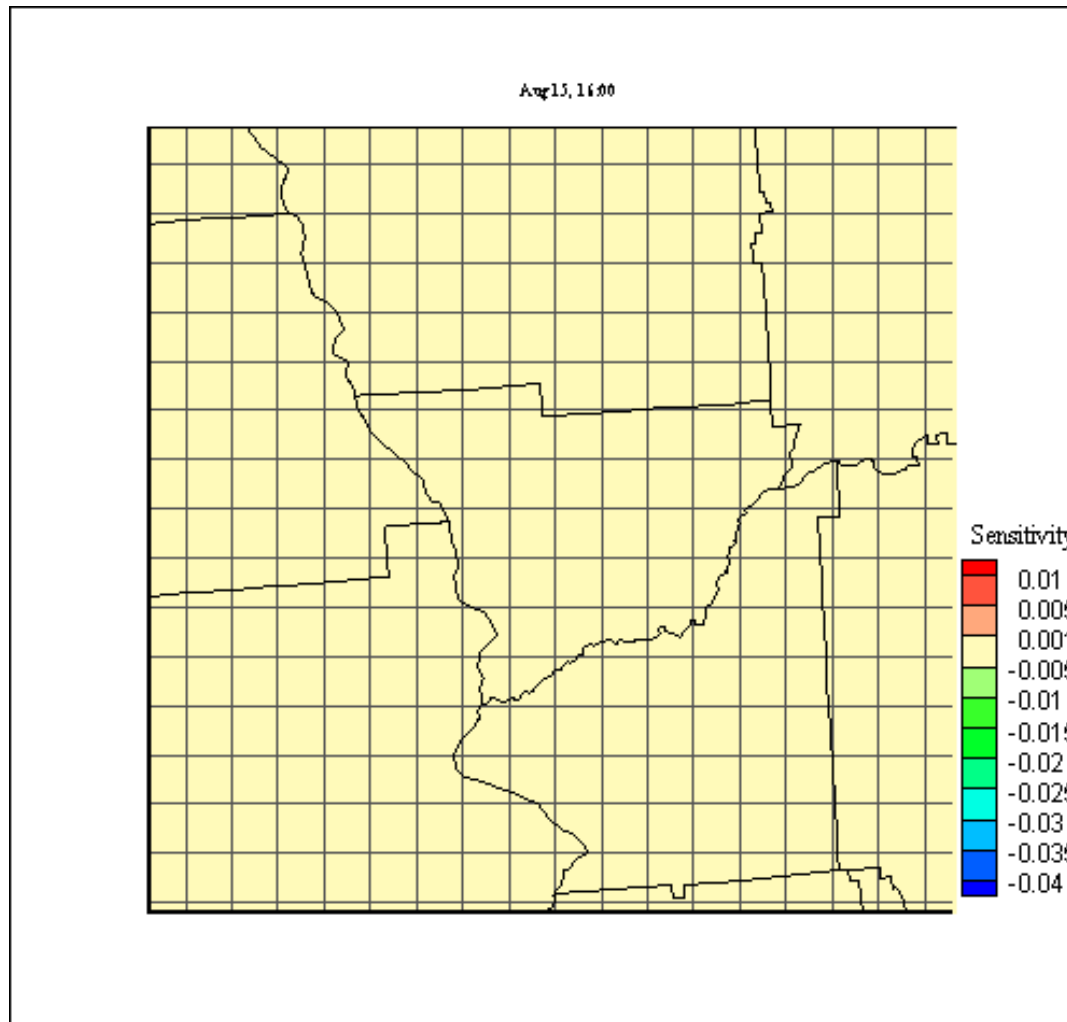
O₃ Sensitivity to FIRE
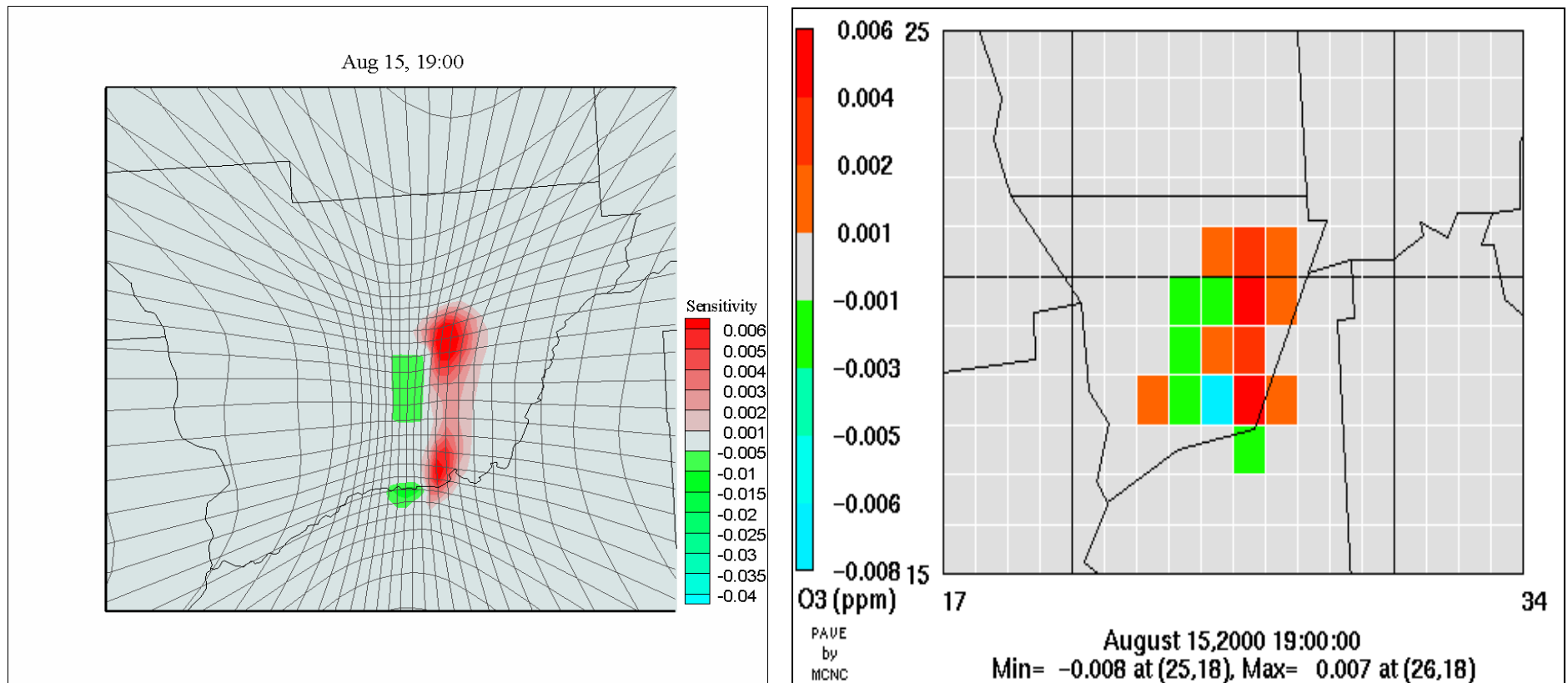
O₃ Sensitivity to FIRE
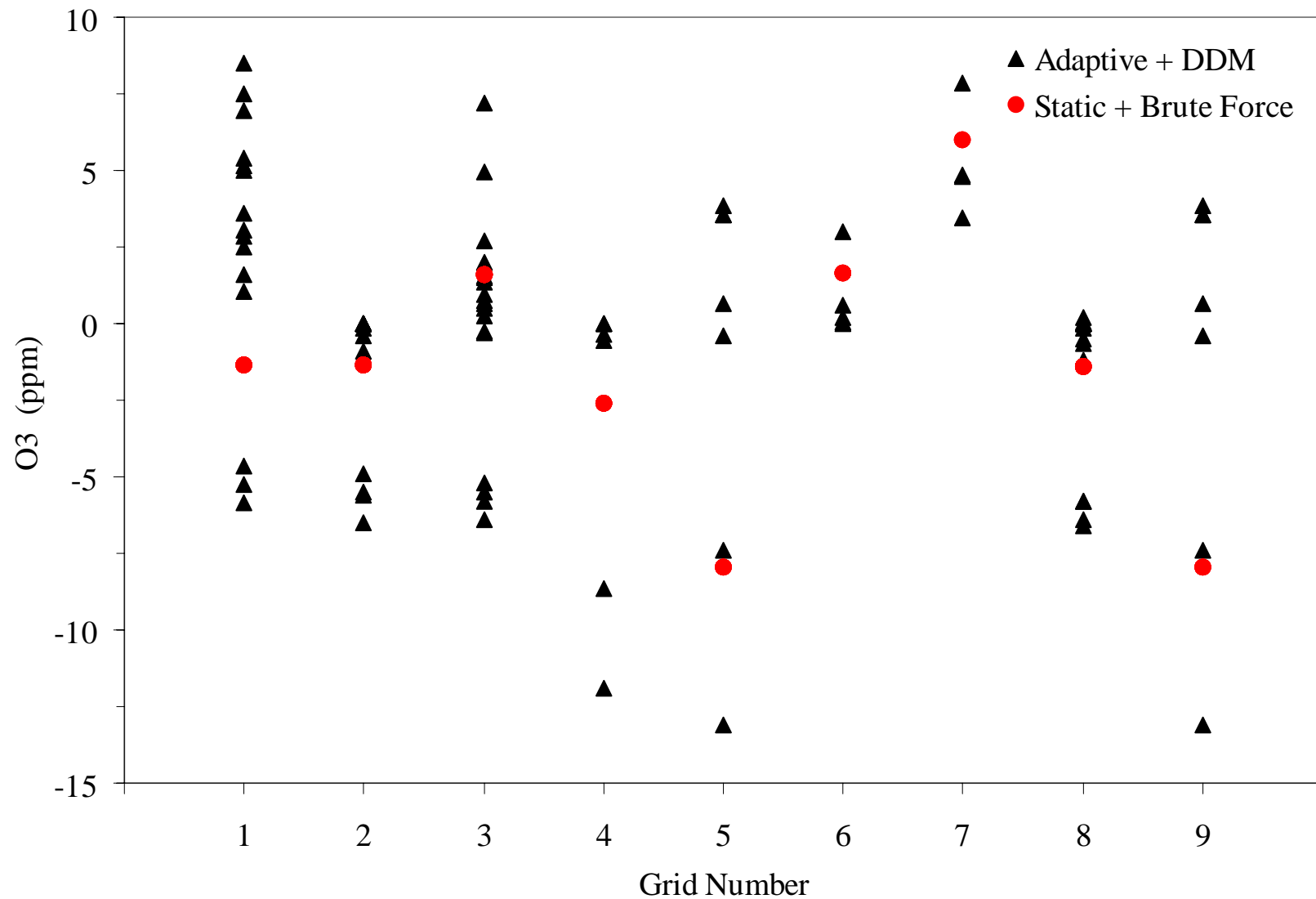
Conclusions

- Adaptive Grid Modeling with Direct Sensitivity Methods were successfully implemented to determine the impact of biomass burning on the surrounding environment
- The impact of fires ranged from 16 ppb reduction to 7 ppb increase in O_3 concentrations. Impact on Columbus area is minimal due to wind directions
- Concentration gradients were better resolved by Adaptive Grid
- Direct Sensitivity compared to Brute Force, better differentiated near and far field impacts

Future Work

- Emissions Inventory:

  - Better emissions estimation for biomass burning

  - Plume Rise calculations

- Comparison with Monitoring Data:

  - **"Prediction of Air Quality Impacts from Prescribed Burning: Model Optimization and Validation by Detailed Emissions Characterization "** with Dr. Karsten Baumann

Acknowledgements

c) Journal Paper (Submitted to either "Journal of Agricultural and Forest Meteorology" or "International Journal of Wildland Fire")

1 **Adaptive Grid Modeling for Predicting the Air Quality**

2 **Impacts of Biomass Burning**

3 Alper Unal and M. Talat Odman

4 School of Civil and Environmental Engineering,

5 Georgia Institute of Technology, Atlanta, Georgia

6 **Abstract**

7 The objective of this study is to improve the ability to model the air quality impacts of biomass

8 burning on the surrounding environment. The focus is on prescribed burning emissions from a

9 military reservation, Fort Benning in Georgia, and their impact on local and regional air quality.

10 The approach taken in this study is to utilize two new techniques we recently developed:

11 1) Adaptive grid modeling and 2) Direct sensitivity analysis. We equipped an advanced air

12 quality model, MAQSIP, with these techniques and conducted regional scale air quality

13 simulations. Grid adaptation reduces the grid sizes in areas that have rapid changes in

14 concentration gradients consequently the results are much more accurate than those of traditional

15 static grid models. Direct sensitivity analysis calculates the rate of change of concentrations with

16 respect to emissions. This enabled us to isolate the effect of emissions from a specific source

17 such as biomass burning.

18 The adaptive grid simulation estimated large variations in O_3 concentrations within 4×4 km^2

19 cells for which the static grid estimates a single average concentration. In one cell, the maximum

20 of adaptive grid values was 28 ppb higher than the static grid value. On the other hand, the

21 average of the adaptive grid O_3 concentrations generally agreed well with the static grid

22 concentration.

23 The differences between adaptive average and static grid values of O_3 sensitivities were more

pronounced. The sensitivity of O_3 to fire is difficult to estimate using the brute-force method with coarse scale (4×4 km^2) static grid models. The qualitative analysis shows that the adaptive grid model equipped with the DDM method can estimate the sensitivity of O_3 to relatively small perturbations such as a prescribed burn more accurately. The static grid can not resolve the difference between the near and far field impacts as adaptive grid does. It was found that the impact of the fires ranged from almost 50 ppb reduction to 8 ppb increase in ozone concentrations. However, the impact of the fires on the air quality in Columbus area was minimal during the selected period.

1. INTRODUCTION

Wildland fires are essential in creating and maintaining functional ecosystems and achieving other land use objectives (Hardy and Leenhouts, 2001). However, biomass burning produces combustion byproducts that are harmful to human health and welfare (Hardy and Leenhouts, 2001; Battye and Battye, 2002). Guided by the Endangered Species Act (ESA), the Department of Interior (DoI) through the Fish and Wildlife Service (FWS) mandates that some military installations and air force bases in the South-Eastern United States use prescribed burning to recreate the natural fire regimes needed to maintain the health of its native long leaf pine forestland thus protecting the habitat of the endangered Red Cockaded Woodpecker (RCW). Proper management may require as much as 1/3 of the forest to undergo treatment by fire each year. These activities, however, can contribute significantly to already burdened local and regional air pollutant loads. In recognition of the conflicting requirements between the ESA and Clean Air Act (CAA) statutes, the Strategic Environmental Research and Development Program (SERDP), supported by Department of Defense (DoD), initiated a program to determine the

1   effects of biomass burning from military installations. As part of this effort, we focused on

2   determining the effects of biomass burning from military reservation, Fort Benning in Georgia,

3   to the local and regional air quality, specifically, in Columbus metropolitan area.

4   Fort Benning, which covers an area of approximately 182,000 acres, is located in the lower part

5   of central Georgia and Alabama, six miles southeast of Columbus, Georgia. Thus emissions from

6   this facility may be affecting the air quality in Columbus, which is reported to violate air quality

7   standards for Ozone (EPD, 2003). The Columbus Environmental Committee is viewing the

8   prescribed burning operation as a potential contributor to the ozone problem. This became a

9   public relations concern for Fort Benning (Larimore, 2000).

10   Approximately 30,000 acres must be prescribed burned each year at Fort Benning, during the

11   growing season (i.e., March through August). This period falls within the "ozone season." In

12   order to restore the RCW habitat, longleaf seedlings are planted. Prescribed burnings continue

13   from August through October for site preparation purposes, which also overlaps with the ozone

14   season. These fires reduce unwanted vegetation that would compete with longleaf seedlings.

15   Operational and safety constraints limit the burnings to an average of 300 acres per day

16   (Environmental Management Division, 2000). For example, although an attempt is made to burn

17   all RCW clusters during the growing season it is logistically impossible due to the number of

18   clusters (75-80 annually) and scheduling conflicts with training. Natural firebreaks, such as

19   roads, trails, drains, and creeks dictate the size of burn areas. All these limitations make it

20   necessary to continue the burnings throughout the year. In realization of the Columbus ozone

21   problem, the majority of the burnings (70-75%) were shifted to the January-April period, which

22   is outside the "ozone season."

1 Currently, the only external constraint on prescribed burning arises as a result of smoke

2 management concerns.   Smoke complaints and the threat of litigation from smoke-related

3 incidents / accidents are the primary concerns. Fort Benning follows voluntary (not mandated by

4 state or federal government) smoke management guidelines in an effort to minimize the adverse

5 impacts from smoke. An additional concern is the effect of prescribed burning on ozone levels in

6 Columbus. Forest fires produce nitrogen oxide and hydrocarbon emissions that form ozone

7 (Cheng *et al.*, 1998; Battye and Battye, 2002; Ottmar, 2001). These pollutants may be

8 transported downwind, mix with emissions from other sources and contribute to the poor air

9 quality in urban areas. Sulfur dioxide and particulate matter emissions from forest fires are also

10 of concern but, in general, they do not have a direct influence on the urban ozone problem. The

11 ozone alert season is from 1 May through 30 September in Georgia. It is during this season that

12 emissions from prescribed burning operations could affect smog levels in Columbus. In

13 collaboration with the Partnership for a Smog-Free Georgia (PSG), Fort Benning is avoiding

14 prescribed burns when meteorological conditions are conducive to ozone buildup. However,

15 more complex methods are required to identify the real effects of biomass burning from Fort

16 Benning on ozone problem in Columbus region.

17 Main objective in this study is to improve the ability to model the air quality impacts of biomass

18 burning on the surrounding environment. For this purpose we equipped an advanced air quality

19 model, Multiscale Air Quality Simulation Platform (MAQSIP) (Odman and Ingram, 1996), with

20 two newly developed techniques; Adaptive Grid Modeling, and Direct Sensitivity Analysis to

21 accurately isolate and determine the effects of biomass burning on ozone formation. In this paper

22 we first describe the methods utilized and then discuss the important findings of the study.

2. METHODOLOGY

The atmospheric and chemical modeling systems currently used by various agencies tend to focus on a single scale that seems to be the most relevant to a particular air pollution problem. Global scale models address climate issues while regional scale models are used for the tropospheric ozone, regional haze or acid deposition studies. Urban scale smog models are being replaced with urban-to-regional scale models in most places where transport from other upwind sources play an important role. On the local scale, models are used to deal with problems such as accidental releases. The domains of local scale models are limited by design; therefore, they cannot be used for regional scale impact studies.

One of the most advanced urban-to-regional scale models is the MAQSIP. Urban-to-regional scale models are used in developing emission control strategies for problems such as urban and regional ozone, acid deposition, or regional haze which is attributed to primary (emitted) and secondary (formed in the atmosphere) fine particulate matter. While these models are equipped with special tools to treat emissions from large power plants (Karamchandani et al, 2000), they lack the ability to resolve emissions from relatively small area sources such as those from prescribed burnings. To account for such area sources, the models rely on grid resolution. Prescribed burnings are performed over areas as small as one square kilometer (approximately 200 acres). This scale is too small for typical regional applications. Therefore, emissions from prescribed fires are blended with emissions from many other sources within the same grid cell of regional scale models. This would make it impossible to conduct an impact study that would target emissions from biomass burnings.

Another limitation of current air quality models is related to numerical errors involved during the

simulations. Let us suppose that the grid cell size could be reduced to one square kilometer by using nested-grid techniques (Odman et al, 1997). In that case, a typical prescribed burning unit would cover a single grid cell. The effect of having or not having prescribed burning emissions from a single grid cell would be a small perturbation for air quality models. As the perturbation gets smaller in size, numerical errors that affect the simulation results become more important. The results of an impact study such as the one proposed here would be highly uncertain if the models were used as is. Therefore, urban-to-regional scale models, in their current state, are not very reliable tools for determining the impact of prescribed burning emissions to the surrounding environment.

The study of the impact of biomass burning from DoD facilities requires investigation of the interaction between various scales due to the fact that both the location of the facilities and the lifetimes of emitted pollutants are conducive to long-range transport. Below, we describe a methodology to improve current urban-to-regional scale air quality models with two modeling techniques. These techniques improve representation of the transport and transformation processes over a wide range of scales and provide more reliable source-receptor relationships. The product is a more reliable tool that can predict accurately the ultimate fate of pollutants emitted from specific sources such as DoD facilities.

2.1.   *Adaptive Grid Modeling*

We developed an adaptive grid modeling approach to reduce the uncertainty in air quality predictions. By clustering the grid nodes in regions that would potentially have large errors in pollutant concentrations, the model is expected to generate much more accurate results than the traditional fixed, uniform grid counterparts. The repositioning of grid nodes is performed

1   automatically through the use of a weight function that assumes large values when the curvature

2   (change of slope) of the pollutant fields is large. The nodes are clustered around regions where

3   the weight function bears large values, thereby increasing the resolution where it is needed. Since

4   the number of nodes is fixed, refinement of grid scales in regions of interest is accompanied by

5   coarsening in other regions where the weight function has smaller values. This yields a

6   continuous multiscale grid where the scales change gradually. Unlike nested grids, there are no

7   grid interfaces, which may introduce numerous difficulties due to the discontinuity of grid scales.

8   The availability of computational resources determines the number of grid nodes that can be

9   afforded in any model application. By clustering grid nodes automatically in regions of interest,

10   the adaptive grid technique uses computational resources in an optimal fashion throughout the

11   simulation.

12   A detailed description of the technique can be found in Srivastava *et al.* (2000). The adaptive

13   technique was applied to problems with increasing complexity and relevance to air quality

14   modeling. First, it was applied to pure advection tests (Srivastava *et al.*, 2000). In a rotating cone

15   test, the adaptive grid solution was more accurate than the fixed uniform grid with the same

16   number of grid nodes. The error in maintaining the peak of the cone was only 13% compared to

17   39% with the fixed grid: an accuracy that could only be achieved by using 22 times more grid

18   nodes with a fixed uniform grid. Srivastava *et al.* (2001a) conducted a third test with concentric

19   conical puffs of NO_x and VOCs reacting in a rotational wind field. The parameters of this

20   problem are such that, after a certain time, ozone levels drop below the background near the base

21   of the conical puffs but they peak near the vertex of the cones. This feature was resolved by the

22   adaptive grid solution while it was completely missed by the uniform fixed grid solution. When

23   nine times more grid nodes were used, the fixed grid was finally able to reveal this feature but

1   not as accurately as the adaptive grid technique.

2   Next, the adaptive grid technique was applied to the simulation of a power plant plume

3   (Srivastava *et al.*, 2001b). A two dimensional plume with a VOC/NO_x emission ratio of 14% was

4   advected with uniform winds and diffused over a background with a VOC/NO_x ratio of 35. Other

5   parameters were chosen to make the dispersion as realistic as possible. After about 12 hours of

6   simulation, the composition of the plume was analyzed taking cross sections at various

7   downwind distances. At 10 km downwind, the adaptive grid solution showed a NO_x rich, but

8   ozone deficient core. This feature, which is also observed in actual power plant plumes, was

9   completely missing in the uniform grid solution, which artificially diffused the NO_x and

10   displayed highest ozone levels at the core of the plume. The adaptive grid, on the other hand, had

11   ozone bulges developing near the plume edges. At a downwind distance of 30 km, these bulges

12   continued to grow as NO_x diffused slowly from the core to the edges (at a rate more in line with

13   physical diffusion) and radicals were entrained into the plume. This plume structure started

14   disappearing after about 80 km. At a downwind distance of 135 km, the plume was fully *matured*

15   with an ozone peak at the center. The peak ozone concentration was larger than one predicted by

16   the fixed uniform grid. A similar evolution of the plume was observed in the fixed uniform grid

17   solution when the number of grid nodes was increased by a factor of nine. However, this solution

18   was about five times more expensive than the adaptive grid solution.

19   After these and other testing of the algorithm (Odman *et al.*, 2001; Khan et al, 2003), finally an

20   adaptive grid AQM was developed (Odman *et al.*, 2002). The model was applied to an ozone

21   simulation in the Tennessee Valley (Khan and Odman 2003). Ozone results from this application

22   were evaluated and showed significant improvement over those from fixed grid models, even

23   those employing up to four times more grid cells. In several cases the agreement with

8

1 observations was better compared to fixed grid models. When the reasons were investigated it

2 was found that the complex source-receptor relationships, especially the long-range ones were

3 much better resolved with the adaptive grid.

2.2. Direct Sensitivity Analysis

5 Sensitivity analysis is essential in determining source-receptor relationships and designing

6 emission control strategies. The traditional "brute-force" method involves running the model

7 several times, each time perturbing one type of emission (e.g., NO_x or VOC) from a different

8 source. If the perturbation is small, the brute-force method may not yield accurate sensitivities

9 due to numerical errors propagating in the model. Our group has developed a new and powerful

10 direct sensitivity analysis technique to study the response of air quality to various types of

11 emissions (Yang et al, 1997; Hakami *et al.*, 2003). Unlike the brute force approach, this

12 technique is not limited by the magnitude of the perturbation and, in theory, it can be used for

13 even infinitesimal changes in emissions. Therefore, the technique has the potential of improving

14 current models to a level where they can be used for impact analysis of relatively small sources

15 such as military installations.

16 Air quality models are based on the atmospheric diffusion equation:

$$\frac{\partial c_i}{\partial t} + \nabla \cdot \left(\mathbf{u} c_i \right) = \nabla \cdot \left(\mathbf{K} \nabla c_i \right) + R_i + S_i \tag{1}$$

18 Here, c_i is the concentration of the *i*th pollutant species, $\mathbf{u}$ describes the velocity field, $\mathbf{K}$ is the

19 diffusivity tensor, $R_i(c_1, c_2, ...)$ is the chemical reaction term and S_i is a source term for certain

20 types of emissions. The local sensitivity of the concentration of a species (e.g., ozone) to a

21 certain emission type (e.g., NO_x or VOC) from a particular source can be defined as:

$$s_{ij}(t) = \frac{\partial c_i(t)}{\partial E_j} \qquad (2)$$

Here, s_{ij} is the sensitivity of c_i to emission E_j. Since the sensitivities to different emissions can vary by many orders of magnitude, it is necessary to define semi-normalized sensitivity coefficients, s^*_{ij}.

$$s^*_{ij}(t) = \tilde{E}_j \frac{\partial c_i(t)}{\partial E_j} \qquad (3)$$

where $\tilde{E}_j$ is the unperturbed emission field (i.e., without fire). Using direct derivatives of Equation (1) the following equation can be obtained for sensitivities.

$$\frac{\partial s^*_{ij}}{\partial t} = -\nabla\left(\mathbf{u} s^*_{ij}\right) + \nabla\left(\mathbf{K}\nabla s^*_{ij}\right) + J_{ik} s^*_{kj} + \frac{\partial R_i}{\partial \varepsilon_j} + \frac{\partial S_i}{\partial \varepsilon_j} - \nabla\left(\mathbf{u} c_i\right)\delta_{ij} + \nabla\left(\mathbf{K}\nabla c_i\right)\delta_{ij} \qquad (4)$$

Here, s^*_{ij} is the semi-normalized sensitivity coefficient, J_{ik} is the Jacobian matrix, ε_j is a scaling variable with a nominal value of 1, and δ_{ij} is a binary variable (either 1 or 0).

The similarity between Equations (1) and (4) allows us to use the same or very similar numerical solution techniques and calculate local sensitivities to emission sources simultaneously along with the species concentrations. This also makes the implementation of the technique in any model relatively straightforward. The technique is also computationally efficient because several of these sensitivities (the number being limited by available core memory) can be calculated simultaneously with a fractional increase in CPU time. The emission sources can be discerned by type as point, area, mobile, or biogenic, and by composition such as SO_2, NO_x, or VOC. Also, the location of the emission source can be specified, for example, as the boundaries of a DoD

10

1   facility (to the grid scale resolution). The technique would predict the sensitivity of air quality at

2   any desired location in the modeling domain (e.g., sensitivity of ozone concentrations at a

3   downwind urban center) to a fractional change in the emissions from the source of interest.

4   The technique has been evaluated in an application to the Southern California where the

5   sensitivities of ozone concentrations to the domain wide reductions of mobile and area sources of

6   NO_x were compared to a brute-force method (Yang *et al.*, 1997). This technique was used in an

7   integrated modeling system focusing, simultaneously, on ozone, particulate matter and acid

8   deposition (Boylan, *et al.*, 2001). We investigated the sensitivity of particulate matter

9   concentrations to the reductions of SO_2 and NO_x emissions in the Southern Appalachian

10   Mountains region. We also investigated the sensitivity of ozone concentrations to NO_x and VOC

11   emissions from different states, using state boundaries as sub-regions. As part of that project, we

12   compared our method to the brute-force approach for ozone sensitivities to domain wide NO_x

13   and VOC emissions. The general agreement between the direct sensitivity and the brute-force

14   method shows that the former is a reliable tool. Whenever we observed differences, we were able

15   to relate the difference to the numerical errors associated with the brute force technique and

16   show that the direct sensitivity method yields results that are more accurate.

17   **3. AIR QUALITY SIMULATIONS**

18   *3.1.   Episode Selection*

19   The episode selection is based primarily on the availability and quality of meteorological and

20   emissions data as well as the impact potential of prescribed burns at Fort Benning on regional air

21   quality. As part of Fall Line Air Quality Study (FAQS), we have already simulated several

22   episodes during summer of 1999 and 2000 in Georgia using MM5 meteorological model and

SMOKE emissions model. The ideal scenario for our case study is one with southeasterly winds, biomass burning performed at Fort Benning and high ozone levels observed at Columbus. Based upon contacts with Land Management Brach at Fort Benning we obtained the locations, date, and time of biomass burning efforts (Westbury, 2002). There were biomass burnings at Fort Benning between August 15 and August 18 2000. Also ozone levels in Columbus region were over the standards at least four times and prevailing winds were southeasterly during the same period. Therefore, we decided to simulate the period from August 15 through August 18, 2000.

3.2.   *Data Preparation*

Data preparation efforts included meteorological and emissions data preparation as well as post-processing. Meteorological data were obtained from FAQS. Detailed information on meteorological data preparation is given elsewhere (Hu *et al.*, 2003). Similarly emissions data were obtained from FAQS study. More information on emissions data can be obtained elsewhere (Unal *et al.*, 2003; Hu *et al.*, 2003). For biomass burning emissions First Order Fire Effects Model (FOFEM) Version 5, developed by Intermountain Fire Sciences Laboratory was utilized. In this model fuel type was assumed as natural fuel with long leaf pine trees. For some of the pollutants, such as speciated VOCs and NOx, emission factors provided by Battye and Battye (2002) were utilized.

3.3.   *Static Grid Simulations*

To verify model efforts, a 4×4 km static grid version of the MAQSIP model was used in simulation for the selected episode. Lambert Conformal projection with parameters of 30^0N, 60^0N, and 90^0W, centered at 40^0N and 90^0W, was utilized for the domain. The 4×4 grid has 102 columns and 78 rows with 13 vertical layers. The results of the static grid run were compared

1   with outputs from the FAQS project for the same location and time period. The comparison

2   showed that static grid results were similar to FAQS results. A separate run was made with

3   emissions including fire as well. The difference between the concentrations of these two

4   simulations yields static grid "brute-force".

5   *3.4.   Adaptive Grid Simulations*

6   The adaptive grid also used the same domain definitions as for the static grid. In adaptive runs

7   inert fire tracer concentrations are used to calculate the weight function that drives the adaption.

8   The tracer is assumed to be a product of the fires at Fort Benning emitted at the same rate as NO

9   emissions from fire. The tracer is transported and deposited the same way as other fire species

10   but it is non reactive. Two different runs were made with the adaptive grid model. These runs

11   include: one run with base emissions; and one run with base emissions plus fire emissions, which

12   also has the direct sensitivity calculations. In both runs the grid adapted to the same fire tracer,

13   therefore the grids are identical in both simulations. The difference between the concentrations of

14   these two simulations yields an adaptive grid "brute-force". DDM sensitivity results were

15   compared with "brute-force" and it was observed that differences were within the bounds of

16   previously reported differences (Hakami *et al.*, 2003). Only DDM sensitivities will be used

17   hereafter.

18   **4.   RESULTS**

19   First we compared the adaptive grid model with the static grid model. The tracer concentrations

20   calculated by the two models as a result of fires at Fort Benning on August 15, 2000 at 19:00

21   Greenwich Mean Time (GMT) are shown in Figures 1 and 2. During this period two different

22   fires happened at two different locations. The fire to the south is emitting at a higher rate than the

1 northern one since the area burnt is almost 1.5 times bigger. The location of these fires can be

2 seen in both static and adaptive simulation results.

3 One of the significant differences between these simulations is the fact that static grid distributes

4 emissions uniformly to the 4-km by 4-km cell area where the fire takes place. Adaptive grid, on

5 the other hand, increases the grid resolution around the fire location as shown in Figure 2. At the

6 points where fires occur, adaptive grid reduces cell size to 400m by 400 m or one tenth of the

7 static grid size. This provides adaptive grid the capability to distinguish two distinct plumes from

8 the fires. For this reason concentration gradients are much better resolved by the adaptive grid

9 model than by the static grid model.

10 Another objective of this study was to utilize direct sensitivity method to estimate sensitivity of

11 ozone to NO emissions from fires. We made a comparison between static "brute-force" and

12 adaptive direct sensitivity results. Figures 3 and 4 present sensitivity of ozone concentration to

13 fire emissions as estimated by static and adaptive grids respectively, in the afternoon of August

14 15, 19:00 PM (UTM). While the fires reduce the ozone concentrations near the source by as

15 much as 8 ppb, they result in an increase by as much as 7 pbb further downwind for this

16 particular time period. Such a distinction between the near and the far field impacts is not so

17 clear in the "brute-force" sensitivities calculated by the static grid model, as shown in Figure 3.

18 **5. DATA ANALYSIS**

19 *5.1.   Comparison of Ozone Estimates*

20 We performed statistical analysis to determine the differences between static and adaptive

21 simulation results. For this purpose, we identified the adaptive cells that intersect with each static

22 cell. Figure 5 presents an example for intersection of static grid cell with adaptive cells. For this

1   particular case, there are about 40 adaptive cells that fall in one static cell. For the intersected

2   cells we recorded individual adaptive cell concentrations and also estimated a weighted average,

3   based upon area, in order to compare to static cell values. Note that in this analysis we selected a

4   region where changes in O_3 concentration occurred due to fire events. Adaptive grid O_3

5   concentrations are very similar to static grid simulation results in the rest of the domain.

6   Figure 6 presents a scatter plot of O_3 concentration values for static and corresponding adaptive

7   cell values for August 15, 21:00 PM (GMT). In this figure both average values as well as

8   minimum and maximum values of adaptive cells within each 4-km by 4-km static cell are shown.

9   One of the important finding in Figure 6 is that O_3 concentrations of adaptive cell averages are

10   very close to static cell results. The correlation coefficient of the regression is 0.9 and has a slope

11   of 0.9 which is an indication of a strong linear relationship between average adaptive and static

12   cell results. However, it should also be noted that adaptive cell averages tends to over predict

13   lower concentrations and under predict higher concentrations as compared to static cell values.

14   The variation in average adaptive results is slightly lower than static cell results. For this

15   particular case, coefficient of variation, which is defined as the ratio of the standard deviation to

16   the mean, is 8.1 percent in adaptive case and 8.6 percent in static case. The coefficient of

17   variation in maximum and minimum values together is slightly greater with a value of 8.9

18   percent. These values suggest that variability is about the same with maximum-minimum values

19   of adaptive cells having the highest variability. It should be noted however that the number of

20   data for this category is twice the static and average adaptive cells. Another important point is

21   the range of variability. Static grid O_3 concentrations change between 62 ppb and 95 ppb,

22   whereas average adaptive cells range between 63 ppb and 92 ppb. For the max/min values this

23   range is between 62 ppb and 96 ppb. Similar results were obtained for other periods of

1   simulation where fire events were observed.

2   Table 1 summarizes the comparison between adaptive and static grids for 20 different hours

3   when fires occurred. As seen in Table 1, the range of variation is similar in adaptive

4   maximum/minimum values and static values. The range is slightly smaller in adaptive averages.

5   Parameters of regression between adaptive averages and static values are also given in Table 1.

6   In most cases (15 out of 20) R^2 values are greater than or equal to 0.9, and slopes are between 0.9

7   and 1.04. There are, however, nighttime fire events where R^2 is less than 0.85 and slope is less

8   than 0.8. In general, it is observed that there is a strong linear relationship between adaptive

9   averages and static values. In 16 cases, the slope of regression is less than 1.0 indicating that the

10   adaptive average O_3 concentration is less than the static cell values. These results are in

11   agreement with the study conducted by Jang *et al.* (1995) where they found that lumped finer-

12   scale grid (i.e., 20km) produced less O_3 than coarser grid (i.e., 80km) for equal size area.

13   Another implication of the differences in adaptive and static predictions is at the local scale.

14   Figure 7 shows O_3 concentrations from adaptive and static grid simulations at a cell near the fires

15   for selected time periods. Adaptive cell averages as well as minimum and maximum values of

16   adaptive cells that fall in the 4-km by 4-km static cell are presented. Adaptive averages are 4 ppb

17   more than static values on the average, and the difference ranges from -2 ppb to 18 ppb. For

18   minimum and maximum adaptive values the average difference from static concentration is +6

19   ppb, and it ranges from -6 ppb to 28 ppb. These findings suggest that there can be significant

20   differences in O_3 between adaptive and static grids at the local scale. For example, one static grid

21   O_3 is 47 ppb whereas one of the adaptive cells inside that static cell has a value of 75. This 28

22   ppb difference may have important implications from a policy perspective.

16

1   *5.2.   Comparison of Ozone Sensitivities*

2   We did a similar analysis to compare sensitivity results from static and adaptive simulations.

3   Figure 8 presents the comparison for the selected region on August 15, 21:00 (UTM). As in the

4   case for O_3 predictions, R^2 and slope values indicate that there is a linear relationship between

5   adaptive averages and static values for sensitivity. However, there is a high variability in

6   individual adaptive cell values as shown by the minimum and maximum sensitivity values.

7   Variation ranges from -8 ppb to 6 ppb for the maximum-minimum adaptive values, whereas it is

8   between -6 ppb to 5 ppb in static grid. For the adaptive averages the range of variation is

9   between -6 ppb to 5 ppb. Similar results were obtained for other periods of simulation where fire

10 events were occurred. Table 2 presents a summary of these events. As seen in Table 2, variability

11 in O_3 sensitivity is smallest in adaptive averages. Maximum-minimum adaptive values have a

12 higher variability than static values. Table 2 also presents parameters of regression between

13 adaptive averages and static values. It is seen that most of the cases (15 out of 20) have R^2 values

14 greater than 0.85 and slope values are greater than 0.70. There are several fire events where there

15 is weak correlation between adaptive averages and static values. One R^2 value is 0.14 at the

16 beginning of a fire. Others are during the nighttime events. In all these cases the sensitivity is

17 mostly negative. The differences in the sensitivities estimated by static and adaptive grids are

18 indicative of the scale-related uncertainty in modeling the impact of prescribed burns.

19 **6. CONCLUSIONS AND FUTURE WORK**

20 The objective of this study was to determine the air quality impacts of biomass burning on the

21 surrounding environment. Fort Benning military reservation, Georgia, was utilized as a case

22 study.

17

1 Current air quality models lack the capability of dealing with multi-scale air quality problems. In

2 this study we utilized an adaptive grid model which inherently has the ability of continuous

3 multiscale gridding. This method also reduces uncertainty in air quality predictions by clustering

4 the grid nodes in regions that would potentially have large errors in pollutant concentrations.

5 We successfully implemented the adaptive grid model in our study and observed that

6 concentration gradients are much better resolved by the adaptive grid model than the static grid

7 version. This is due to the fact that adaptive grid model has 400m by 400m grid cells at locations

8 where fires occur compared to 4km by 4km static grid cells.

9 The adaptive grid simulation estimated large variations in O_3 concentrations within 4×4 km^2

10 cells for which the static grid estimates a single average concentration. In one cell, the maximum

11 of adaptive grid values was 28 ppb higher than the static grid value. On the other hand, the

12 average of the adaptive grid O_3 concentrations generally agreed well with the static grid

13 concentration. The correlation coefficient between adaptive average and static grid values was

14 about 0.9. The average O_3 of adaptive cells had a slightly smaller range than the O_3 of

15 corresponding static cells with lower values on the upper end and higher values on the lower end.

16 The differences between adaptive average and static grid values of O_3 sensitivities were more

17 pronounced. The sensitivity of O_3 to fire is difficult to estimate using the brute-force method

18 with coarse scale (4×4 km^2) static grid models. Qualitative analysis showed that the adaptive grid

19 model equipped with the DDM method can estimate the sensitivity of O_3 to relatively small

20 perturbations such as a prescribed burn more accurately. The static grid cannot resolve the

21 difference between the near and far field impacts as adaptive grid does. It was found that the

22 impact of the fires ranged from almost 50 ppb reduction to 8 ppb increase in ozone

18

concentrations. However, the impact of the fires on the air quality in Columbus area was minimal during the selected period. These findings have to be supported with quantitative analysis in the future. A monitoring program is underway to collect air quality data to support our modeling efforts.

Overall, we successfully incorporated two new techniques into a regional-scale air quality model. This study showed that adaptive grid model equipped with direct sensitivity method can accurately determine the impact of small-scale emission events on the air quality in larger scales. We showed that these techniques can be utilized to determine the impact of biomass burning.

7. REFERENCES

Battye, W. and Battye, R. (2002) "*Development of Emissions Inventory Methods for Wildland Fires*", Report Prepared for U.S. Environmental Protection Agency, Durham, NC.

Boylan, J., Wilkinson, J., Odman, T., Russell, A., Imhoff, R. (2001) Response and sensitivity of $PM_{2.5}$ in the southern Appalachian mountains. *A&WMA Annual Conference and Exhibition*, Orlando, Florida, June 24-28, 2001.

Cheng L., McDonald K.M., Angle R.P. and Sandhu H.S. (1998) Forest fire enhanced photochemical air pollution: A case study. *Atmospheric Environment* **32**, 673-681.

EPD (2003) "*Exceedances of Federal Air Quality Standards in Georgia, 2000*" Georgia Environmental Protection Division, http://www.air.dnr.state.ga.us/tmp/00exceedances/ ,Located: 08/22/2003.

Hakami A., Odman M. T. and Russell A. G., "High-order, direct sensitivity analysis of multidimensional air quality models," Environmental Science and Technology, vol. 37, no. 11,

1   pp. 2442-2452, June 2003.

2   Hardy, C. C. and Leenhouts, B. (2001) "Introduction Section", *2001 Smoke Management Guide*

3   *for Prescribed and Wildland Fire*, Prepared by National Wildfire Coordinating Group, NFES-

4   1279.

5   Hu, Y., Odman, M. T., and Russell, A. (2003a) "*Air Quality Modeling of the First Base Case*

6   *Episode for the Fall Line Air Quality Study*," Prepared for Georgia Department of Natural

7   Resources, Environmental Protection Division, June 2003.

8   Hu, Y., Odman, M. T., and Russell, A. (2003b) "*Meteorological Modeling of the First Base Case*

9   *Episode for the Fall Line Air Quality Study*," Prepared for Georgia Department of Natural

10   Resources, Environmental Protection Division, February 2003.

11   Jang, J. C., Jeffries, H. E., Byun, D., and Pleim, J. E. (1995) "Sensitivity of Ozone to Model Grid

12   Resolution-I. Application of High-Resolution Regional Acid Deposition Model," *Atmospheric*

13   *Environment*, **Vol. 29**, No. 21, 3085-3100.

14   Karamchandani, P., Santos, I., Sykes, I., Zhang, Y., Tonne, C. and Seigneur, C. (2000)

15   Development and evaluation of a state-of-the-science reactive plume model. *Environmental*

16   *Science and Technology* **34**, 870-880.

17   Karsten, B., Zheng, M., Chang, M., and Russell, A. (2003) "Study of Air Quality Impacts

18   Resulting from Prescribed Burning on Military Facilities" Presentation given at Georgia

19   Institute of Technology.

20   Khan, M. N. and Odman, M. T. (2003) Application and performance evaluation of an adaptive

21   grid air quality model, in preparation.

1   Khan, N. K., Odman, M. T. and Karimi, H. (2003) Evaluation of algorithms developed for

2   adaptive grid air quality modeling using surface elevation data," *Computers, Environment and*

3   *Urban Systems*, in press.

4   Larimore, R. (2000) *Prescribed Burning on the Fort Benning Military Reservation.* Presentation

5   to the Columbus Environmental Committee, August 8, 2000

6   Odman, M. T. and Ingram, C. L. (1996), *Multiscale Air Quality Simulation Platform (MAQSIP):*

7   *Source Code Documentation and Validation*. Technical Report, ENV-96TR002, MCNC—North

8   Carolina Supercomputing Center, Research Triangle Park, NC, 83 pp.

9   Odman, M. T., Khan M. N., and McRae, D. S. (2000b) Adaptive grids in air pollution modeling:

10   Towards an operational model. *Millennium NATO/CCMS International Technical Meeting on*

11   *Air Pollution Modelling and Its Application*, Boulder, Colorado, May 15-19, 2000.

12   Odman, M. T., Khan M. N., and McRae, D. S. (2001) Adaptive grids in air pollution modeling:

13   Towards an operational model," in <u>Air Pollution Modeling and Its Application XIV</u>, pp. 541-

14   549, (S.-E. Gryning and F. A. Schiermeier, Eds.), New York: Kluwer Academic/Plenum

15   Publishers.

16   Odman, M. T., Khan, M. N., Srivastava, R. K. and McRae, D. S. (2002a) Initial application of

17   the adaptive grid air pollution model," in <u>Air Pollution Modeling and its Application XV</u>, pp.

18   319-328 (C. Borrego and G. Schayes, Eds.), New York: Kluwer Academic/Plenum Publishers

19   Odman, M. T., Mathur, R., Alapaty, K., Srivastava, R. K., McRae, D. S. and Yamartino, R. J.

20   (1997) Nested and adaptive grids for multiscale air quality modeling. *Next Generation*

21   *Environmental Models Computational Methods*, G. Delic and M. F. Wheeler, SIAM,

1   Philadelphia, p. 59-68.

2   Ottmar, R. D. (2001) "Smoke Source Characteristics" *2001 Smoke Management Guide for*

3   *Prescribed and Wildland Fire*, Prepared by National Wildfire Coordinating Group, NFES-1279.

4   Srivastava, R. K., McRae, D. S. and Odman, M. T. (2000) An adaptive grid algorithm for air

5   quality modeling. *Journal of Computational Physics* **165**, 437-472.

6   Srivastava, R. K., McRae, D. S. and Odman, M. T. (2001a) Simulation of a reacting pollutant

7   puff using an adaptive grid algorithm. *Journal of Geophysical Research*, in press.

8   Srivastava, R. K., McRae, D. S. and Odman, M. T. (2001b) Simulation of dispersion of a power

9   plant plume using an adaptive grid algorithm. *Atmospheric Environment*, revisions submitted.

10   Unal, A., Tian, D., Hu, Y., Russell, T. "*2000 Emissions Inventory for Fall Line Air Quality Study*

11   *(FAQS),*" Prepared for Georgia Department of Natural Resources, Environmental Protection

12   Division, April 2003.

13   Westbury, H. (2002) Personal communication on 10-21-2002.

14   Yang, Y.-J., J. G. Wilkinson and A. G. Russell, Fast direct sensitivity analysis of

15   multidimensional photochemical models, *Environ. Sci. Technol*. **31**, 2859-68, 1997.
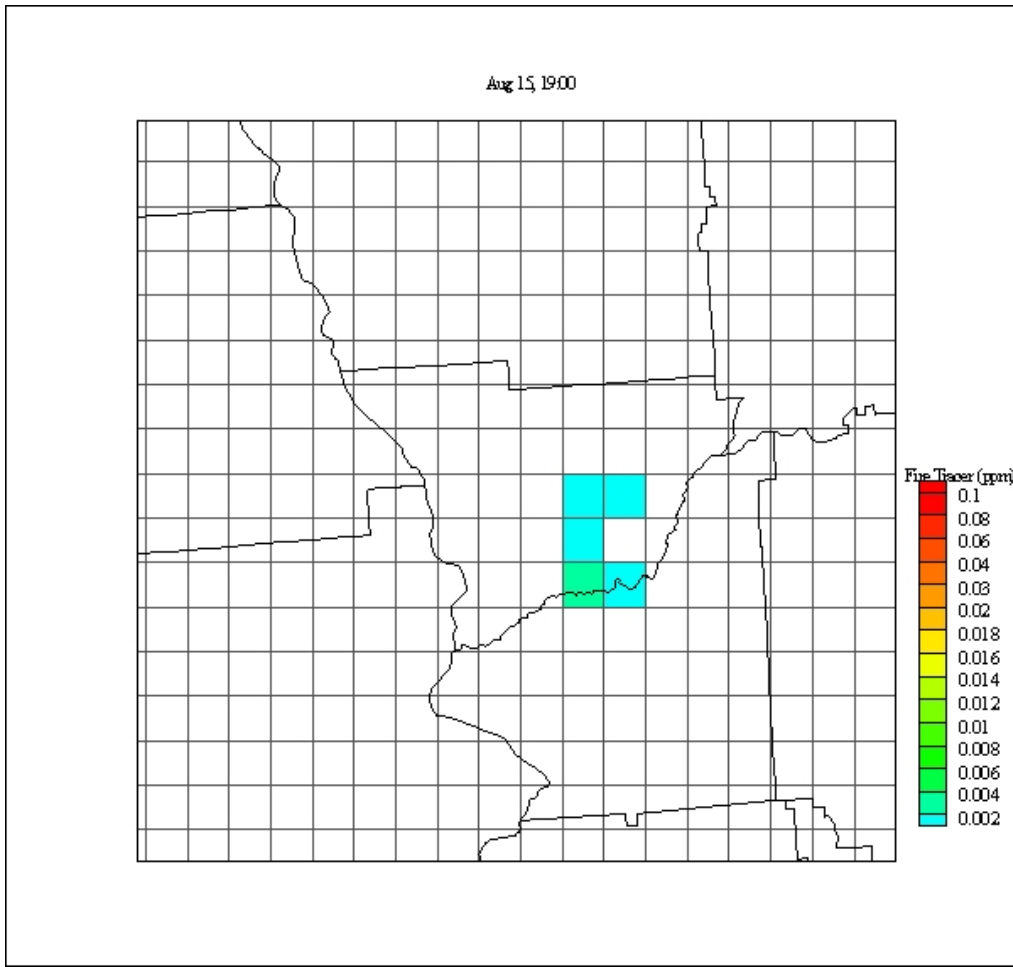
Figure 1 Static Grid Result for Inert Fire Tracer Concentrations (ppm)
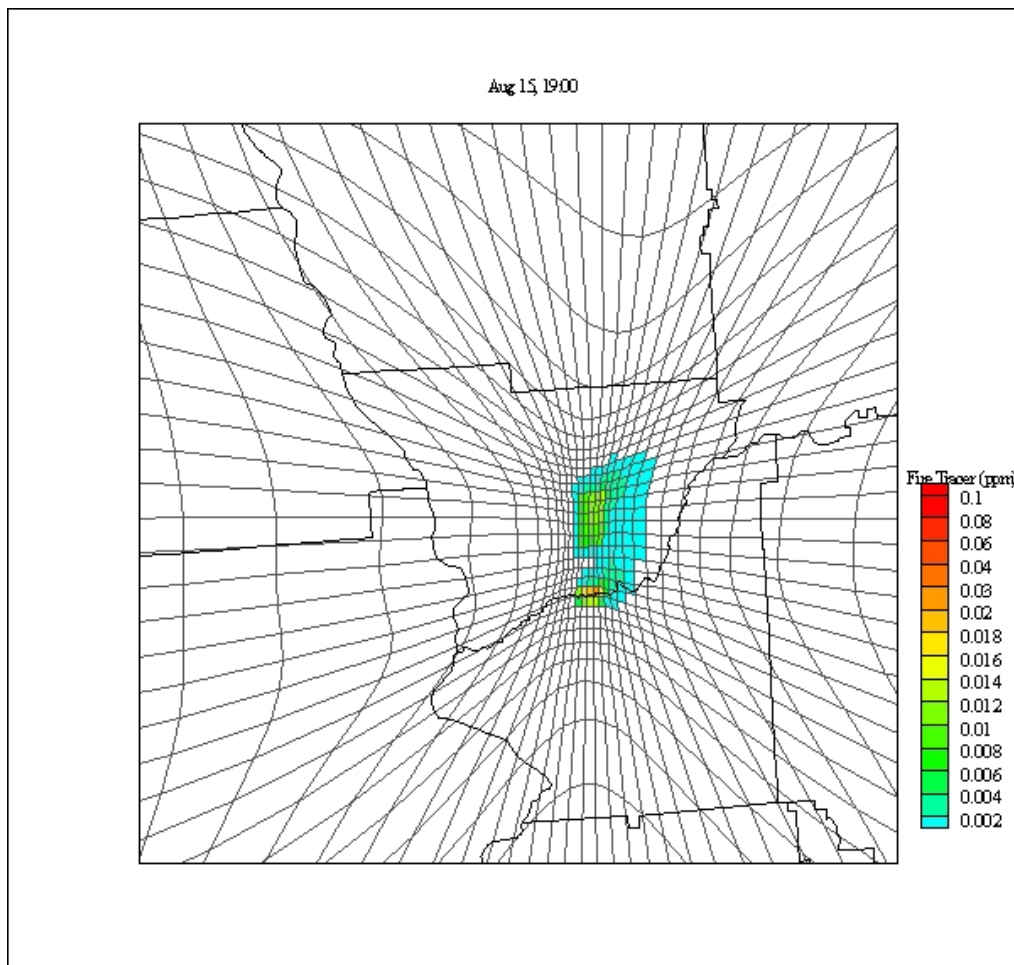
Figure 2 Adaptive Grid Result for Inert Fire Tracer Concentrations (ppm)

Figure 3 Static Grid Result for Brute-Force Sensitivity of O_3 (ppm) to Fire Emissions

Figure 4 Adaptive Grid Result for Direct Sensitivity of O_3 (ppm) to Fire Emissions

Static Cell
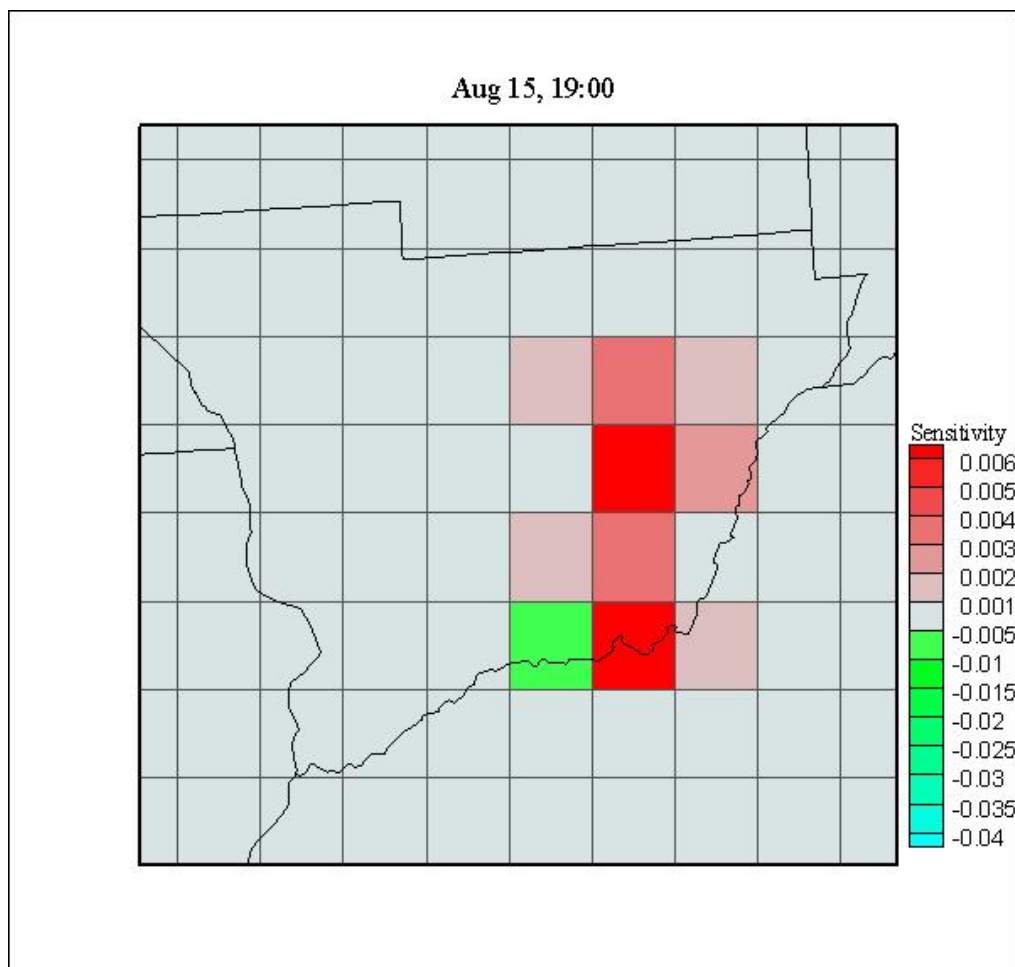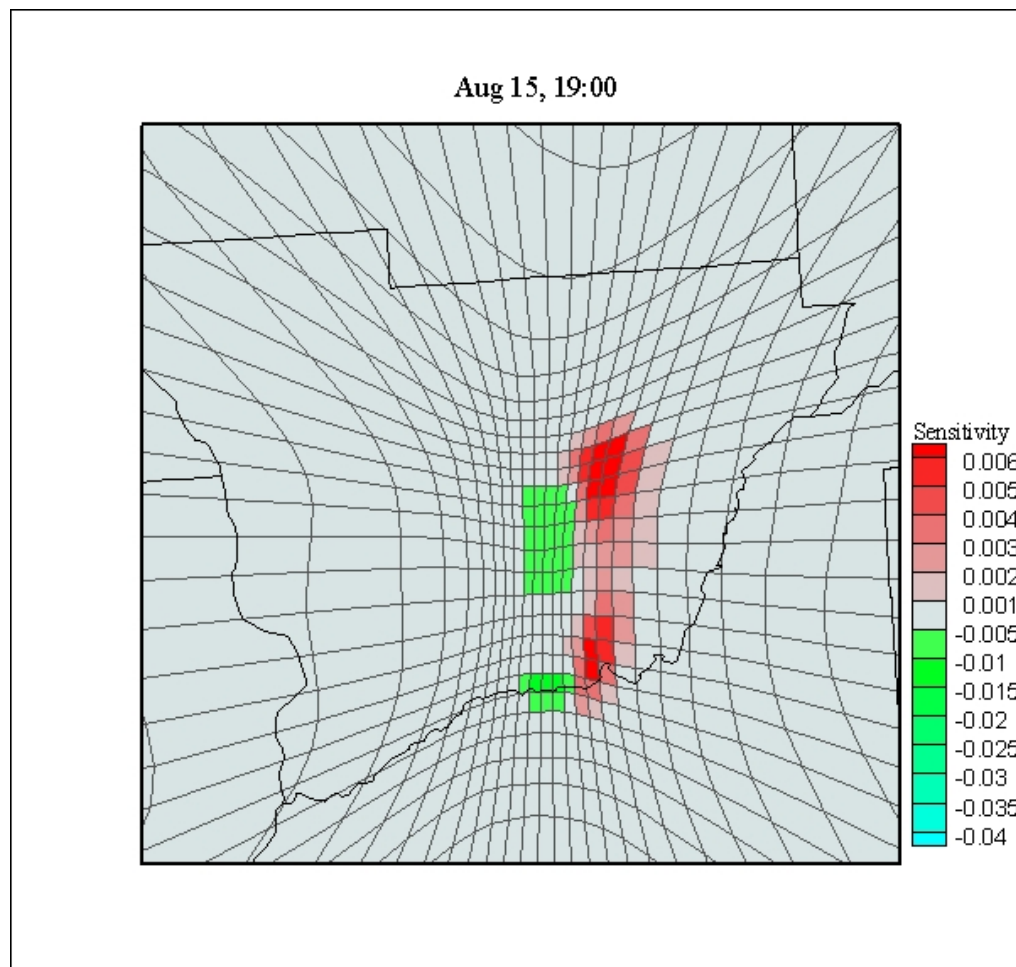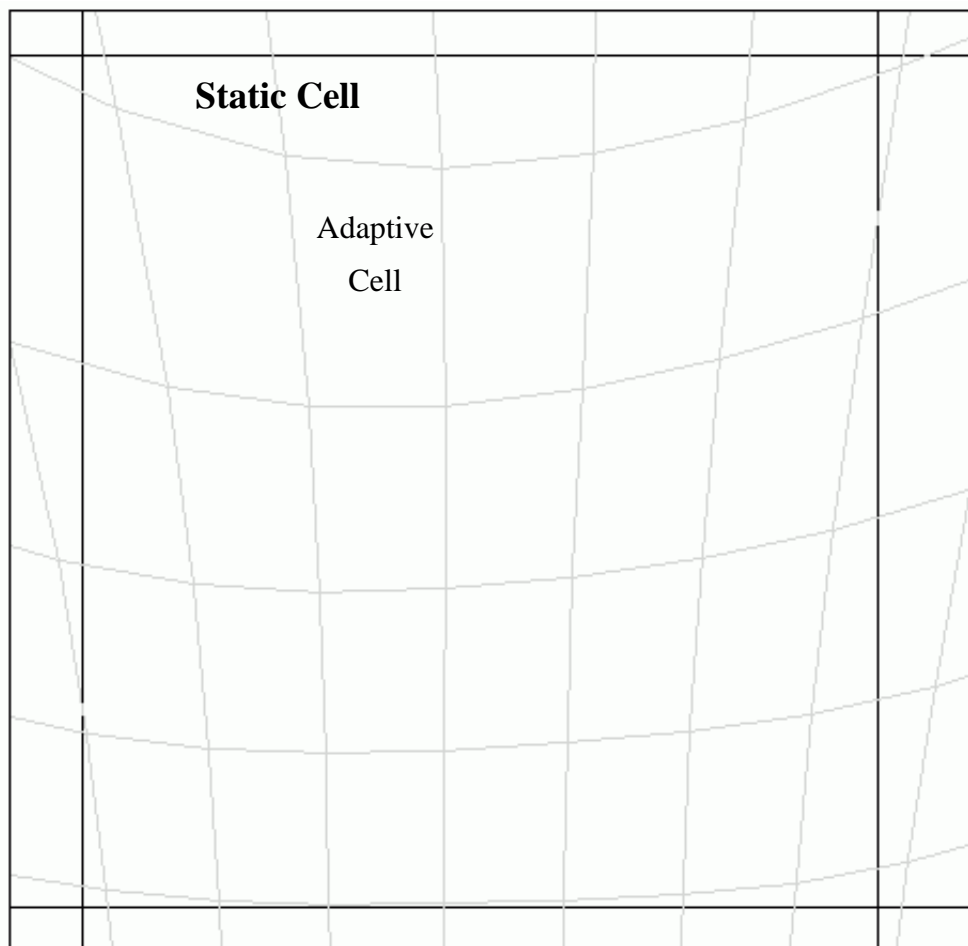
Adaptive
Cell

Figure 5 Intersections of Static and Adaptive Cells
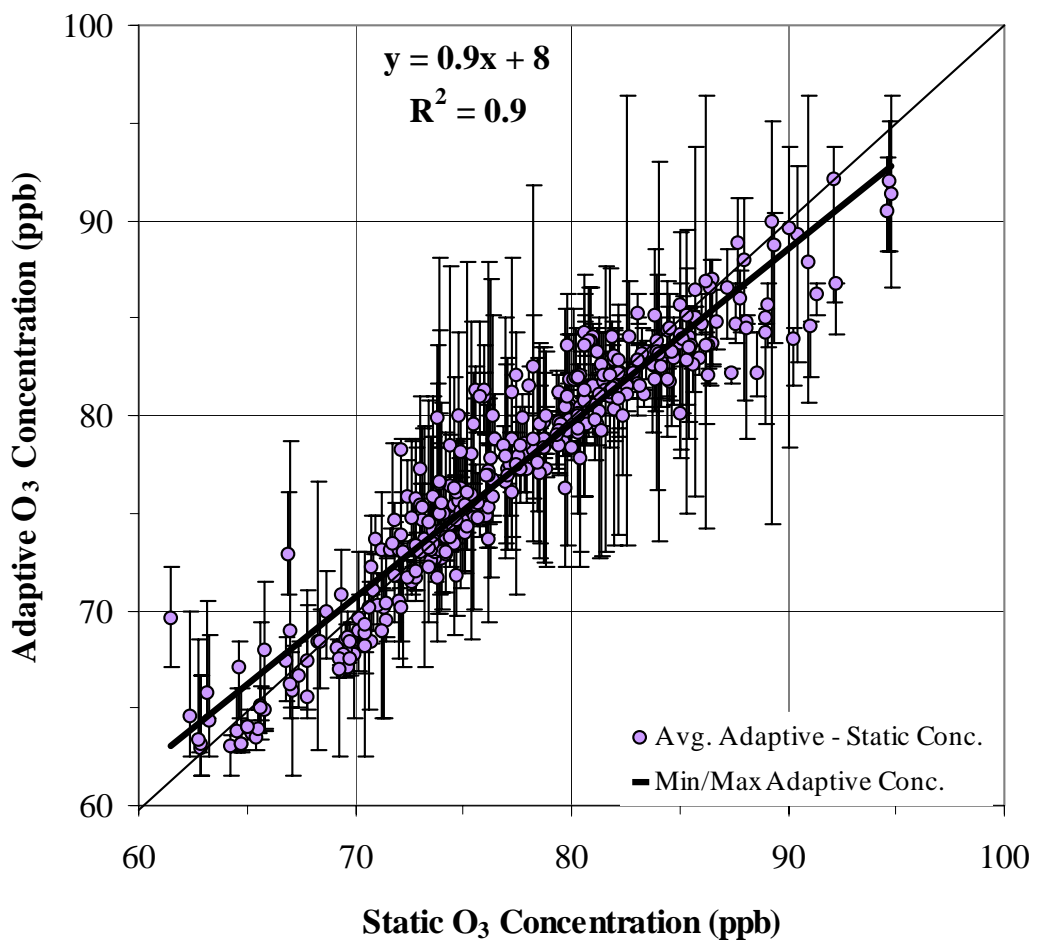
Figure 6 Adaptive versus Static Grid O$_3$ Concentrations (ppb) for August 15, 21:00

Table 1 Comparison of Static versus Adaptive for O_3 Concentration

| Date	Time	Range of O_3 (ppb)			Linear Regression (Adaptive Average vs. Static)	
		Adaptive Average	**Adaptive Max/Min**	**Static**	**R^2**	**Slope**
15	19:00	69 – 100	66 – 106	68 – 103	0.96	0.94
15	20:00	66 – 99	66 – 104	67 – 101	0.92	0.92
15	21:00	63 – 92	61 – 96	62 – 95	0.90	0.90
16	18:00	55 – 99	55 – 101	55 – 100	0.97	1.04
16	19:00	55 -100	54 – 103	55 – 97	0.95	1.01
16	20:00	54 – 101	54 – 106	54 – 97	0.96	1.02
16	21:00	54 – 102	54 – 104	53 – 101	0.96	1.00
16	22:00	48 – 104	47 – 108	39 – 103	0.95	0.97
16	23:00	26 – 103	18 – 105	10 – 100	0.90	0.94
18	2:00	10 – 68	3 – 73	2 – 76	0.92	0.90
18	3:00	7 – 64	2 – 72	2 – 75	0.91	0.91
18	4:00	5 – 64	1 – 64	1 – 72	0.91	0.91
18	5:00	32 – 64	27 -70	31 – 61	0.83	0.97
18	6:00	45 – 63	43 – 65	40 – 61	0.65	0.82
18	7:00	47 – 64	44 – 64	41 – 62	0.68	0.72
18	8:00	43 – 60	42 – 61	39 – 59	0.66	0.73
18	9:00	42 – 57	42 – 58	37 – 55	0.69	0.69
18	10:00	35 – 58	34 – 58	31 – 55	0.93	0.82
18	13:00	38 – 67	36 – 67	29 – 66	0.93	0.91
18	14:00	53 – 75	51 – 77	44 – 74	0.91	0.90

Figure 7 Static versus Adaptive O_3 predictions (ppb) for a specific cell near the fires
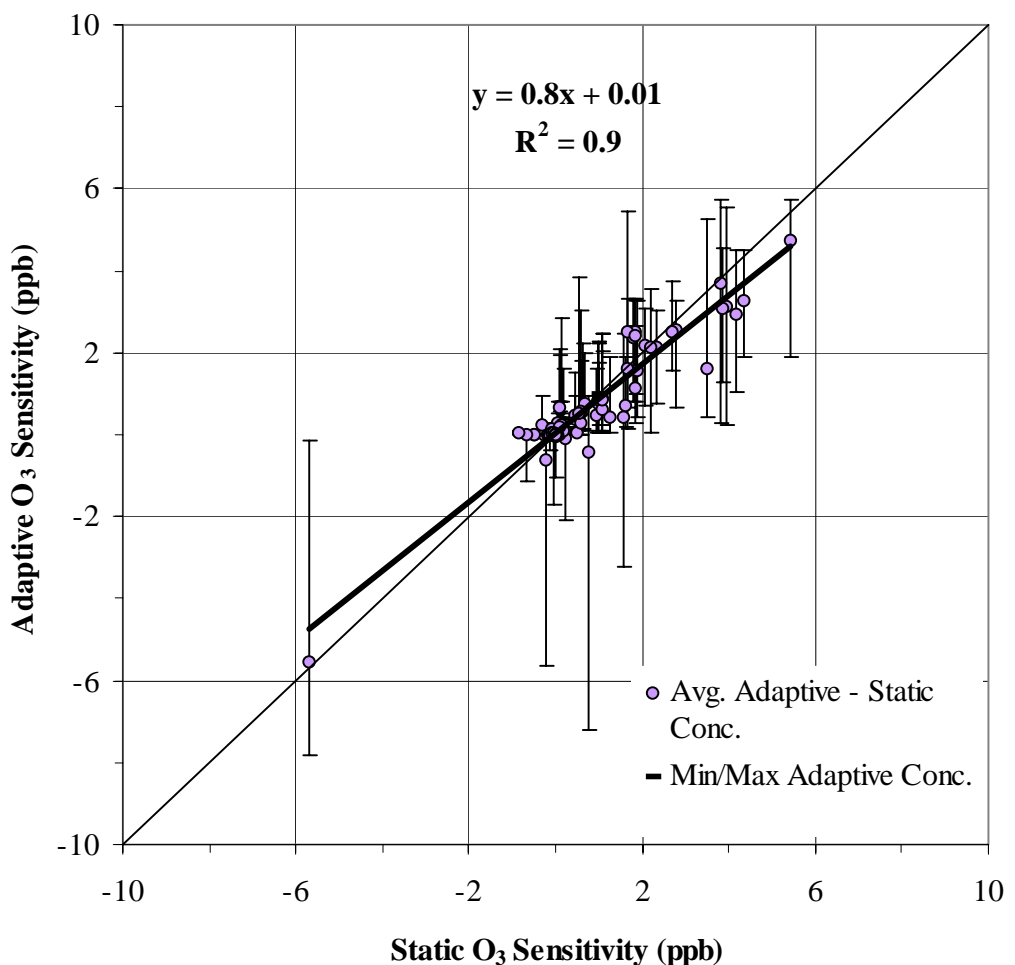
Figure 8 Static versus Adaptive O_3 Sensitivities (ppb) for August 15, 21:00 PM

Table 2 Comparison of Static versus Adaptive for O_3 Sensitivity

Date	Time	Range of O_3 Sensitivity (ppb)			Linear Regression (Adaptive Average vs. Static)	
		Average Adaptive	**Max/Min Adaptive**	**Static**	R^2	**Slope**
15	19:00	-9 – 4	-13 – 8	-8 – 7	0.69	0.77
15	20:00	-5 – 5	-7 – 8	-5 – 6	0.88	0.78
15	21:00	-6 – 5	-8 – 6	-6 – 5	0.90	0.85
16	18:00	-2 – 2	-5 – 3	-2 – 4	0.14	0.23
16	19:00	0 – 6	0 – 8	0 – 6	0.77	0.71
16	20:00	0 – 3	0 – 5	0 – 4	0.93	0.81
16	21:00	0 – 2	0 – 3	0 – 3	0.90	0.73
16	22:00	0 – 2	0 – 3	0 – 2	0.88	0.74
16	23:00	0 – 1	0 – 2	0 – 1	0.91	0.74
18	2:00	-30 – 0	-33 – 0	-48 – 0	0.84	0.52
18	3:00	-33 – 0	-38 – 0	-48 – 0	0.78	0.54
18	4:00	-35 – 0	-40 – 0	-47 – 0	0.76	0.58
18	5:00	-15 – 0	-18 – 0	-15 – 0	0.98	0.96
18	6:00	-8 – 0	-9 – 0	-8 – 0	0.98	0.98
18	7:00	-4 – 0	-4 – 0	-4 – 0	0.97	1.00
18	8:00	-3 – 0	-3 – 0	-3 – 0	0.97	0.97
18	9:00	-2 – 0	-2 – 0	-2 – 0	0.96	0.95
18	10:00	-1 – 0	-1 – 0	-1 – 0	0.96	0.89
18	13:00	-9 – 0	-12 – 0	-16 – 0	0.87	0.49
18	14:00	0 – 2	0 – 2	0 – 3	0.95	0.67